
Electronic Thesis and Dissertation Repository

5-7-2012 12:00 AM

Plasticity in Photosynthetic Performance and Energy Utilization Efficiency in *Triticum aestivum* L., *Secale cereale* L. and *Brassica napus* L. in Response to Low Temperature and High CO₂

Keshav Prasad Dahal, *The University of Western Ontario*

Supervisor: Prof. Dr. Norman PA Hüner, *The University of Western Ontario*

A thesis submitted in partial fulfillment of the requirements for the Doctor of Philosophy degree in Biology

© Keshav Prasad Dahal 2012

Follow this and additional works at: <https://ir.lib.uwo.ca/etd>



Part of the [Biology Commons](#)

Recommended Citation

Dahal, Keshav Prasad, "Plasticity in Photosynthetic Performance and Energy Utilization Efficiency in *Triticum aestivum* L., *Secale cereale* L. and *Brassica napus* L. in Response to Low Temperature and High CO₂" (2012). *Electronic Thesis and Dissertation Repository*. 524.
<https://ir.lib.uwo.ca/etd/524>

This Dissertation/Thesis is brought to you for free and open access by Scholarship@Western. It has been accepted for inclusion in Electronic Thesis and Dissertation Repository by an authorized administrator of Scholarship@Western. For more information, please contact wlsadmin@uwo.ca.

PLASTICITY IN PHOTOSYNTHETIC PERFORMANCE AND ENERGY UTILIZATION
EFFICIENCY IN *TRITICUM AESTIVUM* L., *SECALE CEREALE* L. AND *BRASSICA*
NAPUS L. IN RESPONSE TO LOW TEMPERATURE AND HIGH CO₂

(Spine title: Plasticity in photosynthetic performance and energy utilization efficiency)

(Thesis format: Integrated Article)

by

Keshav Dahal

Graduate Program in Biology

A thesis submitted in partial fulfillment
of the requirements for the degree of
Doctor of Philosophy

The School of Graduate and Postdoctoral Studies
The University of Western Ontario
London, Ontario, Canada

© Keshav Dahal 2012

CERTIFICATE OF EXAMINATION

Supervisor

Examiners

Dr. Norman PA Hüner

Dr. Robert D. Guy

Supervisory Committee

Dr. Eric H. Ball

Dr. Bernard Grodzinski

Dr. Mark Bernards

Dr. Mark Bernards

Dr. Denis Maxwell

The thesis by

Keshav Dahal

entitled:

**Plasticity in Photosynthetic Performance and Energy Utilization
Efficiency in *Triticum aestivum* L., *Secale cereale* L. and *Brassica
napus* L. in Response to Low Temperature and High CO₂**

is accepted in partial fulfillment of the
requirements for the degree of
Doctor of Philosophy

Date

Chair of the Thesis Examination Board

Abstract

I assessed the effects of cold acclimation and long-term elevated CO₂ on photosynthetic performance and energy conversion efficiency of winter (cv Musketeer, cv Norstar) and spring (cv SR4A, cv Katepwa) rye (*Secale cereale*) and wheat (*Triticum aestivum*) as well as wild type (WT) and *BnCBF17*-over-expressing line (*BnCBF17*-OE) of *Brassica napus* cv Westar. Plants were grown at either 20/16°C (non-acclimated, NA) or 5/5°C (cold acclimated, CA) and at either ambient (380 μmol C mol⁻¹) or elevated (700 μmol C mol⁻¹) CO₂. Compared to NA controls, CA winter cereals, Norstar and Musketeer, exhibited compact dwarf phenotype, increased rates of light-saturated CO₂ assimilation (42%) and photosynthetic electron transport (48%) and higher levels of *rbcL*, cytosolic FBPase, *Lhcb1*, *PsbA* and *PsaA* at ambient CO₂. This was associated with enhanced energy conversion efficiency into biomass (31%) and seed yield (20%) coupled to decreased excitation pressure and decreased energy dissipation through non-photochemical quenching (NPQ) for a given irradiance and a given CO₂ concentration in CA versus NA winter cereals. The increased photosynthetic performance and energy conversion efficiency of CA winter cereals at ambient CO₂ were maintained under long-term growth and development at elevated CO₂. In contrast, CA spring cereals, SR4A and Katepwa, exhibited decreased CO₂ assimilation rates (35%) and decreased energy conversion efficiency in biomass (40%) not only at ambient CO₂ but also at long-term elevated CO₂. *BnCBF17*-over-expression in *Brassica napus* resulted into dwarf phenotype, increased rates of light-saturated CO₂ assimilation (38%) and photosynthetic electron transport (18%), an enhanced energy conversion efficiency with concomitant decreased reliance on photoprotection to dissipate absorbed energy through NPQ for a given irradiance and a given CO₂. Compared to WT *Brassica napus*, *BnCBF17*-over-expression reduced sensitivity to feedback-limited photosynthesis during long-term growth of *B. napus* under elevated CO₂. *CBFs* (C-repeat binding factors) are transcriptional activators that induce the expression of cold-regulated genes. We suggest that *CBFs* regulate not only freezing tolerance but also control the photosynthetic performance and energy conversion efficiency in biomass and grain yield through morphological, physiological and biochemical adjustments. Hence, targeting the *CBF* pathways in major crop species can be a novel approach to improve crop yield and productivity.

Keywords

Cold acclimation, CBF transcription factors, *BnCBF17*-over-expression, energy conversion efficiency, light-saturated rates of photosynthesis, long-term elevated CO₂, short-term elevated CO₂, winter and spring cereals, *Brassica napus*

Co-Authorship Statement

Chapter 2:

Dahal K, Kane K, Gadapati W, Webb E, Savitch LV, Singh J, Sharma P, Sarhan F, Longstaffe FJ, Grodzinski B, Hüner NPA (2012a) The effects of phenotypic plasticity on photosynthetic performance in winter rye, winter wheat and *Brassica napus*. *Physiol Plant* 144: 169-188

Winona Gadapati measured CO₂ gas exchange rates in *Brassica napus*. Pooja Sharma counted stomata in cereal leaves. Dr. Savitch and Dr Singh generated transgenic *Brassica napus* and contributed on editing the manuscript. Dr. Sarhan and Mr. Kane were involved in carrying out qRT-PCR and immunoblot assay for COR-genes and interpreting results. Dr. Longstaffe and Dr. Webb granted access for carbon isotope measurements and provided comments on manuscript. Dr. Grodzinski provided feedback on manuscript. Dr. Hüner was involved in designing research, interpreting results and editing the manuscript.

Chapter 3

Dahal K, Kane K, Sarhan F, Grodzinski B, Hüner NPA (2012b) Cold acclimation inhibits CO₂-dependent stimulation of photosynthesis in spring wheat and spring rye. *Botany (in press)*

All co-authors contributed on editorial comments on the manuscript. Dr. Sarhan and Mr. Kane were involved in performing qRT-PCR and interpreting results.

Chapter 4

Dahal K, Gadapati W, Savitch LV, Singh J, Hüner NPA (2012) Cold acclimation and *BnCBF17*-over-expression enhance photosynthetic performance and energy conversion efficiency during long-term growth of *Brassica napus* under elevated CO₂ conditions. *Planta (accepted with minor revisions)*. Manuscript ID: Planta-2012-03-0133

Winona Gadapati measured CO₂ gas exchange rates. Dr. Savitch and Dr. Singh generated transgenic *Brassica napus* and provided comments on the manuscript. Dr. Hüner guided on research design, result interpretation and provided feedback on the manuscript.

Chapter 5

Dahal K, Kane K, Sarhan F, Hüner NPA (2012) Cold acclimated winter wheat and winter rye maintain enhanced photosynthetic performance, energy conversion efficiency and grain yield under long-term growth at elevated CO₂. *Plant Physiology (In preparation)*

Dr. Sarhan and Mr. Kane were involved in performing micro-array and qRT-PCR as well as interpreting results. Dr. Hüner guided in designing research, interpreting results and editing the manuscript.

DEDICATION

I dedicate this research work to
my respected parents

Mr. Hom Prasad Dahal and late Mrs. **Nanda Kumari Dahal**

Acknowledgments

First and foremost, I would like to sincerely thank my respected supervisor Dr. Norman PA Hüner for his incredible guidance and suggestions throughout the entire research work. The successful accomplishment of my PhD thesis would not have been possible without the continuous supports and supervision of Dr. Hüner. In the framework of his laboratory research work, Dr. Hüner always encouraged me to independently plan, implement and conduct my experimental tasks. In addition, Dr. Hüner always inspired me: (i) to be an independent researcher, (ii) to assimilate complex plant physiological, morphological and molecular relationships (iii) to work with great care and skill in a laboratory and (iv) to timely evaluate and interpret the analytical results of my research. Besides his outstanding research guidance, Dr. Hüner always helped me in many aspects with chores always quickly and efficiently. His friendly and open manner, especially towards international students, inspired me to promptly integrate myself in his research team. I am extremely proud to be his PhD student and would like to sincerely salute him for his unique assistance to me.

I would like to gratefully acknowledge members of my advisory committee Dr. Bernard Grodzinski, University of Guelph, and Dr. Mark Bernards, University of Western Ontario for their creative advice and direction to improve the quality of my research. My thanks are also due to Dr. Fathey Sarhan and Khalil Kane, University of Quebec for providing me data on wheat micro-array, qRT-PCR and COR polypeptides.

I am deeply indebted to all members of the Hüner lab and environmental stress biology group for their time, supports and friendship. In this regard, I am especially grateful to Dr. Marianna Kröl, Dr. Alex Ivanov and Dr. Florian Busch for facilitating me in growth chamber and laboratory works. Further, my gratitude goes to Dr. Denis Maxwell for his contribution to me either as an examiner or a course teacher. Dr. Maxwell always encouraged me by appreciating my research work and oral presentation.

I have no words to gratitude my dearest wife Jyoti Dahal for her indispensable supports and love to me during my study. In fact, she sacrificed quite many opportunities for the betterment of my research and involved actively in taking care of our kids and running our

home smoothly during my study. This is incredibly important as I was able to entirely concentrate on my research and get the work done in time.

I am profoundly indebted to my family and relatives especially my father Hom Prasad Dahal and my late mother Nanda Kumari Dahal for always encouraging me to pursue higher level study in North America. Thanks for their patience and supports during my study.

At last but not least, I would like to acknowledge the Natural Sciences and Engineering Research Council (NSERC) Canada for financially supporting my PhD research through Green Crop Network and Dr. Hüner's grant. Moreover, I am thankful to the Department of Biology, University of Western Ontario for providing me an opportunity to undertake my PhD study, financially supporting me through Western Graduate Research Scholarship (WGRS) and decorating me with Dr. Irene Uchida Fellowship.

Table of Contents

CERTIFICATE OF EXAMINATION	ii
Abstract and Key words.....	iii
Co-Authorship Statement.....	v
Dedication.....	vii
Acknowledgments.....	viii
Table of Contents.....	x
List of Tables.....	xvi
List of Figures.....	xviii
List of Appendices.....	xxii
List of Abbreviations.....	xxvi
Chapter 1: General introduction	
1.1 Background.....	1
1.2 Photosynthetic pigments and associated photosystems.....	1
1.3 Photosynthetic Intersystem Electron Transport and Production of Assimilatory Power (NADPH and ATP).....	3
1.4 Photosynthetic CO ₂ assimilation.....	8
1.5 Feedback inhibition of rates of CO ₂ assimilation	10
1.6 Dark respiration rates	11
1.7 Cold acclimation and photosynthesis.....	12
1.8 Elevated CO ₂ and photosynthesis	
1.8.1 Short-term response of photosynthesis to elevated CO ₂	16
1.8.2 Long-term response of photosynthesis to elevated CO ₂	17
1.9 Chlorophyll a fluorescence	18
1.10 Energy partitioning.....	22

1.11 Objective of the thesis.....	25
1.12 References	27
Chapter 2: The effects of phenotypic plasticity on photosynthetic performance in winter rye, winter wheat and <i>Brassica napus</i>	
2.1 Introduction.....	34
2.2 Materials and methods	
2.2.1 Plant materials and growth conditions	36
2.2.2 Comparative growth kinetics	37
2.2.3 Scanning electron microscopy	38
2.2.4 CO ₂ gas exchange measurements.....	38
2.2.5 Room temperature Chl a Fluorescence	39
2.2.6 Carbon isotope discrimination ($\delta^{13}\text{C}$)	40
2.2.7 Determination of total leaf protein and immunodetection	40
2.2.8 Analyses of gene expression.....	41
2.2.9 Statistical analysis	42
2.3 Results	
2.3.1 Effects of cold acclimation on phenotypic plasticity of rye and wheat cultivars	42
2.3.2 Effects of cold acclimation on CO ₂ assimilation in rye and wheat cultivars	46
2.3.3 Differential effects of increased SLW and Chl on photosynthetic light and CO ₂ response curves	51
2.3.4 Effects of cold acclimation on stomatal conductance and water use efficiency .	54
2.3.5 Effects of cold acclimation on $\delta^{13}\text{C}$ values of leaf tissues	56
2.3.6 Effects of cold acclimation on dark respiration rates.....	56
2.3.7 Effects of cold acclimation on ETR, EP and NPQ	57
2.3.8 Effects of cold acclimation on photosynthetic gene expression and polypeptide accumulation	59
2.3.9 Effects of over-expression of <i>BnCBF17</i> on phenotypic plasticity and photosynthetic performance in <i>Brassica napus</i>	61

2.4 Discussion	68
2.5 References	74
2.6 Appendices	80
Chapter 3: Cold acclimation inhibits CO ₂ -dependent stimulation of photosynthesis in spring wheat and spring rye	
3.1 Introduction.....	89
3.2 Materials and methods	
3.2.1 Plant materials and growth conditions	91
3.2.2 Comparative growth kinetics	92
3.2.3 CO ₂ gas exchange measurements	92
3.2.4 Determination of total leaf protein and immunodetection	93
3.2.5 Analyses of gene expression	94
3.2.6 Statistical analysis	94
3.3. Results	
3.3.1 Effects of cold acclimation on growth characteristics at ambient CO ₂	95
3.3.2 Effects of cold acclimation and measuring temperatures on light-saturated rates of photosynthesis, A _{sat} , and stomatal conductance at ambient CO ₂	95
3.3.3 Effects of short-term elevated CO ₂ on light response curves and light-saturated CO ₂ response curves	98
3.3.4 Kinetics for the CO ₂ stimulation of the light-saturated rates of gross photosynthesis.....	101
3.3.5 Effects of short-term elevated CO ₂ on stomatal conductance.....	104
3.3.6 Temperature sensitivity of CO ₂ -stimulated A _{sat}	105
3.3.7 Effects of short- term elevated CO ₂ on dark respiratory rates.....	110
3.3.8 Effects of short-term elevated CO ₂ and high temperature on leaf protein content, photosynthetic gene expression and polypeptide content.....	110
3.4 Discussion	114
3.5 References	117

3.6 Appendices.....	121
Chapter 4: Cold acclimation and <i>BnCBF17</i> -over-expression enhance photosynthetic performance and energy conversion efficiency during long-term growth of <i>Brassica napus</i> under elevated CO ₂ conditions	
4.1 Introduction.....	129
4.2 Materials and methods	
4.2.1 Plant growth.....	132
4.2.2 CO ₂ gas exchange.....	134
4.2.3 Room temperature Chl a fluorescence.....	135
4.2.4 Determination of total leaf protein and immunodetection.....	135
4.2.5 Statistical analysis.....	136
4.3 Results	
4.3.1 Growth characteristics.....	137
4.3.2 Light response curves for CO ₂ assimilation.....	140
4.3.3 CO ₂ -response curves for CO ₂ assimilation.....	142
4.3.4 Light response curves for ETR, EP and NPQ.....	144
4.3.5 CO ₂ response curves for ETR, EP and NPQ.....	146
4.3.6 Photosynthetic polypeptide abundance.....	148
4.3.7 Stomatal characteristics.....	149
4.3.8 Dark respiratory rates.....	152
4.4 Discussion.....	152
4.5 References.....	156
4.6 Appendices.....	161
Chapter 5: Cold acclimated winter wheat and winter rye maintain enhanced photosynthetic performance, energy conversion efficiency and grain yield under long-term growth at elevated CO ₂	
5.1 Introduction.....	162
5.2 Materials and methods	

5.2.1 Plant materials and growth conditions.....	166
5.2.2 Pot size experiment.....	167
5.2.3 Comparative growth kinetics.....	167
5.2.4 CO ₂ gas exchange measurements.....	167
5.2.5 Room temperature Chl a fluorescence.....	168
5.2.6 Determination of total leaf protein and immunodetection.....	169
5.2.7 Micro-array analysis.....	170
5.2.8 Flowering time and grain yield.....	170
5.2.9 Statistical analysis.....	171
5.3 Results	
5.3.1 Effects of cold acclimation and elevated CO ₂ on growth characteristics.....	171
5.3.2 Effects of cold acclimation and elevated CO ₂ on photosynthetic light response curves.....	176
5.3.3 Effects of cold acclimation and elevated CO ₂ on photosynthetic CO ₂ response curves.....	178
5.3.4 Effects of cold acclimation and elevated CO ₂ on light response curves for ETR, EP and NPQ.....	181
5.3.5 Effects of cold acclimation and elevated CO ₂ on photosynthetic CO ₂ response curves for ETR, EP and NPQ.....	182
5.3.6 Effects of cold acclimation and elevated CO ₂ on stomatal characteristics.....	185
5.3.7 Effects of cold acclimation and elevated CO ₂ on dark respiratory rates.....	185
5.3.8 Effects of cold acclimation and elevated CO ₂ on gene expression in wheat.....	187
5.3.9 Effects of cold acclimation and elevated CO ₂ on leaf protein and polypeptide contents.....	191
5.3.10 Effects of elevated CO ₂ on flowering time and grain yield.....	193
5.4 Discussion.....	196
5.5 References.....	201
5.6 Appendices.....	207

Chapter 6: General discussions and future perspectives	
6.1 Major contributions	
6.1.1 CBF enhances energy conversion efficiency.....	217
6.1.2 CO ₂ -induced feedback-limited photosynthesis is species dependent.....	219
6.1.3 Phenotypic plasticity accounts for the increased CO ₂ assimilation.....	221
6.1.4 Elevated CO ₂ can not compensate for decreased A _{sat} of CA spring cereals.....	221
6.1.5 CBF is a master regulator: A model.....	222
6.2 References.....	228
Curriculum Vitae.....	232

List of Tables

Table 2.1. Effects of growth temperatures on growth characteristics of winter and spring rye and wheat cultivars grown at 20/16°C and 5/5°C and at ambient CO ₂ conditions.....	43
Table 2.2. Light-saturated rates of net CO ₂ assimilation (A_{sat}) and dark respiratory rates (R_{dark}) for winter and spring wheat and rye cultivars grown at either 20/16°C or 5/5°C and at ambient CO ₂ conditions.....	47
Table 2.3. Light-saturated rates ETR and J_{max} , the initial linear slope of the light response curves (Q) and the initial linear slope of the light-saturated A/C _i response curves (carboxylation efficiency), for winter and spring wheat and rye cultivars.....	50
Table 2.4. Stomatal conductance, transpiration rates and leaf water use efficiency for winter and spring wheat and rye cultivars grown at either 20/16°C or 5/5°C and at ambient CO ₂	55
Table 2.5. Morphological and physiological characteristics of wild type and <i>BnCBF17</i> -over-expressing transgenic <i>Brassica napus</i> grown at 20/16°C and at ambient CO ₂ conditions.....	63
Table 3.1. Effects of cold acclimation on exponential growth rates (EGR) and specific leaf weight (SLW) for winter and spring cereals grown at ambient CO ₂ at either 20/16°C or 5/5°C.....	96
Table 3.2. Effects of short-term elevated CO ₂ (700 $\mu\text{mol C mol}^{-1}$) on V_{cmax} , J_{max} , Q and the carboxylation efficiency for winter and spring cereals grown at ambient CO ₂ (380 $\mu\text{mol C mol}^{-1}$) and at either 20/16°C or 5/5°C.....	100
Table 3.3. Effects of short-term shift to elevated CO ₂ (700 $\mu\text{mol C mol}^{-1}$) on stomatal conductance, transpiration rates and water use efficiency for winter and spring cereals grown at ambient CO ₂ (380 $\mu\text{mol C mol}^{-1}$) and at either 20/16°C or 5/5°C.....	106
Table 3.4. Effects of short-term shift to elevated CO ₂ (700 $\mu\text{mol C mol}^{-1}$) and /or high temperature (40°C) on leaf protein content for winter and spring cereals grown at ambient CO ₂ (380 $\mu\text{mol C mol}^{-1}$) and at either 20/16°C or 5/5°C.....	111

Table 4.1. Effects of cold acclimation and elevated CO ₂ on morphological and photosynthetic characteristics of WT and <i>BnCBF17</i> -over-expressing <i>B. napus</i> grown at either ambient (380 μmol C mol ⁻¹) or elevated (700 μmol C mol ⁻¹) CO ₂ and at either 20/16°C or 5/5°C.....	139
Table 4.2. Effects of cold acclimation and elevated CO ₂ on stomatal characteristics of WT and <i>BnCBF17</i> -over-expressing <i>B. napus</i> grown at either ambient (380 μmol C mol ⁻¹) or elevated (700 μmol C mol ⁻¹) CO ₂ and at either 20/16°C or 5/5°C.....	151
Table 5.1. Effects of cold acclimation and elevated CO ₂ on growth characteristics of winter and spring cereals grown at either ambient CO ₂ (380 μmol C mol ⁻¹) or elevated CO ₂ (700 μmol C mol ⁻¹) and at either 20/16°C or 5/5°C.....	173
Table 5.2. Effects of cold acclimation and elevated CO ₂ on V _{cmax} , J _{max} , Q and the carboxylation efficiency (CE) for winter and spring cereals grown at either ambient CO ₂ (380 μmol C mol ⁻¹) or elevated CO ₂ (700 μmol C mol ⁻¹) and at either 20/16°C or 5/5°C.....	179
Table 5.3. Effects of cold acclimation and elevated CO ₂ on stomatal characteristics of winter and spring cereals grown at either ambient CO ₂ (380 μmol C mol ⁻¹) or elevated CO ₂ (700 μmol C mol ⁻¹) and at either 20/16°C or 5/5°C.....	186
Table 5.4. List of the genes differentially expressed upon growth at low temperature (5/5°C vs 20/16°C) or at elevated CO ₂ (700 versus 380 μmol C mol ⁻¹) or combination of both for Norstar winter wheat obtained through the Affymetrix wheat micro-array.....	189
Table 5.5. Effects of elevated CO ₂ on grain yield and its components in winter and spring wheat grown at either ambient (380 μmol C mol ⁻¹) or elevated CO ₂ (700 μmol C mol ⁻¹)....	195

List of Figures

Figure 1.1. A schematic of photosynthetic linear electron transport chain in thylakoid membrane of the chloroplast.....	4
Figure 1.2. Schematic illustrations of photosynthetic CO ₂ assimilation and feedback inhibition of photosynthesis.....	9
Figure 1.3. Measurements of fluorescence parameters under dark-adapted and illuminated conditions and upon application of saturating flashes.....	20
Figure 1.4. A diagrammatic description of fate of absorbed light energy in thylakoid membrane of the chloroplast.....	24
Figure 2.1. Specific leaf weight for winter and spring rye and wheat cultivars grown at either 20/16°C or 5/5°C and at ambient CO ₂	45
Figure 2.2. Temperature response curves of light-saturated net CO ₂ assimilation expressed on either leaf area or leaf chlorophyll or leaf dry weight basis for Musketeer winter and SR4A spring rye cultivars grown at either 20/16°C or 5/5°C and at ambient CO ₂	49
Figure 2.3. Light response curves of gross CO ₂ assimilation expressed on either leaf area or leaf chlorophyll or leaf dry weight basis for Musketeer winter and SR4A spring rye cultivars grown at either 20/16°C or 5/5°C and at ambient CO ₂	52
Figure 2.4. Light-saturated rates of net CO ₂ assimilation versus internal CO ₂ concentrations expressed on either leaf area or leaf chlorophyll or leaf dry weight basis for Musketeer winter and SR4A spring rye grown at either 20/16°C or 5/5°C and at ambient CO ₂	53
Figure 2.5. Light response curves of electron transport rates (ETR), excitation pressures (1-qP) and non photochemical quenching of excess energy (NPQ) for Musketeer winter and SR4A spring rye cultivars grown at either 20/16°C or 5/5°C and at ambient CO ₂	58
Figure 2.6. (A) Relative transcript levels of <i>rbcL</i> , <i>cFBPase</i> , <i>lhcb1</i> , <i>psbA</i> , and <i>psaA</i> and (B) Immunoblot analysis of SDS – PAGE for Norstar winter and Katepwa spring wheat grown at either 20/16°C or 5/5°C and at ambient CO ₂	60

Figure 2.7. Effects of <i>BnCBF17</i> -over-expression on plant morphology, growth habit and leaf anatomy of <i>Brassica napus</i> grown at 20/16°C and at ambient CO ₂	62
Figure 2.8. Light response curves of gross CO ₂ assimilation and light-saturated rates of net CO ₂ assimilation versus internal CO ₂ concentrations expressed on either leaf area or leaf chlorophyll or leaf dry weight basis for WT and <i>BnCBF17</i> -over-expressing <i>Brassica napus</i> grown at 20/16°C and at ambient CO ₂	64
Figure 2.9. Temperature response curves of light-saturated net CO ₂ assimilation and electron transport rates expressed on either leaf area or leaf chlorophyll or leaf dry weight basis for WT and <i>BnCBF17</i> transgenic <i>Brassica napus</i> grown at 20/16°C and at ambient CO ₂	66
Figure 2.10. Light response curves of electron transport rates , excitation pressures and non photochemical quenching of excess energy for WT and <i>BnCBF17</i> -over-expressing transgenic <i>Brassica</i> grown at 20/16°C and at ambient CO ₂	67
Figure 3.1. Effects of measuring temperatures on gross A _{sat} and stomatal conductance of NA and CA winter and spring cereals.....	97
Figure 3.2. Light response curves of gross CO ₂ assimilation at either ambient (380 μmol C mol ⁻¹) or after 80 h of exposure to elevated CO ₂ (700 μmol C mol ⁻¹) for Musketeer and SR4A rye.....	99
Figure 3.3. CO ₂ response curves of net CO ₂ assimilation at either ambient (380 μmol C mol ⁻¹) or after 80 h of exposure to elevated CO ₂ (700 μmol C mol ⁻¹) for Musketeer and SR4A rye.....	102
Figure 3.4. Light-saturated rates of gross CO ₂ assimilation at either ambient (380 μmol C mol ⁻¹) or over 80 h of exposure to elevated CO ₂ (700 μmol C mol ⁻¹) for Musketeer and SR4A rye.....	103
Figure 3.5. Temperature sensitivity of net A _{sat} at either ambient (380 μmol C mol ⁻¹) or after 1 h shift to elevated CO ₂ (700 μmol C mol ⁻¹) for Musketeer and SR4A rye.....	107
Figure 3.6. Temperature sensitivity of net A _{sat} at either ambient (380 μmol C mol ⁻¹) or after 80 h shift to elevated CO ₂ (700 μmol C mol ⁻¹) for Musketeer and SR4A rye.....	109

Figure 3.7. Effects of high temperature (40°C) and elevated CO ₂ (700 μmol C mol ⁻¹) on transcript levels of photosynthetic genes isolated from Norstar and Katepwa wheat.....	112
Figure 3.8. Effects of high temperature (40°C) and elevated CO ₂ (700 μmol C mol ⁻¹) on photosynthetic proteins isolated from Norstar and Katepwa wheat.....	113
Fig. 4.1. Effects of cold acclimation and elevated CO ₂ on plant morphology and growth habit of WT <i>B. napus</i> and <i>BnCBF17</i> -OE grown at either ambient (380 μmol C mol ⁻¹) or elevated (700 μmol C mol ⁻¹) CO ₂ and at either 20/16°C or 5/5°C.....	138
Fig. 4.2. Light response curves of gross CO ₂ assimilation for WT <i>B. napus</i> and the <i>BnCBF17</i> -OE grown at either ambient (380 μmol C mol ⁻¹) or elevated (700 μmol C mol ⁻¹) CO ₂ and at either 20/16°C or 5/5°C.....	141
Fig. 4.3. CO ₂ response curves of net CO ₂ assimilation for WT <i>B. napus</i> and the <i>BnCBF17</i> -OE grown at either ambient (380 μmol C mol ⁻¹) or elevated (700 μmol C mol ⁻¹) CO ₂ and at either 20/16°C or 5/5°C.....	143
Fig. 4.4. Light response curves of electron transport rates, excitation pressures and non photochemical quenching of excess energy for non-acclimated WT, <i>BnCBF17</i> -OE and cold acclimated WT <i>B. napus</i> grown at either ambient (380 μmol C mol ⁻¹) or elevated (700 μmol C mol ⁻¹) CO ₂ and at either 20/16°C or 5/5°C.....	145
Fig. 4.5. CO ₂ response curves of electron transport rates, excitation pressures and non photochemical quenching of excess energy for non-acclimated WT, <i>BnCBF17</i> -OE and cold acclimated WT <i>B. napus</i> grown at either ambient (380 μmol C mol ⁻¹) or elevated (700 μmol C mol ⁻¹) CO ₂ and at either 20/16°C or 5/5°C.....	147
Fig. 4.6. Immunoblot analysis of SDS - PAGE probed with antibodies raised against: rbcL, cFBPase and Lhcb1, isolated from WT and <i>BnCBF17</i> -OE grown at either ambient (380 μmol C mol ⁻¹) or elevated (700 μmol C mol ⁻¹) CO ₂ and at either 20/16°C or 5/5°C.....	150
Fig. 5.1. Effects of cold acclimation and elevated CO ₂ on shoot dry weight of Musketeer winter and SR4A spring rye grown at either ambient CO ₂ (380 μmol C mol ⁻¹) or elevated CO ₂ (700 μmol C mol ⁻¹) and at either 20/16°C or 5/5°C.....	175

Fig. 5.2. Light response curves of gross CO ₂ assimilation for Musketeer winter and SR4A spring rye grown at either ambient CO ₂ (380 μmol C mol ⁻¹) or elevated CO ₂ (700 μmol C mol ⁻¹) and at either 20/16°C or 5/5°C.....	177
Fig. 5.3. CO ₂ response curves of light-saturated net CO ₂ assimilation for Musketeer winter and SR4A spring rye grown at either ambient CO ₂ (380 μmol C mol ⁻¹) or elevated CO ₂ (700 μmol C mol ⁻¹) and at either 20/16°C or 5/5°C.....	180
Fig. 5.4. Light response curves of electron transport rates, excitation pressures and non photochemical quenching of excess energy for Musketeer winter and SR4A spring rye grown at either ambient CO ₂ (380 μmol C mol ⁻¹) or elevated CO ₂ (700 μmol C mol ⁻¹) and at either 20/16°C or 5/5°C.....	183
Fig. 5.5. CO ₂ response curves of electron transport rates, excitation pressures and non photochemical quenching of excess energy for Musketeer winter and SR4A spring rye grown at either ambient CO ₂ (380 μmol C mol ⁻¹) or elevated CO ₂ (700 μmol C mol ⁻¹) and at either 20/16°C or 5/5°C.....	184
Fig. 5.6. Number of genes differentially expressed by cold acclimation at either ambient or elevated CO ₂ conditions (A) and by elevated CO ₂ at either NA or CA state (B) for Norstar winter wheat obtained through Affymetrix wheat micro-array.....	188
Fig. 5.7. Effects of elevated CO ₂ on immunoblot analysis of SDS - PAGE probed with antibodies raised against: rbcL, cFBPase, Lhcb1, psbA and psaA isolated from fully developed third leaves of Musketeer winter and SR4A spring rye.....	192
Fig. 5.8. Effects of elevated CO ₂ on flowering time of Norstar winter and Katepwa spring wheat grown at either ambient (380 μmol C mol ⁻¹) or elevated CO ₂ (700 μmol C mol ⁻¹)....	194
Fig. 6.1. Proposed model for CBF as a master regulator of morphological, physiological and biochemical adjustments.....	227

List of Appendices

Appendix 2S1. List of the primers used to analyze the transcript levels of major photosynthetic enzymes and components of photosynthetic electron transport in Norstar winter and Katepwa spring wheat.....	80
Appendix 2S2. Effects of growth temperatures on plant morphology and growth habit of winter versus spring wheat and rye cultivars grown at 20/16°C and 5/5°C and at ambient CO ₂	81
Appendix 2S3. Effects of pot size on growth of NA and CA Musketeer winter rye.....	82
Appendix 2S4. Temperature response curves of light-saturated net CO ₂ assimilation expressed on either leaf area or leaf chlorophyll or leaf dry weight basis for Norstar and Katepwa wheat cultivars grown at either 20/16°C or 5/5°C and at ambient CO ₂	83
Appendix 2S5. Temperature response curves of light-saturated rates of electron transport measured on a leaf area basis for winter and spring rye and wheat cultivars grown at either 20/16°C or 5/5°C and at ambient CO ₂	84
Appendix 2S6. Light response curves of gross CO ₂ assimilation expressed on either leaf area or leaf chlorophyll or leaf dry weight basis for Norstar winter and Katepwa spring wheat grown at either 20/16°C or 5/5°C and at ambient CO ₂	85
Appendix 2S7. Light-saturated rates of net CO ₂ assimilation versus internal CO ₂ concentrations expressed on either leaf area or leaf chlorophyll or leaf dry weight basis for Norstar winter and Katepwa spring wheat grown at either 20/16°C or 5/5°C and at ambient CO ₂	86
Appendix 2S8. Light response curves of electron transport rates, excitation pressures and non- photochemical quenching of excess energy for Norstar winter and Katepwa spring wheat grown at either 20/16°C or 5/5°C and at ambient CO ₂	87
Appendix 2S9. Immunoblot analyses of WCS120, WCOR410 and WCS19 in Norstar winter and Katepwa spring wheat grown at either 20/16°C or 5/5°C and at ambient CO ₂	88

Appendix 3S1. List of primers used to analyze the transcript levels of photosynthetic genes isolated from Norstar and Katepwa wheat grown at either 20/16°C or 5/5°C and at ambient CO ₂	121
Appendix 3S2. Effects of pot size on dry matter accumulation of Musketeer winter rye grown at either 20/16°C or 5/5°C at ambient CO ₂	122
Appendix 3S3. Light response curves of gross CO ₂ assimilation at either ambient (380 μmol C mol ⁻¹) or after 80 h of exposure to elevated CO ₂ (700 μmol C mol ⁻¹) for Norstar and Katepwa wheat.....	123
Appendix 3S4. CO ₂ response curves of net CO ₂ assimilation at either ambient (380 μmol C mol ⁻¹) or after 80 h of exposure to elevated CO ₂ (700 μmol C mol ⁻¹) for Norstar and Katepwa wheat.....	124
Appendix 3S5. Light-saturated rates of gross CO ₂ assimilation at either ambient (380 μmol C mol ⁻¹) or over 80 h of exposure to elevated CO ₂ (700 μmol C mol ⁻¹) for Norstar and Katepwa wheat.....	125
Appendix 3S6. Temperature sensitivity of net A _{sat} at either ambient (380 μmol C mol ⁻¹) or after 1 h shift to elevated CO ₂ (700 μmol C mol ⁻¹) for NA and CA Norstar and Katepwa wheat.....	126
Appendix 3S7. Temperature sensitivity of net A _{sat} at either ambient (380 μmol C mol ⁻¹) or after 80 h shift to elevated CO ₂ (380 μmol C mol ⁻¹) for Norstar and Katepwa wheat.....	127
Appendix 3S8. Effects of short-term shift to elevated CO ₂ (7000 μmol C mol ⁻¹) and /or high temperature (40°C) on dark respiratory rates for winter and spring cereals grown at ambient CO ₂ (380 μmol C mol ⁻¹) and at either 20/16°C or 5/5°C.....	128
Appendix 4S1. Effects of pot size on total dry matter accumulation of non-acclimated WT and <i>BnCBF17</i> -OE <i>B. napus</i> grown at elevated CO ₂ (700 μmol C mol ⁻¹).....	161
Appendix 5S1. Effect of pot size on total dry matter accumulation of Musketeer winter rye grown in 0.5L, 2L, 4L and 6L-sized pots at either ambient CO ₂ (380 μmol C mol ⁻¹) or elevated CO ₂ (700 μmol C mol ⁻¹) and at either 20/16°C and 5/5°C	207

Appendix 5S2. Effects of elevated CO ₂ and growth temperatures on plant morphology and growth habit of winter versus spring wheat and rye cultivars grown at either ambient CO ₂ (380 μmol C mol ⁻¹) or elevated CO ₂ (700 μmol C mol ⁻¹) and at either 20/16°C and 5/5°C.....	208
Appendix 5S3. Effects of cold acclimation and elevated CO ₂ on shoot dry weight of Norstar winter and Katepwa spring wheat grown at either ambient CO ₂ (380 μmol C mol ⁻¹) or elevated CO ₂ (700 μmol C mol ⁻¹) and at either 20/16°C or 5/5°C.....	209
Appendix 5S4. Light response curves of gross CO ₂ assimilation for Norstar winter and Katepwa spring wheat grown at either ambient CO ₂ (380 μmol C mol ⁻¹) or elevated CO ₂ (700 μmol C mol ⁻¹) and at either 20/16°C or 5/5°C.....	210
Appendix 5S5. CO ₂ response curves of light-saturated net CO ₂ assimilation for Norstar winter and Katepwa spring wheat grown at either ambient CO ₂ (380 μmol C mol ⁻¹) or elevated CO ₂ (700 μmol C mol ⁻¹) and at either 20/16°C or 5/5°C.....	211
Appendix 5S6. Light response curves of electron transport rates, excitation pressures and non photochemical quenching of excess energy for Norstar winter and Katepwa spring wheat grown at either ambient CO ₂ (380 μmol C mol ⁻¹) or elevated CO ₂ (700 μmol C mol ⁻¹) and at either 20/16°C or 5/5°C.....	212
Appendix 5S7. CO ₂ response curves of electron transport rates, excitation pressures and non photochemical quenching of excess energy for Norstar winter and Katepwa spring wheat grown at either ambient CO ₂ (380 μmol C mol ⁻¹) or elevated CO ₂ (700 μmol C mol ⁻¹) and at either 20/16°C or 5/5°C.....	213
Appendix 5S8. Effects of elevated CO ₂ on dark respiratory rates (R _{dark}) of winter and spring cereals grown at either ambient (380 μmol C mol ⁻¹) or elevated CO ₂ (700 μmol C mol ⁻¹) and at either 20/16°C or 5/5°C.....	214
Appendix 5S9. Effects of elevated CO ₂ on immunoblot analysis of SDS - PAGE probed with antibodies raised against: rbcL, cFBPase, Lhcb1, psbA and psaA isolated from fully developed third leaves of Norstar winter and Katepwa spring wheat.....	215

Appendix 5S10. Effects of elevated CO₂ on panicle and grain size in Norstar winter and
Katepwa spring wheat.....216

List of Abbreviations

ADP,	adenosine diphosphate
A_{sat} ,	light-saturated rates of CO ₂ assimilation
ATP,	adenosine 5'-triphosphate
<i>BnCBF17</i> ,	gene encoding the <i>Brassica napus</i> <u>C</u> old- <u>B</u> inding Transcription <u>F</u> actor, CBF17
<i>BnCBF17</i> -OE,	<i>B. napus</i> line over-expressing <u>C</u> old- <u>B</u> inding Transcription <u>F</u> actor, <i>BnCBF17</i>
CA,	cold acclimated
CBFs/DREBs,	Cold-Binding/ <u>D</u> ehydration- <u>R</u> esponsive <u>E</u> lement <u>B</u> inding Transcription <u>F</u> actors
CE,	carboxylation efficiency
<i>cFBPase</i> ,	gene encoding cytosolic fructose-1,6-bisphosphatase, cFBPase
C_i ,	internal leaf CO ₂ concentrations
COR polypeptides,	polypeptides encoded by cold-regulated genes (<i>COR</i> genes)
CP43/47,	chlorophyll binding proteins from the core antenna complex of PSII
Cyt <i>b</i> ₆ ,	cytochrome b ₆ found in the Cyt <i>b</i> ₆ <i>f</i> complex
Cyt <i>f</i> ,	cytochrome f found in the in the Cyt <i>b</i> ₆ <i>f</i> complex
D1/D2,	reaction centre proteins of PSII
ECL,	enhanced chemiluminescence
EP,	excitation pressure measured as 1-qP, the proportion of closed PSII reaction centres
ETR,	maximum rate of photosynthetic electron transport estimated from room temperature Chl a fluorescence induction
Fd,	ferredoxin
FeS,	a Rieske iron-sulphur protein of the Cyt <i>b</i> ₆ <i>f</i> complex
F_m ,	maximal fluorescence of a dark-adapted leaf
F'_m ,	maximal fluorescence of a light-adapted leaf

FNR,	ferredoxin-NADP ⁺ reductase
F _o ,	minimal fluorescence of a dark-adapted leaf
F' _o ,	minimal fluorescence of a light-adapted leaf
F _s ,	steady state fluorescence under steady state photosynthesis
F _v ,	variable fluorescence
F _v /F _m ,	maximum PSII photochemical efficiency measured in the dark-adapted state
g _s ,	stomatal conductance
J _{max} ,	maximum rate of photosynthetic electron transport calculated from CO ₂ gas exchange
LHC,	light harvesting complex
Lhca,	PSI light harvesting complex
Lhca1-4,	chlorophyll a/b binding proteins of the PSI light harvesting complex
Lhcb,	PSII light harvesting complex
Lhcb1-6,	chlorophyll a/b binding proteins of the PSII light harvesting complex
<i>Lhcb1</i> ,	gene encoding the major PSII light harvesting protein, Lhcb1
NA,	non-acclimated
NADP ⁺ ,	nicotinamide adenine dinucleotide phosphate (oxidized form)
NADPH,	nicotinamide adenine dinucleotide phosphate (reduced form)
NPQ,	non-photochemical quenching associated with the PS II light harvesting complex
OEC,	oxygen evolving complex
PSI,	photosystem I
PSII,	photosystem II
P ₆₈₀ ,	reaction centre Chl a of PSII (reduced form)
P ₆₈₀ ⁺ ,	reaction centre Chl a of PSII (oxidized form)
P ₇₀₀ ,	reaction centre Chl a of PSI (reduced form)
P ₇₀₀ ⁺ ,	reaction centre Chl a of PSI (oxidized form)

PAGE,	polyacrylamide gel electrophoresis
PC,	plastocyanin
PCO,	photosynthetic carbon oxidation
PCR,	photosynthetic carbon reduction
Pheo,	pheophytin
P _i ,	inorganic phosphate
PPFD,	photosynthetic photon flux density
PQ,	plastoquinone (oxidized form)
PQH ₂ ,	plastoquinone (reduced form)
PsaA/B,	reaction centre protein of PSI
<i>psaA</i> ,	gene encoding the PSI reaction centre polypeptide, PsaA
<i>psbA</i> ,	gene encoding the PSII reaction centre polypeptide, PsbA (D1)
Q,	apparent maximum quantum efficiency for CO ₂ assimilation
Q _A ,	primary electron acceptor quinone of PSII (reduced form)
Q _A ⁻ ,	primary electron acceptor quinone of PSII (oxidized form)
Q _B ,	secondary electron acceptor quinone of PSII
qP,	relative redox state of Q _A
qRT-PCR,	quantitative reverse transcriptase polymerase chain reaction
<i>rbcL</i> ,	gene encoding the large subunit of Rubisco, rbcL
R _{dark} ,	dark respiration rates
Rubisco,	ribulose 1,5-bisphosphate carboxylase/oxygenase
SDS,	sodium dodecyl sulphate
V _{cmax} ,	maximum capacity of Rubisco carboxylation
<i>Wcs120</i> ,	gene encoding the wheat cold-specific protein, WCS120
<i>Wcs19</i> ,	gene encoding the wheat cold-specific protein, WCS19
<i>Wcor410</i> ,	gene encoding the wheat cold-regulated protein, WCOR410

WT, wild type *Brassica napus*;
WUE, water use efficiency
Y_Z, electron donor to P₆₈₀⁺, a tyrosine in the D1 of PSII

Chapter 1

General introduction

1.1 Background

Photosynthesis is a vital physiological process through which green plants synthesize carbohydrates with the help of photosynthetic pigments in the presence of light (Blankenship 2002, Hopkins and Hüner 2009). It is a coordinated oxidation-reduction process in which a water molecule is oxidized to O_2 producing H^+ ions and electrons, and the CO_2 is reduced to carbohydrates. Photosynthesis consists of two stages: a series of primary light-dependent photophysical processes and photochemical reactions that generate assimilatory power (ATP and NADPH) through photosynthetic electron transport coupled to a series of light independent reactions that reduce CO_2 to carbohydrates utilizing the assimilatory power (Blankenship 2002, Ensminger et al. 2007).

1.2 Photosynthetic pigments and associated photosystems

The chlorophyll (Chl) molecules, Chl a and Chl b, are the most abundant pigments in higher plants that absorb predominantly in the blue and red regions of the visible spectrum (Sandmann and Scheer 1998, Nelson and Yukum 2006, Rochaix 2011). The other major classes of photosynthetic pigments in higher plants are the carotenoids (Sandmann and Scheer 1998, Demmig-Adams and Adams 1996). Carotenoids chiefly absorb in the blue and green regions of the spectrum and are bound to the chlorophyll-protein complexes in the thylakoid membrane. The major carotenoid molecules in higher plants are the carotenes and the xanthophylls (Sandmann and Scheer 1998, Demmig-Adams and Adams 1996). The carotenes consist of β -carotene and α -carotene, and the xanthophylls consist of lutein, violaxanthin, neoxanthin, cryptoxanthin, anthraxanthin and zeaxanthin. Chl molecules are primarily involved in the absorption of light energy, transfer of excitation energy to reaction centers and induction of photochemistry. Carotenoids, while they contribute in light harvesting and transferring excitations to Chl

molecules, are mainly associated with the dissipation of excess light energy to photoprotect the photosynthetic apparatus from photodamage through the xanthophyll cycle (Demmig-Adams and Adams 1996, Horton et al. 1999). The xanthophyll cycle is discussed later in the energy partitioning section.

The photosynthetic pigments are organized as pigment-protein complexes referred to as photosystem I (PSI) and photosystem II (PSII) within the thylakoid membrane (Morishige and Dreyfus 1998, He and Malkin 1998, Rochaix 2011, Nelson and Yukum 2006). Both PSI and PSII are composed of reaction centers (RCs), core antenna complexes and light harvesting complexes (LHCs). Each reaction center contains a dimer of specialized Chl a molecules with specific maximum absorption. The reaction centre Chl a of PSI is P₇₀₀, which maximally absorbs at 700 nm whereas that of PSII is P₆₈₀, which maximally absorbs at 680 nm. Since the reaction center chlorophylls have the longest wavelengths, they are the lowest energy absorbing chlorophylls in the complexes (Hüner et al. 1998, 2003). These reaction center Chl a molecules are the sites of the primary photochemical reactions that convert light energy to chemical potential energy through photochemical charge separation (He and Malkin 1998, Rochaix 2011). The PSI reaction center consists of PsaA and PsaB proteins encoded by chloroplastic genes, *psaA* and *psaB* respectively (He and Malkin 1998). The PsaA and PsaB exist as PsaA-PsaB heterodimer which binds P₇₀₀. The PSII reaction centers contain D1 and D2 proteins encoded by chloroplastic genes, *psbA* and *psbD* respectively (He and Malkin 1998). D1 binds P₆₈₀, Pheo and Q_B. D2 binds P₆₈₀, Pheo and Q_A.

Closely linked with the PSI and PSII reaction centers are the core antenna complexes (Blankenship 2002). The core antenna complex of PSI consists of a chlorophyll-protein (CP) complex, CP1 and that of PSII consists of two CP complexes, CP43 and CP47. CP1 contains about 90 Chl a molecules whereas CP43 and CP47 each consists of 20 to 25 Chl a molecules but no Chl b. CP43 and CP47 are encoded by chloroplastic genes, *psbC* and *psbB* respectively. The functions of the core antenna are to absorb light and to funnel the energy resulting from light absorption to the corresponding reaction centers.

Associated with the PSI and PSII core antennae are the light harvesting complexes (LHCs). The light harvesting complex of PSI is designated as LHCI and that of PSII as LHCII. The LHCs are extended antenna systems which are predominantly involved in intercepting light energy and in funneling the excitation energy resulting from light absorption to the associated reaction center Chl a molecules via the core antennae (Morishige and Dreyfus 1998, Hüner et al. 2003). LHCI and LHCII together consist of more than 70% of the total chloroplast pigment content, including almost all of the Chl b (Hopkins and Hüner 2009). LHCI consists of up to 120 Chl a and Chl b molecules per reaction center with a Chla/b ratio of around 4. The major light harvesting Chl a/b binding proteins of PSI are Lhca1, Lhca2, Lhca3 and Lhca4. Compared to LHC1, LHCII is relatively larger containing about 50-60% of the total chlorophyll with Chl a/b ratio of about 1.2. LHCII includes most of the Chl b and also contains xanthophylls as the major caretonoids (Demmig-Adams and Adams 1996, Horton et al. 1999). It comprises the major light harvesting Chl a/b containing proteins such as Lhcb1, Lhcb2 and Lhcb3 as well as several accessory Chl a/b binding proteins, Lhcb4, Lhcb5 and Lhcb6.

1.3 Photosynthetic intersystem electron transport and production of assimilatory power (NADPH and ATP)

Figure 1.1 illustrates the components of the photosynthetic intersystem electron transport chain, their locations in the thylakoid membrane and the path of electron transport from them. The two photosystems, PSII and PSI linked by the cytochrome *b₆f* complex, are involved in the linear electron transfer from H₂O to NADP⁺ through a series of oxidation-reduction reactions (Blankenship 2002, Hopkins and Hüner 2009, Rochaix 2011). Also shown in the figure is the phosphorylating complex known as the ATP synthase or CF₀-CF₁ coupling factor involved in ATP synthesis. PSI as well as CF₀-CF₁ coupling factor is predominantly found in unstacked regions of thylakoid membrane exposed to the stroma, known as stroma lamellae. In contrast, PSII is exclusively located in stacked regions of thylakoid membrane known as grana lamellae. The cytochrome *b₆f* complex is uniformly distributed in grana and stroma.

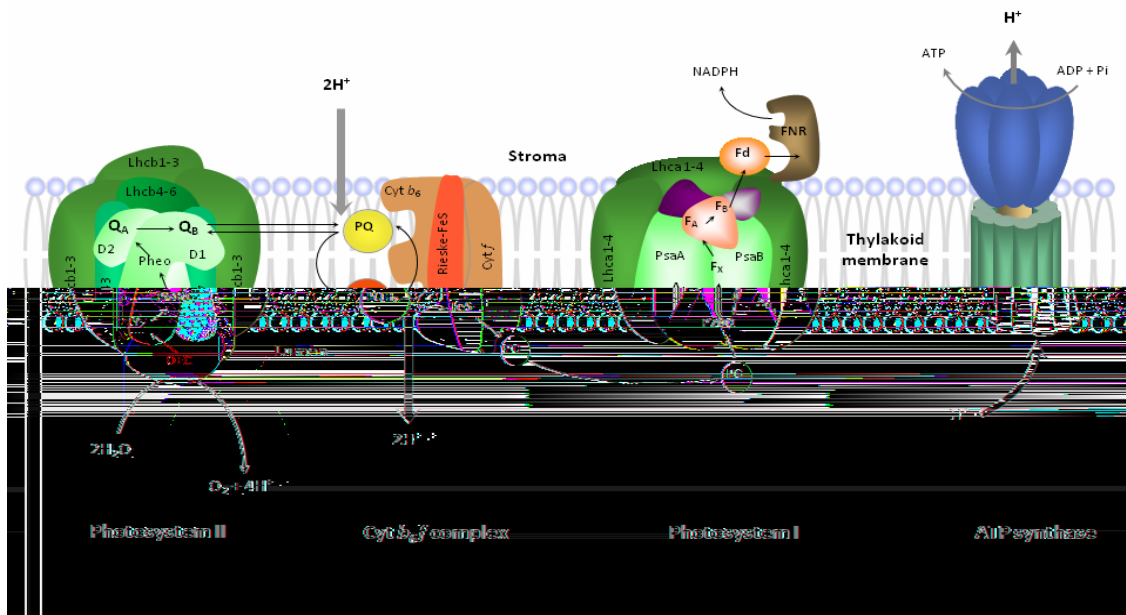


Fig. 1.1. A schematic of photosynthetic linear electron transport chain in the thylakoid membrane of chloroplasts. The two photosystems, PSII and PSI, linked by the *Cyt b₆f* complex, are involved in the linear electron transport from H₂O to NADP⁺ through a series of oxidation-reduction reactions. The PSI, PSII and *Cyt b₆f* complexes cooperate via a series of mobile electron carriers. Plastoquinone links the PSII complex to the *Cyt b₆f* complex, which is further linked to PSI complex by another electron carrier, plastocyanin. The electron transport from PSI to NADP⁺ is mediated by ferredoxin and the membrane-bound ferredoxin-NADP⁺ oxidoreductase. Also shown in the figure is the phosphorylating complex known as the ATP synthase or CF₀-CF₁ coupling factor involved in ATP synthesis. FNR = Ferredoxin (Fd) NADP⁺ Reductase; OEC = Oxygen Evolving Complex; PQ = Plastoquinone; PC = Plastocyanin. (Courtesy of Dr. Denis Maxwell).

The PSI, PSII and Cyt *b₆f* complexes cooperate via a series of mobile electron carriers (Fig. 1.1). Plastoquinone is a shuttle molecule that links the PSII complex to the cytochrome *b₆f* complex, which is further linked to the PSI complex by another electron carrier, plastocyanin (Rochaix 2011). Plastoquinone, which is hydrophobic, diffuses through the thylakoid membrane, and plastocyanin, which is hydrophilic, moves through the thylakoid lumen. The electron transport from PSI to NADP⁺ is mediated by ferredoxin and the membrane-bound ferredoxin-NADP⁺ oxidoreductase (Fig. 1.1).

Linear electron transport begins with light-induced charge separation at PSII and PSI reaction centers (Rutherford 1989) (Fig. 1.1). Light energy absorbed by the antenna pigments is transferred to the PSII reaction center Chl a, P₆₈₀, hence the P₆₈₀ gets excited (Morishige and Dreyfus 1998, Whitmarsh 1998, Rochaix 2011). The excited P₆₈₀ molecule undergoes photooxidation with ejection of an electron and thus, becomes oxidized (P₆₈₀⁺). Hence, an electron 'hole' or deficiency is left behind in PSII. From P₆₈₀, the electron is rapidly trapped by the first electron acceptor, pheophytin (Pheo) within picoseconds. From Pheo, the electron is transferred to Q_A, a primary quinone electron acceptor also within picoseconds. The electron is then transferred from Q_A⁻ to the secondary quinone acceptor Q_B within microseconds (Hüner et al. 1998). Once Q_B receives two electrons, it is fully reduced and becomes protonated to plastoquinol (PQH₂) on the stromal side of PSII (Fig. 1.1). PQ is a plastoquinone molecule that transiently binds to Q_B binding sites on the D1 reaction center protein. The double reduction and protonation of PQ to PQH₂ reduces the affinity of D1 for PQH₂ and hence, PQH₂ dissociates from the D1 binding site and diffuses through the thylakoid membrane to the PQ pool on the luminal side.

Since P₆₈₀⁺ is a strong oxidant, the electron "hole" or deficiency left behind in PSII is filled by an electron coming from the oxidation of water (Ferreira et al. 2004). The oxidation of 2H₂O by P₆₈₀⁺ through the oxygen evolving complex (OEC) associated with the luminal surface of the PSII complex, generates 4H⁺ and 4e⁻ and releases one molecule of O₂ (Fig. 1.1). Water here acts as an electron donor. The electrons generated through splitting of water reduce 4Mn ions in the OEC, which in turn reduce Y_Z, a tyrosine in the D1 or reaction center binding protein of PSII (Rutherford 1898, Ferreira et al. 2004). The Y_Z⁻ in turn reduces P₆₈₀⁺ to P₆₈₀, on the time scale of picoseconds.

The reduction of Q_A to Q_A^- by $Pheo^-$ results in 'closed' PSII reaction centers [$Y_Z P_{680}^+ Pheo Q_A^- Q_B$] (Hüner et al. 1998). Conversion of "closed" to "open" PSII reaction centers [$Y_Z P_{680} Pheo Q_A Q_B$] requires the reduction of P_{680}^+ to P_{680} by Y_Z^- and oxidation of Q_A^- by the PQ pool. The rate-limiting step in the photosynthetic electron transport chain is thought to be the conversion of 'closed' PSII RCs to 'open' PSII RCs (Hüner et al. 1998). The relative redox state of Q_A , that is, $[Q_A^-] / [Q_A] + [Q_A^-]$, is a measure of the proportion of closed PSII reaction centers which is an estimate of the relative PSII excitation pressure (Hüner et al. 1998). This can be quantified *in vivo* from room temperature Chl a fluorescence induction curves (Fig. 1.3).

After their release from PSII binding sites, the PQH_2 molecules in the free PQ pool are oxidized by cytochrome *b₆f* complex (Fig. 1.1). The cytochrome *b₆f* complex is a multiprotein complex that contains cytochrome *b₆* (Cyt *b₆*), cytochrome *f* (Cyt *f*) and a Rieske iron-sulphur protein (FeS). Cyt *f*, and FeS are exposed on the luminal face of the membrane. From PQH_2 , the electrons are transferred to Cyt *b₆* which is oxidized by the Rieske-FeS. The reduced Rieske-FeS then transfers the electrons to Cyt *f* which in turn reduces plastocyanin on the luminal side of the thylakoid membrane (Blankenship 2002, Hopkins and Hüner 2009). The oxidation of PQH_2 by Cyt *b₆f* complex is diffusion limited; consequently, this is the slowest step in the photosynthetic intersystem electron transport chain, occurring in milliseconds.

Meanwhile in PSI, light is absorbed by light harvesting pigments (Morishige and Dreyfus 1998, Whitmarsh 1998, Rochaix 2011) and transferred to the PSI reaction centers; hence, the P_{700} form of Chl a molecule becomes excited (Fig. 1.1). Upon excitation, P_{700} undergoes charge separation and ejects an electron that is transferred through a series of electron acceptors, ultimately to ferredoxin (Fd) (Amunts et al. 2007). Thus, an electron "hole" or deficiency is left behind PSI. This electron "hole" is filled by the electron from reduced plastocyanin. Reduced Fd is oxidized by the ferredoxin-NADP⁺ reductase (FNR) which reduces NADP⁺ to NADPH.

Thus, the linear electron transport results in photo-oxidation of water by P_{680}^+ and the photo-reduction of NADP⁺ by P_{700} . Since both photosystems must be excited for an

electron to be transferred through this pathway from H₂O to NADP⁺, four photons are required to transfer two electrons in order to reduce one molecule of NADP⁺ to NADPH.

Photosynthetic electron transport from water to NADP⁺ is coupled to the chemi-osmotic synthesis of ATP molecules (Whitmarsh 1998, Allen 2003, Rochaix 2011) (Fig. 1.1). The transfer of each electron from Q_B to cytochrome *b₆f* complex via the PQ cycle is associated with translocation of one proton from the stroma to the thylakoid lumen. The oxidation of each water molecule and each PQH₂ generates a trans-thylakoid proton gradient. This creates a proton motive force which is used to phosphorylate a molecule of ADP with inorganic phosphate (P_i) to form one ATP molecule in a process known as photophosphorylation. ATP synthesis is catalyzed by an enzyme complex called ATP synthase, which consists of two parts; CF₀ and CF₁ (Fig. 1.1). CF₀ is a hydrophobic membrane bound protein that forms a channel across the membrane through which protons can pass from thylakoid membrane to stroma. CF₁ is made up of numerous peptides which synthesize ATP in the stroma.

However, linear electron transport is not the only path of photosynthetic electron transport. Electrons can be transferred by a cyclic transport mechanism around PSI and the cytochrome *b₆f* complex via ferredoxin and plastoquinone (Allen 2003). In contrast to linear electron transport, the cyclic electron transport does not generate NADPH. In the cyclic electron transport, the electrons ejected from P₇₀₀ and captured by ferredoxin are not used to reduce NADP⁺. Instead, these electrons ultimately cycle back to its origin, P₇₀₀⁺ by travelling through plastoquinone and the Cyt *b₆f* complex, releasing protons which are used to drive ATP synthesis. Cyclic electron transport is thought to be involved in synthesizing additional ATP required for CO₂ assimilation and in regulating ATP/NADPH ratios in the chloroplast. Linear photosynthetic electron transport generates 1.3 ATP per NADPH. However, 1.5 ATP per NADPH are required to fix each molecule of CO₂. The additional ATP is thought to be supplied by cyclic electron transport.

1.4 Photosynthetic CO₂ assimilation

The assimilatory power (NADPH and ATP) generated in the light-dependent reactions of photosynthesis is utilized in reducing CO₂ to carbohydrates (Taiz and Zeiger 2002, Hopkins and Hüner 2009). Figure 1.2 illustrates an overview of the stromal reduction of CO₂ to triose phosphate (Triose-P) and biosynthesis of sucrose from this triose-P in the cytoplasm. In the stroma of chloroplasts, the enzyme, ribulose 1,5-bisphosphate carboxylase/oxygenase (Rubisco), combines CO₂ with ribulose 1,5-bisphosphate (RuBP) to form two molecules of the first stable three carbon product of photosynthesis, 3-phosphoglyceric acid (PGA) (Fig. 1.2). Subsequently, 3PGA is reduced to glyceraldehyde-3-P (Triose- phosphate) through a two step reaction while consuming the assimilatory power, ATP and NADPH, through the enzyme 3-phosphoglycerate kinase and NADP: glyceraldehyde-3-phosphate dehydrogenase. The continuous assimilation of CO₂ requires the continuous regeneration of RuBP. This is the role of the Calvin cycle and requires additional ATP to convert ribulose-5-P to ribulose 1,5- bisphosphate via the enzyme ribulose-5-P kinase. The triose-P is subsequently used to synthesize starch in the chloroplast or is exported to the cytosol via the triose-P translocator in exchange for the import of cytosolic P_i. The cytosolic triose-P is first converted to fructose 1,6-bisphosphate and subsequently to hexose-P (Fig. 1.2). The first reaction is catalyzed by the enzyme aldolase and the second by cytosolic fructose 1,6 - bisphosphatase (cFBPase). The hexose-P is converted to sucrose-P by the enzyme, sucrose phosphate synthase (SPS) (Fig. 1.2). With the enzyme sucrose phosphate phosphatase, sucrose phosphate is cleaved into sucrose and P_i. Thus, sucrose biosynthesis generates cytosolic P_i.

As the name indicates, Rubisco not only catalyzes carboxylation of RuBP (photosynthetic carbon reduction, PCR) but also an oxygenation reaction of RuBP (photosynthetic carbon oxidation, PCO). The oxygenation reaction of RuBP by Rubisco is the initial reaction of the process, known as photorespiration. The photorespiratory cycle involves oxidation of RuBP to one molecule of 3 - PGA and one molecule of 2 - phosphoglycolate. Each 3 - PGA enters the PCR cycle, whereas 2 - phosphoglycolate is metabolized in a series of reactions in the peroxisome and mitochondria ultimately releasing CO₂. The partial pressure of CO₂ and O₂ in the chloroplast primarily determines

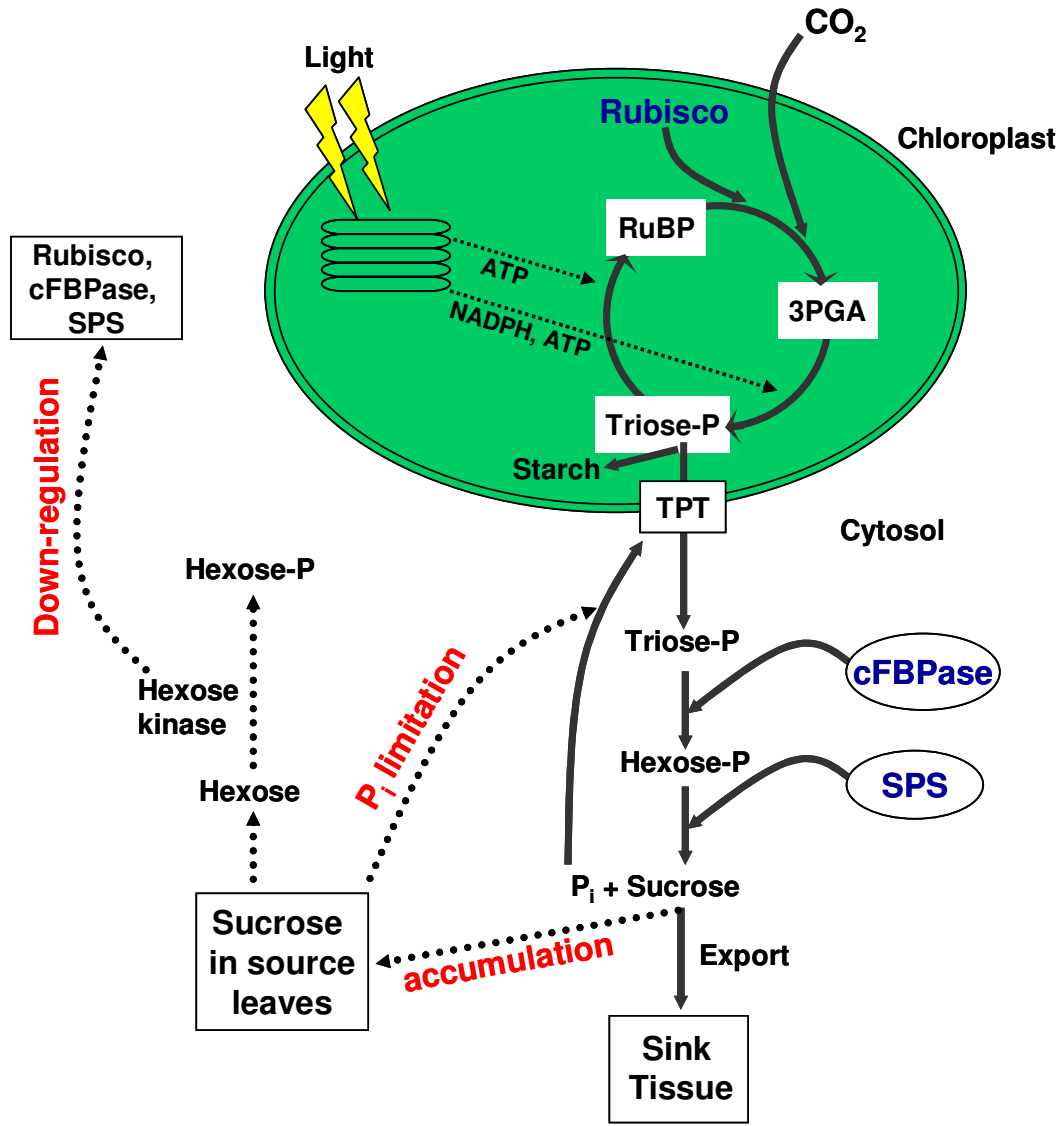


Fig. 1.2. Schematic illustration of photosynthetic CO₂ assimilation and feedback inhibition of photosynthesis. CO₂ is incorporated into a pentose sugar, ribulose 1,5-bisphosphate (RuBP) catalyzed by the enzyme, RubP carboxylase/oxygenase (Rubisco) generating 3-phosphoglycerate (3PGA). 3PGA is reduced to triose-P using NADPH and ATP generated in the light-dependent reactions of photosynthesis. Most of the triose-P is used to regenerate RuBP in the chloroplast. The surplus is either converted to starch in the chloroplast or exported to cytosol in exchange for inorganic phosphate (P_i) via the triose phosphate transporter (TPT). In the cytosol, the triose-P is converted to hexose phosphate and thereby to photosynthetic end product, sucrose. The former reaction is catalyzed by cytosolic fructose-1,6-bisphosphatase (cFBPase) and the later by sucrose phosphate synthase (SPS). Sucrose is either exported to sink tissues or accumulates in the source leaves. The accumulation of sucrose in the source leaves results in the feedback inhibition of photosynthesis due to P_i regeneration limitation in the short-term and down-regulation of expression and activities of major photosynthetic enzymes in the long-term.

whether Rubisco catalyzes carboxylation or oxygenation reaction. An increase in relative concentration of CO₂ (or decrease in O₂) favors carboxylation, whereas an increase in O₂ concentration (or decrease in CO₂) decreases carboxylation and, as a consequence, increases photorespiration. In addition, an increase in temperature also favors oxygenation compared to carboxylation, due to the differential aqueous solubilities of CO₂ and O₂ and kinetic properties of Rubisco (Long et al. 2004). Although a moderate increase in temperature stimulates catalytic activity of Rubisco, the decreased solubilities of CO₂ relative to O₂ at high temperatures limit the possible increase in net CO₂ assimilation with increased temperature (Salvucci and Crafts-Brandner, 2004).

1.5 Feedback inhibition of rates of CO₂ assimilation

The photosynthetic end product, sucrose is either exported to sink tissues or may accumulate in the source leaves as determined by the sink-source relationship (Fig. 1.2). The source tissues are net carbon exporters (photosynthetically active leaves) that assimilate carbon at a greater rate than they respire and consequently export surplus carbon to the sinks. The sink tissues are net carbon importers that assimilate carbon at a lower rate than they respire, and are usually young developing leaves, shoot apex, roots, stems, flowers, fruits and seeds which depend on the source leaf for additional carbon.

Sucrose is not only a photosynthesis end product but also the chief form of translocated carbon in most plants, and the principal substrate for sink respiratory metabolism. Any factors that lead to alteration in the homeostasis between the source capacity to supply versus sink capacity to utilize sucrose may result in the accumulation of sucrose in the source leaf. Such accumulation of sucrose due to either increased source capacity or decreased sink strength to utilize carbon results in feedback inhibition of photosynthesis, also known as end product inhibition of photosynthesis (Arp 1991, Stitt 1991, Drake et al. 1997). In the short-term, the feedback inhibition of photosynthesis is attributed to a decrease in utilization of phosphorylated intermediates and concomitant depletion in stromal P_i (Stitt and Quick 1989, Sharkey and Vadever 1989, Foyer 1990) (Fig. 1.2). The accumulation of sucrose in the cytosol prevents cytosolic P_i recycling owing to decreased sucrose synthesis and consequently, accumulation of the

phosphorylated intermediates, hexose - P and triose - P. This decreases the level of cytosolic P_i and thereby decreases the exchange of triose - P for P_i across the chloroplast envelope (Fig. 1.2). Consequently, the decreased availability of stromal P_i reduces ATP synthesis. The limited ATP synthesis reduces RuBP regeneration as well as the conversion of PGA to triose - P, and eventually photosynthesis (Sharkey and Vadever 1989). It has been revealed that the low availability of P_i concentrations in the stroma may also lower the activation state of Rubisco due to decreased ATP synthesis required to activate Rubisco activase (Crafts-Brandner and Salvucci 2000). In the long-term, the feedback inhibition of photosynthesis may also result in the down-regulation of the expression of genes that encode key regulatory photosynthetic enzymes such as Rubisco, cFBPase and SPS (Drake et al. 1997, Pego et al. 2000) (Fig. 1.2).

How does increased sucrose accumulation in source leaves downregulate photosynthetic gene expression? Long et al. (2004) has suggested a sucrose cycling model for molecular control of Rubisco protein content. The increased level of sucrose in a source leaf is sensed by vacuolar invertase which hydrolyses sucrose to hexose (Long et al. 2004) (Fig. 1.2). Hexose stimulates a hexokinase sensing system that phosphorylates hexose to hexose-P, which is used to resynthesize sucrose (Long et al. 2004). Hexokinase reduces Rubisco content by downregulation of *rbcL/S* gene expression at the levels of transcription, post-transcription, translation and post-translation (Webber et al. 1994, Long et al. 2004) (Fig. 1.2). This is reflected in decreased carboxylation efficiency in addition to decreased CO_2 -saturated photosynthetic capacity.

1.6 Dark respiration rates

Dark respiration is an integral physiological process through which free energy is released and stored in an ATP molecule via oxidation of organic compounds. The ATP generated can be instantly used in maintenance of cellular homeostasis and growth and development of an organism. Contrary to photosynthesis, O_2 is consumed and CO_2 is released in the process of dark respiration. Dark respiration takes place in mitochondria, hence, it is also called mitochondrial respiration. It has been suggested that low temperature stimulates dark respiratory rates in a wide range of plant species (Campbell

et al. 2007). This stimulation of dark respiration rates is associated with increased metabolic demand, increased substrate availability, enhanced activities of respiratory enzymes or increased mitochondrial density and mitochondrial cristae per mitochondria during cold acclimation (Talts et al. 2004, Campbell et al. 2007).

The effects of elevated CO₂ on dark respiratory rates have been a subject of much contradiction. Studies done so far have suggested that elevated CO₂ may either increase or decrease or may not change dark respiratory rates. Previous studies have suggested about 10-20% loss of dark respiratory rates at 700 μmol C mol⁻¹ compared to at ambient CO₂ of 372 μmol C mol⁻¹ (Reviewed by Long et al. 2004). Recent studies have reported that the apparent inhibition of dark respiratory rates in response to growth at elevated CO₂ is likely an artifact of the measuring apparatus and measuring system used causing CO₂ leakage through the leaf intercellular air spaces and chamber seals (Jahnke 2001, Jahnke and Krewitt 2002). To avoid these limitations observed for CO₂ evolution, Davey et al. (2004) used an alternative means of assessing respiratory rates by measuring O₂ uptake in a wide range of plant species. They concluded that dark respiratory rates of plant species tested were insensitive to CO₂ from 0 - 2000 μmol C mol⁻¹.

1.7 Cold acclimation and photosynthesis

The effects of low, non-freezing temperatures on the acclimatory capacity of photosynthetic apparatus has been extensively studied in both cold-sensitive and cold-tolerant species (Falk et al. 1996, Adams et al. 2002, Ensminger et al. 2006). It has been well documented that the photosynthetic apparatus is capable of acclimating to low growth temperatures (Hüner 1985, 1998, Öquist and Hüner 1993). During the course of evolution, plant species have developed several acclimatory strategies to survive the consequences of stress and acclimation to cold temperatures (Öquist and Hüner 2003). However, the plasticity of acclimation to low temperature is dependent on plant species, cultivar or variety and determined by whether the strategy is to maintain active photosynthesis throughout the cold acclimation period as seen in cold-tolerant species or to inhibit photosynthesis during the acclimation period as in cold-sensitive species (Öquist and Hüner 2003, Savitch et al. 2002). On the other hand, conifers such as

lodgepole pine (*Pinus contorta* L.) enter dormancy with cessation of growth during cold acclimation, that is during early fall, when days become shorter and temperatures decrease (Öquist and Hüner 2003). Consequently, conifers substantially inhibit rates of photosynthesis during cold acclimation period and increase dissipation of absorbed light energy as heat through xanthophyll mediated non-photochemical quenching (NPQ). The mechanisms involved in acclimation to low growth temperature range from modifications at the molecular and biochemical level (Hüner et al. 1998, Stitt and Hurry 2002) to modifications at the physiological and morphological levels (Hüner et al. 1981, 1985).

Although cold-sensitive cultivars and species such as spring wheat (Hurry and Hüner 1991), spring rape (Hurry et al. 1995) and tomato (Yakir et al. 1986) can grow and develop at low temperatures, they exhibit decreased light-saturated rates of carbon assimilation (photosynthetic capacity, A_{sat}) compared to growth and development at warm temperatures. In contrast, cold tolerant cultivars and species such as winter wheat, winter rye, barley, spinach, Brassica and *Arabidopsis thaliana* are able to differentially acclimate to low temperatures and exhibit an increased A_{sat} once leaves are cold acclimated (Hurry and Hüner 1991, Hurry et al. 1995, 2000, Hüner et al. 1998, Öquist and Hüner 2003).

The differential stimulation of photosynthetic capacity of cold-tolerant versus cold-sensitive species is associated with differential stimulation of sink capacity and concomitant carbon export to the sinks during cold acclimation (Hurry et al. 1994, Gray et al. 1996, Leonardos et al. 2003) (Fig. 1.2). Consequently, cold acclimation of cold-tolerant and cold-sensitive species results in differential stimulation of carbon metabolism as a result of differential expression of key regulatory photosynthetic genes coding for rbcL, SPS and cFBPase and subsequent activities of corresponding proteins in response to low growth temperatures (Stitt and Hurry 2002). These adjustments at the physiological, biochemical and molecular levels are associated with coordinated changes in phenotype (Hüner et al. 1985; Gray et al. 1996; Strand et al. 1999). With respect to phenotypic plasticity, cold acclimation of winter wheat, winter rye and spinach as well as *Arabidopsis thaliana* generally results in a compact, dwarf phenotype, altered leaf morphology and anatomy with increased leaf thickness and specific leaf weight relative

to their non-acclimated counterparts (Hüner et al. 1981, 1985; Boese and Hüner 1990; Strand et al. 1999; Savitch et al. 2005; Gorsuch et al. 2010a, 2010b).

Spring wheat and spring rape exhibit a limited sink demand and concomitant retardation of carbon export to sink tissues during cold acclimation (Hurry et al. 1995). As a consequence, the photosynthetic end-product, sucrose, accumulates in source leaves (Fig. 1.2). This leads to feedback inhibition of photosynthesis due to P_i regeneration limitation and down-regulation of the expression and activities of key regulatory photosynthetic enzymes such as Rubisco, cFBPase, and SPS (Hurry et al. 1995, Strand et al. 1999, Savitch et al. 2002) (Fig. 1.2). Therefore, spring cultivars appear to exhibit decreased plasticity to low growth temperatures and exhibit reduced photosynthetic capacity during cold acclimation (Hurry et al. 1995, Savitch et al. 2002).

In contrast, winter cultivars of wheat and rye (Savitch et al. 2002, Leonardos et al. 2003) and *Arabidopsis thaliana* (Stitt and Hurry 2002) have an ability to enhance sink capacity and concomitant carbon export to the sinks during cold acclimation. These cultivars store photosynthates as sucrose or fructans in the crown tissue as well as in the leaf vacuoles during cold acclimation. Consequently, these species and cultivars enhance carbon assimilation through up-regulation of carbon metabolism in order to support increased sink demand in response to low growth temperatures. The up-regulation of carbon metabolism and the concomitant increase in carbon fixation of cold-grown, cold-tolerant species appear to be associated with increased expression and subsequent activities of CO_2 -fixing enzyme Rubisco as seen in winter rye (Hurry et al. 1994, Strand et al. 1999) as well as enhanced activities of the cytosolic sucrose biosynthetic enzymes, cFBPase and SPS (Hurry et al. 1995, Strand et al. 1999, Savitch et al. 2002, Rapacz et al. 2008) during cold acclimation (Fig. 1.2). Consequently, cold acclimation of winter wheat, winter rape (Hurry et al. 1995) and *Arabidopsis thaliana* (Stitt and Hurry 2002) results in enhanced P_i cycling and increased capacity for RuBP regeneration through increased utilization of phosphorylated intermediates. Furthermore, Savitch et al. (2002) reported that cold acclimation of winter wheat results in the suppression of photorespiration, thus, diverting ATP and NADPH from oxygenation to carboxylation. Consequently, it was suggested that cold acclimation of winter wheat and rye leads to a feed-forward up-

regulation of photosynthetic carbon assimilation through the global reprogramming of photosynthetic carbon metabolism (Hurry et al. 1994, 1995, Strand et al. 1999, Stitt and Hurry 2002) (Fig. 1.2). This is supported by detailed, comparative metabolic fingerprinting of the cold acclimated state versus the non-acclimated state in *Arabidopsis thaliana* (Gray and Heath 2005). This is reflected in enhanced leaf biomass, altered leaf morphology and cell ultrastructure (Hüner et al. 1985, 1993, Gray et al. 1996, Strand et al. 1999) and a decreased susceptibility to low temperature-induced photoinhibition (Öquist et al. 1993, Gray et al. 1996, Pocock et al. 2001).

In addition, these changes at the physiological, biochemical and molecular levels during cold acclimation result in the induction of differential freezing tolerance in cold-tolerant and cold-sensitive species (Pocock et al. 2001). Molecular and biochemical analyses have revealed that cold acclimation induces the expression of cold-regulated (COR) genes and subsequent accumulation of corresponding proteins associated with freezing tolerance. Cold-regulated genes have been identified in many plant species such as *Arabidopsis thaliana*, barley, wheat and *Brassica napus* (Sarhan et al. 1997, Thomashow 2001, Savitch et al. 2005, Chinnuswamy et al. 2007, Rapacz et al. 2008). In wheat and other cereals, cold acclimation-induced expression of several genes is positively correlated with the capacity of each genotype to develop freezing tolerance measured as LT50 (Öquist and Hüner 1993). Among these, the *Wcs* and *Wcor* gene families are coordinately regulated by low temperature at the transcriptional level and winter cereals exhibit higher levels of expression than do spring cereals (Sarhan et al. 1997). Although the COR gene, *Wcs19*, was originally considered to be regulated by low temperature, Gray et al. (1996) showed that this gene was also regulated by excitation pressure rather than low temperature per se.

What regulates this complex integrated phenomenon in overwintering plants? Previous studies have suggested that CBFs/DREBs (Cold- Binding Transcription Factors/Dehydration Responsive Element Binding Factors) appear to control the phenotypic plasticity, biochemical changes and photosynthetic performance in cold-tolerant species. For instance, the *BnCBF17*-over-expressing transgenic *Brassica napus* grown at 20°C mimicked the effects of cold acclimation in WT Brassica (Savitch et al.

2005). Compared to WT *Brassica napus*, *BnCBF17*-over-expressing lines exhibited enhanced freezing tolerance, compact dwarf phenotype, increased specific leaf weight, increased CO₂ assimilation and concomitant photosynthetic electron transport as associated with cold acclimation of WT *Brassica napus* (Savitch et al. 2005). Thus, the over-expression of a single transcription factor, *BnCBF17*, in *Brassica napus* appears to convert the non-acclimated WT to a cold acclimated state although it has not been exposed to low growth temperature. Similar results have been observed for *Arabidopsis* over-expressing CBF3 (Gilmour et al. 2000a, 2000b). CBFs/DREBs are a family of transcriptional factors responsible for the expression of cold-regulated genes (COR) that enhance plant freezing tolerance (Liu et al. 1998, Kasuga et al. 1999, Gilmour et al. 2000, van Buskirk and Thomashow 2006, Chinnuswamy et al. 2007, Badawi et al. 2008). Thus, CBFs/DREBs appear to be critical factors that govern plant phenotypic plasticity during cold acclimation from the level of gene expression and freezing tolerance to whole plant architecture, photosynthetic electron transport and CO₂ assimilation.

1.8 Elevated CO₂ and photosynthesis

1.8.1 Short-term response of photosynthesis to elevated CO₂

Plants sense and respond directly to increased CO₂ concentrations through photosynthesis (Sage et al. 1989, Long & Drake 1992, Long et al. 2004). In the short term (minutes-hours), the photosynthetic rates of C₃ plants are stimulated following shifts to an elevated CO₂ (Cheng et al. 1998, Long et al. 2004, Ainsworth and Rogers 2007). This photosynthetic stimulation following a short-term shift to elevated CO₂ is attributed to two reasons: (i) Rubisco is CO₂ substrate-limited at ambient CO₂ as indicated by the K_m (CO₂) for Rubisco which is close to the current atmospheric CO₂ concentration of 380 μmol CO₂ mol⁻¹ (Long et al. 2004, Tcherkez et al. 2006). Thus, an immediate increase in carboxylation velocity is expected by increased CO₂ substrate availability. (ii) Elevated CO₂ competitively inhibits photorespiratory CO₂ drain because CO₂ is a competitive inhibitor of the oxygenation of RuBP by Rubisco (Long et al. 2004). Consequently, the assimilatory power, NADPH and ATP, is used preferentially in the carboxylation reaction to fix CO₂ as opposed to the oxygenation reaction.

1.8.2 Long-term response of photosynthesis to elevated CO₂

The effects of long-term growth and development at elevated CO₂ on photosynthesis, respiration and biomass accumulation have been extensively studied in several plant species for decades, but experimental results have varied widely. It has been revealed that a decrease in the photosynthetic capacity is a common, but not a universal phenomenon of photosynthetic acclimation to long term growth and development of plants at elevated CO₂ (Stitt 1991, Long and Drake 1992, Drake 1997).

The photosynthetic response of C₃ leaves to internal CO₂ concentration (C_i) has been theoretically modeled by Farquhar et al. (1980). According to their model, at lower C_i, the light-saturated rates of photosynthesis (A_{sat}) is limited by the rate at which Rubisco consumes RuBP in CO₂ fixation (Rubisco carboxylation efficiency). At higher C_i, A_{sat} is limited by RuBP regeneration capacity associated either with (i) photosynthetic electron-transport capacity to supply ATP and NADPH or (ii) the capacity of starch and sucrose synthesis to regenerate P_i from phosphorylated intermediates (Sage et al. 1989, Stitt and Quick 1989).

The increased carbon assimilation resulting from initial stimulation of photosynthesis by elevated CO₂ results in the accumulation of sucrose in the source leaf (Fig. 1.2). This leads to feedback inhibition of photosynthesis due to P_i regeneration limitation and down-regulation of the expression and activities of key regulatory photosynthetic enzymes such as Rubisco, cFBPase, and SPS (Stitt and Quick 1989, Sharkey and Vadever 1989, Foyer 1990, Arp 1991, Stitt 1991, Drake et al. 1997, Pego et al. 2000) (Fig. 1.2).

It has been suggested that sensitivity to feedback inhibition of photosynthesis at elevated CO₂ is predominantly determined by sink strength. Any factors that limit sink capacity leads to a greater inhibition of feedback-limited photosynthetic capacity at elevated CO₂. One of the most limiting factors among others (genetic, environmental) is the experimental pot size. It has been suggested that the feedback inhibition of photosynthetic CO₂ assimilation at elevated CO₂, would be severe in plants grown at small pot size due to inadequate sink size and rooting volume constraints (Arp 1991,

Thomas and Strain 1991, Long et al. 2004, Ainsworth and Rogers 2007). Therefore, in order to assess the effects of elevated CO₂ in controlled experiments, the selection of proper pot size is critical to prevent rooting volume constraints and sink limitation.

Most C₃ plants exhibit decreased carboxylation efficiency in response to growth at elevated CO₂ (Stitt 1991, Long and Drake 1992). This inhibition of carboxylation efficiency is attributed to either a decrease in total amount of Rubisco or decrease in its activation state (Sage et al. 1989, Long and Drake 1992, Drake et al. 1997, Crafts-Brandner and Salvucci 2000, Araya et al. 2006). The decrease in the amount of Rubisco is associated with photosynthetic end product induced- downregulation of *rbcL/S* gene expression in response to growth at elevated CO₂.

Rubisco activase is an enzyme that activates Rubisco by promoting the ATP-dependent release of competitive inhibitors such as 2-Carboxy-D-arabitol 1-phosphate (CAIP), RuBP and sugar bisphosphates from the catalytic sites of Rubisco. The activity of Rubisco activase is determined by the ATP:ADP ratio in the chloroplast. Elevated CO₂ inactivates Rubisco activase and consequently lowers the Rubisco activation state (Crafts-Brandner and Salvucci 2000). Rubisco activase requires energy in the form of ATP to become activated. Under elevated CO₂ conditions, ATP synthesis is limited by P_i regeneration limitation causing inactivation of Rubisco activase. However, the down-regulation of photosynthetic capacity in response to elevated CO₂ is not associated with Rubisco activity. This is because photosynthesis is limited by RuBP regeneration capacity rather than Rubisco capacity at elevated CO₂. Thus, decreased photosynthesis under long-term elevated CO₂ is accounted for by decreased rates of electron transport, P_i regeneration limitation and decreased activities of key regulatory photosynthetic enzymes associated with starch and sucrose synthesis (Fig. 1.2).

1.9 Chlorophyll a fluorescence

Room temperature Chl a fluorescence measurements are extremely useful tool in assessing the structure and function of PSII and overall process of photosynthesis *in vivo* (Schreiber et al. 1998). The phenomenon of Chl a fluorescence has greatly helped our understanding of the fate of absorbed light energy that is, its flux into the photochemistry

and thermal dissipation mechanisms (Schreiber et al. 1998). Chl a fluorescence can be measured *in vitro* or *in vivo* by using a fluorometer such as the LI-COR leaf chamber fluorometer. Modern fluorescence technology enables the use of this technique as a non-destructive method of monitoring photosynthetic performance in intact leaves.

Fig. 1.3 illustrates the fluorescence induction curve for 25 day old fully expanded third leaves of wheat under dark-adapted and illuminated conditions. Fluorescence parameters were measured by using a LI-COR portable photosynthesis system (LI-6400 XRT, LI-COR Biosciences, Lincoln, NE, USA) according to the manufacturer's instruction manual. Leaves were dark-adapted for 20 min prior to fluorescence measurements to ensure that all electrons were drained out of the photosynthetic electron transport chain causing all PSII reaction centers to be in the "open" configuration. Minimal fluorescence (F_o) was measured by illuminating dark-adapted leaves with a low irradiance measuring beam (PPFD $< 1 \mu\text{mol photons m}^{-2} \text{s}^{-1}$) from a light emitting diode. Maximum fluorescence for the dark-adapted leaf (F_m) was determined by application of a saturating flash of light (PPFD $> 5000 \mu\text{mol photons m}^{-2} \text{s}^{-1}$) with a pulse duration of 0.8 s. Afterwards, an actinic light was applied. Superimposed on the actinic beam was another saturating light flash (PPFD $> 5000 \mu\text{mol photons m}^{-2} \text{s}^{-1}$; 0.8 s) applied repetitively at 20 s intervals to determine maximal fluorescence (F_m') under steady state illumination. F_s was determined as the steady state fluorescence under steady state illumination. Finally, light-adapted minimal fluorescence (F_o') was measured by turning off the actinic light. This allowed us to quantify maximal photochemical efficiency of PSII reaction centers (F_v/F_m), maximum potential rates of photosynthetic electron transport (ETR), excitation pressure (EP), which estimates the relative reduction state of PSII reaction centers, and non-photochemical quenching (NPQ), an estimate of the capacity to dissipate energy as heat (Hüner et al. 1998).

The maximal photochemical efficiency of PSII reaction centers is the ratio of F_v/F_m , where, $F_v = F_m - F_o$. F_v/F_m is a rapid measurement of photoinhibition induced by excess light stress and follows a similar pattern to photosynthetic efficiency.

Excitation pressure is measured as $1 - qP$,

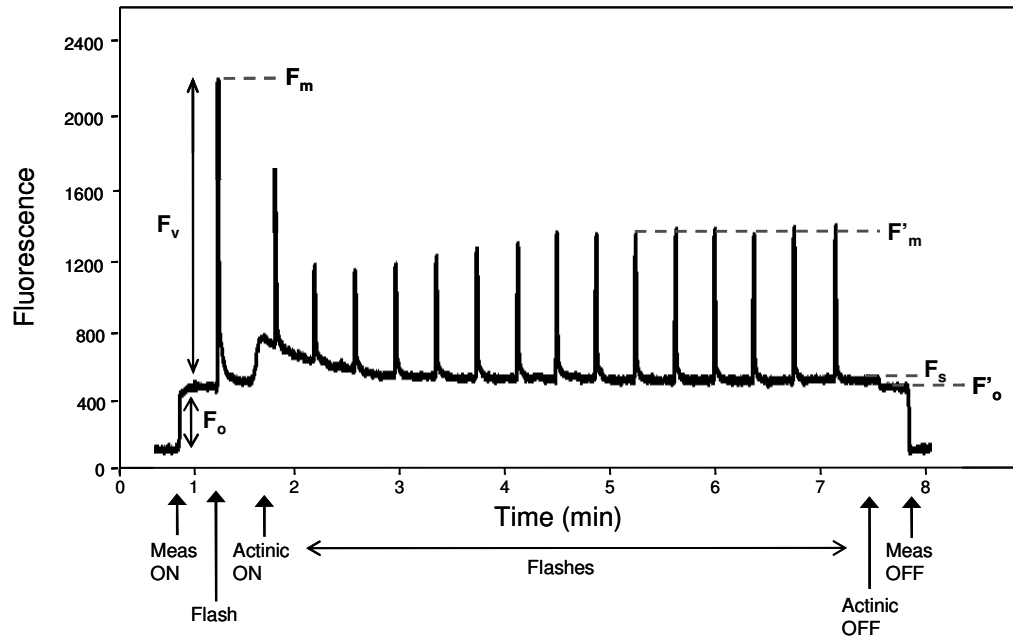


Fig. 1.3. Measurements of fluorescence parameters under dark-adapted and illuminated conditions and upon application of saturating flashes. The dark-adapted leaves were illuminated with a low irradiance measuring beam ($\text{PPFD} < 1 \mu\text{mol photons m}^{-2} \text{s}^{-1}$) from a light emitting diode to measure minimum fluorescence (F_o). Maximal fluorescence (F_m) was determined by application of saturating flash of light ($\text{PPFD} > 5000 \mu\text{mol photons m}^{-2} \text{s}^{-1}$) with a pulse duration of 0.8 s. Afterwards, an actinic light ($\text{PPFD} 1300 \mu\text{mol photons m}^{-2} \text{s}^{-1}$) was applied. Superimposed on the actinic beam was another saturating light flash applied repetitively at 20 s intervals to determine maximal fluorescence in the light-adapted leaf (F'_m). Light adapted steady state fluorescence (F_s) was determined by measuring the level of fluorescence during steady-state photosynthesis. Finally, minimal fluorescence (F'_o) in the light-adapted leaf was measured by turning off the actinic light.

Where, $qP = (F'_m - F_s) / (F'_m - F_o)$

Non-photochemical quenching is calculated as,

$$NPQ = (F_m - F'_m) / F'_m$$

Rates of electron transport is calculated as,

$$ETR = \Phi_{PSII} \cdot PAR \cdot f \cdot a$$

Where, Φ_{PSII} = quantum efficiency of PSII under light-adapted state, $(F'_m - F_s) / F'_m$,

PAR = photosynthetic active radiation ($1300 \mu\text{mol photons m}^{-2} \text{s}^{-1}$),

f = energy partitioning between PSI and PSII (0.5),

a = proportion of light absorbed (0.85)

Excitation pressure or excessive excitation energy is a relative measure of the reduction state of Q_A , which is the proportion of the closed reaction centers. Thus, $1 - qP$ is approximately equal to $[Q_A^-] / [Q_A] + [Q_A^-]$ and is an estimate of the relative PSII excitation pressure to which an organism is exposed (Hüner 1998). The relative reduction state of Q_A is estimated *in vivo* (as described above) or *in vitro* by using LI-COR or any other pulse modulated fluorometer, as $1 - qP$.

In general, chlorophyll fluorescence is minimal (F_o) when all PSII reaction centers are "open" [$Y_Z P_{680} \text{Pheo } Q_A Q_B$] and maximal (F_m) when PSII reaction centers are "closed" [$Y_Z P_{680}^+ \text{Pheo } Q_A^- Q_B$] (Hüner et al. 1998). Since the quantity of the light supplied by LED light is insufficient ($PPFD < 1 \mu\text{mol photons m}^{-2} \text{s}^{-1}$) to close the "open" reaction center, the fluorescence observed by supplying LED light is minimal. Minimal fluorescence is also known as background fluorescence as it occurs irrespective of photochemistry. When the dark-adapted leaf is exposed to a saturating flash of light, all reaction centers are "closed" and thus, the leaf fluoresces maximally. This is due to the fact that the absorbed light energy closes PSII reaction centers through photochemistry much faster than they can be reopened by PSI. Secondly, under dark-adapted condition numerous enzymes associated with the Calvin cycle are inactive and the metabolites associated with CO_2 assimilation are insufficient and thus, there is no way that electrons can be drained out to the metabolic sink, causing PSII reaction centers to be closed.

Moreover, under dark-adapted conditions, the xanthophyll cycle is inactive and no excess energy is dissipated as heat. In general, F_o and F_m account for about 0.6% and 3% of the absorbed light respectively.

Actinic light is any continuous light intensity that drives photosynthesis. Once the actinic light is turned on, the Calvin cycle gets activated and xanthophyll cycle becomes active. This causes subsequent decrease in fluorescence yield due to reopening of PSII reaction centers (Fig. 1.3). Thus, upon illumination of a dark-adapted leaf with actinic light, the fluorescence can be quenched in two ways. First, the fluorescence is quenched photochemically by PSII reaction centers to yield electron that is used in metabolic sink and growth, known as photochemical quenching (Fig. 1.4). Secondly, the fluorescence can be quenched non-photochemically resulting in heat dissipation (Fig. 1.4). This will be discussed in detail in next section under energy partitioning. Thus, the maximal fluorescence (F_m') obtained for a light-illuminated leaf is lower than that of dark-adapted leaf because it is impossible to close all reaction centers under light-illuminated condition as the Calvin cycle as well as xanthophyll cycle is active.

1.10 Energy partitioning

Plants are frequently exposed to irradiance that is in excess of that used for CO_2 assimilation and growth. If plants continue to be exposed to prolonged excess light, they become prone to photoinhibition that is, the light-dependent inhibition of photosynthesis. The photoinhibitory loss of photosynthesis due to excess light can be measured by either monitoring maximum PSII photochemical efficiency (F_v/F_m , Fig. 1.3) or by assessing photosynthetic efficiency and photosynthetic capacity. Plants have evolved several mechanisms to dissipate excess light energy to photoprotect the photosynthetic apparatus from photodamage. Dynamic photoinhibition results in the reversible short-term reduction of photosynthetic efficiency with unchanged photosynthetic capacity and is considered a photoprotective mechanism. In contrast, chronic photoinhibition results in the very slowly reversible reduction of photosynthetic efficiency as well as photosynthetic capacity. Chronic photoinhibition results in photodamage of the PSII reaction center polypeptide, D1 resulting in a decreased efficiency in charge separation

that can be monitored as decreased F_v/F_m . Repair of photodamage to D1 requires de novo biosynthesis of the D1 polypeptide.

Photoprotection through dynamic photoinhibition involves mechanisms to dissipate excitation energy through heat loss as NPQ within the LHCII (Fig. 1.4). NPQ in the LHCII occurs through the xanthophyll cycle (Demmig-Adams and Adams 1996, Horton et al. 1999). The xanthophyll cycle is the reversible, light-dependent enzymatic interconversion of the light-harvesting pigment, violaxanthin, to the quenching pigments, antheraxanthin and zeaxanthin (Ensminger et al. 2006). Under high light conditions, violaxanthin is converted to zeaxanthin through de-epoxidation reaction via antheraxanthin. Violaxanthin transfers absorbed energy to Chl a, however, antheraxanthin and zeaxanthin are unable to transfer their excitation energy to Chl a and thus, dissipate excess energy in the form of heat (Horton et al. 1999, Niyogi et al. 2005). De-epoxidation is induced by low pH in the lumen associated with electron transport under excess light conditions. It has been suggested that the zeaxanthin is bound to *PsbS*-encoded PSII polypeptide. On the other hand, under low light conditions, the zeaxanthin is converted back to violaxanthin through epoxidation reaction. Thus, while carotenoids harvest light energy and transfer excitation energy to Chl molecules they play a pivotal role in photoprotecting PSII from chronic photoinhibition by dissipating excess energy as heat through xanthophyll cycle.

In addition to dissipation through NPQ, the excess energy can also be lost through xanthophyll-independent constitutive energy quenching (Hendrickson et al. 2004) (Fig. 1.4). Although the molecular mechanism of constitutive quenching remains equivocal, recent evidence indicates that it is associated with reaction centre quenching (Ivanov et al. 2008). Reaction centre quenching involves modulation of the redox potential difference between QA and QB such that the redox potential of QA equals to that of QB. This increases the probability of reverse electron transport and charge recombination between $P680^+$ and $Pheo^-$ within PSII reaction centres resulting in the nonphotochemical release of energy (Ivanov et al. 2008).

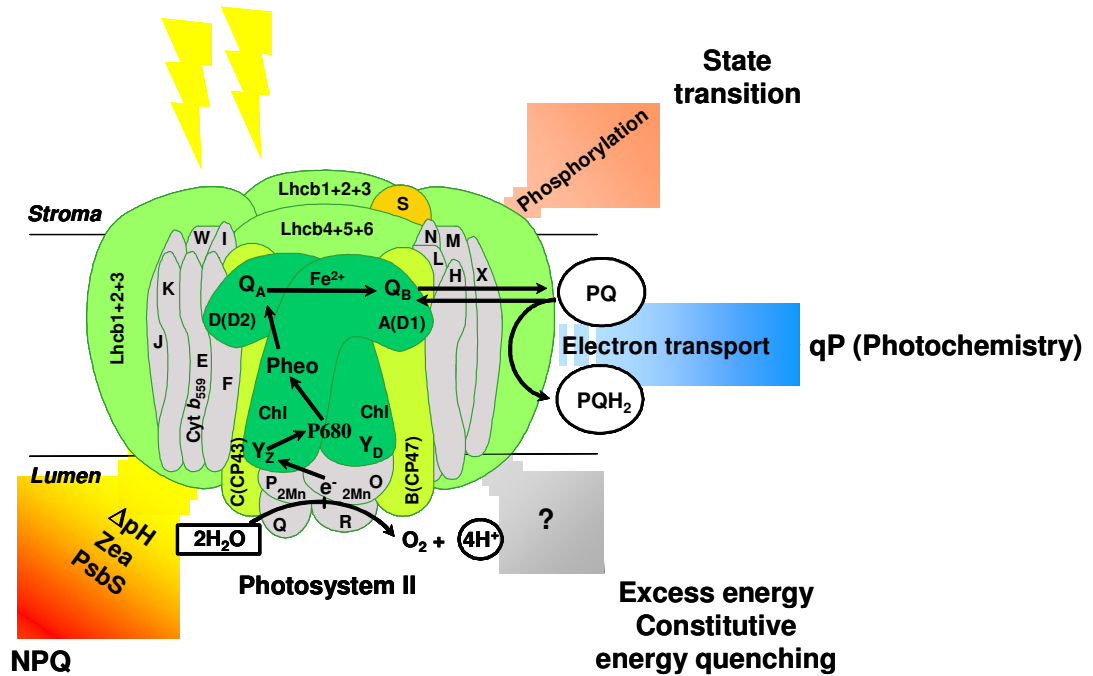


Fig. 1.4. Fate of absorbed light energy. The light harvesting antenna complex absorbs the light energy and becomes excited. The excitation energy resulting from light absorption is basically used in the photochemistry initiating linear electron transport and finally used in CO₂ assimilation and growth. The irradiance that is in excess of what is used for CO₂ assimilation and growth is dissipated as heat. The heat loss of excess energy occurs through either zeaxanthin dependent non photochemical quenching (NPQ) or zeaxanthin independent constitutive energy quenching. The light energy can be transiently distributed between PSII and PSI through state transitions. Courtesy of Dr. Norm Hüner.

State transitions are another crucial mechanism to prevent excess excitation of PSII (Fig. 1.4). This occurs via reversible phosphorylation of LHCII proteins by protein kinase, for instance, Stt7 kinase in *C. reinhardtii* and STN7 kinase in *Arabidopsis thaliana* (Rochaix 2011). The activity of these kinases is regulated by the redox state of the plastoquinone pool. When PSII is preferentially excited relative to PSI during high light stress, the rate at which the PQ is reduced to PQH₂ exceeds the rate at which PSI can oxidize PQH₂. Hence, the PQ pool becomes reduced, which is a condition referred to as state 2. The reduced plastoquinone pool is sensed by thylakoid Stt7/STN7 kinase. The activation of Stt7/STN7 kinase results in the phosphorylation of LHCII protein and causes a part of LHCII to dissociate from PSII and move towards PSI. This reduces the amount of PSII photosynthetic pigments resulting in decreased fluorescence emission. In contrast, under condition of low light energy, PSI is preferentially excited than PSII, referred to as state 1. This causes plastoquinone to be reoxidized resulting in deactivation of the protein kinase and consequently, activation of thylakoid protein phosphatases, PPH1/TAP38 (Rochaix 2011). PPH1/TAP38 dephosphorylates LHCII protein and causes LHCII to dissociate from PSI and become associated with PSII.

1.11 Objective of the thesis

The objective of my Ph.D. thesis is to test the following hypotheses.

1. Previous studies have suggested that cold acclimation of winter wheat, winter rye and *Brassica napus* as well as *BnCBF17*-over-expression in *Brassica napus* results in enhanced light-saturated rates of photosynthesis (A_{sat}), increased activities of key regulatory photosynthetic enzymes and altered plant phenotype with leaves that exhibit increased specific leaf weight compared to NA controls. This leads to the question: does altered plant phenotype contribute to the increase in A_{sat} of CA winter cereals and *Brassica napus* when measured on a leaf area basis? I hypothesize that the altered leaf morphology and leaf anatomy significantly contribute to increased A_{sat} of CA versus NA winter cereals, *BnCBF17*- over-expressor versus NA wild type *Brassica napus* as well as CA versus NA wild type *B. napus* especially when measured on a leaf area basis.

2. In contrast to CA winter cereals, CA spring cereals exhibit a decreased A_{sat} relative to their NA controls. The decreased A_{sat} of CA spring cultivars appears to be due to down-regulation of carbon metabolism associated with decreased sink capacity during cold acclimation. This leads to the questions: does the cold acclimation-induced increase in CO_2 assimilation of winter cultivars at ambient CO_2 translate into enhanced potential for CO_2 assimilation under short-term exposure to elevated CO_2 ? Does short-term elevated CO_2 compensate for the cold acclimation-induced decrease in CO_2 assimilation of spring cereals? I hypothesize that CA winter wheat and winter rye exhibit enhanced potential for CO_2 assimilation during short-term exposure to elevated CO_2 relative to NA controls. Further, I hypothesize that short-term elevated CO_2 cannot compensate for the cold acclimation-induced inhibition of photosynthetic capacity of spring cultivars.

3. The feedback inhibition of photosynthesis following long-term growth and development at elevated CO_2 has been reported in a wide range of plant species. This leads to the question: does cold acclimation of winter wheat and rye cultivars and *Brassica napus* decrease sensitivity to feedback inhibition of photosynthetic capacity induced by long-term growth and development at elevated CO_2 ? Since CA winter cereals and *Brassica napus* as well as *BnCBF17*-over-expressing *Brassica napus* exhibit enhanced sink capacity and increased activities of major photosynthetic enzymes and components of photosynthetic electron transport, I hypothesize that the feedback inhibition of photosynthetic capacity in response to growth and development at elevated CO_2 will be less in CA versus NA winter cereals, CA versus NA wild type *Brassica napus* as well as *BnCBF17*- over-expressor versus NA wild type *Brassica napus*.

1.12 References

- Adams III WW, Demmig-Adams B, Rosenstiel TN, Brightwell AK, Ebbert V (2002) Photosynthesis and photoprotection in overwintering plants. *Plant Biol* 4: 545-557
- Ainsworth EA, Rogers A (2007) The response of photosynthesis and stomatal conductance to rising CO₂: mechanisms and environmental interactions. *Plant Cell Environ* 30: 258-270
- Allen JF (2003) Cyclic, pseudocyclic and noncyclic photophosphorylation: new links in the chain. *Trends Plant Sci* 8: 15-19
- Amunts A, Drory O, Nelson N (2007) The structure of a plant photosystem I supercomplex at 3.4 Å resolution. *Nature* 447: 58–63
- Araya T, Noguchi K, Terashima I (2006) Effects of carbohydrate accumulation on photosynthesis differ between sink and source leaves of *Phaseolus vulgaris* L. *Plant Cell Physiol* 47: 644–652
- Arp WJ (1991) Effects of source–sink relations on photosynthetic acclimation to elevated CO₂. *Plant Cell Environ* 14: 869-875
- Badawi M, Reddy YV, Agharbaoui Z, Tominaga Y, Danyluk J, Sarhan F, Houde M (2008) Structure and functional analysis of wheat *ICE* (Inducer of CBF Expression) genes. *Plant Cell Physiol* 49: 1237-1249
- Blankenship RE (2002) Photosynthesis: the light reactions. In Taiz L, Zeiger E (eds) *Plant Physiology*. 3rd edition, Sinauer Associates Inc, Sunderland, MA, pp 111-143
- Campbell C, Atkinson L, Zaragoza-Castells J, Lundmark M, Atkin O, Hurry V (2007) Acclimation of photosynthesis and respiration is asynchronous in response to changes in temperature regardless of plant functional group. *New Phytol* 176: 375-389
- Cheng SH, Moore BD, Seemann JR (1998) Effects of short and long-term elevated CO₂ on the expression of Ribulose-1,5-bisphosphate carboxylase/oxygenase genes and carbohydrate accumulation in leaves of *Arabidopsis thaliana* (L.) Heynh. *Plant Physiol* 116: 715-723
- Chinnusamy V, Zhu J, Zhu JK (2007) Cold stress regulation of gene expression in plants. *Trends Plant Sci* 12: 1360-1385
- Crafts-Brandner SJ, Salvucci ME (2000) Rubisco activase constrains the photosynthetic potential of leaves at high temperature and CO₂. *Proc Natl Acad Sci* 97: 13430-13435

- Davey P, Hunt S, Hymus G, Drake B, DeLucia E, (2004). Respiratory oxygen uptake is not decreased by an instantaneous elevation of CO₂, but is increased by long-term growth in the field at elevated CO₂. *Plant Physiol.* 134: 520–27
- Demmig-Adams B, Adams WW (1996) The role of xanthophyll cycle carotenoids in the protection of photosynthesis. *Trends Plant Sci* 1: 21–26
- Drake BG, González-Meler MA, Long SP (1997) More efficient plants: a consequence of rising atmospheric CO₂? *Annu Rev Plant Physiol Plant Mol Biol* 48: 609-639
- Ensminger I, Busch F, Hüner NPA (2006) Photostasis and cold acclimation: sensing low temperature through photosynthesis. *Physiol Plant* 126: 28-44
- Falk S, Maxwell DP, Laudenbach DE, Hüner NPA (1996) Photosynthetic adjustment to temperature. In: Baker NR (eds) *Advances in photosynthesis: photosynthesis and the environment*, Vol. 5. Dordrecht: Kluwer Academic Publishers, PP 367-385
- Farquhar GD, Caemmerer S, Berry JA (1980) A biochemical model of photosynthetic CO₂ assimilation in leaves of C₃ species. *Planta* 149: 78–90
- Ferreira KN, Iverson TM, Maghlaoui K, Barber J, Iwata S (2004) Architecture of the photosynthetic oxygen-evolving center. *Science* 303: 1831–1838
- Foyer C (1990) The effect of sucrose and mannose on cytoplasmic protein phosphorylation sucrose phosphate synthetase activity and photosynthesis in leaf protoplasts from spinach. *Plant Physiol Biochem* 28: 151-160
- Gilmour SJ, Fowler SG, Thomashow MF (2000a) Arabidopsis transcriptional activators CBF1, CBF2 and CBF3 have matching functional activities. *Plant Mol Biol* 54: 767-781
- Gilmour SJ, Sebolt AM, Salazar MP, Everard JD, Thomashow MF (2000b) Over-expression of the Arabidopsis CBF3 transcriptional activator mimics multiple biochemical changes associated with cold acclimation. *Plant Physiol* 124: 1854-1865
- Gray GR, Savitch LV, Ivanov A, Hüner NPA (1996) Photosystem II excitation pressure and development of resistance to photoinhibition II. Adjustment of photosynthetic capacity in winter wheat and winter rye. *Plant Physiol* 110: 61-71
- Gray GR, Heath D (2005) A global reorganization of the metabolome in *Arabidopsis* during cold acclimation is revealed by metabolic fingerprinting. *Physiol Plant* 124: 236 - 248

- Hendrickson L, Furbank RT, Chow WS (2004) A simple alternative approach to assessing the fate of absorbed light energy using chlorophyll fluorescence. *Photosyn Res* 82: 73–81
- He WZ, Malkin R (1998) Photosystem I and II. In: Raghavendra AS (eds) *Photosynthesis: a Comprehensive Treatise*. Cambridge Univ Press, Cambridge, UK, pp 29-43
- Hopkins WG, Hüner NPA (2009) *Introduction to Plant Physiology*. 4th edition, John Wiley and Sons, Inc, Hoboken, NJ, pp 109-150
- Horton P, Ruban AV, Young AJ (1999) Regulation of the structure and function of the light harvesting complexes of photosystem II by the xanthophyll cycle. In: Frank HA, Young AJ, Britton G, Cogdell RJ (eds) *Advances in Photosynthesis and Respiration: the Photochemistry of Carotenoids*, Vol. 8. Kluwer Academic Publishers, The Netherlands, pp 271–291
- Hüner NPA (1985) Morphological, anatomical and molecular consequences of growth and development at low temperature in *Secale cereale* L. cv Puma. *Amer J Bot* 72: 1290-1306
- Hüner NPA, Öquist G, Sarhan F (1998) Energy balance and acclimation to light and cold. *Trend Plant Sci* 3: 224-230
- Hüner NPA, Öquist G, Melis A (2003) Photostasis in plants, green algae and cyanobacteria: the role of light harvesting antenna complexes. In: Green BR, Parson WW (eds) *Advances in Photosynthesis and Respiration Light Harvesting Antennas in Photosynthesis*. Kluwer Academic Publishers, Dordrecht, pp 401-421
- Hüner NPA, Palta JP, Li PH, Carter JV (1981) Anatomical changes in leaves of Puma rye in response to growth at cold hardening temperatures. *Bot Gaz* 142: 55-62
- Hurry VM, Hüner NPA (1991) Low growth temperature effects a differential inhibition of photosynthesis in spring and winter wheat. *Plant Physiol* 96: 491-497
- Hurry VM, Malmberg G, Gardeström P, Öquist G (1994) Effects of a short-term shift to low temperature and of long-term cold hardening on photosynthesis and ribulose-1,5-bisphosphate carboxylase/oxygenase and sucrose phosphate synthase activity in leaves of winter rye (*Secale cereale* L.). *Plant Physiol* 106: 983-990

- Hurry V, Strand A, Furbank R, Stitt M (2000) The role of inorganic phosphate in the development of freezing tolerance and the acclimatization of photosynthesis to low temperature is revealed by the pho mutants of *Arabidopsis thaliana*. *Plant J* 24: 383-96
- Hurry VM, Strand A, Tabiaeson M, Gardeström P, Öquist G (1995) Cold hardening of spring and winter wheat and rape results in differential effects on growth, carbon metabolism, and carbohydrate content. *Plant Physiol* 109: 697-706
- Ivanov AG, Sane PV, Hurry V, Öquist G, Hüner NPA (2008) Photosystem II reaction center quenching: mechanisms and physiological role. *Photosynth Res* 98: 565-574
- Jahnke S (2001). Atmospheric CO₂ concentration does not directly affect leaf respiration in bean or poplar. *Plant Cell Environ* 24: 1139-1151
- Jahnke S, Krewitt M (2002) Atmospheric CO₂ concentration may directly affect leaf respiration measurement in tobacco, but not respiration itself. *Plant Cell Environ* 25: 641-651
- Kasuga M, Liu Q, Miura S, Yamaguchi-Shinozaki K, Shinozaki K (1999) Improving plant drought, salt, and freezing tolerance by gene transfer of a single stress-inducible transcription factor. *Nat Biotech* 17: 287-291
- Leonardos ED, Savitch LV, Hüner NPA, Öquist G, Grodzinski B (2003) Daily photosynthetic and C-export patterns in winter wheat leaves during cold stress and acclimation. *Physiol Plant* 117: 521-531
- Liu Q, Kasuga M, Sakuma Y, Abe H, Miura S, Yamaguchi-Shinozaki K, Shinozaki K (1998) Two transcription factors, DREB1 and DREB2, with an EREBP/AP2 DNA binding domain separate two cellular signal transduction pathways in drought- and low-temperature-responsive gene expression, respectively, in *Arabidopsis*. *Plant Cell* 10: 1391-1406
- Long SP, Drake BG (1992) Photosynthetic CO₂ assimilation and rising atmospheric CO₂ concentrations. In NR Baker, H Thomas (eds) *Crop Photosynthesis: Spatial and Temporal Determinants*. Elsevier, Amsterdam, pp 69-95
- Long SP, Ainsworth EA, Rogers A, Ort DR (2004) Rising atmospheric carbon dioxide: plants FACE the future. *Ann Rev Plant Biol* 55: 591-628

- Morishige and Dreyfus (1998) Light-harvesting complexes of higher plants. In: Raghavendra AS (eds) *Photosynthesis: a Comprehensive Treatise*. Cambridge Univ Press, Cambridge, UK, pp 18-28
- Nelson N, Yukum CF (2006) Structure and function of photosystems I and II. *Annu Rev Plant Biol*. 57: 521-65
- Öquist G, Hüner NPA (2003) Photosynthesis of overwintering evergreen plants. *Ann Rev Plant Biol* 54: 329-355
- Öquist G, Hurry VM, Hüner NPA (1993) Low-temperature effects on photosynthesis and correlation with freezing tolerance in spring and winter cultivars of wheat and rye. *Plant Physiol* 101: 245-250
- Pego JV, Kortstee AJ, Huijser C, Smeekens SCM (2000) Photosynthesis, sugars and the regulation of gene expression. *J Exp Bot* 51: 407-416
- Pocock TH, Hurry VM, Savitch LV, Hüner NPA (2001) Susceptibility to low-temperature photoinhibition and the acquisition of freezing tolerance in winter and spring wheat: The role of growth temperature and irradiance. *Physiol Plant* 113: 499-506
- Rapacz M, Wolanin B, Hura K, Tyrka M (2008) The effects of cold acclimation on photosynthetic apparatus and the expression of COR14b in four genotypes of barley (*Hordeum vulgare*) contrasting in their tolerance to freezing and high-light treatment in cold conditions. *Ann Bot* 101: 689-699
- Rochaix JD (2011) Reprint of: Regulation of photosynthetic electron transport. *Biochimica et Biophysica Acta* 1807: 878-886
- Rutherford AW (1989) Photosystem II, the water-splitting enzyme. *Trends Biochem Sci* 14: 227-232
- Sage RF, Sharkey TD, Seemann JR (1989) Acclimation of photosynthesis to elevated CO₂ in five C₃ species. *Plant Physiol* 89: 590-596
- Sandmann G, Scheer H (1998) Chloroplast pigments: chlorophylls and carotenoids. In: Raghavendra AS (eds) *Photosynthesis: a Comprehensive Treatise*. Cambridge Univ Press, Cambridge, UK, pp 44-57

- Sarhan F, Ouellet F, Vazquez-Tello A (1997) The wheat *Wcs120* gene family: a useful model to understand the molecular genetics of freezing tolerance in cereals. *Physiol Plant* 101: 439-445
- Savitch LV, Allard G, Seki M, Robert LS, Tinker NA, Hüner NPA, Shinozaki K, Singh J (2005) The effect of over-expression of two Brassica CBF/DREB1-like transcription factors on photosynthetic capacity and freezing tolerance in *Brassica napus*. *Plant Cell Physiol* 46: 1525-1539
- Savitch LV, Leonardos ED, Krol M, Jansson S, Grodzinski B, Hüner NPA, Öquist G (2002) Two different strategies for light utilization in photosynthesis in relation to growth and cold acclimation. *Plant Cell Environ* 25: 761-771
- Schreiber, U., Bilger, W., Hormann, H., Neubauer, C (1998) Chlorophyll fluorescence as a diagnostic tool: basics and some aspects of practical relevance. In: Raghavendra AS (ed) *Photosynthesis: a Comprehensive Treatise*. Cambridge Univ Press, Cambridge, UK, pp 320-336
- Sharkey TD, Vanderveer PJ (1989) Stromal phosphate concentration is low during feedback limited photosynthesis. *Plant Physiol* 91: 679-684
- Stitt M (1991) Rising CO₂ levels and their potential significance for carbon flow in photosynthetic cells. *Plant Cell Environ* 14: 741-762
- Stitt M, Quick WP (1989) Photosynthetic carbon partitioning: its regulation and possibilities for manipulation. *Physiol Plant* 77: 633-641
- Stitt M, Hurry VM (2002) A plant for all seasons: alterations in photosynthetic carbon metabolism during cold acclimation in *Arabidopsis*. *Curr Opin Plant Biol* 5: 199-206
- Strand A, Hurry V, Gustafsson P, Gardestrom P (1997) Development of *Arabidopsis thaliana* leaves at low temperature releases the suppression of photosynthesis and photosynthetic expression despite the accumulation of soluble carbohydrates. *Plant J* 12: 605-614
- Strand A, Hurry VM, Henkes S, Hüner NPA, Gustafsson P, Gardeström P, Stitt M (1999) Acclimation of *Arabidopsis* leaves developing at low temperatures. Increasing cytoplasmic volume accompanies increased activities of enzymes in the Calvin cycle and in the sucrose-biosynthesis pathway. *Plant Physiol* 119: 1387-1398

- Talts P, Parnik T, Gardestrom P, Keerberg O (2004) Respiratory acclimation in *Arabidopsis thaliana* leaves at low temperature. *J Plant Physiol* 161: 573-579
- Tcherkez GGB, Farquhar GD, Andrews TJ (2006) Despite slow catalysis and confused substrate specificity, all ribulose biphosphate carboxylases may be nearly perfectly optimized. *Proc Nat Acad Sci* 103: 7246-7251
- Thomas RB, Strain BR (1991) Root restriction as a factor in photosynthetic acclimation of cotton seedlings grown in elevated carbon dioxide. *Plant Physiol* 1991 96: 627-634
- Thomashow MF (2001) So what's new in the field of plant cold acclimation? Lots! *Plant Physiol* 125: 89-93
- Van Buskirk HA, Thomashow MF (2006) *Arabidopsis* transcription factors regulating cold acclimation. *Physiol Plant* 126: 72-80
- Whitmarsh J (1998) Electron transport and energy transduction. In: Raghavendra AS (eds) *Photosynthesis: a Comprehensive Treatise*. Cambridge Univ Press, Cambridge, UK, pp 87-107
- Webber AN, Nie G-Y, Long SP (1994) Acclimation of photosynthetic proteins to rising atmospheric CO₂. *Photosyn Res* 39: 413-425
- Yakir D, Rudich J, Bravdo BA (1986) Adaptation to chilling: Photosynthetic characteristics of the cultivated tomato and a high altitude wild species. *Plant Cell Environ* 9: 477-484

Chapter 2

The effects of phenotypic plasticity on photosynthetic performance in winter rye, winter wheat and *Brassica napus*

2.1 Introduction

At the molecular level, cold acclimation induces the expression of cold-regulated (COR) genes and subsequent accumulation of corresponding proteins associated with freezing tolerance. Cold-induced genes have been identified in many plant species such as *Arabidopsis thaliana*, barley, wheat and *Brassica napus* (Sarhan et al. 1997, Thomashow 2001, Chinnuswamy et al. 2007, Rapacz et al. 2008). In wheat and other cereals, cold acclimation-induced expression of several genes is positively correlated with the capacity of each genotype to develop freezing tolerance. Among these, the *Wcs* and *Wcor* gene families are coordinately regulated by low temperature at the transcriptional level and winter cereals exhibit higher levels of expression than do spring cereals (Sarhan et al. 1997). Previous studies in *Arabidopsis thaliana*, *Brassica napus* and wheat revealed a family of CBF/DREB1 transcriptional activators (Jaglo-Ottosen et al. 1998, Thomashow 2001, Savitch et al. 2005, Badawi et al. 2008) and CAMTA transcription factors (Doherty et al. 2009) that are crucial in cold-regulation of gene expression and subsequent freezing tolerance. However, Gray et al. (1997) showed that the attainment of maximum freezing tolerance in winter rye is the result of a complex interaction between light and low temperature acclimation (Gray et al. 1997). In fact, the expression of *Wcs19*, previously assumed to be regulated by low temperature, is regulated by excitation pressure (Gray et al. 1997).

At the biochemical and physiological levels, the effects of cold acclimation on the structure and function of the photosynthetic apparatus have been extensively studied in cold-tolerant winter cultivars of wheat, rye and barley as well as spinach, *Arabidopsis thaliana*, and *Brassica napus* (Krause 1988, Hüner et al. 1993, Adams et al. 2002, Stitt and Hurry 2002, Öquist and Hüner 2003, Ensminger et al. 2006). Cold acclimation requires

long-term growth and development at low temperature (5°C) in contrast to cold stress which can be imposed within minutes by a rapid, short-term shift from a moderate temperature (20° - 25°C) to a low temperature regime. Based on these distinctions, cold acclimation of cold tolerant plant species generally results in enhanced light-saturated rates of photosynthesis (A_{sat}) whereas cold stress inhibits A_{sat} compared to NA controls when measured on a leaf area basis (Hurry and Hüner 1991, Boese and Hüner 1992, Öquist et al. 1993, Hurry et al. 1994, 1995, Hüner et al. 1998, Savitch et al. 2002). The cold acclimation-induced increase in A_{sat} of cold-tolerant herbaceous species is correlated with a stimulation of carbon metabolism as a result of the enhanced activities of key regulatory photosynthetic enzymes such as Rubisco, cFBPase, and SPS in response to low growth temperatures when measured on a leaf area basis (Hurry et al. 2000, Stitt and Hurry 2002). There is a strong, positive correlation between the cold acclimation-induced increase in A_{sat} and the development of freezing tolerance as well as an increased resistance to low temperature-induced photoinhibition in spinach (Krause 1988, Somersalo and Krause 1989, Boese and Hüner 1992), winter rye and winter wheat (Hüner et al. 1993, Öquist et al. 1993, Pocock et al. 2001) and *Arabidopsis thaliana* (Savitch et al. 2001). Although spring cereals can grow and develop at low temperatures, unlike winter cultivars, cold acclimation decreases A_{sat} and spring cultivars remain susceptible to low temperature-induced photoinhibition of photosynthesis (Hüner et al. 1993, Hurry et al. 1996).

At the leaf and whole plant levels, cold acclimation of winter rye (Hüner et al. 1981, 1985), spinach (Boese and Hüner 1990) as well as *Arabidopsis thaliana* (Strand et al. 1999, Gorsuch et al. 2010a, 2010b) results in significant alterations in plant phenotype. Growth and development of cold-tolerant plants at low temperature generally results in a compact, dwarf growth habit with leaves that exhibit increased thickness relative to NA controls. The dwarf growth habit appears to be controlled by overexpression of *CBF3* in *Arabidopsis thaliana* (Gilmour et al. 2000a, 2000b) and overexpression of *BnCBF17* in *Brassica napus* (Savitch et al. 2005). The increased leaf thickness associated with the cold acclimated state can be accounted for by either increases in leaf mesophyll cell size (Hüner et al. 1981, Gorsuch et al. 2010a) and/or increases in the number of palisade layers (Boese and Hüner 1990). At the ultrastructural

level, cold acclimated winter rye and *Arabidopsis thaliana* exhibit an apparent increase in cytoplasmic volume and an apparent decrease in vacuolar volume (Hüner et al. 1984, Strand et al. 1999). This is accompanied by an increase in the content of sucrose and other structural carbohydrates (Steponkus 1984, Guy 1990, Guy et al. 1992, Hurry et al. 1995, Strand et al. 1997, 2003, Savitch et al. 2000, Gorsuch et al. 2010b).

Research in plant cold acclimation has focussed primarily on events at the molecular and biochemical levels (Sarhan et al. 1997, Hüner et al. 1998, Thomashow 2001, Stitt and Hurry 2002, van Buskirk and Thomashow 2006, Wilson et al. 2006, Chinnuswamy et al. 2007, Rapacz et al. 2008). Although the regulation of photosynthesis, respiration and transpiration in a changing environment are critical for plant survival and productivity, few studies have attempted to integrate changes observed at the leaf and whole plant levels with those at the biochemical and molecular levels during cold acclimation (Lapointe and Hüner 1993, Gilmour et al. 2000a, Savitch et al. 2005, Gorsuch et al. 2010a, 2010b). The objective of this study was to delineate the potential contributions of phenotypic plasticity at the leaf and whole plant levels versus those at the biochemical and molecular levels to the photosynthetic performance, transpiration and water use efficiency of winter and spring cultivars of rye (*Secale cereale* L.) and wheat (*Triticum aestivum* L.) during cold acclimation. To accomplish this objective, we measured leaf morphology (stomatal density, leaf thickness), transpiration, and light- / CO₂-dependence of photosynthetic gas exchange using three frames of reference (leaf area, leaf Chl, leaf dry weight). These measurements were coupled with photosynthetic gene expression, polypeptide accumulation and in vivo Chl a fluorescence quenching analyses in NA and CA winter and spring cultivars of wheat and rye as well as WT and a *BnCBF17*-over-expressing line of *Brassica napus*. The apparent energetic costs and benefits of phenotypic plasticity are discussed in terms of the potential for winter survival and subsequent reproductive fitness.

2.2 Materials and methods

2.2.1 Plant materials and growth conditions

One cultivar each of winter (cv Norstar) and spring (cv Katepwa) wheat (*Triticum aestivum* L.) and one each of winter (cv Musketeer) and spring (cv SR4A) rye (*Secale cereale* L) was used. Seeds were germinated and grown in the controlled environmental growth chambers (Model: GCW15 chamber, Environmental Growth Chambers, Chargin Falls, Ohio, USA) at ambient CO₂ (380 ± 15 µmol C mol⁻¹), a PPFD of 250 ± 20 µmol photons m⁻² s⁻¹, 55 ± 5% relative humidity, a 16 h photoperiod and at day/night temperature regimes of 20/16°C for non-acclimated (NA) and 5/5°C for cold acclimated (CA) plants. The temperature, relative humidity, irradiance level and photoperiod in each chamber were computer-controlled and monitored and recorded continuously. Rye and wheat seedlings were grown in coarse vermiculite in 500mL-sized plastic pots at a density of three plants per pot and watered with Hoagland's solution.

Brassica napus cv. Westar (WT) and the *Brassica napus* *BnCBF17*-over-expressing transgenic line, generated as described in detail elsewhere (Savitch et al. 2005), were grown in controlled environmental growth chambers (Model: GCW15 chamber, Environmental Growth Chambers, Chargin Falls, Ohio, USA) with a 16 h photoperiod and at day/night temperature regimes of 20/16°C as described above except that the seedlings were grown in organic soil (Promix) in 300mL-sized pots with one plant each and watered with all-purpose fertilizer (Plant Prod 20-20-20, Sure-Gro IP Inc. Brampton, ON, Canada). The WT plants were grown for 3 weeks and the *BnCBF17*-over-expressing line for 4 weeks. At these ages, the third leaves were fully expanded in both WT and the transgenic plants.

2.2.2 Comparative growth kinetics

Since minimal data are available for the growth and photosynthetic characteristics of NA and CA Norstar winter wheat, Katepwa spring wheat and SR4A spring rye, comparative growth kinetics were performed to ensure that all comparisons of photosynthetic measurements and biochemical analyses between NA and CA plants were assessed at a comparable developmental stage. NA plants were harvested every week and CA plants every two weeks until the full stem elongation stage. Total tiller number, leaf number and leaf blade area were recorded on each harvest. Total root and shoot fresh biomass were

weighed, and the tissues were dried at 80°C to constant weight for the determination of dry weight. Exponential growth rates ($\text{g g}^{-1} \text{ dry mass day}^{-1}$) were calculated from plots of the natural logarithm (\ln) of shoot dry mass over time in days. Specific leaf weight (SLW) was calculated as leaf dry weight in g m^{-2} leaf blade area. Leaf blade area was measured by using a LI-COR portable area meter (LI-3000A, LI-COR Biosciences, Lincoln, Nebraska, USA). The photosynthetic pigments, chlorophyll a and b, were determined according to Arnon (1949).

2.2.3 Scanning electron microscopy

In order to assess the effect of *BnCBF17*- over-expression on *Brassica napus* leaf anatomy, leaf surface and leaf cross sections were examined by scanning electron microscope. Leaf samples from WT and the *BnCBF17*-over-expressing line were cut into small pieces (2mm^2) and fixed in 2.5% (w/v) glutaraldehyde: 2% (w/v) paraformaldehyde in 20 mM phosphate buffer (pH 7.2) for 12 h at 4°C. The samples were washed and postfixed in 2% (v/v) osmium tetroxide in the same phosphate buffer for 2 h at room temperature. The samples were then washed thoroughly in the buffer and dehydrated in graded series of alcohol (50%, 70%, 90% and 100%) for about 20 min at each concentration. The leaf samples were then dried using a critical point drier (Tousimis Samdri PVT B). The samples were then mounted vertically on stubs and coated with gold/palladium in a Hummer VI sputter coater. The leaf surface and leaf cross sections were then viewed using a Hitachi S-3400 scanning electron microscope operating at 5kV.

2.2.4 CO₂ gas exchange measurements

CO₂ gas exchange rates were measured on fully expanded third leaves of 25-day-old NA and 75-day-old CA plants. At these ages, the plants were considered to be at comparable physiological stages of development based on growth kinetics. CO₂ gas exchange rates were measured by using the LI-COR portable infrared CO₂ gas analyzer (LI-6400 XRT Portable Photosynthesis System, LI-COR Biosciences, Lincoln, NE, USA). The apparent maximum quantum efficiency (Q) and the maximal photosynthetic capacity (A_{sat}) for the NA and CA plants were determined as the maximum initial slope of the linear portion of the light response curves and maximum light-saturated rates of photosynthesis

respectively from light response curves using 12 irradiance values over the range of 0 to 1500 $\mu\text{mol photons m}^{-2} \text{s}^{-1}$ PPFD. Light response curves were measured from high to low light intensity with 8 min of waiting time between the measurements. Maximum rate of photosynthetic electron transport for CO_2 gas exchange (J_{max}) was calculated by using computer software “Photosyn Assistant” (Dundee scientific, University of Dundee, UK). Rubisco-limited carboxylation efficiency (CE) was determined as the maximum initial slope of the linear portion of the CO_2 response curves and the CO_2 - saturated carboxylation capacity was calculated from CO_2 response curves measured by supplying 11 different CO_2 concentrations over the range of 50 to 1200 $\mu\text{mol C mol}^{-1}$ at a saturating irradiance. Respiration rates (R_{dark}) were measured in the dark. In addition, stomatal conductance and leaf transpiration rates were measured simultaneously with CO_2 gas exchange measurements. Leaf water use efficiency was calculated as the rate of CO_2 assimilated divided by the stomatal conductance (A_{sat}/g_s).

Stomatal density was estimated on both adaxial and abaxial leaf surfaces of NA and CA wheat and rye cultivars using a Leica microscope (Leica ATCTM 2000, Buffalo, NY, USA) equipped with a stage micrometer (1mm^2) at a magnification of 100X. Stomatal density for WT and the *BnCBF17* -over-expressing line of *Brassica napus* was estimated from micrographs of leaf surfaces obtained by scanning electron microscope as described above.

2.2.5 Room Temperature Chl a Fluorescence

Chl a fluorescence was measured concomitantly with CO_2 gas exchange on fully expanded third leaves using the LI-COR portable photosynthesis system (LI-6400 XRT, LI-COR Biosciences, Lincoln, NE, USA). All measurements of Chl a fluorescence were carried out by using the standard fluorescence leaf chamber (2 cm^2). Prior to fluorescence measurements the leaves were dark-adapted for 20 min. Minimum fluorescence (F_0) was measured by illuminating dark-adapted leaves with a low irradiance measuring beam ($\text{PPFD} < 1\mu\text{mol photons m}^{-2} \text{s}^{-1}$) from a light emitting diode. Maximal fluorescence (F_m) was determined by application of a second flash of light ($\text{PPFD} > 5000\mu\text{mol photons m}^{-2} \text{s}^{-1}$) with a pulse duration of 0.8 s. Afterwards, an actinic light ($\text{PPFD} 1300\mu\text{mol photons}$

$\text{m}^{-2} \text{s}^{-1}$) was applied. Superimposed on the actinic beam was another saturating light flash (PPFD > 5000 $\mu\text{mol photons m}^{-2} \text{s}^{-1}$; 0.8 s) applied repetitively at 20 s intervals to determine maximal fluorescence in the light-adapted leaf (F_m'). Light-adapted steady state fluorescence (F_s) was determined by measuring the level of fluorescence immediately before the saturating flash. Finally, minimal fluorescence (F_o') in the light-adapted leaf was measured by turning off the actinic light. This allowed us to calculate maximum photochemical efficiency (F_v/F_m), photochemical quenching (qP), non-photochemical quenching (NPQ), excitation pressure (1-qP) and photosynthetic electron transport rate (ETR).

2.2.6 Carbon isotope discrimination ($\delta^{13}\text{C}$)

Leaf samples were harvested, freeze-dried and ground into a fine powder using a ball mill. About 0.1 mg of homogenized fine powder was sealed into a 5 x 3.5 mm-sized tin capsule. Samples were combusted using Costech ECS 4010 elemental analyzer coupled to a Thermo Finnigan Delta V Plus isotope ratio mass spectrometer in continuous flow mode. The carbon isotope ratios ($R = {}^{13}\text{C}/{}^{12}\text{C}$) of the samples (R_{sample}) and standard (R_{standard}) were determined. R values were converted to $\delta^{13}\text{C}$ values (in ‰ or per mil) using the relationship: $\delta^{13}\text{C} (\text{‰}) = [R_{\text{sample}}/R_{\text{standard}} - 1] \times 1000$. The $\delta^{13}\text{C}$ values were calibrated to VPDB using NBS - 22 (accepted value = -30.0 ‰) and IAEA - CH - 6 (accepted value: -10.5 ‰), to yield the accepted value of 1.95 ‰ for NBS-19 (Coplen, 1994).

2.2.7 Determination of total leaf protein and immunodetection

After each CO_2 gas exchange measurement, the fully expanded third leaves of 25-day-old NA and 75-day-old CA plants were harvested, immediately frozen in liquid N_2 and stored at -80°C . The frozen leaf samples were ground into a fine powder using liquid N_2 in a mortar and pestle. About 30 - 35 mg of ground leaf samples were added to 800 μl of cold (4°C) extraction buffer containing 1M Tris-HCl (pH 6.8), 10% (w/v) SDS, 15% (w/v) sucrose and 50 mM DTT. The samples were vortexed briefly, solubilized at 70°C for 10 min and centrifuged to remove debris. Total leaf protein concentrations of the supernatant were quantified using the RC-DC protein assay kit (Bio-Rad) according to the

manufacturer's instructions. While quantifying the total leaf protein content, the addition of 1 µg of bovine serum albumin (Invitrogen) in the extraction buffer was used as an internal standard.

The extracted proteins were electrophoretically separated using NuPAGE Novex 10% (w/v) Bis-Tris precast, polyacrylamide gels (Invitrogen) with MES SDS running buffer (Invitrogen) in an XCell4 SureLock Midi Cell (Invitrogen) according to manufacturer's instructions. Samples were loaded for SDS-PAGE on an equal protein basis (8 µg protein per lane). Gels were electrophoresed at 80V for about 3 h. For immunodetection, separated polypeptides were electroblotted onto nitrocellulose membranes (0.2 µM pore size, Bio - Rad) in transfer buffer for 1 h at 100V as described by Gray et al. (1996). The membranes were blocked with 5% (w/v) fat free, dried milk powder overnight at 4°C and then probed with primary antibodies raised against the target proteins; *rbcL*, *cFBPase*, *Lhcb1*, *PsbA* (D1) and *PsaA* at a dilution of 1:2000-5000. The blots were rinsed briefly and washed in TBS wash buffer at room temperature with agitation. The blots were probed with secondary antibody (anti-rabbit IgG Peroxidase antibody, Sigma-Aldrich) at 1:10000-20000 dilutions for 1 h at room temperature with agitation. The blots were washed as described above and the target proteins were visualized with enhanced chemiluminescence immunodetection (ECL Detection Kit; GE Healthcare, UK) on X-ray film (Fujifilm, Fuji Corporation, Tokyo). Immunoblots were quantified by using a computer software program (Scion Image, Scion Corporation, Frederick, Maryland 21701, USA).

2.2.8 Analyses of gene expression

Quantitative real-time polymerase chain reaction (qRT-PCR) was carried out to assess the effects of cold acclimation on photosynthetic gene expression. The transcript levels for *rbcL*, *cFBPase*, *Lhcb1*, *PsbA* and *PsaA* were quantified by qRT-PCR. Total RNA was extracted from wheat leaves (200mg fresh weight) with Trizol reagent (Invitrogen). For qRT-PCR, 10 µg of total RNA was digested with DNASE I (Invitrogen) and half of the digested RNA was used for cDNA synthesis with random hexamers and Superscript Reverse Transcriptase (Invitrogen). The cDNA obtained was diluted ten-fold in deionized

water and 2 µl were used as template for real-time PCR. The polymerase chain reaction was performed with SYBR-Green PCR Mastermix (Invitrogen) and amplification was monitored on an ABI PRISM 7000 (Applied Biosystem). The 18S ribosomal gene was used as an internal standard for normalization of expression levels. The PCR amplification efficiency was 1.4 for all the genes tested. The primers used for the different genes are listed in Appendix 2S1.

2.2.9 Statistical analysis

In all experiments, 20 replicate pots with three plants per pot for each cultivar in either the NA or CA state were grown in a completely randomized design. Out of the 20 replicate pots, three pots for each cultivar at each growth condition were randomly selected for all photosynthetic measurements and biochemical analyses. Thus, all data are the averages of measurements made on nine different plants from three replicate pots.

Results were subjected to analysis of variance (ANOVA). When conducting ANOVA, growth parameters, leaf protein content, CO₂ gas exchange rates and photosynthetic characteristics were considered as dependent variables while the growth temperatures were considered as independent variables. Means were compared at the 5% level of significance ($P \leq 0.05$) by using the statistical package SPSS version 17.

2.3 Results

2.3.1 Effects of cold acclimation on phenotypic plasticity of rye and wheat cultivars

Except for Musketeer winter rye, minimal data are available for the growth and photosynthetic characteristics of Norstar winter wheat, SR4A spring rye and Katepwa spring wheat grown at either 20/16°C or 5/5°C. Therefore, comparative growth kinetics were performed to ensure that all comparisons of photosynthetic measurements, biochemical and molecular analyses for NA and CA plants were assessed at comparable physiological stage of development. The exponential growth rates for all CA cultivars were about 1/3 of those observed for NA counterparts (Table 2.1). The third leaves of all NA cultivars were fully expanded between 20-25 days and those of CA cultivars between

Table 2.1. Effects of growth temperatures on growth characteristics of winter (cv Musketeer rye; cv Norstar wheat) and spring (cv SR4A rye; cv Katepwa wheat) rye and wheat cultivars grown at 20/16°C (NA) and 5/5°C (CA). Samples were collected from fully expanded third leaves of 25-day-old NA and 75-day-old CA plants. Data represent the mean of nine plants from three different pots \pm SD. Significant differences of the means between the growth temperatures within each cultivar are indicated by the symbol * ($P \leq 0.05$). na = Not available.

Growth characteristics	Acclimation state	Musketeer	Norstar	SR4A	Katepwa
Exponential growth rates ($\text{g g}^{-1} \text{DM day}^{-1}$)	NA	0.223 \pm 0.041	0.215 \pm 0.024	0.229 \pm 0.029	0.212 \pm 0.036
	CA	0.072 \pm 0.010*	0.069 \pm 0.008*	0.075 \pm 0.02*	0.065 \pm 0.014*
Leaf water content (%)	NA	87 \pm 3	88 \pm 3	88 \pm 4	86 \pm 3
	CA	67 \pm 6*	71 \pm 8*	82 \pm 5	83 \pm 4
Total shoot dry mass (mg plant^{-1})	NA	266 \pm 38	219 \pm 19	310 \pm 55	202 \pm 23
	CA	228 \pm 27	181 \pm 32	271 \pm 41	136 \pm 20*
Dry weight : fresh weight ratio	NA	0.13 \pm 0.03	0.12 \pm 0.03	0.12 \pm 0.02	0.14 \pm 0.03
	CA	0.33 \pm 0.05*	0.29 \pm 0.06*	0.18 \pm 0.02*	0.17 \pm 0.04
Shoot : root ratio	NA	3.26 \pm 0.24	3.31 \pm 0.23	4.51 \pm 0.46	2.90 \pm 0.51
	CA	4.02 \pm 0.41*	3.43 \pm 0.30	4.85 \pm 0.72	2.29 \pm 0.19
Total chlorophyll (mg m^{-2})	NA	599 \pm 58	645 \pm 46	602 \pm 45	531 \pm 34
	CA	861 \pm 79*	784 \pm 38*	561 \pm 24	480 \pm 59
Chl a/chl b	NA	2.65 \pm 0.18	2.60 \pm 0.19	2.81 \pm 0.13	2.58 \pm 0.36
	CA	2.63 \pm 0.25	2.45 \pm 0.11	3.08 \pm 0.20	2.21 \pm 0.29
Total leaf protein (g m^{-2} leaf area)	NA	2.70 \pm 0.46	2.32 \pm 0.31	3.33 \pm 0.54	2.89 \pm 0.45
	CA	12.65 \pm 2.20*	9.84 \pm 1.60*	4.01 \pm 0.51	3.27 \pm 0.42
Protein/Chl Ratio	NA	4.5 \pm 0.8	3.6 \pm 0.2	5.5 \pm 0.8	5.4 \pm 0.4
	CA	14.7 \pm 1.2*	12.5 \pm 1.5*	7.1 \pm 0.9	6.8 \pm 1.1
$\delta^{13}\text{C}$ (‰, VPDB)	NA	-29.5 \pm 0.2	na	-29.2 \pm 0.4	na
	CA	-27.2 \pm 0.4*	na	-29.1 \pm 0.3	na

70-80 days. Consequently, all subsequent comparisons were made in fully expanded third leaves of 25-day-old NA and 75-day-old CA plants for all cultivars. With respect to plant morphology, CA Musketeer winter rye and Norstar winter wheat exhibited a dwarf, compact growth habit whereas NA counterparts exhibited the typical elongated growth habit (Appendix 2S2). In contrast, growth of SR4A spring rye and Katepwa spring wheat resulted in an elongated growth habit irrespective of growth temperature (Appendix 2S2).

Cold acclimation significantly reduced the leaf water content of the winter cultivars, Musketeer rye and Norstar wheat, by about 20% and, as a result, the dry weight to fresh weight ratio (Dwt : Fwt) increased by about 150% in both cultivars (Table 2.1). In contrast, cold acclimation had minimal effects on leaf water content, and thus Dwt:Fwt ratio, in the spring cultivars, SR4A rye and Katepwa wheat (Table 2.1). Consequently, the specific leaf weight (SLW, g dry weight m⁻² leaf area) increased by about 2.5-fold in CA versus NA winter cultivars whereas the SLW changed minimally between CA and NA spring cultivars (Fig. 2.1). Cold acclimation resulted in a 23% increase in the shoot/root ratio in CA compared to NA winter rye, but no significant changes in this ratio were observed upon cold acclimation of the other cultivars tested (Table 2.1). CA Norstar and Musketeer exhibited a 1.21-1.44-fold increase in Chl per leaf area relative to NA counterparts with no changes in Chl a/b. Minimal changes in Chl per unit area were observed upon cold acclimation of the spring cultivars tested (Table 2.1).

We observed a comparable leaf protein content of 2.3 - 3.3 g m⁻² leaf area in all cultivars tested when grown under NA conditions (Table 2.1). However, CA winter wheat and winter rye exhibited a 4.2 to 4.7-fold increase in total leaf protein content when measured on a leaf area basis and a 3.3 to 3.5-fold increase in the protein/Chl ratio compared to NA controls (Table 2.1). In contrast, CA spring wheat and spring rye exhibited minimal changes in total leaf protein content per leaf area and protein/Chl ratio relative to NA controls (Table 2.1). The effects of growth temperature on total plant dry matter accumulation and plant morphology were not affected by variations in pot size (Appendix 2S3).

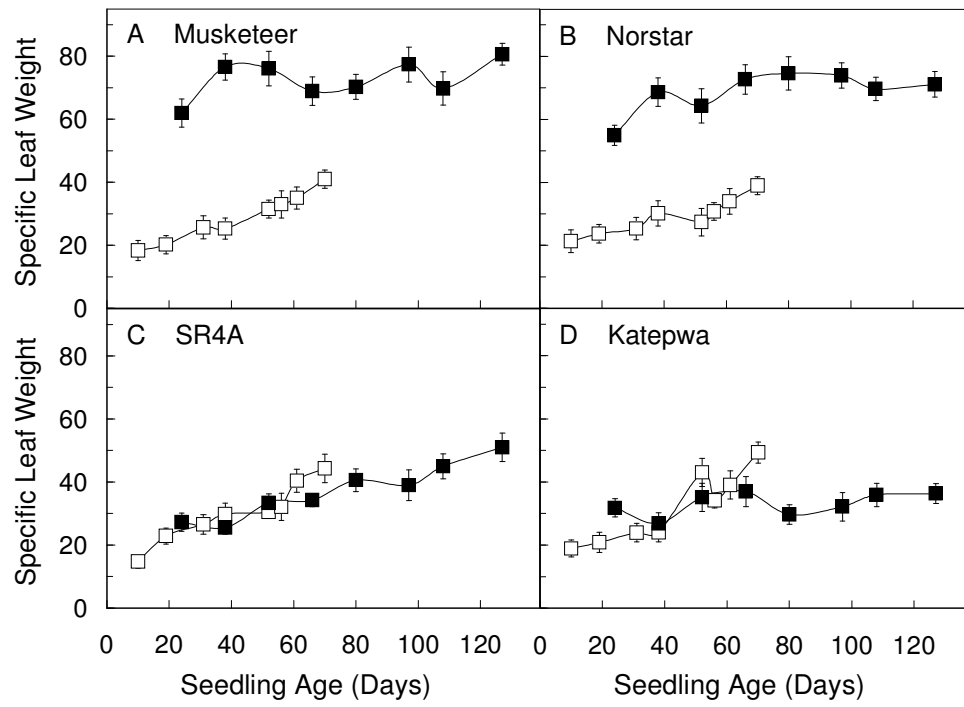


Fig. 2.1. Specific leaf weight (dry weight g m⁻² leaf area) for winter (cv Musketeer rye, cv Norstar wheat) and spring (cv SR4A rye, cv Katepwa wheat) rye and wheat cultivars grown at either 20/16°C (□) or 5/5°C (■) and at ambient CO₂. Each point represents the mean of nine plants from three different pots. Bars represent SD.

2.3.2 Effects of cold acclimation on CO₂ assimilation in rye and wheat cultivars

Since leaf surfaces regulate photosynthetic CO₂ gas exchange, rates of photosynthetic CO₂ assimilation are typically calculated on a per unit leaf area basis. All cultivars exhibited comparable light-saturated rates of net CO₂ assimilation (A_{sat}) of 17- 20 $\mu\text{mol CO}_2 \text{ m}^{-2} \text{ s}^{-1}$ when grown and measured at 20°C and measured on a leaf area basis (Table 2.2, A_{sat} , NA, 20). Cold stress imposed by an immediate reduction in the measuring temperature from 20° to 5°C inhibited these rates by about 35 - 50% in all NA winter and spring cereals (Table 2.2, A_{sat} , NA, 5). However, the CA winter cultivars, Musketeer rye and Norstar wheat, were able to maintain net CO₂ assimilation rates at 5°C (Table 2.2, A_{sat} , CA, 5) that were comparable to or slightly higher than those rates observed for NA controls but measured at 20°C (Table 2.2, A_{sat} , NA, 20). Light- saturated rates of photosynthesis of CA winter cultivars measured at 20°C (Table 2.2, A_{sat} , CA, 20) were 16-20% higher than those measured at 5°C (Table 2.2, A_{sat} , CA, 5). In addition, rates of net CO₂ assimilation measured at 5°C (Table 2.2, A_{sat} , CA, 5) resulted in 60 - 80% higher rates in CA Musketeer and Norstar compared to NA controls measured at 5°C (Table 2.2, A_{sat} , NA, 5). Thus, cold acclimation of Musketeer and Norstar enhanced light-saturated rates of net CO₂ assimilation on a leaf area basis irrespective of the measuring temperature.

In contrast to the CA winter cultivars, the CA spring cultivars, SR4A rye and Katepwa wheat, exhibited a 30 - 35% decrease in the light-saturated rates of net CO₂ assimilation (Table 2.2, A_{sat} , CA, 5) relative to NA controls (Table 2.2, A_{sat} , NA, 20) when measured on a leaf area basis. The assimilation rates observed for CA spring cultivars were comparable to those rates observed for NA controls that were cold-stressed at 5°C. Hence, the CA-induced increase in light-saturated rates of net CO₂ assimilation measured on a leaf area basis appeared to be specific for the winter cultivars tested.

The data in Fig. 2.2 illustrate the temperature dependence of light-saturated rates of net CO₂ assimilation in winter Musketeer and spring (SR4A) rye. Although both NA and CA Musketeer exhibited a temperature maximum of about 25°C, the low temperature sensitivity of CO₂ assimilation rates (5° to 25°C) was less for CA ($Q_{10} = 1.05$) than that of

Table 2.2. Light-saturated rates of net CO₂ assimilation (A_{sat}) and dark respiratory rates (R_{dark}) for winter and spring wheat and rye cultivars grown at either 20/16°C (NA) or 5/5°C (CA) at ambient CO₂ conditions. Photosynthetic and dark respiratory rates were measured on attached, fully developed third leaves of 25-day-old NA and 75-day-old CA plants at measuring temperatures of either 20° or 5°C and at ambient CO₂. Data represent the mean of nine plants from three different pots \pm SD. Significant differences among the means within each cultivar are indicated by the superscripted letters ($P \leq 0.05$).

Cultivars	Acclimation state	A_{sat} ($\mu\text{mol CO}_2$ fixed $\text{m}^{-2} \text{s}^{-1}$)		R_{dark} ($\mu\text{mol CO}_2$ evolved $\text{m}^{-2} \text{s}^{-1}$)	
		Measuring temperatures (°C)		Measuring temperatures (°C)	
		20	5	20	5
Musketeer	NA	18.1 \pm 1.6 ^b	11.8 \pm 1.2 ^a	3.24 \pm 0.14 ^b	2.7 \pm 0.21 ^a
	CA	25.4 \pm 1.5 ^c	20.9 \pm 1.8 ^b	4.06 \pm 0.18 ^c	3.88 \pm 0.23 ^c
Norstar	NA	16.8 \pm 0.9 ^b	9.9 \pm 1.6 ^a	2.28 \pm 0.11 ^b	1.71 \pm 0.15 ^a
	CA	20.5 \pm 1.8 ^c	17.7 \pm 1.3 ^{bc}	2.96 \pm 0.23 ^c	2.85 \pm 0.18 ^c
SR 4A	NA	20.4 \pm 1.7 ^b	12.6 \pm 1.0 ^a	3.05 \pm 0.12 ^b	2.56 \pm 0.19 ^a
	CA	14.6 \pm 1.5 ^a	13.9 \pm 1.4 ^a	3.59 \pm 0.24 ^c	3.43 \pm 0.13 ^c
Katepwa	NA	17.6 \pm 1.1 ^c	9.2 \pm 1.2 ^a	2.07 \pm 0.24 ^b	1.52 \pm 0.15 ^a
	CA	12.1 \pm 0.8 ^b	11.3 \pm 1.9 ^{ab}	2.55 \pm 0.31 ^b	2.35 \pm 0.25 ^b

NA Musketeer ($Q_{10} = 1.38$) (Fig. 2.2A). However, CO_2 assimilation in CA Musketeer exhibited minimal differences in sensitivity to high temperature (25° to $40^\circ C$) from that of NA Musketeer (Fig. 2A). In contrast to winter rye, CA spring rye exhibited lower rates of CO_2 assimilation at all temperatures between 15° and $40^\circ C$ than that of NA spring rye (Fig. 2.2B). Thus, although NA Musketeer and SR4A exhibited similar temperature profiles for net CO_2 assimilation, CA winter rye maintained rates of photosynthesis that were about 1.8-fold higher than NA winter rye as well as CA SR4A at temperatures between 5° and $25^\circ C$ when measured on a leaf area basis (Fig. 2.2A). These results are consistent with the data in Table 2.2, which indicated that cold acclimation of SR4A caused an inhibition of CO_2 assimilation whereas CA Musketeer exhibited a stimulation of CO_2 assimilation relative to NA counterparts. When CO_2 assimilation rates were calculated on a per unit Chl basis (Fig. 2.2C), CA Musketeer exhibited higher rates at temperatures below $15^\circ C$ whereas NA plants exhibited higher rates of photosynthesis at temperatures above $15^\circ C$. Similar trends were observed for Norstar winter wheat (Appendix 2S4). In contrast to Musketeer, calculation of CO_2 assimilation rates on a per unit Chl basis had minimal effects on the temperature response profiles for SR4A spring rye (compare Fig. 2.2B and 2D) as well as Katepwa spring wheat (Appendix 2S4).

The difference in the calculated Q_{10} for CO_2 assimilation between 5° and $25^\circ C$ for CA and NA Musketeer was unaffected by the method of calculating light-saturated rates of photosynthesis. However, when light-saturated rates of CO_2 assimilation in Musketeer (Fig. 2.2E) and SR4A (Fig. 2.2F) were normalized on a leaf dry weight basis, minimal differences were observed in the temperature profiles of Musketeer versus SR4A in either the cold acclimated or non-acclimated state. Similar trends were observed for Norstar winter wheat versus Katepwa spring wheat (Appendix 2S4).

The results for the effects of cold acclimation on light-saturated rates of photosynthetic electron transport associated with CO_2 assimilation (Table 2.3, J_{max}) and ETR (Table 2.3; Appendix 2S5) are consistent with the results for light-saturated rates of net CO_2 assimilation based on leaf area (Table 2.2). CA Musketeer and Norstar generally exhibited higher J_{max} relative to NA controls irrespective of the measuring temperature. However, J_{max} was inhibited by 14-20% upon exposure to a low measuring temperature

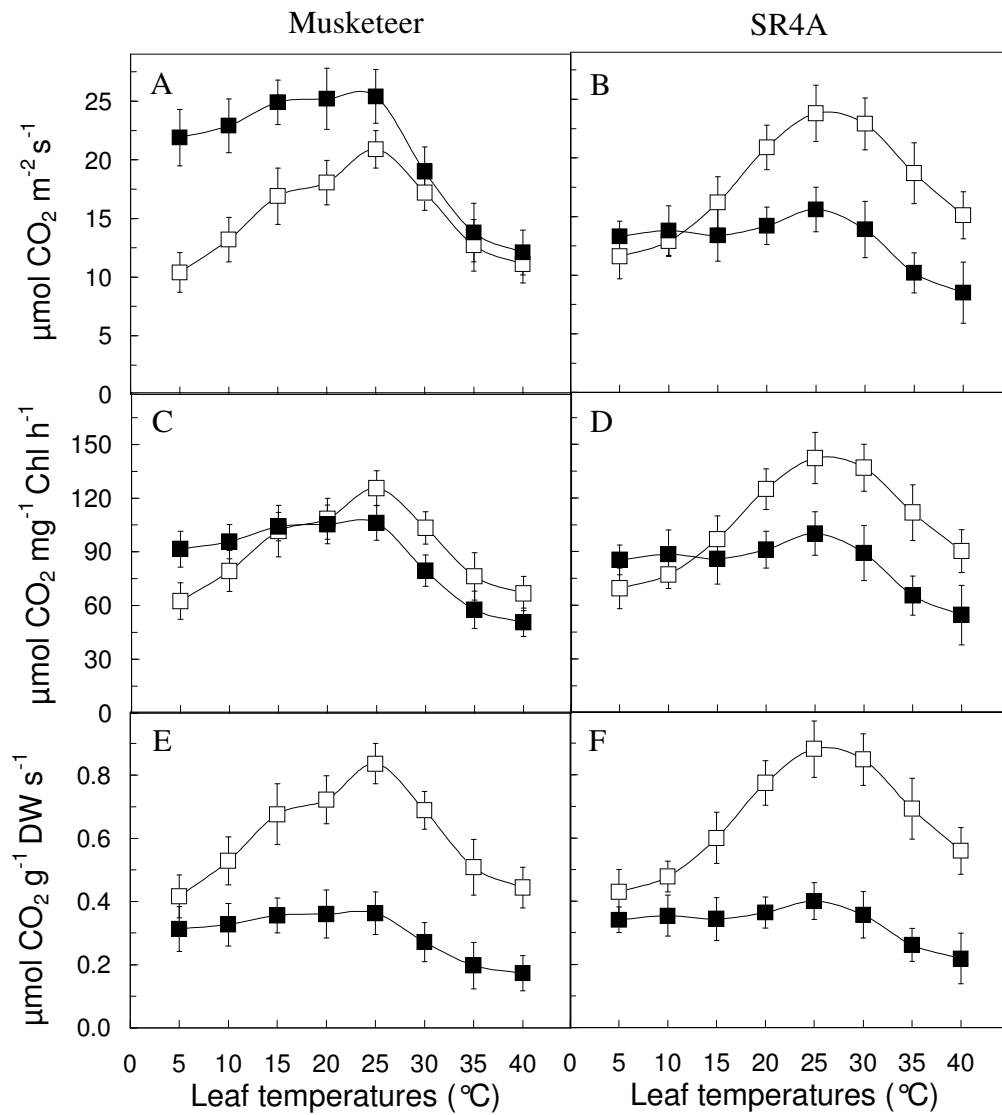


Fig. 2.2. Temperature response curves of light-saturated net CO₂ assimilation expressed on either leaf area (A, B) or leaf chlorophyll (C, D) or leaf dry weight (E, F) basis for Musketeer winter (A, C, E) and SR4A spring rye (B, D, F) cultivars grown at either 20/16°C (□) or 5/5°C (■) and at ambient CO₂. Photosynthetic rates for both NA and CA plants were measured on attached, fully developed third leaves at varying leaf temperatures ranging from 5° to 40°C and at ambient CO₂. Each point represents the mean of nine plants from three different pots. Bars represent standard deviation.

Table 2.3. Light-saturated rates of maximum electron transport for Chl a fluorescence (ETR) and for CO₂ gas exchange (J_{max}), the initial linear slope of the light response curves (the apparent maximum quantum efficiency, Q), the initial linear slope of the light-saturated A/C_i response curves (carboxylation efficiency, CE), for winter and spring cultivars. The measurements were carried out on attached, fully developed third leaves of 25-day-old NA and 75-day-old CA plants at measuring temperatures of either 20° or 5°C and at ambient CO₂. Each point represents the mean of nine plants from three different pots ± SD. Significant differences among the means within each cultivar are indicated by the superscripted letters (P ≤ 0.05).

Cultivars	Acclimation state	Measuring temp. (°C)	ETR (μmol e ⁻ m ⁻² s ⁻¹)	J _{max} (μmol e ⁻ m ⁻² s ⁻¹)	Q (CO ₂ /photon)	CE (CO ₂ m ⁻² s ⁻¹ /mol ⁻¹ CO ₂)
Musketeer	NA	20	166 ± 12 ^b	137 ± 8 ^b	0.048 ± 0.006 ^b	0.083 ± 0.007 ^{ab}
		5	122 ± 17 ^a	109 ± 14 ^a	0.033 ± 0.004 ^a	0.073 ± 0.005 ^a
	CA	20	235 ± 25 ^c	178 ± 21 ^c	0.059 ± 0.004 ^c	0.093 ± 0.006 ^b
		5	223 ± 28 ^c	162 ± 11 ^c	0.053 ± 0.008 ^{bc}	0.091 ± 0.016 ^b
Norstar	NA	20	157 ± 10 ^b	139 ± 10 ^a	0.045 ± 0.006 ^b	0.078 ± 0.012 ^{ab}
		5	128 ± 11 ^a	118 ± 16 ^a	0.034 ± 0.003 ^a	0.065 ± 0.008 ^a
	CA	20	202 ± 18 ^b	172 ± 13 ^b	0.049 ± 0.007 ^b	0.088 ± 0.006 ^b
		5	208 ± 17 ^b	167 ± 9 ^b	0.047 ± 0.005 ^b	0.084 ± 0.009 ^b
SR 4A	NA	20	197 ± 15 ^b	142 ± 17 ^b	0.058 ± 0.004 ^b	0.094 ± 0.007 ^b
		5	142 ± 9 ^a	115 ± 9 ^a	0.035 ± 0.004 ^a	0.079 ± 0.011 ^{ab}
	CA	20	161 ± 13 ^a	109 ± 11 ^a	0.041 ± 0.005 ^a	0.064 ± 0.008 ^a
		5	148 ± 9 ^a	106 ± 14 ^a	0.045 ± 0.007 ^a	0.069 ± 0.01 ^a
Katepwa	NA	20	182 ± 20 ^b	148 ± 13 ^b	0.052 ± 0.009 ^b	0.087 ± 0.011 ^b
		5	116 ± 15 ^a	108 ± 15 ^a	0.029 ± 0.005 ^a	0.060 ± 0.008 ^a
	CA	20	127 ± 8 ^a	115 ± 10 ^a	0.037 ± 0.004 ^a	0.052 ± 0.005 ^a
		5	122 ± 13 ^a	113 ± 14 ^a	0.044 ± 0.006 ^b	0.061 ± 0.008 ^a

in NA controls whereas it was inhibited by only 3-8% in CA winter cultivars (Table 2.3, 20 vs 5). Consequently, the Q_{10} for J_{\max} in CA Musketeer (1.06) and Norstar (1.01) were lower than those of the NA rye (1.16) and wheat counterparts (1.11). Similar trends were observed when light-saturated rates of photosynthetic electron transport were calculated from Chl fluorescence data (Table 2.3, ETR; Appendix 2S5), which are indicative of maximum rates of electron transport. Furthermore, similar trends with respect to the relative effects of cold acclimation and sensitivity to measuring temperature were observed for both apparent maximum quantum efficiency (Table 2.3, Q) as well as carboxylation efficiency (Table 2.3, CE).

In contrast to the winter cultivars, the CA spring cultivars, SR4A rye and Katepwa wheat, exhibited a significant inhibition of J_{\max} and ETR relative to NA controls (Table 2.3; Appendix 2S5). These results are consistent with the inhibition of light-saturated rates of CO_2 assimilation induced by cold acclimation of SR4A spring rye and Katepwa spring wheat (Table 2.2). J_{\max} and ETR observed for CA spring cultivars were comparable to those rates observed for NA controls measured at 5°C. However, both CA winter and spring cultivars exhibited decreased sensitivity of CO_2 assimilation (Fig. 2.2; Appendix 2S4) as well as ETR (Appendix 2S5) to low measuring temperatures between 5° and 25°C relative to NA control plants.

2.3.3 Differential effects of increased SLW and Chl on photosynthetic light and CO_2 response curves

Increases in light-saturated rates of photosynthetic CO_2 assimilation between NA and CA winter rye and wheat based on leaf area ignores potential contributions of differences in SLW, Chl per unit area and leaf thickness to CO_2 gas exchange. Since cold acclimation caused a 2.5-fold and 1.44-fold increase in SLW and Chl per unit area in winter Musketeer rye (Fig. 2.1, Table 2.1), we tested the possible contributions of increased SLW and Chl per unit leaf area on the light (Fig. 2.3) and CO_2 response curves (Fig. 2.4) for NA and CA rye cultivars when measured at the same temperature (20°C). The results illustrated in Fig. 2.3 indicate that, although light-saturated rates of CO_2 assimilation were about 1.4-fold higher in CA than in NA Musketeer when expressed on the leaf area

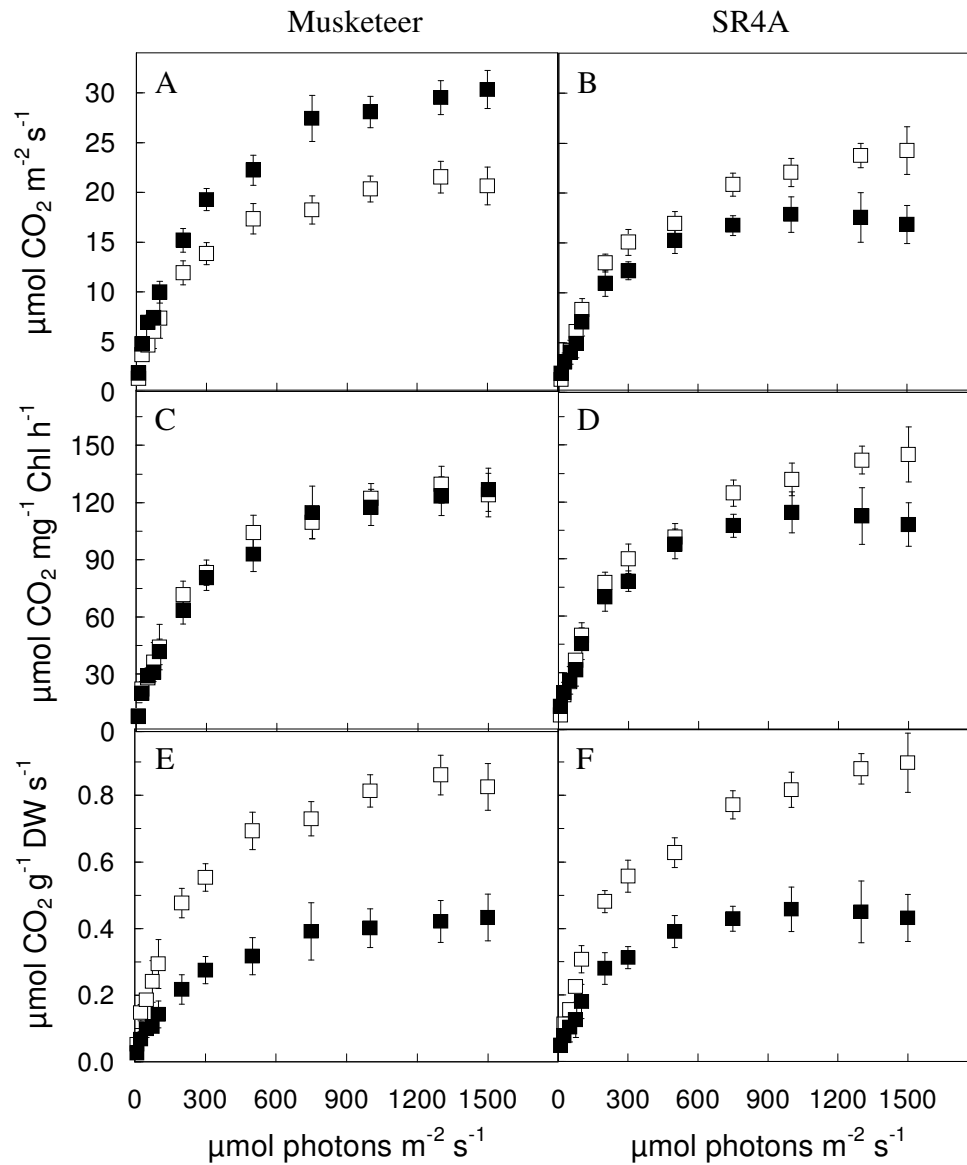


Fig. 2.3. Light response curves of gross CO₂ assimilation expressed on either leaf area (A, B) or leaf chlorophyll (C, D) or leaf dry weight (E, F) basis for Musketeer winter (A, C, E) and SR4A spring rye (B, D, F) cultivars grown at either 20/16°C (□) or 5/5°C (■) and at ambient CO₂. Photosynthetic rates for both NA and CA plants were measured on attached, fully developed third leaves at 20°C. Each point represents the mean of nine plants from three different pots. Bars represent SD.

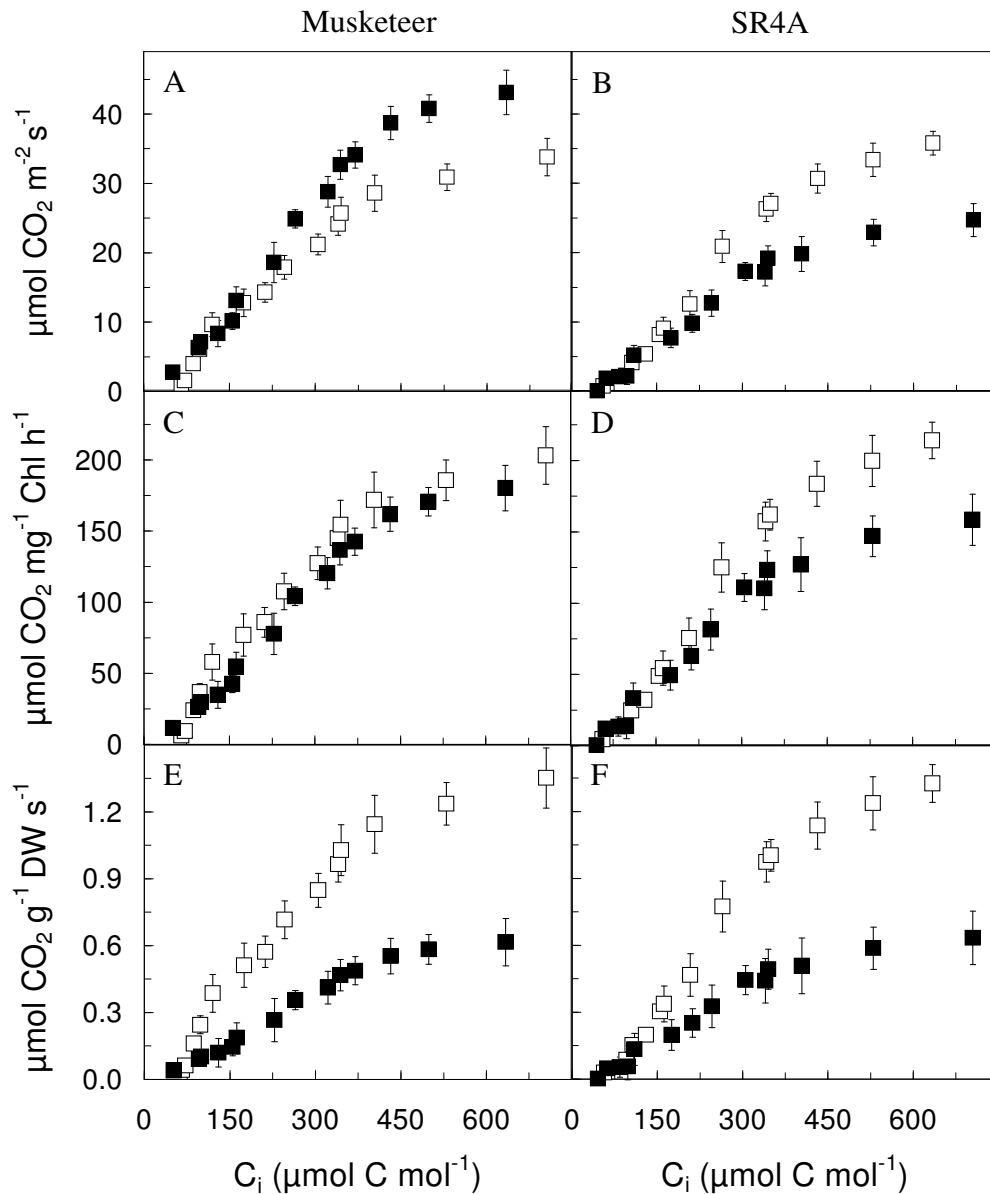


Fig. 2.4. Light-saturated rates of net CO₂ assimilation versus internal CO₂ concentrations (C_i) expressed on either leaf area (A, B) or leaf chlorophyll (C, D) or leaf dry weight (E, F) basis for Musketeer winter (A, C, E) and SR4A spring rye (B, D, F) cultivars grown at either 20/16°C (\square) or 5/5°C (\blacksquare) and at ambient CO₂. Photosynthetic rates for both NA and CA plants were measured on attached, fully developed third leaves at 20°C. Each point represents the mean of nine plants from three different pots. Bars represent SD.

basis (Fig. 2.3A), this difference was eliminated when CO₂ assimilation was expressed on a Chl basis (Fig. 2.3C). Furthermore, the light-saturated rates of CO₂ assimilation were approximately 50% lower in CA than in NA Musketeer when expressed on a leaf dry weight basis (Fig. 2.3E). Since the growth of spring rye, SR4A, at low temperature resulted in minimal changes on Chl per unit area (Table 2.1), cold acclimation of spring rye, SR4A, inhibited light-saturated rates of CO₂ assimilation irrespective of whether CO₂ assimilation was expressed either on a leaf area (Fig. 2.3B) or per unit Chl basis (Fig. 2.3D). However, the light response curves for CA and NA Musketeer were indistinguishable from those of CA and NA SR4A when calculated on a leaf dry weight basis (Fig. 2.3E and F). Similar trends were observed for the CO₂ response curves for NA and CA Musketeer winter rye (Fig. 2.4A, C and E) and NA and CA spring rye (Fig. 2.4B, D and F). Comparable results were observed for winter and spring cultivars of wheat (Appendix S6 and S7).

2.3.4 Effects of cold acclimation on stomatal conductance and water use efficiency

Since the rates of leaf gas exchange and rates of water loss through transpiration are under stomatal control, we examined the effects of cold acclimation on stomatal conductance (gs) and stomatal density. Cold acclimation suppressed stomatal conductance by 60 - 70% in the winter cultivars, Musketeer and Norstar, when measured at 20°C but only by 30-35% when measured at 5°C (Table 2.4). As a result, leaf transpiration rates were 35 - 50% lower in these cultivars during cold acclimation irrespective of the measuring temperature (Table 2.4). Thus, the stimulation of light-saturated (Fig. 2.3A) and CO₂-saturated rates of CO₂ assimilation in CA winter cultivars (Fig. 2.4A) measured on a leaf area basis can not be due to a stomatal effect.

In contrast to the winter cultivars, cold acclimation suppressed stomatal conductance by 30 - 40% and transpiration rates by about 20% in the spring cultivars, SR4A and Katepwa (Table 2.4). Furthermore, stomatal conductance of the CA winter cultivars appeared to be less temperature sensitive than their NA counterparts whereas CA and NA spring cultivars appeared to be equally sensitive to measuring temperature. Consequently, CA Norstar and Musketeer exhibited approximately a 3-fold increase in

Table 2.4. Stomatal conductance, transpiration rates and leaf water use efficiency (WUE) of fully developed third leaves of winter and spring wheat and rye cultivars grown at either 20/16°C (NA) or 5/5°C (CA) and at ambient CO₂. The measurements were carried out on attached, fully developed third leaves of 25-day-old NA and 75-day-old CA plants at measuring temperatures of either 20° or 5°C and at ambient CO₂. Data represent the mean of nine plants from three different pots ± SD. Significant differences among the means within each cultivar are indicated by the superscripted letters ($P \leq 0.05$).

Cultivars	Acclimation state	Measuring temperatures (°C)	Stomatal conductance gs (mol m ⁻² s ⁻¹)	Transpiration (mmol H ₂ O m ⁻² s ⁻¹)	WUE (A/gS)
Musketeer	NA	20	0.61 ± 0.09 ^c	2.65 ± 0.30 ^b	29.7 ± 1.9 ^a
		5	0.40 ± 0.05 ^b	2.23 ± 0.19 ^b	29.5 ± 2.6 ^a
	CA	20	0.25 ± 0.03 ^a	1.68 ± 0.11 ^a	98 ± 10.4 ^c
		5	0.27 ± 0.04 ^a	1.79 ± 0.12 ^a	77.4 ± 5.1 ^b
Norstar	NA	20	0.68 ± 0.11 ^c	3.42 ± 0.24 ^c	24.7 ± 3.2 ^a
		5	0.36 ± 0.06 ^b	2.86 ± 0.16 ^b	27.5 ± 1.3 ^a
	CA	20	0.22 ± 0.03 ^a	1.93 ± 0.18 ^a	93.2 ± 8.7 ^c
		5	0.25 ± 0.05 ^{ab}	1.76 ± 0.41 ^a	70.8 ± 5.3 ^b
SR4A	NA	20	0.81 ± 0.13 ^b	3.09 ± 0.22 ^b	25.2 ± 1.8 ^b
		5	0.73 ± 0.10 ^{ab}	2.51 ± 0.15 ^a	17.2 ± 2.5 ^a
	CA	20	0.61 ± 0.04 ^a	2.44 ± 0.32 ^a	23.9 ± 3.2 ^{ab}
		5	0.56 ± 0.06 ^a	2.39 ± 0.29 ^a	24.8 ± 2.2 ^b
Katepwa	NA	20	0.54 ± 0.07 ^b	3.24 ± 0.49 ^b	32.6 ± 2.9 ^b
		5	0.62 ± 0.11 ^b	2.30 ± 0.31 ^a	14.8 ± 1.2 ^a
	CA	20	0.35 ± 0.05 ^a	2.39 ± 0.16 ^a	34.6 ± 2.1 ^b
		5	0.32 ± 0.05 ^a	2.56 ± 0.17 ^a	35.3 ± 3.1 ^b

leaf water use efficiency (WUE) relative to NA controls whereas CA Katepwa and SR4A exhibited a minimal change in leaf WUE relative to NA controls irrespective of the measuring temperature (Table 2.4). These data indicate that the differential enhancement of WUE induced by cold acclimation of Musketeer winter rye and Norstar winter wheat is primarily associated with an increase in A_{sat} and decrease in stomatal conductance. Unlike winter cultivars, spring cultivars, Katepwa wheat and SR4A rye inhibited A_{sat} in addition to stomatal conductance upon cold acclimation and, thus, had minimal changes on A_{sat}/g_s ratio, that is, water use efficiency.

It appears that the suppressed stomatal conductance observed in CA plants can be accounted for, in part, by a decrease in stomatal density on both the abaxial and adaxial leaf surfaces for all four cultivars tested. For example, CA Musketeer winter rye exhibited a 55% reduction in adaxial stomatal density (72 ± 22 stomates mm^{-2}) compared to NA Musketeer (159 ± 14 stomates mm^{-2}). In contrast, CA SR4A spring rye exhibited only a 27% reduction in adaxial stomatal density (101 ± 15) compared to NA SR4A (137 ± 6). Similar trends were observed for the effects of cold acclimation on adaxial and abaxial stomatal densities in Norstar winter wheat compared to Katepwa spring wheat (data not shown).

2.3.5 Effects of cold acclimation on $\delta^{13}\text{C}$ values of leaf tissues

Alterations in stomatal density and WUE should be reflected in changes in $^{13}\text{C}/^{12}\text{C}$ carbon isotope ratios measured as $\delta^{13}\text{C}$ (‰) (O'Leary 1988). The results illustrated in Table 2.1 indicate that CA Musketeer exhibited a 2.3‰ increase (less negative) in $\delta^{13}\text{C}$ compared to NA winter rye. In contrast, we detected no significant differences in the $\delta^{13}\text{C}$ values between CA and NA SR4A (Table 2.1). These results are consistent with the differential effects of cold acclimation on WUE in winter versus spring cultivars (Table 2.4).

2.3.6 Effects of cold acclimation on dark respiration rates

Respiration is another important process that contributes to leaf net CO_2 gas exchange. All four cultivars exhibited comparable dark respiration rates of about 2.1 - 3.2 $\mu\text{mol CO}_2$

evolved $\text{m}^{-2}\text{s}^{-1}$ at 20°C and ambient CO_2 (Table 2.2, R_{dark} , NA, 20). An immediate reduction in measuring temperature from 20° to 5°C inhibited these rates by 15 – 25% in all NA cultivars (Table 2.2, R_{dark} , NA, 5). However, unlike photosynthesis, cold acclimation significantly increased dark respiration rates (17 – 30%) not only in winter cultivars but also in spring cultivars irrespective of the measuring temperatures (Table 2.2, R_{dark} , CA). Thus, we did not detect any differential effects of cold acclimation on rates of respiration in winter versus spring cultivars of rye and wheat.

2.3.7 Effects of cold acclimation on ETR, EP and NPQ

In vivo Chl a fluorescence provides a convenient means to quantify maximum potential rates of photosynthetic electron transport (ETR), excitation pressure (EP), which estimates the relative reduction state of PSII reaction centers, and non-photochemical quenching (NPQ), an estimate of the capacity to dissipate energy as heat. However, differences in leaf morphology have minimal impact on measurements of ETR, EP and NPQ by Chl a fluorescence. The amount of light absorbed by Chl decreases as the light penetrates into the leaf with the fluorescence signal being strongest near the leaf surface. Light response curves for 1-qP and NPQ are useful to estimate the apparent quantum requirement to close PSII reaction centers and to induce energy dissipation by NPQ, respectively (Rosso et al. 2009). Apparent quantum requirement is the inverse of apparent quantum efficiency and is estimated as the inverse of the initial slopes calculated from the linear portion of the light response curve for either 1-qP (Fig. 2.5 C and D) or NPQ (Fig. 2.5 E and F). Fig. 2.5 illustrates the light response curves of ETR, 1-qP and NPQ for NA and CA Musketeer winter and SR4A spring rye. The light response curves for ETR in Musketeer indicate that cold acclimation stimulated both the apparent quantum efficiency (maximum initial slope) as well as the light-saturated rates of photosynthetic electron transport by about 50% relative to NA Musketeer (Fig. 2.5A). This was associated with a 13% increase in the apparent quantum requirement for PSII closure (Fig. 2.5C) coupled with a concomitant 40% increase in the apparent quantum requirement to induce NPQ (Fig. 2.5E) in CA versus NA Musketeer. In contrast, cold acclimation of spring rye, SR4A, resulted in a 25% decrease in the apparent quantum efficiency as well as the light-saturated rates of ETR (Fig. 2.5B). This was associated with a 40% decrease in the

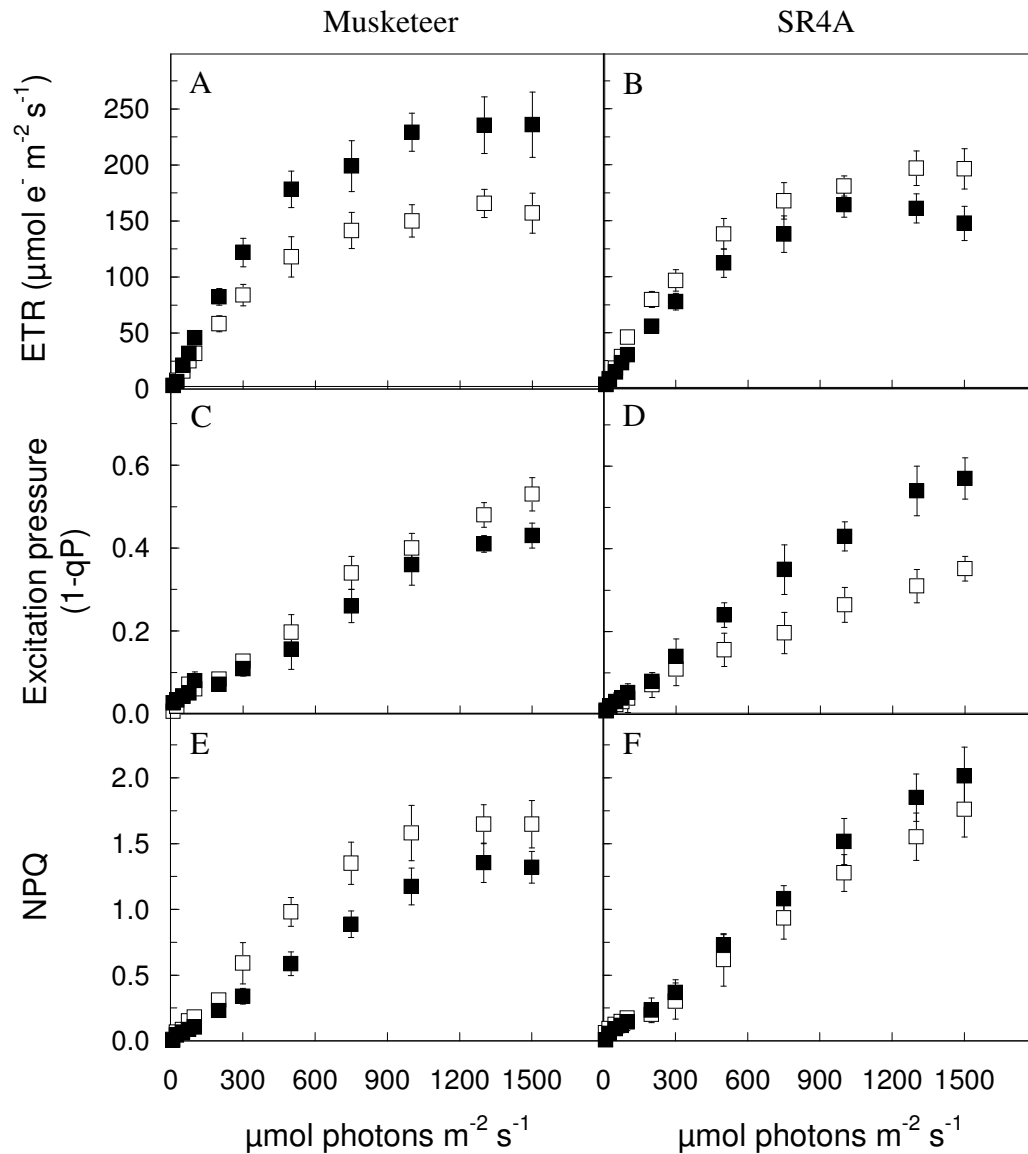


Fig. 2.5. Light response curves of electron transport rates (ETR; A, B), excitation pressures (1-qP; C, D) and non photochemical quenching of excess energy (NPQ; E, F) for Musketeer winter (A, C, E) and SR4A spring rye (B, D, F) cultivars grown at either 20/16°C (□) or 5/5°C (■) and at ambient CO₂. Measurements were carried out at 20°C for both NA and CA plants. Each point represents the mean of nine plants from three different pots. Bars represent SD.

apparent quantum requirement for PSII closure (Fig. 2.5D) and a 12% decrease in the apparent quantum requirement to induce NPQ (Fig. 2.5F) in CA relative to NA SR4A. Similar trends in ETR, EP and NPQ were observed in NA and CA Norstar winter wheat versus NA and CA Katepwa spring wheat (Appendix 2S8).

2.3.8 Effects of cold acclimation on photosynthetic gene expression and polypeptide accumulation

To confirm that the winter and spring cultivars tested were differentially cold acclimated, the accumulation of three COR protein markers (Wcs120, Wcor410 and Wcs19) in Norstar winter and Katepwa spring wheat were measured. None of the COR proteins were detected in either wheat cultivars in the NA state (Appendix 2S9, lane 1 and 3). However, we observed the accumulation of all three COR proteins tested in CA Norstar but not in CA Katepwa (Appendix 2S8, lane 2 and 4). Therefore, the differential accumulation of COR proteins in winter versus spring wheat cultivars in response to low growth temperature confirms that these cereals were indeed differentially cold acclimated.

Cold acclimation also appeared to alter photosynthetic gene expression. Transcript abundance either increased (*rbcL*, *cFBPase*, *psbA*) or remained about the same (*Lhcb1*, *psaA*) in CA versus NA Norstar wheat (Fig. 2.6A). Similar trends were observed in CA Katepwa spring wheat except that *cFBPase* expression was significantly inhibited during cold acclimation (Fig. 2.6A). However, at the protein level, cold acclimation induced minimal changes (10 - 15%) in the relative amount of major photosynthetic enzymes and components of photosynthetic electron transport such as *rbcL*, *cFBPase*, *Lhcb1*, *psbA* and *psaA* in either Musketeer winter rye (Fig. 2.6B, Musketeer, CA versus NA) or Norstar winter wheat (Fig. 2.6B, Norstar, CA versus NA) when expressed on total leaf protein basis. However, cold acclimation appeared to reduce the level of *psbA*, the PSII reaction center polypeptide, in both SR4A (59%) (Fig. 2.6B, SR4A, CA versus NA) and Katepwa (32%) (Fig. 2.6B, Katepwa, CA versus NA). Minimal changes in both *Lhcb1* expression and *Lhcb1* accumulation are consistent with minimal differences in the Chl a/b ratios between CA and NA winter and spring cultivars (Table 2.1). We conclude

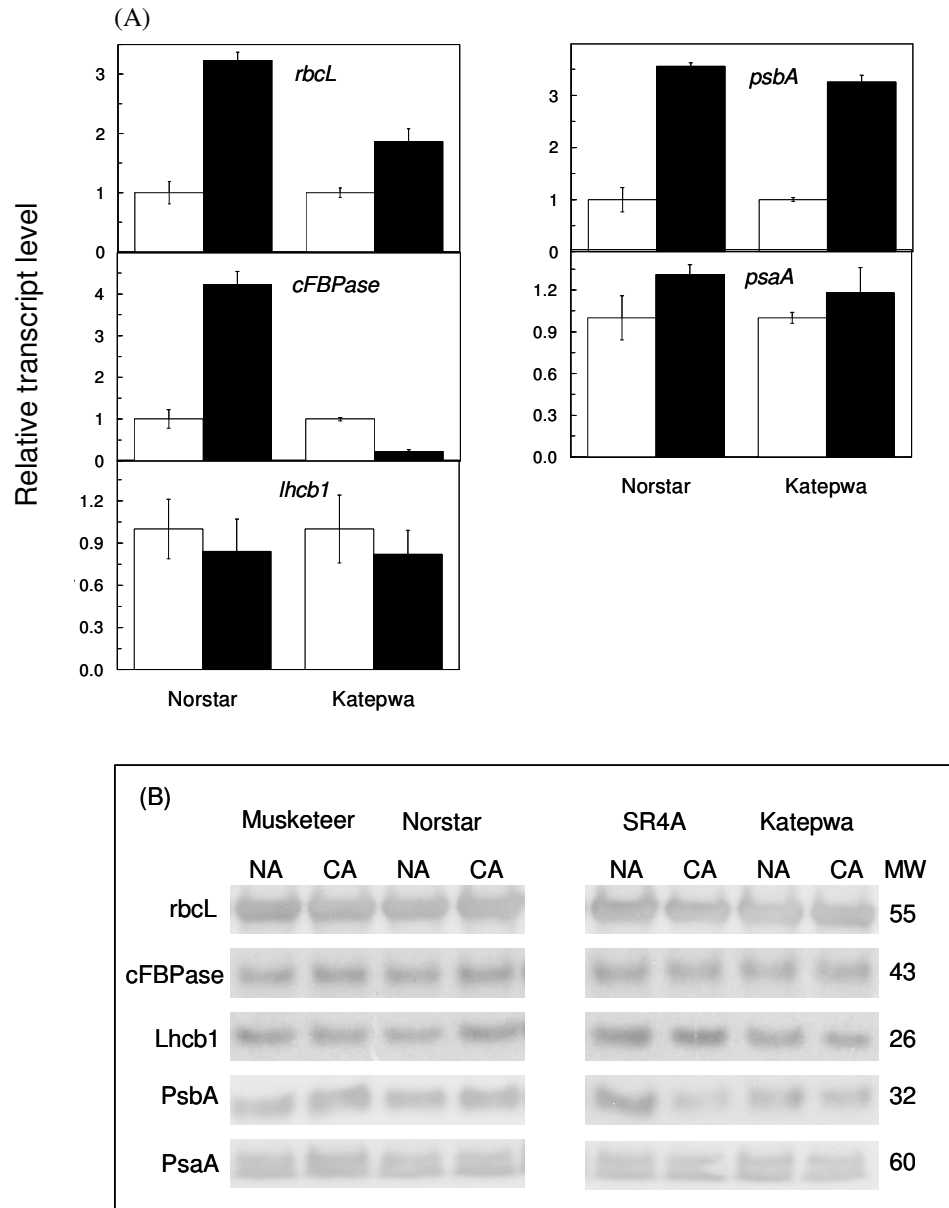


Fig. 2.6. (A) Relative transcript levels of *rbcL*, *cFBPase*, *lhcb1*, *psbA*, and *psaA* isolated from Norstar winter and Katepwa spring wheat grown at either 20/16°C (□) or 5/5°C (■) and at ambient CO₂. Samples were collected from fully developed third leaves. 18S gene was used as an internal control. (B) Immunoblot analysis of SDS – PAGE probed with antibodies raised against: *rbcL*, *cFBPase*, *Lhcb1*, *PsbA* and *PsaA* isolated from winter and spring rye and wheat cultivars grown at either 20/16°C (NA) or 5/5°C (CA) and at ambient CO₂. Lanes of SDS – PAGE were loaded on equal protein basis (8 µg protein/lane). The bovine serum albumin (1µg on each lane) was used as an internal control. Numbers on the right indicate molecular weight (MW, kDa) of markers.

that the levels of rbcL and cFBPase as well as the other components of the photosynthetic apparatus are 3-fold greater in CA than NA winter cereals on the basis of a 3-fold increase in the protein/Chl ratio (Table 2.1). In contrast, this was not observed in the spring varieties since cold acclimation affected the protein/Chl ratio minimally in these cultivars (Table 2.1). Although winter cultivars exhibited a 3-fold increase in the amount of rbcL, no apparent changes in the catalytic properties of Rubisco were detected as indicated by minimal changes in the carboxylation efficiencies upon cold acclimation (Table 2.3).

2.3.9 Effects of over-expression of BnCBF17 on phenotypic plasticity and photosynthetic performance in Brassica napus

Overexpression of *CBFs* induces a dwarf growth habit and increases freezing tolerance in *Arabidopsis thaliana* (Gilmour et al. 2000a, 2000b) as well as *Brassica napus* (Savitch et al 2005). Fig. 2.7 illustrates that over-expression of *BnCBF17* in *Brassica napus* resulted in a dwarf growth habit and approximately a 1.7-fold increase in leaf thickness (330 μ m) compared to WT (191 μ m) which appeared to be primarily due to an increased thickness of the palisade layer.

The changes in leaf anatomy and plant phenotype in the *BnCBF17*-over-expressing line were associated with a 1.7-fold increase in SLW, a 2.7-fold increase in Chl per unit leaf area (Table 2.5) and a 1.3-fold increase in light-saturated rates of gross CO₂ assimilation measured on a leaf area basis compared to WT (Fig. 2.8A). This was coupled with a significant increase in apparent quantum yield (Q) of CO₂ assimilation but no significant change in carboxylation efficiency (CE) (Table 2.5). However, the light response curves illustrated in Fig. 2.8A indicate that the 1.3-fold increase in light-saturated rates of CO₂ assimilation exhibited by the *BnCBF17*-over-expressing transgenic line relative to the WT when expressed on a leaf area basis was eliminated when calculated either on a per unit Chl basis (Fig. 2.8C) or on a leaf dry weight basis (Fig. 2.8E). Although the *BnCBF17* transgenic line exhibited a significant increase in the light and CO₂-saturated rates of CO₂ assimilation on a leaf area basis (Fig. 2.8B), both the carboxylation efficiency as well as the light and CO₂-saturated rates of CO₂ assimilation

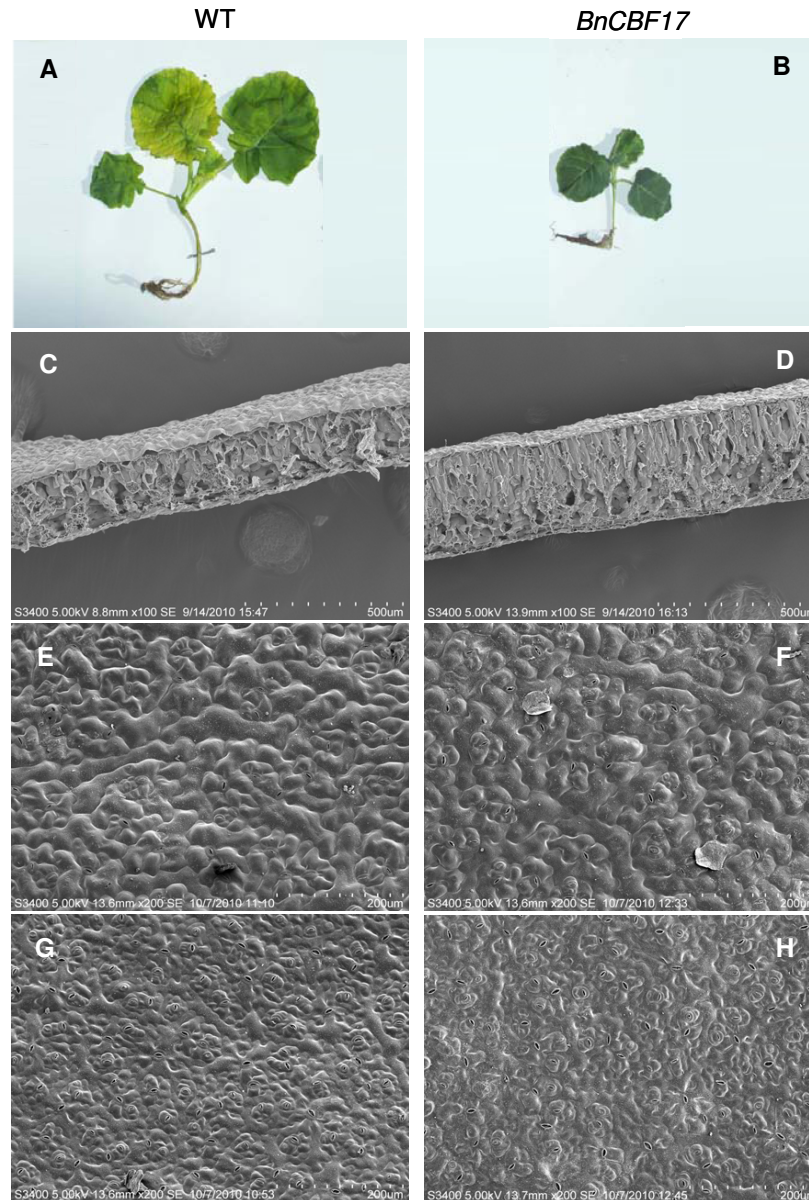


Fig. 2.7. Effects of *BnCBF17*-over-expression on plant morphology, growth habit and leaf anatomy of two *Brassica* lines. Photographs for 3-week-old wild type (WT, A) and four-week-old *BnCBF17*-over-expressing *Brassica* transgenic lines (*BnCBF17*, B) grown at 20/16°C and at ambient CO₂ conditions. Leaf cross sections for WT (C) and *BnCBF17* (D). Upper leaf surfaces for WT (E) and *BnCBF17* (F). Lower leaf surfaces for WT (G) and *BnCBF17* (H). The images for leaf cross sections and leaf surfaces were taken from fully developed third leaves of three-week-old WT and four-week-old *BnCBF17*-over-expressing plants using SEM.

Table 2.5. Morphological and physiological characteristics of wild type (WT) and *BnCBF17* -over-expressing *Brassica* transgenic line (*BnCBF17*) grown at 20/16°C and at ambient CO₂ conditions. All measurements were carried out on fully developed third leaves of three-week-old WT and four-week-old *BnCBF17* at measuring temperatures of 20°C and at ambient CO₂. Data represent the mean of three plants from three different pots ± SD. Significant differences of the means between the two lines are indicated by the symbol * ($P \leq 0.05$).

Morphological and physiological characteristics	Genotypes		
	WT	<i>BnCBF17</i>	
Specific leaf weight (g dry weight m ⁻² leaf area)	24 ± 4	41 ± 6*	
Total Chlorophyll (mg m ⁻²)	367 ± 48	984 ± 74*	
Chl a/Chl b ratio	3.3 ± 0.12	2.8 ± 0.19*	
Q (CO ₂ /photon)	0.051 ± 0.003	0.061 ± 0.004*	
CE (CO ₂ m ⁻² s ⁻¹ /mol ⁻¹ CO ₂)	0.097 ± 0.012	0.115 ± 0.017	
δ ¹³ C	-31.1 ± 0.3	-29.6 ± 0.4*	
R _{dark} (μmol CO ₂ evolved m ⁻² s ⁻¹)	- 3.43 ± 1.18	- 2.58 ± 0.38	
Stomatal conductance gs (mol m ⁻² s ⁻¹)	0.29 ± 0.04	0.32 ± 0.04	
Stomatal frequency (Stomates mm ⁻² leaf area)	Adaxial	126 ± 15	160 ± 28
	Abaxial	375 ± 19	345 ± 37
Transpiration (mmol H ₂ O m ⁻² s ⁻¹)	1.96 ± 0.93	2.14 ± 0.34	
WUE (A _{sat} /gs)	56.6 ± 4	72.6 ± 6*	

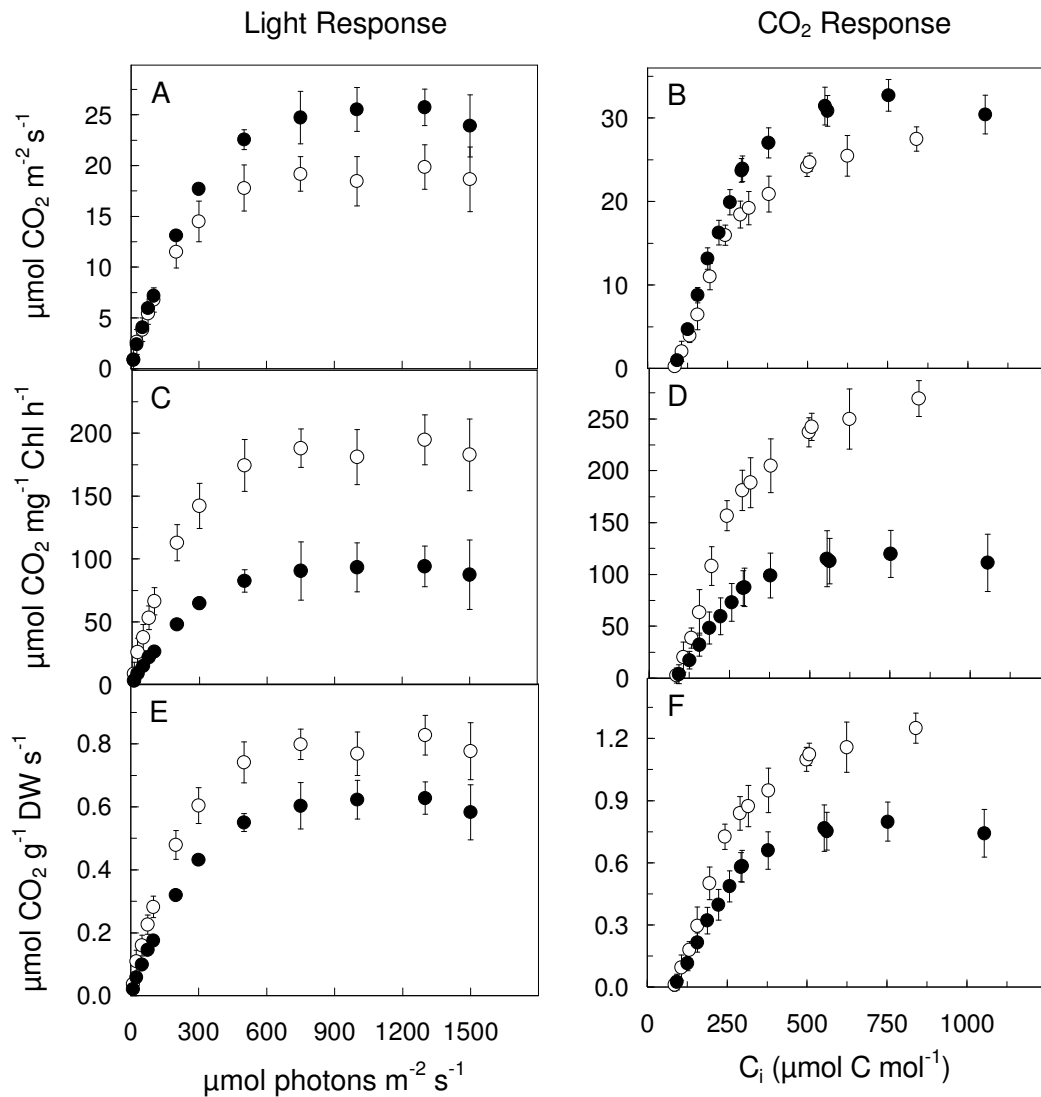


Fig. 2. 8. Light response curves of gross CO₂ assimilation (A, C, E) and light-saturated rates of net CO₂ assimilation versus internal CO₂ concentrations (B, D, F) expressed on either leaf area (A, B) or leaf chlorophyll (C, D) or leaf dry weight (E, F) basis for WT (○) and *BnCBF17*-over-expressing *Brassica* transgenic lines (●) grown at 20/16°C and at ambient CO₂ conditions. Photosynthetic rates were measured on fully developed third leaves of three-week-old WT and four-week-old *BnCBF17*-over-expressing plants at measuring temperature of 20°C and at ambient CO₂. Each point represents the mean of three plants from three different pots. Bars represent SD.

were lower in the *BnCBF17* transgenic line compared to WT when calculated either on a per unit Chl basis (Fig. 2.8D) or on a leaf dry weight basis (Fig. 2.8F).

Fig. 2.9 illustrates the temperature response curves for CO₂ assimilation (Fig. 2.9 A, B, C) and ETR (Fig. 2.9D) for WT and the transgenic *BnCBF17* line of *Brassica napus*. The *BnCBF17* transgenic line exhibited higher light-saturated rates of CO₂ assimilation (Fig. 2.9A) and ETR (Fig. 2.9D) than WT at all temperatures between 5° and 25°C when they were expressed on a leaf area basis. This difference between the WT and the *BnCBF17* transgenic line with respect to of CO₂ assimilation was eliminated when CO₂ assimilation was expressed on either a Chl basis (Fig. 2.9B) or of a leaf dry weight basis (Fig. 2.9C). However, overexpression of *BnCBF17* decreased the low temperature sensitivity of CO₂ assimilation and ETR ($Q_{10_{Asat}} = 1.13$; $Q_{10_{ETR}} = 1.07$) compared to WT ($Q_{10_{Asat}} = 1.47$; $Q_{10_{ETR}} = 1.32$) (Fig. 2.9).

The transgenic *BnCBF17* line exhibited minimal changes in transpiration rates compared to WT (Table 2.5) which were consistent with minimal changes in adaxial (WT : *BnCBF17* = 0.79) and abaxial (WT : *BnCBF17* = 1.09) stomatal frequencies calculated from the SEM micrographs of respective leaf surfaces (Fig. 2.7, Table 2.5). However, WUE was 30% higher and the $\delta^{13}C$ value increased by 1.5‰ in the *BnCBF17* line compared to the WT (Table 2.5).

In vivo Chl a fluorescence indicated that the transgenic line exhibited a small (10%) but significant increase in light-saturated ETR but no change in the apparent quantum efficiency of ETR compared to WT (Fig. 2.10A). However, the apparent quantum requirements for closure of PSII reaction centers (Fig. 2.10B) and for NPQ (Fig. 2.10C) were 25% and 35% higher, respectively, in the *BnCBF17*- over-expressing line than the WT.

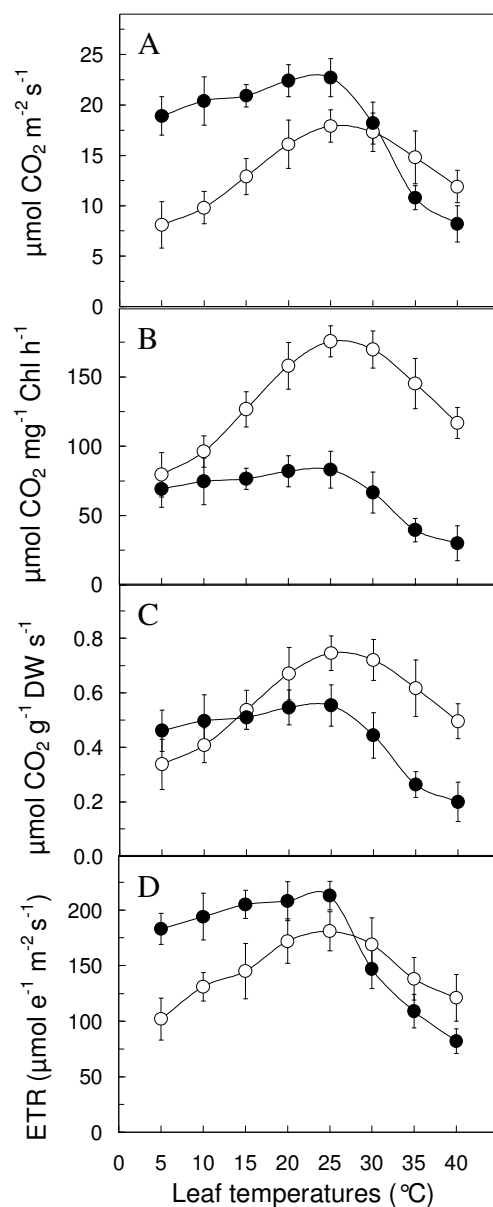


Fig. 2.9. Temperature response curves of light-saturated net CO₂ assimilation expressed on either leaf area (A) or leaf chlorophyll (B) or leaf dry weight (C) basis. (D) Temperature response curves for light-saturated electron transport rates (ETR) measured on leaf area basis for WT (○) and *BnCBF17* transgenic line (●) grown at 20/16°C and at ambient CO₂. Measurements were carried out on fully developed third leaves at varying leaf temperatures ranging from 5° to 40°C at ambient CO₂. Each point represents the mean of three plants from three different pots. Bars represent SD.

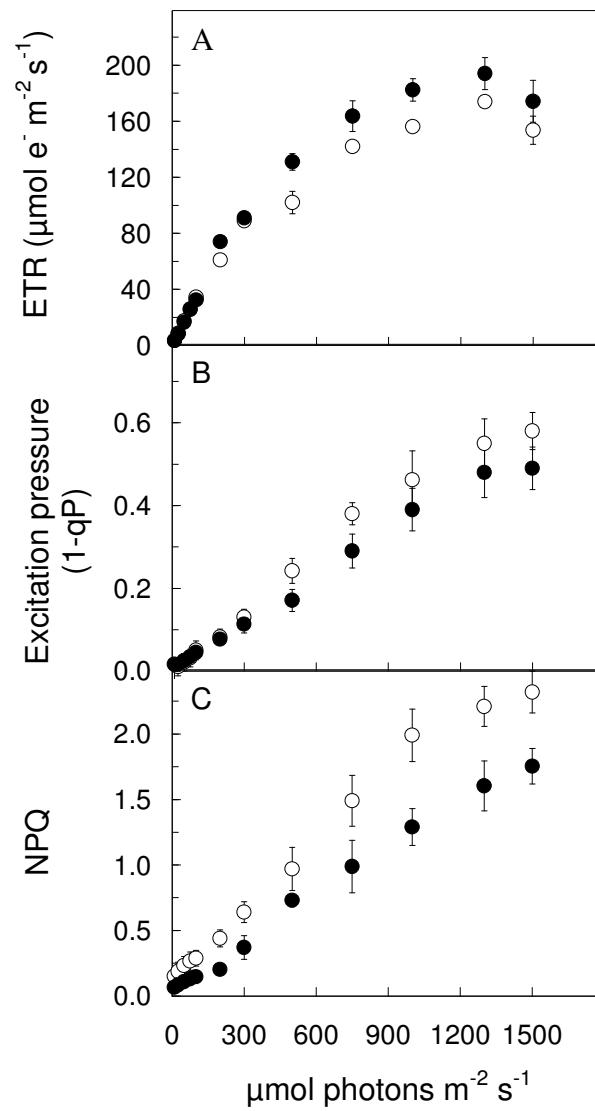


Fig. 2.10. Light response curves of electron transport rates (ETR; A), excitation pressures (1-qP; B) and non photochemical quenching of excess energy (NPQ; C) for WT (○) and *BnCBF17*-over-expressing *Brassica* transgenic lines (●) grown at 20/16°C and at ambient CO₂ conditions. Measurements were carried out at 20°C for both WT and transgenic lines. Each point represents the mean of three plants from three different pots. Bars represent SD.

2.4 Discussion

In this report, we show that the conclusions drawn from a comparison of CO₂ assimilation rates of CA versus NA winter cereals are directly dependent on how one expresses the gas exchange data, that is, are dependent on the frame of reference. All three frames of reference (leaf area; leaf Chl; leaf dry weight) used to calculate photosynthetic gas exchange rates are useful but each frame of reference provides a somewhat different perspective of the effects of cold acclimation on photosynthetic performance in winter cereals. Cold acclimation of winter cereals resulted in significant reductions in stomatal conductance (Table 2.4) and stomatal densities on both leaf surfaces, which are associated with a 1.5-fold increase in leaf thickness (Hüner et al. 1985, Gorsuch et al. 2010a). Thus, CA winter rye and wheat exhibited a significant reduction in the ratio of leaf gas exchange surface area (SA) to leaf volume (V) (SA/V) as compared to NA winter rye and wheat. Despite these significant restrictions regarding the surface area available for CO₂ gas exchange, CA Musketeer (Fig. 2.3A; Fig. 2.4A) and Norstar (Appendix 2S6 and S7) exhibited higher rates of light-saturated as well as CO₂-saturated CO₂ assimilation than NA winter cultivars when expressed on a leaf area basis. This is a consequence, first, of an increased protein/Chl ratio (Table 2.1) which reflects a change in the amount of photosynthetic apparatus at the chloroplast level, and second, of an increased SLW (Fig. 2.1) which reflects an increase in the amount of photosynthetic apparatus available per unit leaf area upon growth at low temperature (compare Fig. 2.3A and C as well as Fig. 2.4A and C). The enhanced photosynthetic efficiency and capacity of CA winter cereals when CO₂ assimilation is expressed on a leaf area basis is consistent with the 3-fold higher protein/Chl ratio (Table 2.1) and the increased quantum requirements for the closure of PSII reaction centers and the induction of energy dissipation through NPQ (Fig. 2.5). This means that CA winter cereals exhibit an increased efficiency to convert absorbed photons into fixed carbon and biomass and concomitantly minimizing energy loss through NPQ. Altering the phenotype and SLW of *Brassica napus* by over-expression of *BnCBF17* (Fig. 2.7, Fig. 2.8, Fig. 2.9, Fig. 2.10) resulted in comparable enhancement of photosynthetic performance as exhibited by CA Musketeer and Norstar. In addition, CA winter cultivars exhibited an enhanced WUE (Table 2.4) irrespective of the measuring temperature relative to NA controls. Thus, we

conclude that the phenotypic plasticity of winter cereals associated with cold acclimation, such as the induction of a dwarf growth habit, increased leaf thickness (Hüner et al. 1985, Gorsuch et al. 2010a) and increased SLW, contribute directly to their enhanced photosynthetic performance when rates of CO₂ assimilation are expressed on a leaf area basis.

In contrast to the photosynthetic performance of CA winter rye (Fig. 2.3; Fig. 2.4) and winter wheat (Appendix 2S6 and S7), the photosynthetic performance of spring rye and spring wheat indicated that cold acclimation resulted in an inhibition of photosynthetic efficiency and photosynthetic capacity when CO₂ assimilation rates were expressed on a leaf area basis (Fig. 2.3; Fig. 2.4). This was associated with decrease in the quantum requirement for both PSII reaction center closure and the concomitant induction of NPQ (Fig. 2.5). This means that, upon cold acclimation, spring cereals exhibit a decreased efficiency to convert absorbed photons into fixed carbon and biomass which is compensated by an increased efficiency for the dissipation of excess absorbed energy through NPQ. In addition, CA spring cultivars did not alter WUE (Table 2.4) and $\delta^{13}\text{C}$ (Table 2.1) relative to NA controls. Furthermore, the inhibition of photosynthesis in the CA spring cultivars was associated with minimal phenotypic plasticity with respect to plant and leaf morphology (Appendix 2S2) and SLW (Fig. 2.1).

However, comparisons of photosynthetic performance between winter and spring cultivars result in alternative conclusions when CO₂ assimilation is calculated on a leaf dry weight basis. First, cold acclimation of winter rye caused a 50% decrease in light-saturated (Fig. 2.3E) as well as light and CO₂-saturated rates of CO₂ assimilation (Fig. 2.4E). Similar results were observed for CA versus NA winter wheat (Appendix 2S6 and S7). Thus, cold acclimation of winter rye and winter wheat induced an inhibition of photosynthetic capacity relative to NA controls when expressed on a leaf dry weight basis (Fig. 2.3E, Fig. 2.4E, Appendix 2S6E and S7E) rather than on a leaf area basis (Fig. 2.3A, Fig. 2.4A, Appendix 2S6A and S7A). Second, when CO₂ assimilation rates were expressed on a leaf dry weight basis, no differences in photosynthetic performance were observed between CA winter and spring cultivars (Fig. 2.3; Fig. 2.4; Appendix 2S6 and S7). CA winter and CA spring cultivars both exhibited an inhibition of photosynthetic

capacity. Thus, the assessment of photosynthetic performance on a leaf dry weight basis appears to eliminate the effects of the differential phenotypic plasticity exhibited by winter and spring cultivars upon cold acclimation. A similar conclusion can be made when photosynthetic rates are expressed on per unit protein basis since cold acclimation increased protein/Chl ratio by 3.5- fold in winter cultivars but had minimal effects on this ratio in spring cultivars (Table 2.1). A similar inhibition of photosynthetic performance is observed when WT *Brassica napus* and the *BnCBF17*- over-expressing line are compared (Fig. 2.8E, Fig. 2.8F). These results provide additional support for our thesis that integration of the changes in plant morphology and leaf anatomy induced during growth at low temperature are important in the interpretation of the comparative photosynthetic performance between winter and spring cultivars during cold acclimation.

How can one rationalize the apparent conundrum between the interpretation of the results for photosynthetic performance expressed on a leaf area basis versus leaf dry weight basis in CA winter and spring cereals? We suggest that this can be explained by an analysis of the potential costs and benefits of phenotypic plasticity associated with cold acclimation. Growth at low temperature induces maximum freezing tolerance in winter cultivars through the induction of cold tolerance-associated genes (Appendix 2S9), which maximizes the probability of survival during the harsh winter conditions. In addition, a characteristic which distinguishes overwintering cereals from spring cereals is that the former increase SLW (Fig. 2.1) and exhibit a dwarf, compact growth habit compared to the latter (Appendix 2S2). The increase in SLW can be explained, in part, by the fact that the equivalent total plant dry matter present in a NA plant accumulates in a much smaller, dwarf CA plant (Table 2.1; Appendix 2S2). Consequently, cold acclimation of winter cereals induces an increase in the ratio of plant biomass / plant volume, that is, an increase in energy per unit volume. We suggest that this reflects a requirement of leaves of cold-acclimated winter cereals to sustain an increased leaf metabolic demand and accumulation of cryoprotectants in order to maintain the cold acclimated state while concomitantly supporting translocation of photoassimilates to critical overwintering sinks such as the crown. Thus, overwintering cereals divert metabolic energy away from vegetative growth and store the fixed carbon as an energy source for the maintenance of the cold acclimated state, which is characterized by

enhanced utilization of absorbed photons and increased resistance to photoinhibition (Hurry et al. 1992, Pocock et al. 2001) as well as increased cryoprotection and freezing tolerance. Consequently, we suggest that a cost of increasing the biomass or energy per unit plant volume is a reduction in photosynthetic capacity when measured on a leaf dry weight basis. However, this apparent cost must be considered in the context of the potential benefit of increasing the biomass or energy per unit volume and WUE, which includes a greater probability of winter survival combined with enhanced reproductive fitness in the following spring due, in part, to the energy accumulated during the cold acclimation period in the preceding autumn.

In contrast to the winter cultivars, cold tolerance-associated genes are not induced in spring cultivars (Appendix 2S9) and hence the spring cultivars are unable to divert energy from vegetative growth to storage required for successful overwintering. Consequently, CA spring cultivars show no changes in plant growth habit (Appendix 2S2), exhibit minimal changes in SLW compared to NA plants (Fig. 2.1) and decrease the efficiency of energy conversion into biomass. Thus, spring cultivars remain susceptible to low temperature photoinhibition (Hurry et al. 1992, Pocock et al. 2001). Thus, the lack of phenotypic plasticity and decreased photosynthetic performance limits the ability of spring cultivars to exploit photosynthesis at low temperatures in the fall and subsequently succumb to the freezing conditions.

What governs phenotypic plasticity, photosynthetic performance and energy storage in overwintering plants? Compared to WT *Brassica napus*, over-expression of *BnCBF17* in *Brassica napus* grown at 20/16°C mimicked the effects of cold acclimation in Musketeer winter rye and Norstar winter wheat with respect to increased SLW (Table 2.5), increased leaf thickness and increased photosynthetic performance (Fig. 2.8A, B). This is also associated with an increase in freezing tolerance (Savitch et al. 2005), which confirms previous published reports for *Arabidopsis thaliana* (Lui et al. 1998, Kasuga et al. 1999, Gilmour et al. 2000). Thus, the over-expression in *Brassica napus* of a single transcription factor, *BnCBF17*, appears to cause the conversion of non-acclimated WT to a cold acclimated state without exposure to low temperature. CBFs/DREBs are a family of transcriptional activators (Liu et al. 1998, Kasuga et al. 1999, Gilmour et al. 2000, van

Buskirk and Thomashow 2006) required for the induction of a suite of cold-regulated genes (*COR*) such as *WCS120*, *WCOR410* and *WCS19* (Appendix 2S9) that enhance plant freezing tolerance (Sarhan et al. 1997). In addition to enhanced freezing tolerance, we confirm that over-expression of *BnCBF17* has much broader effects on leaf anatomy, CO₂ assimilation, photosynthetic electron transport and dry matter accumulation (Savitch et al. 2005). As observed upon cold acclimation of winter rye and winter wheat, over-expression of *BnCBF17* induces a dwarf phenotype with a total dry matter content that is approximately equivalent to the larger, extended phenotype observed in the WT (Table 2.5, Fig, 7A, B). Thus, CBFs/DREBs appear to be critical factors that govern plant phenotypic plasticity during cold acclimation from the level of gene expression and freezing tolerance to whole plant architecture, to photosynthetic electron transport and CO₂ assimilation to resistance to photoinhibition. However, the governance of phenotypic plasticity and photosynthetic performance by CBFs/DREBs in winter cultivars must also be integrated with the process of vernalization (Amasino 2004, Sung and Amasino 2005).

Light-saturated CO₂ assimilation rates and ETR appear to be surprisingly insensitive to temperature between 5° and 25°C in CA compared to NA cultivars (Fig.2, Appendix 2S4, S5). This was observed in both winter and spring cultivars. Thus, cold acclimation appears to stabilize enzymes of the Calvin cycle as well as the thylakoid membrane to a greater extent in CA than in NA winter and spring cultivars. In addition, we show that over-expression of *BnCBF17* in *Brassica napus* also reduces the low temperature sensitivities of light-saturated CO₂ assimilation as well as ETR (Fig. 2.9) in a manner comparable to that observed for cold acclimated winter cereals even though the *BnCBF17*- over-expressing line had never been exposed to low temperature. This is consistent with the thesis that CBFs/DREBs are critical factors governing photosynthetic performance during cold acclimation.

Although alterations in plant morphology, leaf anatomy and SLW in CA winter cultivars as well as *BnCBF17*- over-expressing *Brassica napus* can, by and large, account for the changes in photosynthetic performance, these changes at the leaf level can not account for the differences either in temperature sensitivities (Q₁₀) for CO₂ assimilation (Fig. 2.2; Fig. 2.9; Appendix 2S4) and ETR (Fig. 2.9; Appendix 2S5) or the

differences in the light response curves for ETR, excitation pressure and NPQ in CA versus NA plants (Fig. 2.5, see Appendix 2S8) or between WT versus the *BnCBF17*-over-expressing line (Fig. 2.10). This indicates that growth temperature must also influence the processes of CO₂ assimilation and photosynthetic electron transport at the biochemical level. This, in part, may be a reflection of the increased amounts of the different components of the photosynthetic apparatus in CA compared to NA winter cultivars to enhance energy utilization versus energy dissipation through NPQ. This is consistent with the 3-fold increase in the protein/Chl ratio and the increased quantum requirement for not only PSII closure but also the induction of NPQ (Fig. 2.5, Appendix 8). Consequently, CA Musketeer and Norstar exhibited a lower excitation pressure for a given irradiance, and thus, a greater capacity to keep Q_A oxidized than NA plants (Fig. 2.5, Appendix 8). These results are consistent with published data, which indicate an increased resistance to low temperature-induced photoinhibition in CA versus NA winter cultivars and consistent with the fact that winter and spring cultivars can be discriminated from each other on their differential sensitivities to photoinhibition (Hurry and Hüner 1992, Pocock et al. 2001). Lapointe and Hüner (1993) reported that intact, photosynthetically active, mesophyll cells isolated from cold acclimated rye leaves exhibited a similar increased resistance to photoinhibition as observed for intact CA rye leaves. They concluded that the increased resistance to photoinhibition observed in cold acclimated rye must reside at the cellular level rather than at the level of the intact leaf (Lapointe and Hüner 1993). Thus, both changes in Q₁₀ and the decreased efficiencies of PSII closure and the induction of NPQ as a function of irradiance in either CA versus NA rye and wheat or in WT versus the *BnCBF17*-over-expressing line reflect, in part, the inherent flexibility in energy utilization by photosynthetic electron transport (McDonald et al. 2011) rather than changes in leaf anatomy and plant phenotype.

Acknowledgements

This work was supported, in part, by the Natural Sciences and Engineering Research Council (NSERC) and industrial and government partners, through the Green Crop Research Network (GCN). NPAH, FS, BG and FJL also acknowledge research support through their individual NSERC Discovery Grants. Scanning electron microscopy was

carried out at the Biotron Experimental Climate Change Research Centre, The University of Western Ontario with the help of Richard Gardiner. Stable isotope analyses were performed in the Laboratory for Stable Isotope Science at the University of Western Ontario with the assistance of Kim Law.

2.5 References

- Adams III WW, Demmig-Adams B, Rosenstiel TN, Brightwell AK, Ebbert V (2002) Photosynthesis and photoprotection in overwintering plants. *Plant Biol* 4: 545-557
- Amasino R (2004) Vernalization, Competence, and the Epigenetic Memory of Winter. *Plant Cell* 16: 2553-2559
- Arnon DI (1949) Copper enzymes in isolated chloroplasts. Polyphenoloxidases in *Beta vulgaris*. *Plant Physiol* 24: 1-15
- Badawi M, Reddy YV, Agharbaoui Z, Tominaga Y, Danyluk J, Sarhan F, Houde M (2008) Structure and functional analysis of wheat *ICE* (Inducer of CBF Expression) genes. *Plant Cell Physiol* 49: 1237-1249
- Boese SR, Hüner NPA (1990) Effect of growth temperature and temperature shifts on spinach leaf morphology and photosynthesis. *Plant Physiol* 94: 1830-1836
- Boese SR, Hüner NPA (1992) Developmental history affects the susceptibility of spinach leaves to in vivo low temperature photoinhibition. *Plant Physiol* 99: 1141-1145
- Chinnusamy V, Zhu J, Zhu JK (2007) Cold stress regulation of gene expression in plants. *Trends Plant Sci* 12: 1360-1385
- Coplen TB (1994) Reporting of stable hydrogen, carbon, and oxygen isotopic abundances. *Pure & Appl Chem* 66: 273-276
- Doherty CJ, Buskirk H, Myers SJ, Thomashow MF (2009) Roles for *Arabidopsis* CAMTA transcription factors in cold-regulated gene expression and freezing tolerance. *Plant Cell* 21: 972-984
- Ensminger I, Busch F, Hüner NPA (2006) Photostasis and cold acclimation: sensing low temperature through photosynthesis. *Physiol Plant* 126: 28-44
- Gilmour SJ, Fowler SG, Thomashow MF (2000a) *Arabidopsis* transcriptional activators CBF1, CBF2 and CBF3 have matching functional activities. *Plant Mol Biol* 54: 767-781

- Gilmour SJ, Sebolt AM, Salazar MP, Everard JD, Thomashow MF (2000b) Over-expression of the Arabidopsis CBF3 transcriptional activator mimics multiple biochemical changes associated with cold acclimation. *Plant Physiol* 124: 1854-1865
- Gorsuch PA, Pandey S, Atkin OK (2010a) Thermal de-acclimation: how permanent are leaf phenotypes when cold-acclimated plants experience warming? *Plant Cell Environ* 33: 1124-1137
- Gorsuch PA, Pandey S, Atkin OK (2010b) Temporal heterogeneity of cold acclimation phenotypes in Arabidopsis leaves. *Plant Cell Environ* 33: 244-258
- Gray GR, Chauvin LP, Sarhan F, Hüner NPA (1997) Cold acclimation and freezing tolerance. A complex interaction of light and temperature. *Plant Physiol* 114: 467-474
- Gray GR, Savitch LV, Ivanov A, Hüner NPA (1996) Photosystem II excitation pressure and development of resistance to photoinhibition II. Adjustment of photosynthetic capacity in winter wheat and winter rye. *Plant Physiol* 110: 61-71
- Guy CL (1990) Cold acclimation and freezing tolerance: role of protein metabolism. *Ann Rev Plant Physiol Plant Mol Biol* 41: 187-223
- Guy CL, Huber JLA, Huber SC (1992) Sucrose phosphate synthase and sucrose accumulation at low temperature. *Plant Physiol* 100: 502-508
- Hüner NPA (1985) Morphological, anatomical and molecular consequences of growth and development at low temperature in *Secale cereale* L. cv Puma. *Amer J Bot* 72: 1290-1306
- Hüner NPA, Elfman B, Krol M, MacIntosh A (1984) Growth and development at cold hardening temperatures. Chloroplast ultrastructure, pigment content and composition. *Can J Bot* 62: 53-60
- Hüner NPA, Öquist G, Hurry VM, Krol M, Falk S, Griffith M (1993) Photosynthesis, photoinhibition and low temperature acclimation in cold tolerant plants. *Photosyn Res* 37: 19-39
- Hüner NPA, Öquist G, Sarhan F (1998) Energy balance and acclimation to light and cold. *Trend Plant Sci* 3: 224-230
- Hüner NPA, Palta JP, Li PH, Carter JV (1981) Anatomical changes in leaves of Puma rye in response to growth at cold hardening temperatures. *Bot Gaz* 142: 55-62

- Hurry VM, Hüner NPA (1991) Low growth temperature effects a differential inhibition of photosynthesis in spring and winter wheat. *Plant Physiol* 96: 491-497
- Hurry VM, Hüner NPA (1992) Effects of cold hardening on sensitivity of winter and spring wheat leaves to short-term photoinhibition and recovery of photosynthesis. *Plant Physiol* 100: 1283-1290
- Hurry V, Hüner NPA, Selstam E, Gardestrom P, Öquist G (1996) Photosynthesis at low temperatures. In: Raghavendra AS (ed) *Photosynthesis: a comprehensive treatise*. Cambridge Univ Press, pp 238-249
- Hurry VM, Krol M, Öquist G, Hüner NPA (1992) Effect of long-term photoinhibition on growth and photosynthesis of cold hardened spring and winter wheat. *Planta* 188: 369-375
- Hurry VM, Malmberg G, Gardeström P, Öquist G (1994) Effects of a short-term shift to low temperature and of long-term cold hardening on photosynthesis and ribulose-1,5-bisphosphate carboxylase/oxygenase and sucrose phosphate synthase activity in leaves of winter rye (*Secale cereale* L.). *Plant Physiol* 106: 983-990
- Hurry V, Strand A, Furbank R, Stitt M (2000) The role of inorganic phosphate in the development of freezing tolerance and the acclimatization of photosynthesis to low temperature is revealed by the pho mutants of *Arabidopsis thaliana*. *Plant J* 24: 383-96
- Hurry VM, Strand A, Tabiaeson M, Gardeström P, Öquist G (1995) Cold hardening of spring and winter wheat and rape results in differential effects on growth, carbon metabolism, and carbohydrate content. *Plant Physiol* 109: 697-706
- Jaglo-Ottosen KR, Gilmour SJ, Zarka DG, Schabenberger O, Thomashow MF (1998) *Arabidopsis CBF1* over-expression induces COR genes and enhances freezing tolerance. *Science* 280: 104-106
- Kasuga M, Liu Q, Miura S, Yamaguchi-Shinozaki K, Shinozaki K (1999) Improving plant drought, salt, and freezing tolerance by gene transfer of a single stress-inducible transcription factor. *Nat Biotech* 17: 287-291
- Krause GH (1988) Photoinhibition of photosynthesis. An evaluation of damaging and protective mechanisms. *Physiol Plant* 74: 566-74

- Lapointe L, Hüner NPA (1993) Photoinhibition of intact isolated mesophyll cells from rye. *Plant Cell Environ* 16: 249-58
- Liu Q, Kasuga M, Sakuma Y, Abe H, Miura S, Yamaguchi-Shinozaki K, Shinozaki K (1998) Two transcription factors, DREB1 and DREB2, with an EREBP/AP2 DNA binding domain separate two cellular signal transduction pathways in drought- and low-temperature-responsive gene expression, respectively, in *Arabidopsis*. *Plant Cell* 10: 1391-1406
- McDonald A, Ivanov AG, Bode R, Maxwell D, Rodermel SR, Hüner NPA (2011) Flexibility in photosynthetic electron transport: the physiological role of plastoquinol terminal oxidase (PTOX). *Biochim Biophys Acta (Bioenergetics)*, in press.
- O'Leary MH (1988) Carbon isotopes in photosynthesis: Fractionation techniques may reveal new aspects of carbon dynamics in plants. *Bio Sci* 38: 328-336
- Öquist G, Hüner NPA (2003) Photosynthesis of overwintering evergreen plants. *Ann Rev Plant Biol* 54: 329-355
- Öquist G, Hurry VM, Hüner NPA (1993) Low-temperature effects on photosynthesis and correlation with freezing tolerance in spring and winter cultivars of wheat and rye. *Plant Physiol* 101: 245-250
- Pocock TH, Hurry VM, Savitch LV, Hüner NPA (2001) Susceptibility to low-temperature photoinhibition and the acquisition of freezing tolerance in winter and spring wheat: The role of growth temperature and irradiance. *Physiol Plant* 113: 499-506
- Rapacz M, Wolanin B, Hura K, Tyrka M (2008) The effects of cold acclimation on photosynthetic apparatus and the expression of COR14b in four genotypes of barley (*Hordeum vulgare*) contrasting in their tolerance to freezing and high-light treatment in cold conditions. *Ann Bot* 101: 689–699
- Rosso D, Bode R, Li W, Krol M, Saccon D, Wang S, Schillaci LA, Rodermel SR, Maxwell DP, Hüner NPA (2009) Photosynthetic redox imbalance governs leaf sectoring in the *Arabidopsis thaliana* variegation mutants *immutans*, *spotty*, *var1*, and *var2*. *The Plant Cell* 21: 3473–3492

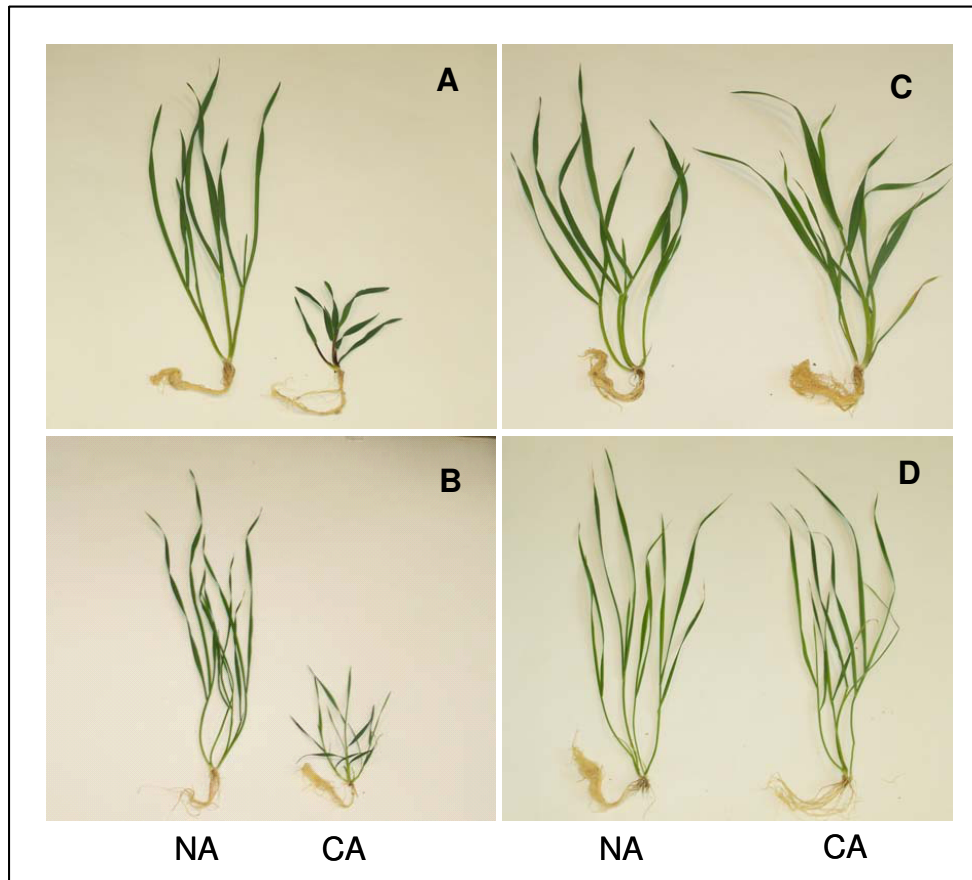
- Sarhan F, Ouellet F, Vazquez-Tello A (1997) The wheat *Wcs120* gene family: a useful model to understand the molecular genetics of freezing tolerance in cereals. *Physiol Plant* 101: 439-445
- Savitch LV, Allard G, Seki M, Robert LS, Tinker NA, Hüner NPA, Shinozaki K, Singh J (2005) The effect of overexpression of two Brassica CBF/DREB1-like transcription factors on photosynthetic capacity and freezing tolerance in *Brassica napus*. *Plant Cell Physiol* 46: 1525-1539
- Savitch LV, Barker-Astrom J, Ivanov A G, Hurry V, Öquist G, Hüner NPA (2001) Cold acclimation of *Arabidopsis thaliana* results in incomplete recovery of photosynthetic capacity which is associated with an increased reduction of the chloroplast stroma. *Planta* 214: 295-301
- Savitch LV, Harney T, Hüner NPA (2000) Sucrose metabolism in spring and winter wheat in response to high irradiance, cold stress and cold acclimation. *Physiol Plant* 108: 270-278
- Savitch LV, Leonardos ED, Krol M, Jansson S, Grodzinski B, Hüner NPA, Öquist G (2002) Two different strategies for light utilization in photosynthesis in relation to growth and cold acclimation. *Plant Cell Environ* 25: 761-771
- Somersalo S, Krause GH (1989) Photoinhibition at chilling temperatures : Fluorescence characteristics of unhardened and cold-hardened spinach leaves. *Planta* 177: 409-416
- Steponkus PL (1984) Role of the plasma membrane in freezing injury and cold acclimation. *Ann Rev Plant Physiol* 35: 543-584
- Stitt M, Hurry VM (2002) A plant for all seasons: alterations in photosynthetic carbon metabolism during cold acclimation in *Arabidopsis*. *Curr Opin Plant Biol* 5: 199-206
- Strand A, Foyer CH, Gustafsson P, Gardestrom P, Hurry V (2003) Altering flux through the sucrose biosynthesis pathway in transgenic *Arabidopsis thaliana* modifies photosynthetic acclimation at low temperatures and the development of freezing tolerance. *Plant Cell Environ* 26: 523-535
- Strand A, Hurry V, Gustafsson P, Gardestrom P (1997) Development of *Arabidopsis thaliana* leaves at low temperature releases the suppression of photosynthesis and photosynthetic expression despite the accumulation of soluble carbohydrates. *Plant J* 12: 605-614

- Strand A, Hurry VM, Henkes S, Hüner NPA, Gustafsson P, Gardeström P, Stitt M (1999) Acclimation of Arabidopsis leaves developing at low temperatures. Increasing cytoplasmic volume accompanies increased activities of enzymes in the Calvin cycle and in the sucrose-biosynthesis pathway. *Plant Physiol* 119: 1387-1398
- Sung S, Amasino RM (2005) Remembering winter: Toward a molecular understanding of vernalization. *Ann Rev Plant Biol* 56: 491-508
- Thomashow MF (2001) So what's new in the field of plant cold acclimation? Lots! *Plant Physiol* 125: 89-93
- Van Buskirk HA, Thomashow MF (2006) Arabidopsis transcription factors regulating cold acclimation. *Physiol Plant* 126: 72-80
- Wilson K E, Ivanov A G, Oquist G, Grodzinski B, Sarhan F, Hüner NPA (2006) Energy balance, organellar redox status and acclimation to environmental stress. *Can J Bot* 84: 1355-1370

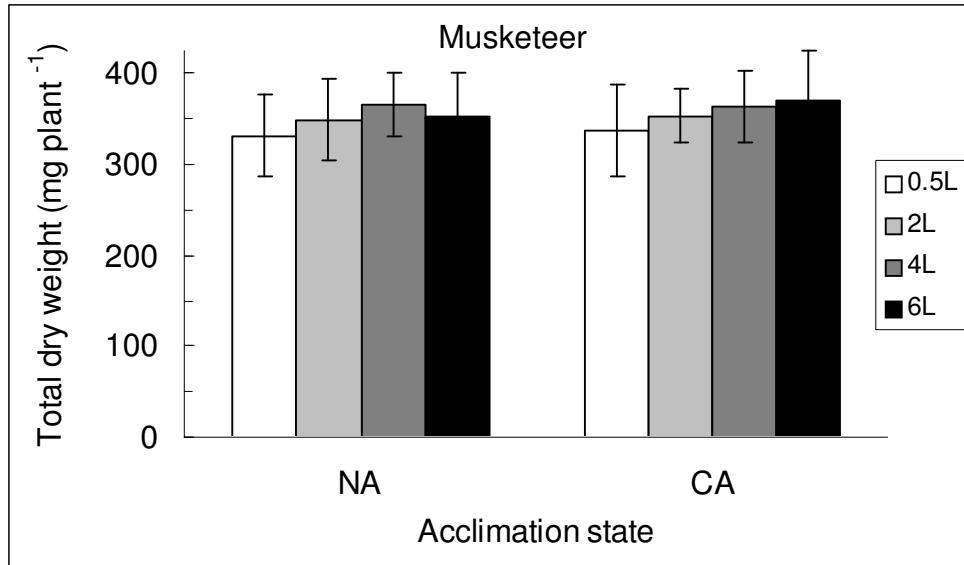
2.6 Appendices

Appendix 2S1. List of the primers used to analyze the transcript levels of major photosynthetic enzymes and components of photosynthetic electron transport in Norstar winter and Katepwa spring wheat cultivars.

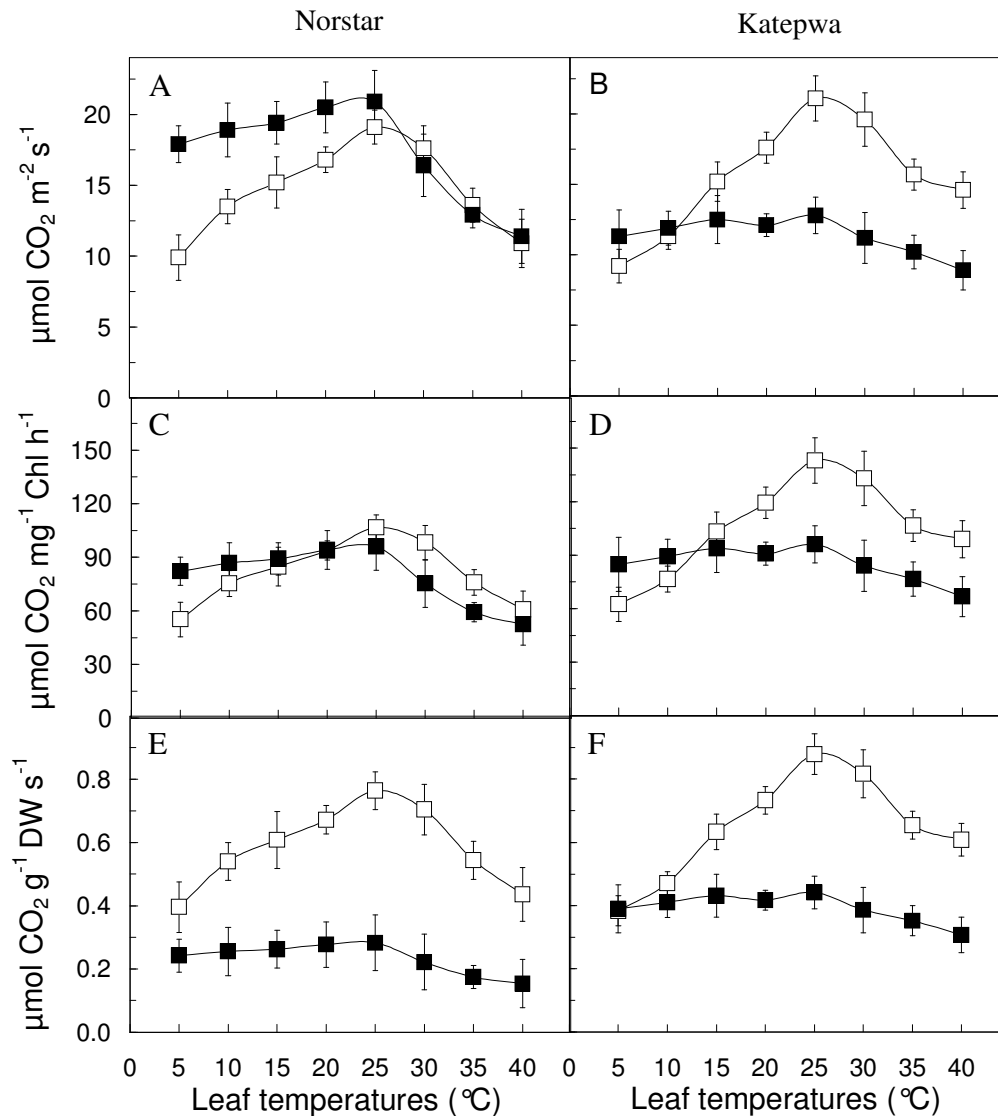
Genes	Sequences
<i>rbcL</i>	5'-CTA CGC GGT GGA CTT GAT TT-3' 3'-ATT TCA CCA GTT TCG GCT TG-5'
<i>cFBPase</i>	5'-AAC AAG AAC GAG GGA GGG ATA C-3' 3'-TCC GCA TCA CAA GAA AAG G-5'
<i>Lhcb1</i>	5'-CGT CCT TCG GAC AAA TAT GC-3' 3'-TAA TGA CAT GGG CCA GCA AG-5'
<i>PsbA</i>	5'-GTG GCT GCT CAC GGT TAT TT-3' 3'-CCA AGC AGC CAA GAA GAA GT-5'
<i>PsaA</i>	5'-GGA AAA TGC AGT CGG ATG TT-3' 3'-AGA AAT CTC GAA GCC AAC CA-5'



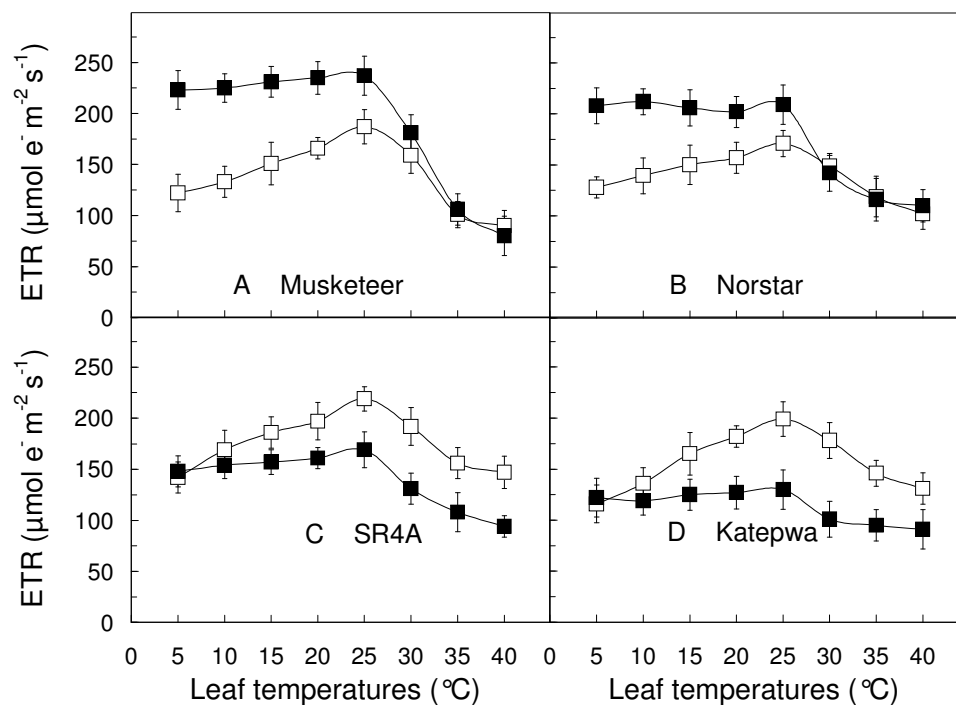
Appendix 2S2. Effects of growth temperatures on plant morphology and growth habit of winter (cv Musketeer rye, A; cv Norstar wheat, B) versus spring cultivars (cv SR4A rye, C; cv Katepwa wheat, D). Plants were grown at 20/16°C (NA) and 5/5°C (CA). Photographs were taken from 25-d-old NA and 75-d-old CA plants. The photographs for NA and CA plants of each cultivar were taken together.



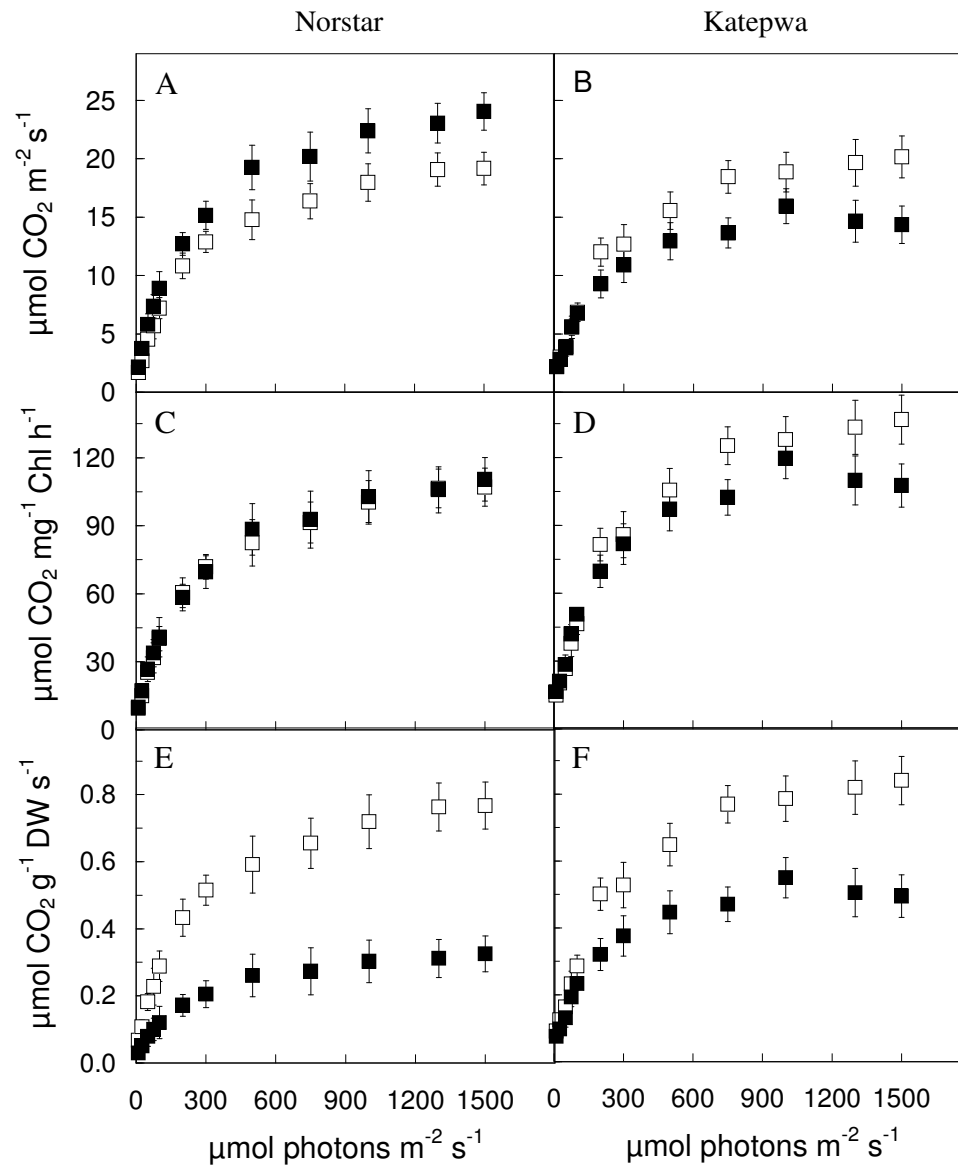
Appendix 2S3. Effect of pot size on plant growth. Musketeer winter rye was grown in 0.5L, 2L, 4L and 6L-sized pots at either 20/16°C (NA) or 5/5°C (CA) and at ambient CO₂. The shoot and root samples were harvested from 25-d-old NA and 75-d-old CA plants. Each point represents the mean of nine plants from three different pots. Bars represent SD.



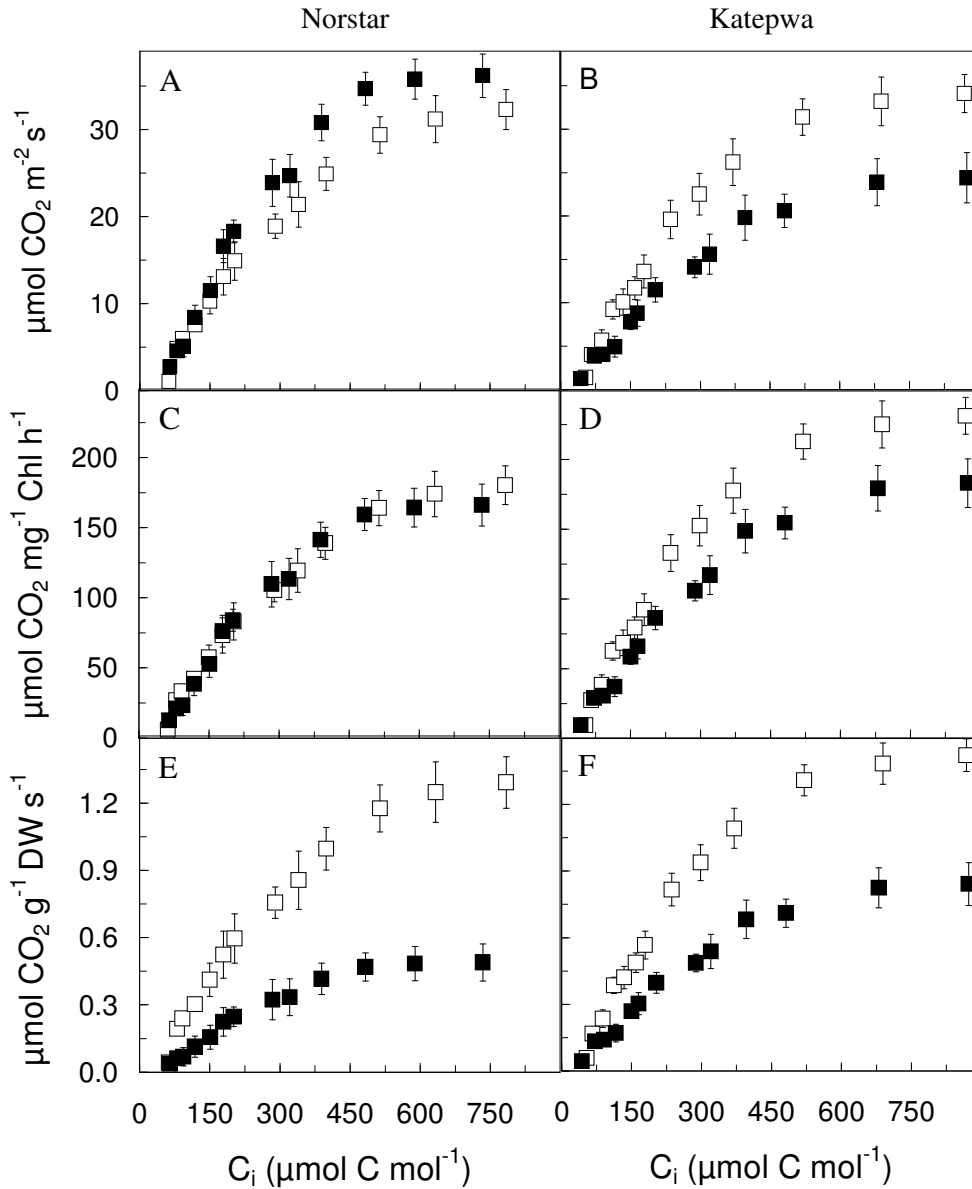
Appendix 2S4. Temperature response curves of light-saturated net CO₂ assimilation expressed on either leaf area (A, B) or leaf chlorophyll (C, D) or leaf dry weight (E, F) basis for Norstar winter (A, C, E) and Katepwa spring wheat (B, D, F) cultivars grown at either 20/16°C (□) or 5/5°C (■) and at ambient CO₂. Photosynthetic rates for both NA and CA plants were measured on attached, fully developed third leaves at varying leaf temperatures ranging from 5° to 40°C and at ambient CO₂. Each point represents the mean of nine plants from three different pots. Bars represent standard deviation.



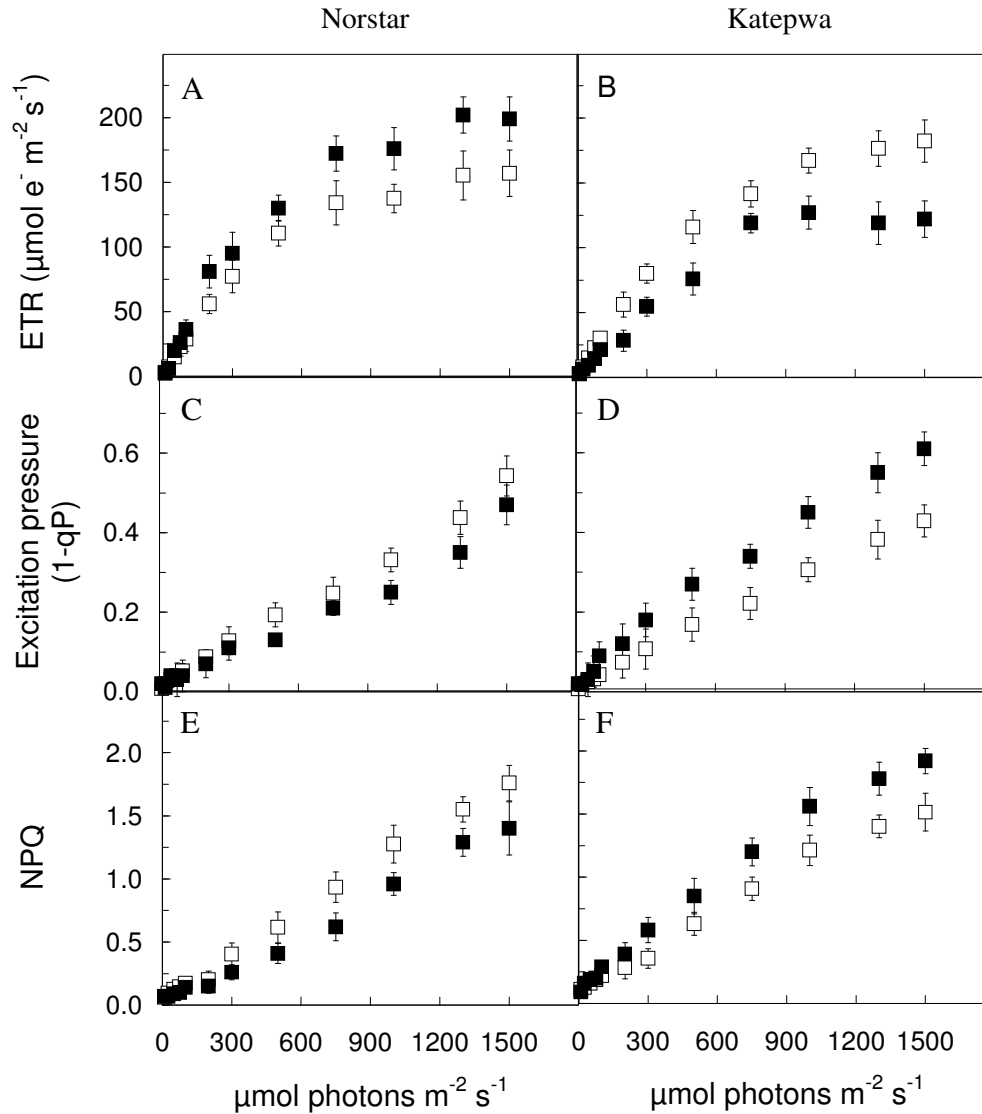
Appendix 2S5. Temperature response curves of light-saturated rates of electron transport (ETR) measured on a leaf area basis for winter (cv Musketeer rye, cv Norstar wheat) and spring (cv SR4A rye, cv Katepwa wheat) rye and wheat cultivars grown at either 20/16°C (□) or 5/5°C (■) and at ambient CO₂. Measurements were carried out on fully developed third leaves at varying leaf temperatures ranging from 5° to 40°C at ambient CO₂. Each point represents the mean of three plants from three different pots. Bars represent SD.



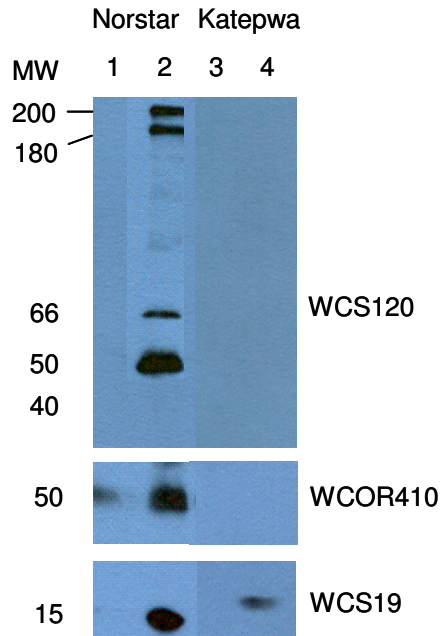
Appendix 2S6. Light response curves of gross CO₂ assimilation expressed on either leaf area (A, B) or leaf chlorophyll (C, D) or leaf dry weight (E, F) basis for Norstar winter (A, C, E) and Katepwa spring wheat (B, D, F) cultivars grown at either 20/16°C (□) or 5/5°C (■) and at ambient CO₂. Photosynthetic rates for both NA and CA plants were measured on attached, fully developed third leaves at 20°C. Each point represents the mean of nine plants from three different pots. Bars represent SD.



Appendix 2S7. Light-saturated rates of net CO₂ assimilation versus internal CO₂ concentrations (C_i) expressed on either leaf area (A, B) or leaf chlorophyll (C, D) or leaf dry weight (E, F) basis for Norstar winter (A, C, E) and Katepwa spring wheat (B, D, F) cultivars grown at either 20/16°C (□) or 5/5°C (■) and at ambient CO₂. Photosynthetic rates for both NA and CA plants were measured on attached, fully developed third leaves at 20°C. Each point represents the mean of nine plants from three different pots. Bars represent SD.



Appendix 2S8. Light response curves of electron transport rates (ETR; A, B), excitation pressures ($1-qP$; C, D) and non- photochemical quenching of excess energy (NPQ; E, F) for Norstar winter (A, C, E) and Katepwa spring wheat (B, D, F) grown at either 20/16°C (\square) or 5/5°C (\blacksquare) and at ambient CO_2 . Measurements were carried out at 20°C for both NA and CA plants. Each point represents the mean of nine plants from three different pots. Bars represent SD.



Appendix 2S9. Immunoblot analyses of WCS120, WCOR410 and WCS19 in winter (cv Norstar) and spring (cv Katepwa) wheat grown at either 20°C (NA) or 5°C (CA). The polypeptides were identified by anti - *WCS120* (1/20000), - *WCOR410* (1/10000), and - *WCS19* (1/5000) antibodies. Molecular weight (MW) is indicated in kDa on the left. Lane 1 = NA Norstar, Lane 2 = CA Norstar, Lane 3 = NA Katepwa, Lane 4 = CA Katepwa.

Chapter 3

Cold acclimation inhibits CO₂-dependent stimulation of photosynthesis in spring wheat and spring rye

3.1 Introduction

Acclimation of the photosynthetic apparatus to low, non-freezing temperatures has been extensively studied in both cold-sensitive and cold-tolerant species (Adams et al. 2002; Ensminger et al. 2006). It is well documented that low growth temperature is often stressful to many cold-sensitive cultivars and species such as spring wheat (Hurry and Hüner 1991), spring rape (Hurry et al. 1995) and tomato (Sassernath and Ort 1990). Spring cereals exhibit decreased photosynthetic capacity estimated as light-saturated rates of carbon assimilation, A_{sat} , in response to growth and development at low temperatures (Hurry and Hüner 1991). Spring cultivars exhibit a limited sink demand and subsequent retardation of carbon export to the sinks during cold acclimation (Hurry et al. 1995). This results in inhibition of sucrose synthesis and concomitant decrease in utilization of phosphorylated intermediates and depletion in stromal P_i which leads to feedback-limited photosynthesis (Hurry et al. 1995, Savitch et al. 2002). Therefore, spring cultivars appear to exhibit decreased plasticity to low growth temperatures and exhibit reduced photosynthetic capacity during cold acclimation (Hurry et al. 1995, Savitch et al. 2002). In addition, spring cultivars exhibit susceptibility to low temperature-induced photoinhibition of photosynthesis during the cold acclimation process (Hüner et al. 1993, Hurry et al. 1995, Pockock et al. 2001) and are unable to attain maximum freezing tolerance in winter (Sarhan et al. 1997).

In contrast, cold-tolerant cultivars and species such as winter wheat, winter rye, winter barley, winter rape, spinach and *Arabidopsis thaliana* exhibit enhanced photosynthetic capacity during the cold acclimation process (Hurry and Hüner 1991, Öquist et al. 1993, Hurry et al. 1994, 1995, Hüner et al. 1998, Savitch et al. 2002, Rapacz et al. 2008). It has been suggested that the increase in photosynthetic capacity upon cold

acclimation of cold-tolerant cultivars and species is, in part, the result of the enhanced activities of key regulatory photosynthetic enzymes such as Rubisco, cFBPase, and SPS (Hurry et al. 1994, 1995, Stitt and Hurry 2002) and concomitant carbon export to the sinks during cold acclimation (Leonardos et al. 2003). These cultivars and species require growth and development at low temperatures and enhanced carbon assimilation in order to attain maximum freezing tolerance (Öquist & Hüner 2003) as well as to develop increased resistance to low temperature-induced photoinhibition (Krause 1988, Somersalo and Krause 1989, Boese and Hüner 1992, Hüner et al. 1993, Öquist et al. 1993, Pocock et al. 2001, Savitch et al. 2001).

It has been well documented that short-term exposure of C₃ plants from ambient to elevated CO₂ results in an immediate increase in the rates of net CO₂ assimilation (Cheng et al. 1998, Long et al. 2004, Ainsworth and Rogers 2007). This stimulation of photosynthesis in C₃ plants due to elevated CO₂ is thought to occur for the following reasons. First, the K_m (CO₂) for Rubisco is close to the current atmospheric CO₂ (Long et al. 2004, Tcherkez et al. 2006) which indicates that Rubisco is CO₂ substrate-limited at ambient CO₂. Thus, an immediate increase in carboxylation velocity is expected by increased CO₂ substrate availability. Second, elevated CO₂ competitively inhibits the light-dependent evolution of CO₂ by photorespiration because CO₂ is a competitive inhibitor of the oxygenation of RuBP by Rubisco (Long et al. 2004).

Much of our present knowledge of photosynthetic acclimation of winter and spring cereals to low temperature has been achieved through comparative studies of plants grown and developed at ambient CO₂. Previous studies have suggested that cold acclimation of winter cereals enhances the light-saturated rates of CO₂ assimilation measured on a leaf area basis primarily due to increased specific leaf weight (Hurry and Hüner 1991, Hurry et al. 1995). In contrast, spring cereals exhibit a decreased A_{sat} in response to low growth temperature. Does a short-term exposure of spring wheat and spring rye to elevated CO₂ compensate for the cold acclimation-induced inhibition of CO₂ assimilation?

To address this question, we compared CO₂ gas exchange rates as well as photosynthetic electron transport coupled with photosynthetic gene expression and polypeptide accumulation in NA and CA spring cultivars of wheat and rye grown at ambient CO₂ (380 μmol C mol⁻¹) and subsequently exposed to short-term (80 h) elevated CO₂ (700 μmol C mol⁻¹). As an additional control, NA and CA winter wheat and winter rye were also exposed to short-term elevated CO₂ for comparison.

3.2 Materials and methods

3.2.1 Plant materials and growth conditions

In all experiments, winter (cv Norstar) and spring (cv Katepwa) wheat (*Triticum aestivum* L.) and winter (cv Musketeer) and spring (cv SR4A) rye (*Secale cereale* L.) cultivars were used. Seeds were obtained from Agriculture and Agri-Food Canada, Indian Head Research Farm, Saskatchewan, Canada. Seeds were germinated and grown in the controlled environmental growth chambers (Model: GCW15 chamber, Environmental Growth Chambers, Chargin Falls, Ohio, USA) at ambient CO₂ of 380 ± 15 μmol C mol⁻¹, a PPFD of 250 ± 30 μmol photons m⁻² s⁻¹, 50 - 60% relative humidity, a 16 h photoperiod and with day/night temperature regimes of 20/16°C for non-acclimated (NA) and 5/5°C for cold acclimated (CA) plants. The seedlings were grown in coarse vermiculite in 500mL-sized plastic pots at a density of three plants per pot and fertilized with Hoagland's solution.

To assess the effects of short-term elevated CO₂ on CO₂ gas exchange rates, the 25-day-old NA and 75-day-old CA plants grown at ambient CO₂ (380 μmol C mol⁻¹) were shifted to elevated CO₂ (700 μmol C mol⁻¹) for up to 80 h in specialized CO₂ chambers (Model: GCW15 chamber, Environmental Growth Chambers, Chargin Falls, Ohio, USA) with all other conditions remaining the same. CO₂ gas exchange rates were measured at different time points during the 80 h shift period at their respective growth temperatures.

To assess the temperature sensitivity of CO₂ gas exchange rates, the NA and CA plants were shifted for up to 80 h to varying day/night temperature regimes of either 5/5,

10/10, 20/20, 25/25, 30/30, 35/35 or 40/40°C at either ambient or elevated CO₂. CO₂ gas exchange rates were measured at different time points during the 80 h shift period at shifted temperatures and CO₂ levels.

Each CO₂ growth chamber was equipped with a computer-controlled CO₂ infrared gas analyzer (Model: WMA-4 CO₂ Analyzer, PP Systems International, Inc. Amesbury, MA 01913 USA) which monitored CO₂ concentrations continuously such that elevated CO₂ concentrations were maintained at $700 \pm 30 \mu\text{mol C mol}^{-1}$. In addition, the temperature, relative humidity, irradiance level and photoperiod in each chamber were computer-controlled and monitored continuously.

3.2.2 Comparative growth kinetics

NA plants were harvested every week and CA plants every two weeks until the full stem elongation stage. The root and shoot fresh biomass were weighed. In order to determine dry weight, the root and shoot tissues were oven-dried at 80°C to constant weight. Exponential growth rates ($\text{g g}^{-1} \text{dry mass day}^{-1}$) were calculated from plots of the natural logarithm (\ln) of shoot dry mass versus time in days. Specific leaf weight (SLW) was calculated as g leaf dry weight m^{-2} leaf blade area. Leaf blade area was measured by using a LI-COR portable area meter (LI-3000A, LI-COR Biosciences, Lincoln, Nebraska, USA).

3.2.3 CO₂ gas exchange measurements

CO₂ gas exchange rates were measured on fully expanded third leaves by using the LI-COR portable infrared CO₂ gas analyzer (LI-6400 XRT Portable Photosynthesis System, LI-COR Biosciences, Lincoln, NE, USA). Light response curves were measured by supplying 12 irradiance values over the range of 0 to 1500 $\mu\text{mol photons m}^{-2} \text{s}^{-1}$ PPFD from high to low light intensity with 8 min of waiting time between each measurement. The apparent maximum quantum efficiency (Q) and the maximal photosynthetic capacity (A_{sat}) were determined as the maximum initial slope (25-200 $\mu\text{mol photons m}^{-2} \text{s}^{-1}$, Q) and the maximum light-saturated rates respectively from the light response curves. CO₂ response curves were measured by supplying 11 different CO₂ values over the range of

50 to 1200 $\mu\text{mol C mol}^{-1}$ at a saturating irradiance of 1000 to 1300 $\mu\text{mol photons m}^{-2} \text{s}^{-1}$. Rubisco-limited carboxylation efficiency (CE) was calculated as the maximum initial slope (50-300 $\mu\text{mol C mol}^{-1}$) of the curves. The maximum Rubisco carboxylation capacity (V_{cmax}) and the maximum rates of electron transport (J_{max}) were calculated using the FCB photosynthesis model (Farquhar et al. 1980). Respiration rates (R_{dark}) were measured in the dark. Measurements were made inside the CO_2 enriched chambers to reduce diffusion errors through the leaf blade and chamber seals as cautioned by Jahnke and Krewitt (Jahnke 2001, Jahnke and Krewitt 2002). In addition, stomatal conductance and leaf transpiration rates were measured simultaneously with CO_2 gas exchange measurements. Leaf water use efficiency was calculated as the ratio of A_{sat} and stomatal conductance (A_{sat}/gs). All measurements for NA and CA plants were carried out on fully expanded third leaves at their respective growth temperatures.

3.2.4 Determination of total leaf protein and immunodetection

The fully expanded third leaves were harvested, immediately frozen in liquid nitrogen and stored at -80°C . The total leaf protein of the leaf tissues was extracted and quantified by using the RC-DC protein assay kit (Bio-Rad) according to the manufacturer's specifications.

The extracted proteins were electrophoretically separated using NuPAGE Novex 10% (w/v) Bis-Tris precast, polyacrylamide gels (Invitrogen) with MES SDS running buffer (Invitrogen) in an XCell4 SureLock Midi Cell (Invitrogen) according to manufacturer's specifications. Samples for SDS-PAGE were loaded on an equal protein basis (8 μg protein per lane). The addition of 1 μg of bovine serum albumin (Invitrogen) in the extraction buffer was used as an internal standard. Gels were electrophoresed and the separated polypeptides were electroblotted onto nitrocellulose membranes (0.2 μM pore size, Bio - Rad). The blots were blocked with 5% (w/v) fat free, dried milk powder overnight at 4°C and then probed with primary antibodies raised against the target proteins; rbcL, cFBPase, Lhcb1, psbA and psaA at a dilution of 1:2000-5000. The blots were probed with secondary antibody (anti-rabbit IgG Peroxidase antibody, Sigma-Aldrich) at 1:10000-20000 dilutions (depending on the target proteins) and visualized

with enhanced chemiluminescence immunodetection (ECL Detection Kit; GE Healthcare, UK) on X-ray film (Fujifilm, Fuji Corporation, Tokyo). Immunoblots were quantified by using a computer software program (Scion Image, Scion Corporation, Frederick, Maryland 21701, USA).

3.2.5 Analyses of gene expression

Quantitative reverse transcriptase polymerase chain reaction (qRT-PCR) was carried out to achieve a wider view of the role of transcript to polypeptide changes that occurred during cold acclimation and short-term exposure to 40°C and/or elevated CO₂. The transcript levels for *rbcL*, *cFBPase*, *Lhcb1*, *psbA* and *psaA* were quantified by qRT-PCR. Total RNA was extracted from wheat leaves (200mg fresh weight) with Trizol reagent (Invitrogen). For qRT-PCR, 10 µg of total RNA was digested with DNASE I (Invitrogen) and half of the digested RNA was used for cDNA synthesis with random hexamers and Superscript Reverse Transcriptase (Invitrogen). The cDNAs obtained were diluted ten-fold in deionized water and 2 µl were used as template for real-time PCR. The polymerase chain reaction was performed with SYBR-Green PCR Mastermix (Invitrogen) and amplification was monitored on an ABI PRISM 7000 (Applied Biosystem). The 18S ribosomal gene was used as an internal standard for normalization of expression levels. The PCR amplification efficiency was 1.4 for all the genes tested. The primers used for the different genes are listed in Appendix 3S1.

3.2.6 Statistical analysis

In all experiments, 20 replicate pots with three plants per pot for each cultivar in either NA or CA state were grown in a completely randomized design. Out of the 20 replicate pots, three pots for each cultivar at each growth condition were randomly selected for all photosynthetic measurements and biochemical analyses. Thus, all data are the averages of measurements made on nine different plants from three replicate pots. Results were subjected to analysis of variance (ANOVA). Means were compared at the 5% level of significance ($P \leq 0.05$) by using the statistical package SPSS version 17.

3.3 Results

3.3.1 Effects of cold acclimation on growth characteristics at ambient CO₂

Cold acclimation reduced growth rates by about 70% relative to the NA counterparts regardless of species or cultivars (Table 3.1). The third leaves of all NA cultivars were fully expanded between 20-25 days and those of CA cultivars between 70-80 days. Consequently, all subsequent comparisons were made on fully expanded third leaves of 25-day-old NA and 75-day-old CA wheat and rye cultivars.

CA winter cultivars exhibited a 1.9 to 2.3-fold increase in the specific leaf weight (SLW, g dry weight m⁻² leaf area) relative to those values observed for NA counterparts whereas the SLW changed minimally in CA versus NA spring cultivars (Table 3.1). These results are consistent with published data on the differential effects of cold acclimation on SLW for winter and spring cereals (Hüner et al. 1981, 1985, Gray et al. 1996, Leonardos et al. 2003). Pot size had minimal effects on cold acclimation-induced changes on plant morphology and total plant dry matter accumulation in all cultivars tested (Appendix 3S2).

3.3.2 Effects of cold acclimation and measuring temperatures on light-saturated rates of photosynthesis, A_{sat}, and stomatal conductance at ambient CO₂

We observed comparable gross A_{sat} of 18 - 22 μmol CO₂ m⁻² s⁻¹ for all NA winter and spring cultivars grown and measured at ambient CO₂ at 20°C (Fig. 3.1A, white bars, 20). A decrease in the measuring temperature from 20° to 5°C inhibited these rates by about 35 - 50% in all NA cultivars (Fig. 3.1A, white bars, 5). However, the CA winter cultivars, Musketeer rye and Norstar wheat, were able to maintain gross CO₂ assimilation rates at 5°C (Fig. 3.1A, black bars, 5) that were comparable to or slightly higher than those rates observed for NA controls measured at 20°C (Fig. 3.1A, white bars, 20). The measuring temperature had minimal effects on gross A_{sat} of CA Musketeer and Norstar (Fig. 3.1A, black bars, 20 versus 5). In addition, gross A_{sat} measured at 5°C was 70-130% higher in CA Musketeer and Norstar (Fig. 3.1A, black bars, 5) as compared to those rates observed for their NA controls measured at the same temperature (Fig. 3.1A, white bars, 5). Thus, cold acclimation of Musketeer winter rye and Norstar winter wheat enhanced the light-saturated rates of gross CO₂ assimilation irrespective of the measuring temperature.

Table 3.1. Effects of cold acclimation on exponential growth rates (EGR) and specific leaf weight (SLW) for winter and spring cereals. Samples were collected from fully expanded third leaves grown at ambient CO₂ (380 μmol C mol⁻¹) at either 20/16°C (NA) or 5/5°C (CA). Significant differences of the means between the acclimation state within each cultivar are indicated by the symbol * (*P* ≤ 0.05). ± SD. DW = Dry weight.

Cultivars	Acclimation state	EGR (g g DW ⁻¹ day ⁻¹)	CA/NA	SLW (g DW m ⁻²)	CA/NA
Musketeer	NA	0.223 ± 0.041		34 ± 3	
	CA	0.072 ± 0.010*	0.323	79 ± 6*	2.32
Norstar	NA	0.215 ± 0.024		28 ± 4	
	CA	0.06 ± 0.008*	0.279	53 ± 6*	1.89
SR4A	NA	0.229 ± 0.029		35 ± 4	
	CA	0.075 ± 0.02*	0.328	42 ± 5	1.2
Katepwa	NA	0.212 ± 0.036		39 ± 2	
	CA	0.065 ± 0.014*	0.307	36 ± 5	0.92

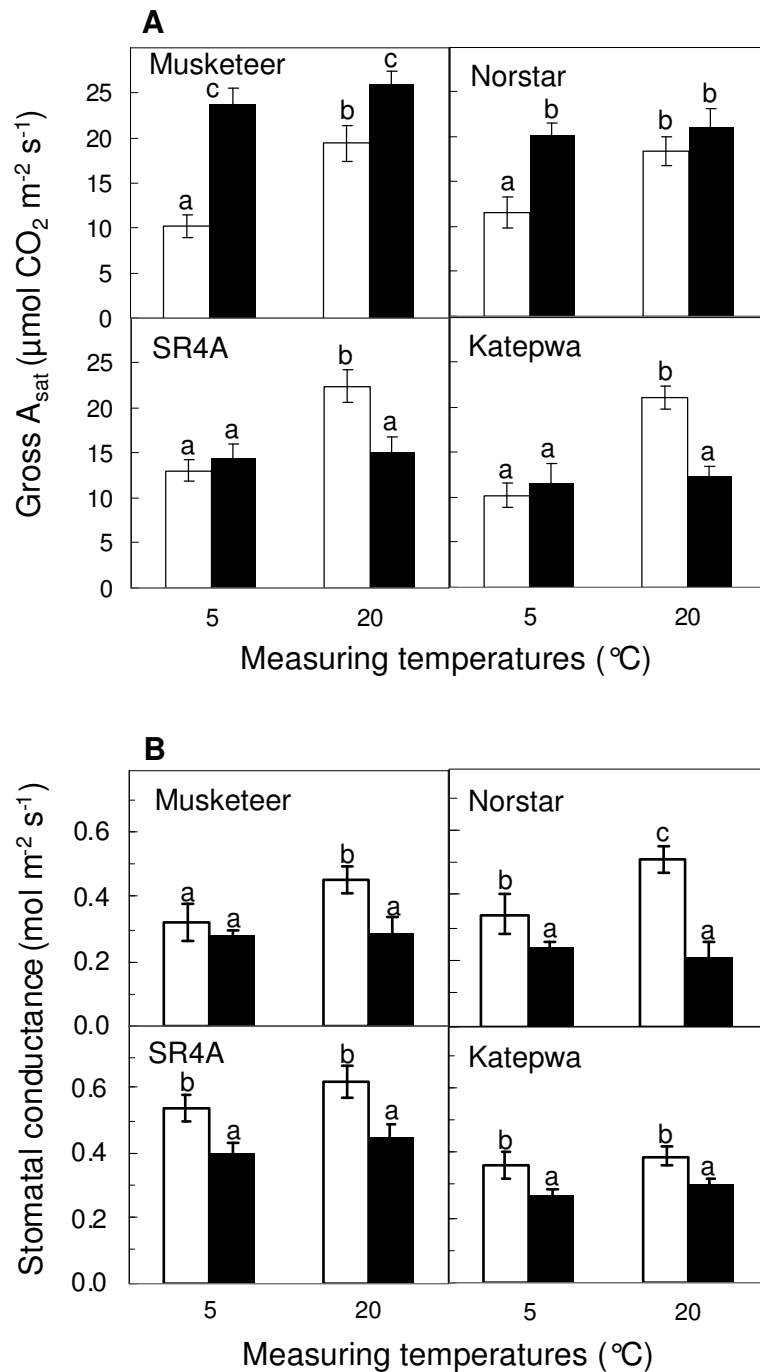


Fig. 3.1. Effects of measuring temperatures on (A) gross A_{sat} and (B) stomatal conductance of NA (\square) and CA (\blacksquare) winter and spring cereals. Bars represent SD.

In contrast to the CA winter cultivars, the CA spring cultivars, SR4A rye and Katepwa wheat, exhibited a 30 - 45% decrease in the light-saturated rates of gross CO₂ assimilation regardless of measuring temperature (Fig. 3.1A, black bars, 5, 20) relative to the NA controls measured at 20°C (Fig. 3.1, white bars, 20). The assimilation rates observed for CA spring cultivars, SR4A and Katepwa were comparable to those rates observed for NA controls but measured at 5°C (Fig. 3.1A, white versus black bars, 5). Hence, the CA-induced decrease in the light-saturated rates of gross CO₂ assimilation appeared to be specific for the spring cultivars tested. However, irrespective of species or cultivar, growth at low temperature appeared to decrease the temperature sensitivity of CO₂ assimilation. A change of measuring temperature affected A_{sat} by only 5-10% in all CA cultivars whereas it affected all NA cultivars by 35-60% (Fig. 3.1A).

Cold acclimation suppressed the stomatal conductance by 30 - 60% when measured at 20°C (Fig. 3.1B, 20, black bars versus white bars) and by 15-25% when measured at 5°C in all four cultivars (Fig. 3.1B, 5, black bars versus white bars). Thus, decrease in stomatal conductance is not due to the fact that CA plants are at lower temperature than NA plants because stomatal conductance was measured at 5°C and at 20°C for both CA and NA plants (Fig. 3.1B). The decrease in stomatal conductance was evident regardless of the leaf measuring temperature. Furthermore, stomatal conductance of the CA winter cultivars appeared to be less temperature sensitive than their NA counterparts whereas CA and NA spring cultivars appeared to be equally sensitive to measuring temperatures (Fig. 3.1B).

3.3.3 Effects of short-term elevated CO₂ on light response curves and light-saturated CO₂ response curves

Fig. 3.2 illustrates the effects of short-term elevated CO₂ on light response curves for Musketeer winter (Fig. 3.2a, b) and SR4A spring rye (Fig. 3.2c, d). Exposure to elevated CO₂ significantly increased the apparent maximum quantum efficiency by about 25-45% compared to that of at ambient CO₂ in NA Musketeer (Fig. 3.2a, closed versus open circles, Table 3.2, Q) and NA SR4A rye (Fig. 3.2c, closed versus open circles, Table 3.2, Q). Whereas elevated CO₂ had minimal effects on Q values for CA Musketeer (Fig. 3.2b,

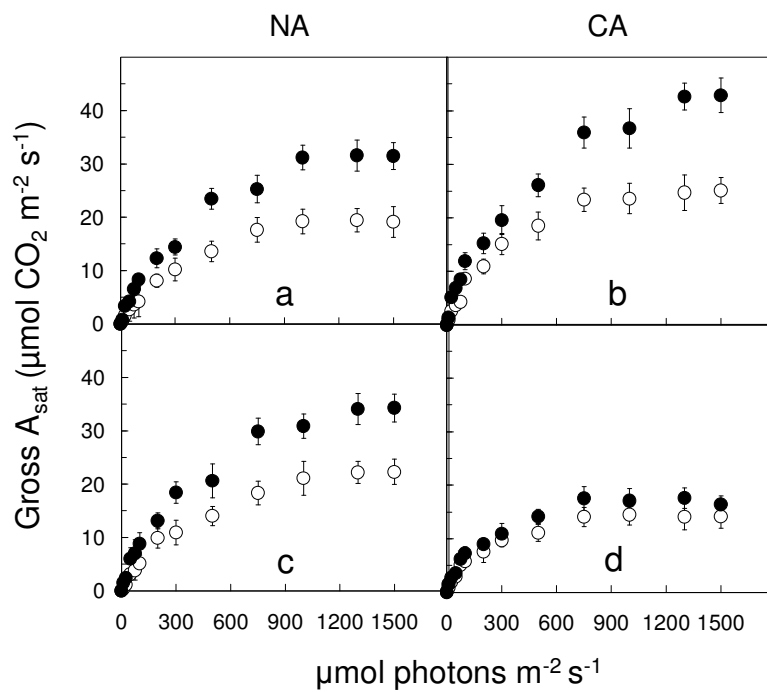


Fig. 3.2. Light response curves of gross CO_2 assimilation at either ambient (○) or after 80 h of exposure to elevated (●) CO_2 for NA (a, c) and CA (b, d) Musketeer (a, b) and SR4A (c, d) rye. Bars represent SD.

Table 3.2. Effects of short-term elevated CO₂ on the maximum Rubisco carboxylation capacity (V_{cmax} , $\mu\text{mol CO}_2 \text{ m}^{-2} \text{ s}^{-1}$), maximum rates of electron transport (J_{max} , $\mu\text{mol e}^- \text{ m}^{-2} \text{ s}^{-1}$), the apparent maximum quantum efficiency (Q , $\text{CO}_2/\text{photon}$) and the carboxylation efficiency (CE, $\text{CO}_2 \text{ m}^{-2} \text{ s}^{-1} / \text{mol}^{-1} \text{ CO}_2$), for winter and spring cereals grown at ambient CO₂ (380 $\mu\text{mol C mol}^{-1}$) and at either 20/16°C (NA) or 5/5°C (CA). Measurements were carried out on fully expanded third leaves at 20°C. Significant differences among the means within each cultivar are indicated by the superscripted letters ($P \leq 0.05$). \pm SD.

Cultivars	Acclimation state	CO ₂	V_{cmax}	J_{max}	Q	CE
Musketeer	NA	380	71 \pm 4 ^a	157 \pm 10 ^a	0.037 \pm 0.002 ^a	0.072 \pm 0.006 ^a
		700	75 \pm 2 ^a	169 \pm 8 ^a	0.053 \pm 0.003 ^b	0.083 \pm 0.009 ^{ab}
	CA	380	98 \pm 7 ^b	220 \pm 15 ^b	0.051 \pm 0.002 ^b	0.098 \pm 0.008 ^b
		700	93 \pm 5 ^b	214 \pm 19 ^b	0.056 \pm 0.004 ^b	0.087 \pm 0.006 ^b
Norstar	NA	380	67 \pm 4 ^a	146 \pm 10 ^a	0.053 \pm 0.003 ^a	0.069 \pm 0.004 ^a
		700	62 \pm 3 ^a	142 \pm 13 ^a	0.068 \pm 0.004 ^b	0.073 \pm 0.007 ^{ab}
	CA	380	79 \pm 3 ^b	173 \pm 9 ^b	0.057 \pm 0.002 ^a	0.084 \pm 0.004 ^b
		700	76 \pm 6 ^b	164 \pm 16 ^{ab}	0.059 \pm 0.005 ^{ab}	0.077 \pm 0.005 ^{ab}
SR4A	NA	380	84 \pm 6 ^b	187 \pm 14 ^b	0.049 \pm 0.003 ^b	0.081 \pm 0.005 ^b
		700	70 \pm 5 ^b	168 \pm 11 ^b	0.061 \pm 0.004 ^c	0.078 \pm 0.004 ^b
	CA	380	48 \pm 3 ^a	121 \pm 17 ^a	0.032 \pm 0.004 ^a	0.062 \pm 0.004 ^a
		700	53 \pm 5 ^a	124 \pm 8 ^a	0.036 \pm 0.001 ^a	0.061 \pm 0.008 ^a
Katepwa	NA	380	65 \pm 8 ^b	161 \pm 12 ^a	0.045 \pm 0.002 ^b	0.087 \pm 0.008 ^b
		700	60 \pm 4 ^b	151 \pm 10 ^a	0.058 \pm 0.004 ^c	0.075 \pm 0.010 ^b
	CA	380	37 \pm 2 ^a	99 \pm 7 ^a	0.034 \pm 0.002 ^a	0.049 \pm 0.004 ^a
		700	31 \pm 3 ^a	89 \pm 9 ^a	0.034 \pm 0.003 ^a	0.053 \pm 0.006 ^a

closed versus open circles, Table 3.2, Q) as well as for CA SR4A (Fig. 3.2d, closed versus open circles, Table 3.2, Q). Exposure to elevated CO₂ enhanced the light-saturated rates of gross photosynthesis (gross A_{sat}) by 55 - 65% in NA Musketeer and SR4A rye (Fig. 3.2a, c, closed versus open circles). In contrast, the gross A_{sat} increased by 70% in CA Musketeer but increased minimally in CA SR4A rye following exposure to elevated CO₂ (Fig. 3.2b, d, closed versus open circles). Comparable results were obtained for light response curves of Norstar winter and Katepwa spring wheat (Appendix 3S3).

Exposure to elevated CO₂ had minimal effects on the CO₂ limited-carboxylation efficiency as well as the light-saturated and CO₂-saturated carboxylation capacity relative to those values observed at ambient CO₂ for all cultivars irrespective of acclimation state (Fig. 3.3, Appendix 3S4, Table 3.2, CE). Similarly, there were no CO₂ effects on the maximum Rubisco carboxylation capacity (V_{cmax}) as well as maximum rates of electron transport (J_{max}) for all cultivars regardless of acclimation state (Table 3.2).

3.3.4 Kinetics for the CO₂ stimulation of the light-saturated rates of gross photosynthesis

All NA cultivars exhibited average gross A_{sat} of 18 - 22 μmol CO₂ m⁻² s⁻¹ when grown and measured at ambient CO₂ and 20°C (Fig. 3.4a,c, Appendix 3S5a, c, open circles). A shift from ambient (Fig. 3.4a, open circles) to elevated CO₂ (Fig. 3.4a, closed circles) at 20°C stimulated average gross CO₂ assimilation by 63% in NA Musketeer winter rye. This CO₂-stimulation of A_{sat} was observed within 30 min of shift from ambient to elevated CO₂ and was fairly stable throughout the entire 80 h shift experiment. Comparable CO₂-stimulation of gross A_{sat} (54%) was observed for NA SR4A spring rye (Fig. 3.4c, open versus closed circles) as well as for NA Norstar winter wheat (49%, Appendix 3S5a, open versus closed circles) and NA Katepwa spring wheat (58%, Appendix 3S5c, open versus closed circles). Thus, NA winter and spring cultivars exhibited a comparable stimulation of A_{sat} upon a short-term exposure from ambient to elevated CO₂.

CA Musketeer winter rye exhibited an average 70% stimulation of light-saturated rates of gross CO₂ assimilation following exposure to elevated CO₂ at 5°C (Fig. 3.4b,

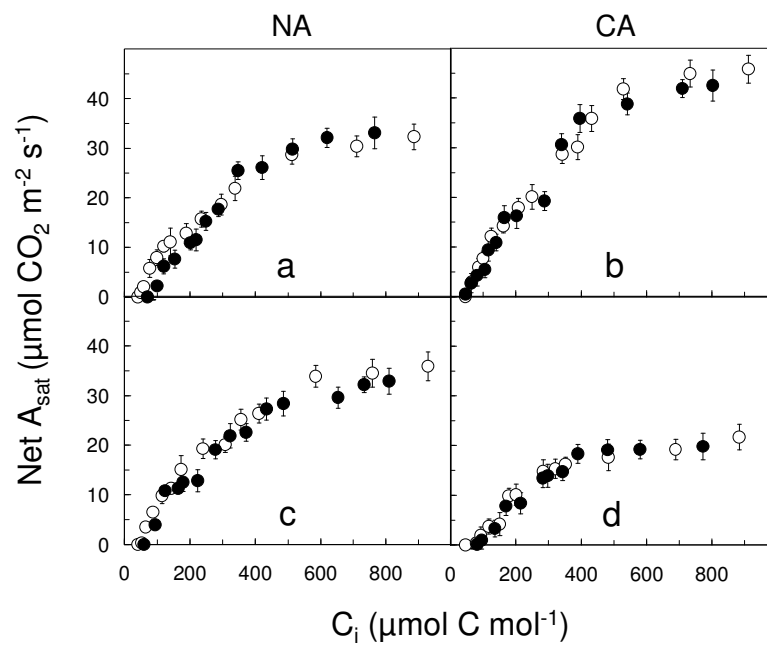


Fig. 3.3. CO₂ response curves of light-saturated net CO₂ assimilation at either ambient (○) or after 80 h of exposure to elevated (●) CO₂ for NA (a, c) and CA (b, d) Musketeer (a, b) and SR4A (c, d) rye. Bars represent SD.

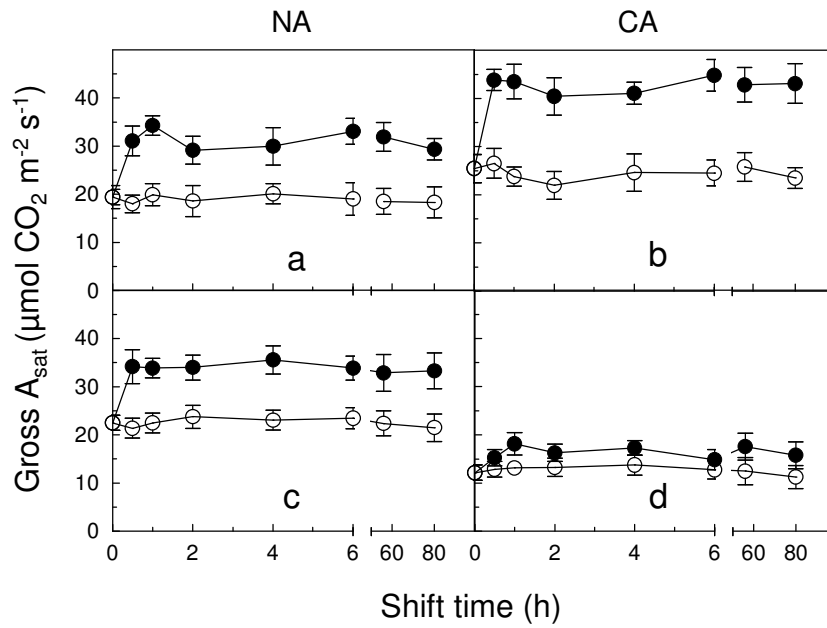


Fig. 3.4. Light-saturated rates of gross CO_2 assimilation at either ambient (\circ) or over 80 h of exposure to elevated (\bullet) CO_2 for NA (a, c) and CA (b, d) Musketeer (a, b) and SR4A (c, d) rye. Bars represent SD.

closed circles) relative to those rates observed at ambient CO₂ at 5°C (Fig. 3.4b, open circles). Even when measured at its growth temperature of 5°C, the average CO₂-stimulated rate of gross CO₂ assimilation was 37% higher for CA Musketeer (Fig. 3.4b, closed circles, 42.8 ± 3.2 μmol CO₂ m⁻² s⁻¹) as compared to the stimulation observed for NA Musketeer but measured at 20°C (Fig 4a, closed circles, 31.3 ± 2.4 μmol CO₂ m⁻² s⁻¹). Similar trends were observed for Norstar winter wheat (Appendix 3S5a versus S5b). Thus, cold acclimation further enhanced the CO₂- stimulation of gross A_{sat} in winter cultivars, Musketeer and Norstar.

In contrast to CA Musketeer winter rye, CA spring rye (SR4A) exhibited minimal stimulation of gross CO₂ assimilation following shift to elevated CO₂ at 5°C (Fig. 3.4d, closed circles) relative to those rates observed at ambient CO₂ at 5°C (Fig. 3.4d, open circles). Hence, since cold acclimation considerably inhibited A_{sat} relative to that of NA spring rye, this minimal stimulation of A_{sat} of CA spring rye at elevated CO₂ (Fig. 3.4d, closed circles) was not sufficient to compensate for the cold acclimation-induced inhibition at ambient CO₂ (Fig. 3.4c versus 4d, open circles). The average CO₂-stimulated rate of gross CO₂ assimilation measured at 5°C was 49% less for CA spring rye (Fig. 3.4d, closed circles, 17.5 ± 3.2 μmol CO₂ m⁻² s⁻¹) as compared to the stimulation observed for NA spring rye measured at 20°C (Fig. 3.4c, closed circles, 34.3 ± 2.4 μmol CO₂ m⁻² s⁻¹). In addition, the stimulation observed for CA spring rye was 59% less than that of CA winter rye measured at 5°C (Fig 4b versus 4d, closed circles). We observed similar trends for CA Katepwa spring wheat (Appendix 3S5c versus S5d) relative to CA Norstar winter wheat. For instance, cold acclimation inhibited CO₂-dependent stimulation of photosynthesis by 58% in Katepwa spring wheat (Appendix 3S5c versus S5d, closed circles) whereas cold acclimation further enhanced the CO₂-dependent stimulation of photosynthesis by 12% in Norstar winter wheat (Appendix 3S5a versus S5b, closed circles). Thus, cold acclimation inhibited the CO₂- stimulation of gross A_{sat} in spring cultivars, SR4A and Katepwa.

3.3.5 Effects of short-term elevated CO₂ on stomatal conductance

Exposure to elevated CO₂ suppressed leaf stomatal conductance by about 40% in all NA cultivars and, as a consequence, leaf transpiration rates decreased by 25 - 40% (Table 3.3). In contrast, except for CA Katepwa spring wheat, elevated CO₂ induced minimal changes in stomatal conductance as well as leaf transpiration rates in all other CA cultivars (Table 3.3). Therefore, the enhanced photosynthetic capacity of all cultivars associated with short-term exposure to elevated CO₂ can not be due to increased stomatal conductance. Leaf water use efficiency (WUE) of all NA cultivars increased by 160 - 180% following exposure to elevated CO₂ whereas leaf WUE of all CA cultivars increased by about 50 - 75% upon exposure to elevated CO₂ (Table 3.3). However, WUE was about 50% lower in CA spring cultivars than in CA winter cultivars irrespective of CO₂ concentrations.

3.3.6 Temperature sensitivity of CO₂-stimulated A_{sat}

Since we observed maximum CO₂ stimulation within an hour of shift from ambient to elevated CO₂, we measured the temperature sensitivity of the 1 h temperature shift on the CO₂-dependent stimulation of light-saturated photosynthetic rates for Musketeer winter and SR4A spring rye (Fig. 3.5). Results in Fig. 3.5 illustrate the temperature response curves for CO₂ assimilation in Musketeer (Fig. 3.5a, b) and SR4A rye (Fig. 3.5c, d) following a 1 h shift to the various temperatures indicated at either ambient (open circles) or elevated CO₂ (closed circles). In the NA state, the temperature sensitivity for net A_{sat} were similar for both cultivars with a maximum A_{sat} at 25°C at either ambient or elevated CO₂ (Fig. 3.5a, c). However, A_{sat} in Musketeer and SR4A appeared to be less sensitive to temperatures between 5° - 25°C in the CA than in the NA state irrespective of CO₂ concentration (Fig. 3.5b, d). As a consequence, the extent of the elevated CO₂-induced stimulation of A_{sat} after 1 h at the respective temperatures was constant between 5° - 25°C in CA Musketeer and CA SR4A whereas the elevated CO₂-induced stimulation of A_{sat} was at a minimum at 5°C and increased to a maximum at 25°C in NA counterparts. At temperatures above 25°C, A_{sat} decreased substantially in NA Musketeer and SR4A at ambient CO₂ (Fig. 3.5a, c, open circles) but changed minimally at elevated CO₂ (Fig. 3.5a, c, closed circles). Similar results were observed for CA Musketeer (Fig. 3.5b). In contrast, A_{sat} in CA SR4A decreased to a comparable extent at either ambient or elevated

Table 3.3. Effects of short-term shift to elevated CO₂ on stomatal conductance, transpiration rates and water use efficiency (WUE) for winter and spring cereals grown at ambient CO₂ (380 μmol C mol⁻¹) and at either 20/16°C (NA) or 5/5°C (CA). Measurements were carried out on fully expanded third leaves at their respective growth CO₂ and at 20°C. Significant differences among the means within each cultivar are indicated by the superscripted letters ($P \leq 0.05$). ± SD.

Cultivars	Acclimation state	CO ₂ (μmol C mol ⁻¹)	Stomatal Conductance g _s (mol m ⁻² s ⁻¹)	Transpiration (mmol H ₂ O m ⁻² s ⁻¹)	WUE (A/gs)
Musketeer	NA	380	0.45 ± 0.04 ^b	2.65 ± 0.30 ^b	38 ± 6 ^a
		700	0.26 ± 0.03 ^a	2.02 ± 0.26 ^a	108 ± 14 ^{bc}
	CA	380	0.28 ± 0.02 ^a	1.79 ± 0.12 ^a	84 ± 9 ^b
		700	0.31 ± 0.03 ^a	1.82 ± 0.35 ^a	136 ± 10 ^c
Norstar	NA	380	0.51 ± 0.04 ^b	3.42 ± 0.24 ^b	30 ± 4 ^a
		700	0.30 ± 0.03 ^a	2.32 ± 0.36 ^a	80 ± 15 ^{bc}
	CA	380	0.24 ± 0.02 ^a	1.76 ± 0.41 ^a	72 ± 7 ^b
		700	0.28 ± 0.02 ^a	1.94 ± 0.21 ^a	107 ± 12 ^c
SR4A	NA	380	0.62 ± 0.05 ^b	3.09 ± 0.22 ^b	32 ± 8 ^a
		700	0.37 ± 0.03 ^a	2.25 ± 0.37 ^a	85 ± 13 ^c
	CA	380	0.40 ± 0.03 ^a	2.39 ± 0.29 ^a	37 ± 4 ^a
		700	0.36 ± 0.02 ^a	2.15 ± 0.12 ^a	56 ± 8 ^b
Katepwa	NA	380	0.39 ± 0.03 ^c	3.24 ± 0.49 ^c	46 ± 6 ^a
		700	0.23 ± 0.02 ^{ab}	2.01 ± 0.32 ^a	128 ± 18 ^c
	CA	380	0.27 ± 0.02 ^b	2.56 ± 0.17 ^b	43 ± 3 ^a
		700	0.18 ± 0.04 ^a	2.17 ± 0.27 ^a	74 ± 10 ^b

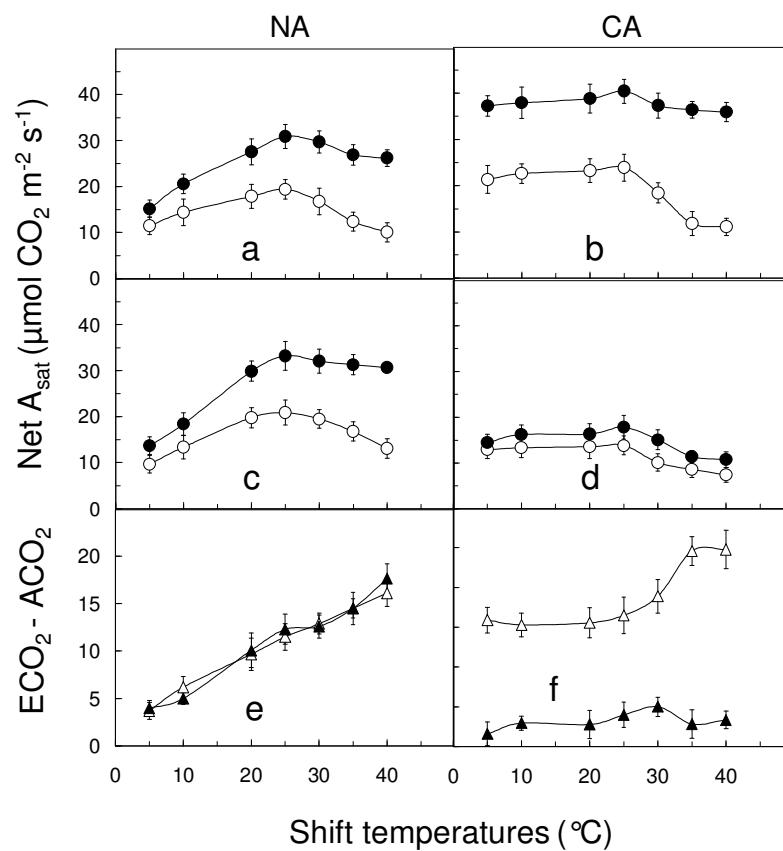


Fig. 3.5. Temperature sensitivity of net A_{sat} at either ambient (○) or after 1 h shift to elevated (●) CO_2 for NA (a, c,) and CA (b, d) Musketeer (a, b) and SR4A (c, d) rye. Difference in net A_{sat} at elevated versus ambient CO_2 ($\text{ECO}_2 - \text{ACO}_2$) for NA (e) and CA (f) Musketeer (Δ) and SR4A (▲). Bars represent SD.

CO₂ at temperatures above 25°C (Fig. 3.5d). Similar trends for the sensitivity of a 1h temperature shift on the CO₂-dependent stimulation of light-saturated photosynthetic rates were observed for winter and spring wheat (Appendix 3S6).

In order to assess the sensitivity of a prolonged shift to high temperature on the CO₂-dependent stimulation of light-saturated photosynthetic rates, we measured the CO₂ assimilation rates for Musketeer winter and SR4A spring rye after 80 h of shift to various temperatures at either ambient or elevated CO₂ (Fig. 3.6). Consistent with the 1 h temperature shift, similar results were observed for an 80 h temperature shift except that, at temperatures above 25°C, A_{sat} decreased substantially not only at ambient CO₂ (Fig. 3.6a, b, c, d, open circles) but also at elevated CO₂ (Fig. 3.6a, b, c, d, closed circles) in both winter and spring rye regardless of acclimation state. Comparable trends were observed for winter and spring wheat (Appendix 3S7a, b, c, d).

To illustrate the relative effects of elevated CO₂ on temperature-dependent inhibition of net A_{sat}, we calculated the difference in net A_{sat} between elevated CO₂ (ECO₂) versus ambient CO₂ (ACO₂) after 1 h of shift to various temperatures (Fig. 3.5e, f). In the NA state, the temperature profile of ECO₂ - ACO₂ for Musketeer (Fig. 3.5e, open triangles) was indistinguishable from that of SR4A (Fig. 3.5e, closed triangles) and increased linearly with increased temperatures between 5° - 40°C. In contrast, ECO₂ - ACO₂ for CA spring rye remained constant but low at all temperatures between 5° - 40°C (Fig. 3.5f, closed triangles), whereas ECO₂ - ACO₂ for CA Musketeer (Fig. 3.5f, open triangles) was at least 3-fold higher between 5° and 25°C and increased between 25° and 40°C relative to that of SR4A.

Similar trends were observed for a 80 h temperature shift except that, at temperatures above 25°C, ECO₂ - ACO₂ decreased substantially in both cultivars regardless of acclimation state and CO₂ concentrations (Fig. 3.6e, f). Comparable results were observed for winter and spring wheat (Appendix 3S6e, f, Appendix 3S7e, f). Thus, the CO₂-dependent stimulation of CO₂ assimilation appeared to be less sensitive to increased temperatures in all CA cultivars relative to their NA counterparts.

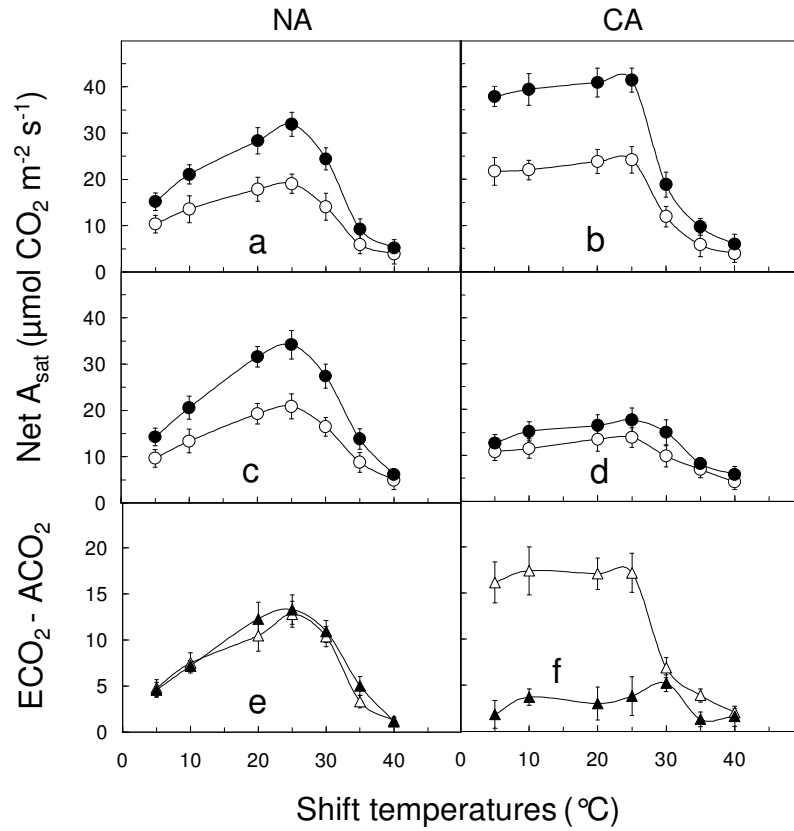


Fig. 3.6. Temperature sensitivity of net A_{sat} at either ambient (○) or after 80 h shift to elevated (●) CO_2 for NA (a, c,) and CA (b, d) Musketeer (a, b) and SR4A (c, d) rye. Difference in net A_{sat} at elevated versus ambient CO_2 ($\text{ECO}_2 - \text{ACO}_2$) for NA (e) and CA (f) Musketeer (Δ) and SR4A (\blacktriangle). Bars represent SD.

3.3.7 Effects of short-term elevated CO₂ on dark respiratory rates

Unlike photosynthesis, 80 h exposure to elevated CO₂ at their respective growth temperature minimally (5-20%) decreased dark respiratory rates in all NA and CA cultivars (Appendix 3S8). However, an 80 h exposure to 40°C at either ambient (380 μmol C mol⁻¹) or elevated (700 μmol C mol⁻¹) CO₂ substantially suppressed respiratory rates (40-70%) in all cultivars irrespective of acclimation state (Appendix 3S8).

3.3.8 Effects of short-term elevated CO₂ and high temperature on leaf protein content, photosynthetic gene expression and polypeptide content

We observed a comparable leaf protein content of 2.3 - 3.3 g m⁻² leaf area for all NA cultivars at ambient CO₂ (Table 3.4). CA winter wheat and winter rye exhibited a 4.2 to 4.7-fold increase in leaf protein content compared to NA controls (Table 3.4). In contrast, CA spring wheat and spring rye exhibited minimal changes in leaf protein content relative to their NA counterparts (Table 3.4). Exposure to elevated CO₂ for 80 h, at their respective growth temperature, induced minimal changes on leaf protein content in all four cultivars regardless of acclimation state (Table 3.4). However, shifting plants to 40°C for 80 h at either ambient or elevated CO₂ decreased the leaf protein content by 40 - 60% in all NA and CA cultivars (Table 3.4).

Quantitative reverse transcriptase polymerase chain reaction (qRT-PCR) indicated that 80 h exposure to 40°C at ambient CO₂ considerably reduced the transcript levels of most of the key chloroplast (*rbcL*, *psbA*, *psaA*) and nuclear encoded (*cFBPase*, *Lhcb1*) photosynthetic genes examined in both Norstar and Katepwa wheat (Fig. 3.7). However, *Lhcb1* expression in Katepwa was the least sensitive to high temperature (Fig.3.7). This general reduction of transcript levels occurred independently of acclimation state. Similar results were obtained for plants exposed to 40°C at elevated CO₂ (Fig.3.7).

Cold acclimation induced minimal changes (10 - 15%) in the protein levels of *rbcL*, *cFBPase*, *Lhcb1*, *PsbA* and *PsaA* in either winter or spring cultivars at ambient CO₂ (Fig. 3.8). This can be explained by the fact that the loading for SDS-PAGE and immunoblotting was based on leaf protein. Our leaf protein results (Table 3.4) have

Table 3.4. Effects of short-term shift to elevated CO₂ and /or high temperature on leaf protein content for winter and spring cereals grown at ambient CO₂ (380 μmol C mol⁻¹) and at either 20/16°C (NA) or 5/5°C (CA). Samples were collected from 25-day-old NA and 75-day-old CA plants; at ambient CO₂ and respective growth temperatures, and after 80 h at (i) elevated CO₂ (700 μmol C mol⁻¹) at constant temperature (ii) ambient CO₂ at 40°C and (iii) elevated CO₂ at 40°C. Significant differences among the means within each cultivar are indicated by the superscripted letters ($P \leq 0.05$). ± SD.

Total Leaf protein Content (g m ⁻² leaf area)					
Cultivars	Acclimation state	Ambient CO ₂	80 h shift to		
			Elevated CO ₂	Ambient CO ₂ + 40°C	Elevated CO ₂ + 40°C
Musketeer	NA	2.70 ± 0.46 ^b	2.40 ± 0.31 ^b	1.12 ± 0.14 ^a	1.08 ± 0.19 ^a
	CA	12.65 ± 2.20 ^d	11.97 ± 1.70 ^d	7.41 ± 1.16 ^c	7.95 ± 1.30 ^c
Norstar	NA	2.32 ± 0.31 ^b	2.14 ± 0.39 ^b	1.10 ± 0.16 ^a	0.98 ± 0.10 ^a
	CA	9.84 ± 1.60 ^d	9.30 ± 1.20 ^d	5.89 ± 0.66 ^c	5.15 ± 0.89 ^c
SR 4A	NA	3.33 ± 0.54 ^{bc}	3.05 ± 0.29 ^b	1.91 ± 0.30 ^a	1.78 ± 0.22 ^a
	CA	4.01 ± 0.37 ^c	3.77 ± 0.26 ^c	2.30 ± 0.34 ^a	2.17 ± 0.38 ^a
Katepwa	NA	2.89 ± 0.45 ^{bc}	2.53 ± 0.22 ^b	1.49 ± 0.26 ^a	1.80 ± 0.31 ^a
	CA	3.27 ± 0.27 ^c	2.74 ± 0.40 ^{bc}	1.60 ± 0.33 ^a	1.78 ± 0.21 ^a

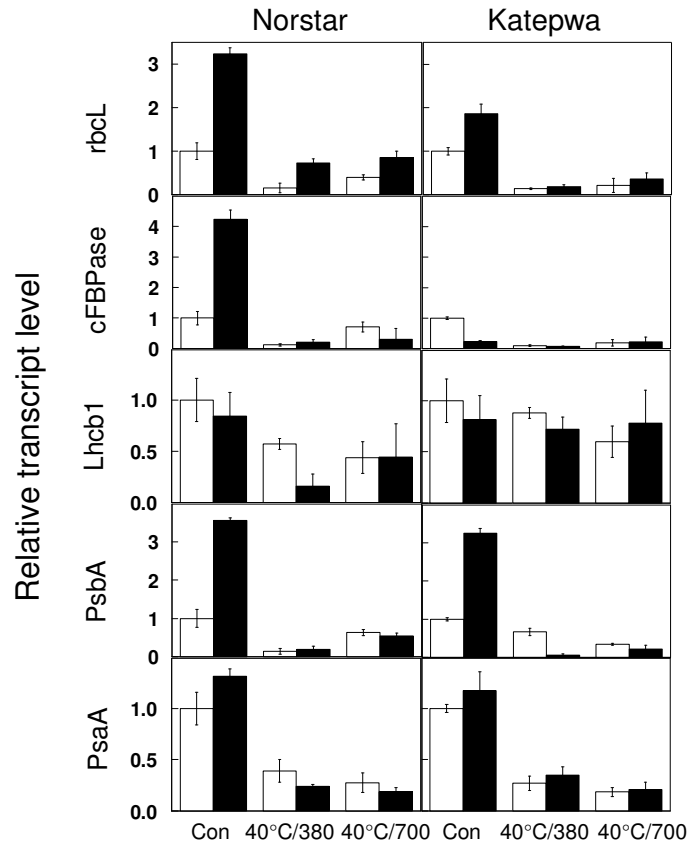


Fig. 3.7. Effects of high temperature (40°C) and elevated CO₂ (700 μmol C mol⁻¹) on transcript levels of photosynthetic genes isolated from NA (□) and CA (■) Norstar and Katepwa wheat. Bars represent SD. Con = controls (growth temperature and CO₂).

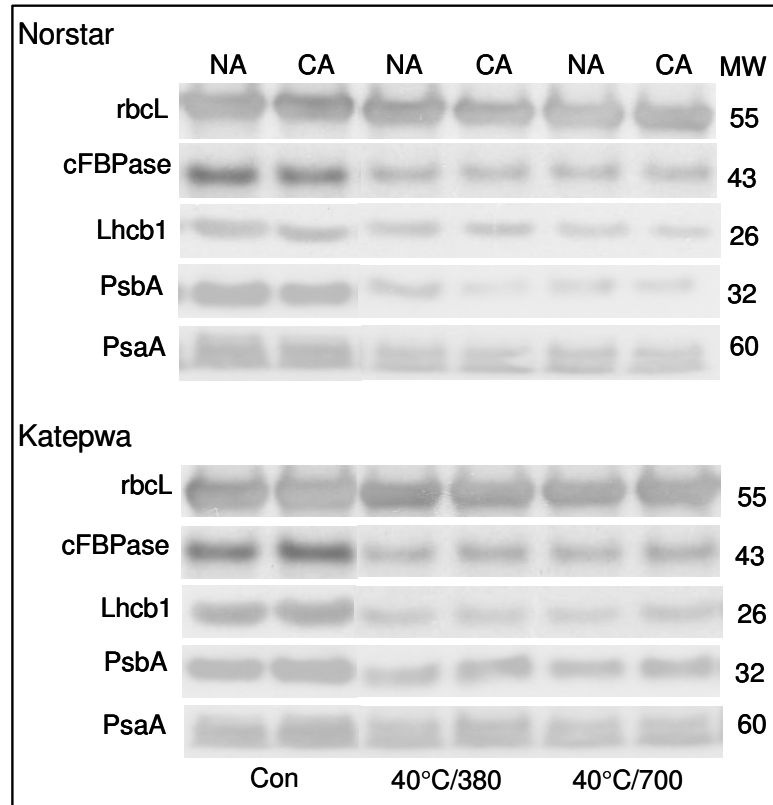


Fig. 3.8. Effects of high temperature (40°C) and elevated CO₂ (700 μmol C mol⁻¹) on photosynthetic proteins isolated from NA and CA Norstar and Katepwa wheat. Numbers on the right indicate molecular masses (kDa) of markers. Con = controls (growth temperature and CO₂).

indicated that CA winter cultivars exhibited a 4.5-fold increase in leaf protein content per unit leaf area relative to NA controls. Hence, the increased leaf protein content is likely in part to reflect the enhanced levels of rbcL, cFBPase, Lhcb1, PsbA and PsaA on a leaf area basis for CA winter cultivars, Norstar and Musketeer. However, the proportion of the photosynthetic polypeptides tested relative to total leaf protein does not change upon cold acclimation. In contrast, CA spring cultivars, Katepwa wheat and SR4A rye exhibited minimal changes in leaf protein content (Table 3.4) and would likely reflect minimal changes in the levels of all five proteins tested on a leaf area basis.

Exposure to 40°C at ambient CO₂ for 80 h substantially reduced the abundance of photosynthetic enzymes, cFBPase and thylakoid proteins, Lhcb1, psbA, psaA by 20 - 40% regardless of acclimation state and cultivars (Fig. 3.8). However, rbcL content appeared to be least sensitive to high temperature (Fig. 3.8). Comparable results were observed for plants exposed to 40°C at elevated CO₂ (Fig. 3.8).

3.4 Discussion

Since spring cereals exhibit a decreased A_{sat} in response to low growth temperature at ambient CO₂, we asked the question whether a short-term exposure of spring wheat and spring rye from ambient to elevated CO₂ could compensate for the cold acclimation-induced inhibition of CO₂ assimilation. Our results have clearly indicated that a short-term exposure of Katepwa spring wheat and SR4A spring rye to elevated CO₂ can not compensate for the cold acclimation-induced inhibition of CO₂ assimilation. The cold acclimation-induced decrease in A_{sat} of spring cultivars, SR4A and Katepwa, at ambient CO₂ resulted in a 45% (SR4A) and a 60% (Katepwa) inhibition of CO₂-dependent stimulation of photosynthesis during the short-term shift to elevated CO₂ relative to NA controls. Therefore, even though spring wheat and rye grow at low temperature, cold acclimation not only inhibits photosynthetic rates at ambient CO₂ but also inhibits the stimulation of photosynthetic rates by short-term exposure to elevated CO₂. In addition, the CA spring wheat and spring rye are not able to recover from the low temperature-induced inhibition of A_{sat} through a short-term exposure to elevated CO₂. Cold acclimation-induced decrease in CO₂ assimilation of CA spring cultivars are consistent

with the decrease in the maximum rates of photosynthetic electron transport, maximal quantum efficiency and maximal Rubisco carboxylation efficiency as well as carboxylation capacity in response to growth at low temperature (Table 3.2). The decreased A_{sat} in CA spring cultivars appears to be associated with a downregulation of carbon metabolism during cold acclimation (Hurry et al. 1995). Previous studies have suggested that spring wheat and spring rape exhibit a limited sink demand and concomitant retardation of carbon export to the sinks during cold acclimation (Hurry et al. 1995). As a consequence, the photosynthetic end-product, sucrose, accumulates in source leaves. This results in inhibition of sucrose synthesis and concomitant decrease in utilization of phosphorylated intermediates and depletion in stromal P_i which leads to feedback-limited photosynthesis (Hurry et al. 1995, Savitch et al. 2002). In addition, the feedback inhibition of photosynthesis is also attributed to down-regulation of the expression and activities of key regulatory photosynthetic enzymes such as Rubisco, cFBPase, and SPS (Hurry et al. 1995, Strand et al. 1999). Therefore, spring cultivars appear to exhibit decreased plasticity to low growth temperatures and exhibit reduced photosynthetic capacity during cold acclimation (Hurry et al. 1995, Savitch et al. 2002). Consequently, spring cultivars, SR4A rye and Katepwa wheat were unable to compensate for the cold acclimation-induced inhibition of CO_2 assimilation following a short-term exposure to elevated CO_2 .

In contrast to spring cultivars, the low temperature-induced increase in A_{sat} for winter cultivars, Musketeer and Norstar, at ambient CO_2 , translated into 12% (Norstar) and 37% (Musketeer) increase in the capacity for carbon assimilation upon short-term exposure to elevated CO_2 relative to NA counterparts at elevated CO_2 . This enhancement of photosynthetic capacity in CA versus NA winter cultivars can be explained by the fact that cold acclimation of the winter wheat and rye cultivars, results in major changes in leaf morphology and leaf anatomy (Hüner et al. 1981, Hüner 1985, Gray et al. 1996, chapter 2), which are associated with significant increases in SLW and the amount of photosynthetic apparatus per unit leaf area (Leonardos et al. 2003, chapter 2). In addition, cold acclimation-induced increase in CO_2 assimilation of CA winter cultivars are consistent with the increase in the maximum rates of photosynthetic electron transport,

maximal quantum efficiency and maximal Rubisco carboxylation efficiency as well as carboxylation capacity in response to growth at low temperature (Table 3.2).

CA spring cultivars appear to be incapable of adjusting the short-term temperature sensitivity of photosynthesis under elevated CO₂ compared to winter cultivars. However, these differences are not reflected in a differential temperature stability of the photosynthetic gene expression either at the transcript level or at the level of photosynthetic polypeptide content associated with Rubisco, PSI and PSII. Thus, this differential temperature sensitivity between spring and winter cultivars is most likely due to differences in the relative temperature sensitivities of other components of both photorespiration and photosynthetic CO₂ assimilation.

It has been suggested that high temperature favors photorespiration compared to photosynthesis, due to differential aqueous solubilities of CO₂ and O₂ and kinetic properties of Rubisco (Long et al. 2004, Salvucci and Crafts-Brandner 2004, Ainsworth and Rogers 2007). Thus, we suggest that the difference in the temperature profiles under ambient versus short-term elevated CO₂ are due to the differential effects of temperature on photosynthesis versus photorespiration. Under elevated CO₂, photorespiration is reduced and does not compete with photosynthesis whereas, under ambient CO₂, photorespiration competes with CO₂ assimilation.

We conclude that the inhibition of photosynthetic capacity after 80 h of exposure to 40°C at either ambient or elevated CO₂ (Fig. 3.6, Appendix 3S7) is attributed to a general denaturation and degradation of leaf protein (Table 3.4) and concomitant decrease in the activities of major photosynthetic enzymes and components of photosynthetic electron transport such as *rbcL*, *cFBPase*, *Lhcb1*, *psbA* and *psaA* (Fig. 3.8). Furthermore, the inhibition of photosynthetic carbon assimilation is also closely correlated with a high temperature-induced decrease in the activation state of Rubisco as well as irreversible PSII damage (Salvucci and Crafts-Brandner 2004, Kumar et al. 2009).

The K_m (CO₂) for Rubisco in air is 420 $\mu\text{mol mol}^{-1}$ (Tcherkez et al. 2006) which is close to the current ambient CO₂ of about 380 $\mu\text{mol C mol}^{-1}$ (Long et al. 2004). Thus,

we suggest that the increased carbon assimilation upon the shift of plants from ambient to elevated CO₂ (700 μmol C mol⁻¹) resulted from increased Rubisco carboxylation activity as a consequence of increased CO₂ substrate availability. Our results clearly showed a marked suppression of stomatal conductance following exposure of NA plants to elevated CO₂ for all four cultivars. Therefore, we confirm that the increased photosynthetic capacity of all cultivars upon exposure to elevated CO₂ can not be accounted for by increased stomatal conductance but must reflect changes at the biochemical level. Since the maximum stimulation occurred in less than 30 min upon shift from ambient to elevated CO₂, we conclude that the short-term shift of plants to elevated CO₂ overcomes Rubisco CO₂ substrate limitations present under ambient CO₂. Cold acclimation of spring wheat and rye appeared to exacerbate this limitation.

In summary, cold acclimation of spring wheat and spring rye not only inhibits CO₂ assimilation under ambient CO₂ but also inhibits the capacity for the stimulation of light-saturated rates of photosynthesis during a short-term exposure to elevated CO₂ relative to winter wheat and winter rye. The cold acclimation-induced inhibition of CO₂ assimilation for spring wheat and spring rye at ambient CO₂ can not be compensated by a short-term exposure to elevated CO₂.

Acknowledgements

This work was supported, in part, by the Natural Sciences and Engineering Research Council (NSERC) and industrial and government partners, through the Green Crop Research Network (GCN). NPAH, FS and BG also acknowledge research support through their individual NSERC Discovery Grants.

3.5 References

- Adams III WW, Demmig-Adams B, Rosenstiel TN, Brightwell AK, Ebbert V (2002) Photosynthesis and photoprotection in overwintering plants. *Plant Biol* 4: 545-557
- Ainsworth EA, Rogers A (2007) The response of photosynthesis and stomatal conductance to rising CO₂: mechanisms and environmental interactions. *Plant Cell Environ* 30: 258-270

- Boese SR, and Hüner NPA (1992) Developmental history affects the susceptibility of spinach leaves to in vivo low temperature photoinhibition. *Plant Physiol* 99: 1141-1145
- Cheng SH, Moore BD, Seemann JR (1998) Effects of short and long-term elevated CO₂ on the expression of Ribulose-1,5-bisphosphate carboxylase/oxygenase genes and carbohydrate accumulation in leaves of *Arabidopsis thaliana* (L.) Heynh. *Plant Physiol* 116: 715-723
- Dahal K, Kane K, Gadapati W, Webb E, Savitch LV, Singh J, Sharma P, Sarhan F, Longstaffe FJ, Grodzinski B, Hüner NPA (2012) The effects of phenotypic plasticity on photosynthetic performance in winter rye, winter wheat and *Brassica napus*. *Physiol Plant* 144: 169-188
- Ensminger I, Busch F, Hüner NPA (2006) Photostasis and cold acclimation: sensing low temperature through photosynthesis. *Physiol Plant* 126: 28-44
- Farquhar GD, von Caemmerer S, Berry JA (1980) A biochemical model of photosynthetic CO₂ assimilation in leaves of C₃ species. *Planta* 149: 78-90
- Gray GR, Savitch LV, Ivanov A, Hüner NPA (1996) Photosystem II excitation pressure and development of resistance to photoinhibition II. Adjustment of photosynthetic capacity in winter wheat and winter rye. *Plant Physiol* 110: 61-71
- Hüner NPA (1985) Morphological, anatomical and molecular consequences of growth and development at low temperature in *Secale cereale* L. cv Puma. *Am J Bot* 72: 1290-1306
- Hüner NPA, Palta JP, Li PH, Carter JV (1981) Anatomical changes in leaves of Puma rye in response to growth at cold hardening temperatures. *Bot. Gaz.* 142: 55-62
- Hüner NPA, Öquist G, Hurry VM, Krol M, Falk S, Griffith M (1993) Photosynthesis, photoinhibition and low temperature acclimation in cold tolerant plants. *Photosyn Res* 37: 19-39
- Hüner NPA, Öquist G, Sarhan F (1998) Energy balance and acclimation to light and cold. *Trends Plant Sci* 3: 224-230
- Hurry VM, Hüner NPA (1991) Low growth temperature effects a differential inhibition of photosynthesis in spring and winter wheat. *Plant Physiol* 96: 491-497

- Hurry VM, Malmberg G, Gardeström P, Öquist G (1994) Effects of a short-term shift to low temperature and of long-term cold hardening on photosynthesis and ribulose-1,5-bisphosphate carboxylase/oxygenase and sucrose phosphate synthase activity in leaves of winter rye (*Secale cereale* L.). *Plant Physiol* 106: 983-990
- Hurry VM, Strand A, Tabiaeson M, Gardeström P, Öquist G (1995) Cold hardening of spring and winter wheat and rape results in differential effects on growth, carbon metabolism, and carbohydrate content. *Plant Physiol* 109: 697-706
- Jahnke S (2001) Atmospheric CO₂ concentration does not directly affect leaf respiration in bean or poplar. *Plant Cell Environ* 24: 1139-1151
- Jahnke S, Krewitt M (2002) Atmospheric CO₂ concentration may directly affect leaf respiration measurement in tobacco, but not respiration itself. *Plant Cell Environ* 25: 641-651
- Krause GH (1988) Photoinhibition of photosynthesis. An evaluation of damaging and protective mechanisms. *Physiol Plant* 74: 566-74
- Kumar A, Li C, Portis AR (2009) Arabidopsis thaliana expressing a thermostable chimeric Rubisco activase exhibits enhanced growth and higher rates of photosynthesis at moderately high temperatures. *Photosyn Res* 100: 143-153
- Leonardos ED, Savitch LV, Hüner NPA, Öquist G, Grodzinski B (2003) Daily photosynthetic and C-export patterns in winter wheat leaves during cold stress and acclimation. *Physiol Plant* 117: 521-531
- Long SP, Ainsworth EA, Rogers A, Ort DR (2004) Rising atmospheric carbon dioxide: plants FACE the future. *Ann Rev Plant Biol* 55: 591-628
- Öquist, G., and Hüner, N.P.A. 2003. Photosynthesis of overwintering evergreen plants. *Ann. Rev. Plant Biol.* 54: 329-355.
- Öquist G, Hurry VM, Hüner NPA (1993) Low-temperature effects on photosynthesis and correlation with freezing tolerance in spring and winter cultivars of wheat and rye. *Plant Physiol* 101: 245-250
- Pocock TH, Hurry VM, Savitch LV, Hüner NPA (2001) Susceptibility to low-temperature photoinhibition and the acquisition of freezing tolerance in winter and spring wheat: The role of growth temperature and irradiance. *Physiol Plant* 113: 499-506

- Rapacz M, Wolanin B, Hura K, Tyrka M (2008) The effects of cold acclimation on photosynthetic apparatus and the expression of COR14b in four genotypes of barley (*Hordeum vulgare*) contrasting in their tolerance to freezing and high-light treatment in cold conditions. *Ann Bot* 101: 689–699
- Salvucci ME, Crafts-Brandner SJ (2004) Inhibition of photosynthesis by heat stress: the activation state of Rubisco as a limiting factor in photosynthesis. *Physiol Plant* 120: 179-186
- Sarhan F, Ouellet F, Vazquez-Tello A (1997) The wheat *Wcs120* gene family: a useful model to understand the molecular genetics of freezing tolerance in cereals. *Physiol Plant* 101: 439–445
- Sassenrath GF, Ort DR (1990) The relationship between inhibition of photosynthesis at low temperature and the inhibition of photosynthesis after rewarming in chill-sensitive tomato. *Plant Physiol Biochem* 28: 457-465
- Savitch LV, Barker-Astrom J, Ivanov AG, Hurry V, Oquist G, Hüner NPA (2001) Cold acclimation of *Arabidopsis thaliana* results in incomplete recovery of photosynthetic capacity which is associated with an increased reduction of the chloroplast stroma. *Planta* 214: 295-301
- Savitch LV, Leonardos ED, Krol M, Jansson S, Grodzinski B, Hüner NPA, Öquist G (2002) Two different strategies for light utilization in photosynthesis in relation to growth and cold acclimation. *Plant Cell Environ* 25: 761-771
- Somersalo S, Krause GH (1989) Photoinhibition at chilling temperatures: Fluorescence characteristics of unhardened and cold-hardened spinach leaves. *Planta* 177: 409-416
- Stitt M, Hurry VM (2002) A plant for all seasons: alterations in photosynthetic carbon metabolism during cold acclimation in *Arabidopsis*. *Curr Opin Plant Biol* 5: 199-206
- Strand A, Hurry VM, Henkes S, Hüner NPA, Gustafsson P, Gardeström P, Stitt M (1999) Acclimation of *Arabidopsis* leaves developing at low temperatures. Increasing cytoplasmic volume accompanies increased activities of enzymes in the Calvin cycle and in the sucrose-biosynthesis pathway. *Plant Physiol* 119: 1387-1398
- Tcherkez GGB, Farquhar GD, Andrews TJ (2006) Despite slow catalysis and confused substrate specificity, all ribulose biphosphate carboxylases may be nearly perfectly optimized. *Proc Nat Acad Sci* 103: 7246-7251

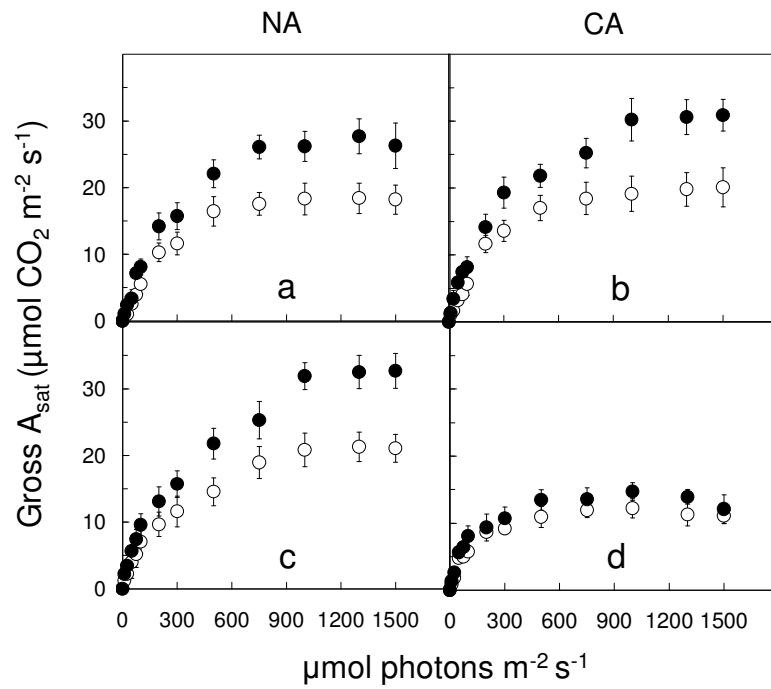
3.6 Appendices

Appendix 3S1. List of primers used to analyze the transcript levels of photosynthetic genes isolated from Norstar and Katepwa wheat.

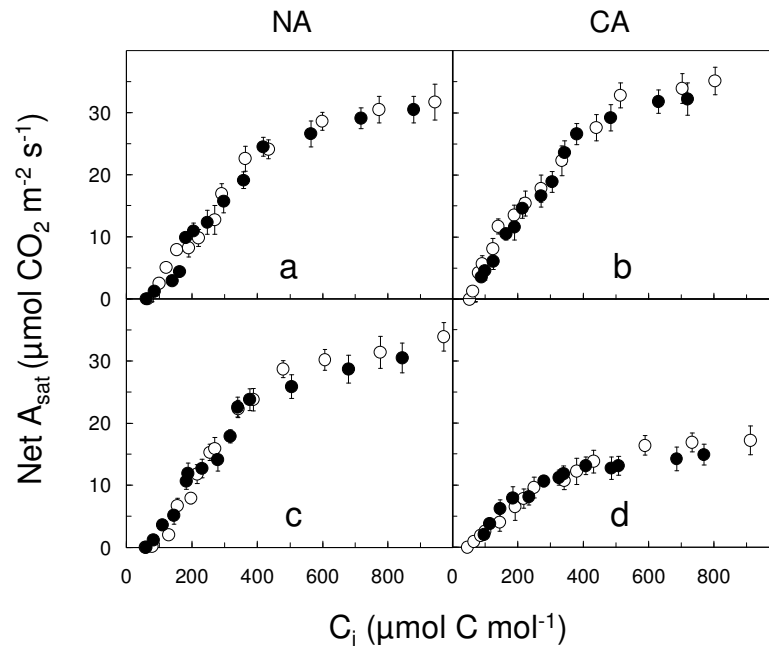
Genes	Sequences
rbcl	5'-CTA CGC GGT GGA CTT GAT TT-3' 3'-ATT TCA CCA GTT TCG GCT TG-5'
cFBPase	5'-AAC AAG AAC GAG GGA GGG ATA C-3' 3'-TCC GCA TCA CAA GAA AAG G-5'
Lhcb1	5'-CGT CCT TCG GAC AAA TAT GC-3' 3'-TAA TGA CAT GGG CCA GCA AG-5'
PsbA	5'-GTG GCT GCT CAC GGT TAT TT-3' 3'-CCA AGC AGC CAA GAA GAA GT-5'
PsaA	5'-GGA AAA TGC AGT CGG ATG TT-3' 3'-AGA AAT CTC GAA GCC AAC CA-5'

Appendix 3S2. Effects of pot size on dry matter accumulation of Musketeer winter rye grown at ambient CO₂. ± SD.

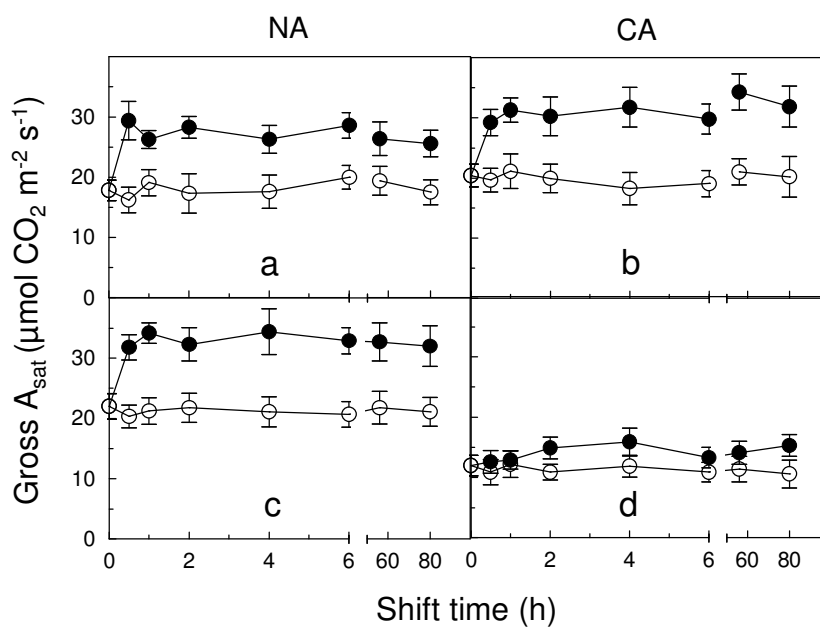
Pot size (L)	Total DW mg plant ⁻¹	
	NA	CA
0.5	331 ± 45	307 ± 29
2	349 ± 22	324 ± 33
4	366 ± 31	348 ± 39
6	352 ± 37	331 ± 21



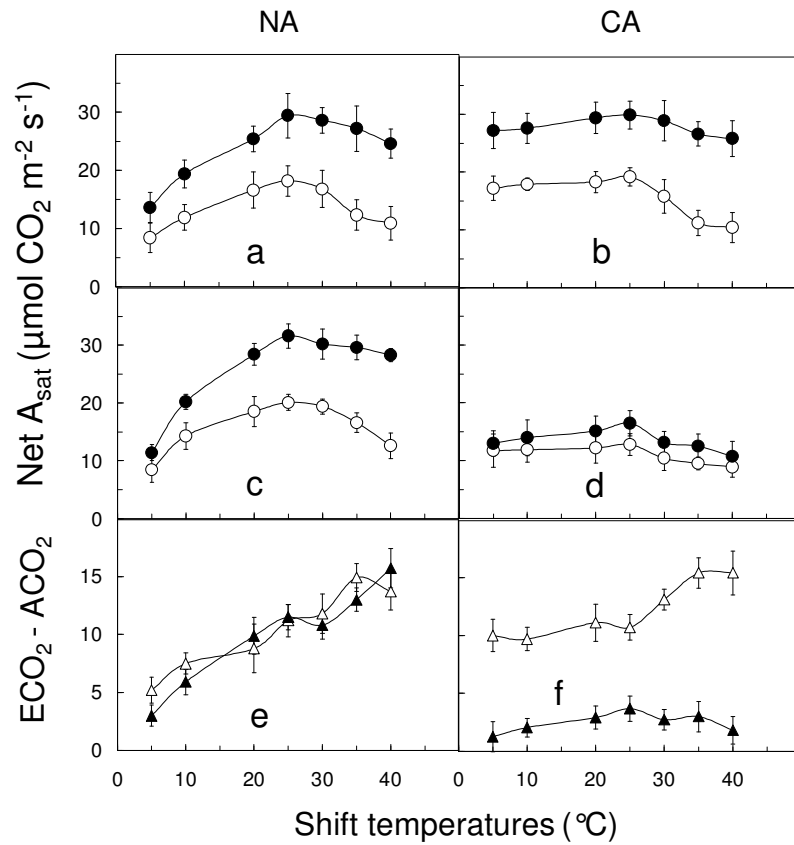
Appendix 3S3. Light response curves of gross CO₂ assimilation at either ambient (○) or after 80 h of exposure to elevated (●) CO₂ for NA (a, c) and CA (b, d) Norstar (a, b) and Katepwa (c, d) wheat. Bars represent SD.



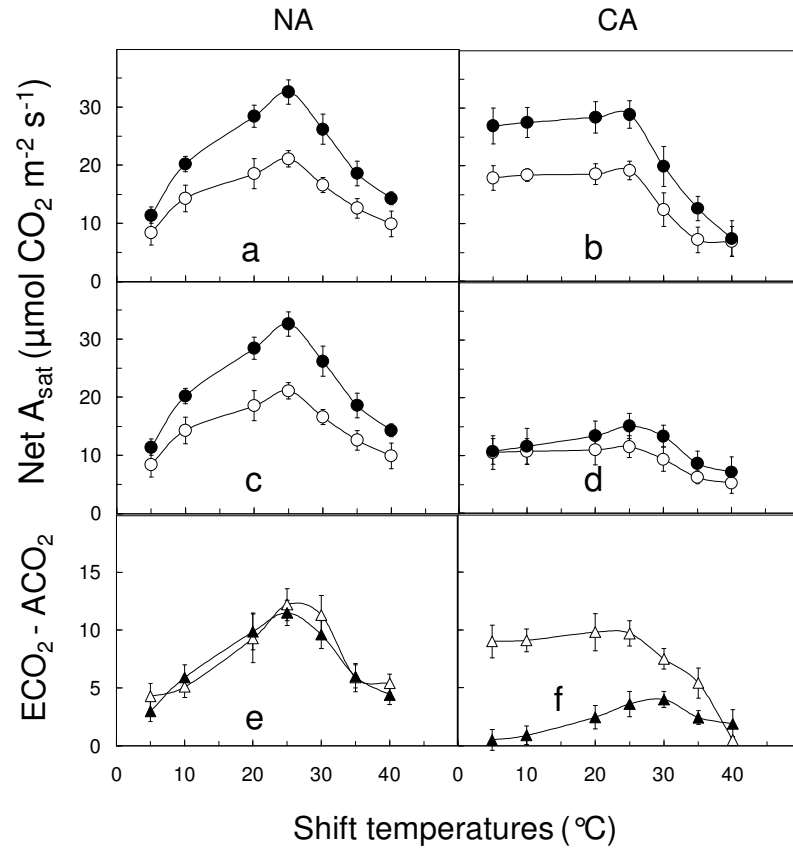
Appendix 3S4. CO₂ response curves of light-saturated net CO₂ assimilation at either ambient (○) or after 80 h of exposure to elevated (●) CO₂ for NA (a, c) and CA (b, d) Norstar (a, b) and Katepwa (c, d) wheat. Bars represent SD.



Appendix 3S5. Light-saturated rates of gross CO₂ assimilation at either ambient (○) or over 80 h of exposure to elevated (●) CO₂ for NA (a, c) and CA (b, d) Norstar (a, b) and Katepwa (c, d) wheat. Bars represent SD.



Appendix 3S6. Temperature sensitivity of net A_{sat} at either ambient (○) or after 1 h shift to elevated (●) CO_2 for NA (a, c,) and CA (b, d) Norstar (a, b) and Katepwa (c, d) wheat. Difference in net A_{sat} at elevated versus ambient CO_2 ($\text{ECO}_2 - \text{ACO}_2$) for NA (e) and CA (f) Norstar (Δ) and Katepwa (▲). Bars represent SD.



Appendix 3S7. Temperature sensitivity of net A_{sat} at either ambient (○) or after 80 h shift to elevated (●) CO_2 for NA (a, c,) and CA (b, d) Norstar (a, b) and Katepwa (c, d) wheat. Difference in net A_{sat} at elevated versus ambient CO_2 ($\text{ECO}_2 - \text{ACO}_2$) for NA (e) and CA (f) Norstar (Δ) and Katepwa (\blacktriangle). Bars represent SD.

Appendix 3S8. Effects of short-term shift to elevated CO₂ and /or high temperature on dark respiratory rates for winter and spring cereals grown at ambient CO₂ (380 μmol C mol⁻¹) and at either 20/16°C (NA) or 5/5°C (CA). Respiratory rates for NA and CA plants were measured at ambient CO₂ and respective growth temperatures, and after 80 h at (i) elevated CO₂ (700 μmol C mol⁻¹) at constant temperature (ii) ambient CO₂ at 40°C and (iii) elevated CO₂ at 40°C. Significant differences among the means within each cultivar are indicated by the superscripted letters ($P \leq 0.05$). ± SD.

Respiration (μmol CO ₂ evolved m ⁻² s ⁻¹)					
Cultivars	Acclimation state	Ambient CO ₂	80 h shift to		
			Elevated CO ₂	Ambient CO ₂ + 40°C	Elevated CO ₂ + 40°C
Musketeer	NA	3.24 ± 0.14 ^c	2.83 ± 0.13 ^b	1.51 ± 0.24 ^a	1.37 ± 0.08 ^a
	CA	3.88 ± 0.23 ^d	3.13 ± 0.29 ^{bc}	1.22 ± 0.11 ^a	1.31 ± 0.16 ^a
Norstar	NA	2.28 ± 0.11 ^c	2.14 ± 0.39 ^c	1.30 ± 0.28 ^{ab}	0.98 ± 0.13 ^a
	CA	2.85 ± 0.18 ^d	2.38 ± 0.20 ^c	1.39 ± 0.21 ^b	1.35 ± 0.10 ^b
SR 4A	NA	3.05 ± 0.12 ^d	2.54 ± 0.18 ^c	1.77 ± 0.12 ^b	1.41 ± 0.20 ^{ab}
	CA	3.43 ± 0.13 ^e	2.89 ± 0.21 ^{cd}	1.35 ± 0.16 ^a	1.51 ± 0.35 ^{ab}
Katepwa	NA	2.07 ± 0.24 ^{bc}	1.63 ± 0.28 ^b	1.28 ± 0.19 ^a	1.26 ± 0.11 ^a
	CA	2.35 ± 0.29 ^c	2.31 ± 0.17 ^c	1.12 ± 0.14 ^a	1.23 ± 0.22 ^a

Chapter 4

Cold acclimation and *BnCBF17*-over-expression enhance photosynthetic performance and energy conversion efficiency during long-term growth of *Brassica napus* under elevated CO₂ conditions

4.1 Introduction

The effects of cold acclimation at morphological, physiological and biochemical levels have been widely studied in cold-tolerant wheat, rye and barley as well as spinach, *Arabidopsis thaliana*, and *Brassica napus* (Krause 1988, Hüner et al. 1993, 1998, Adams et al. 2002, Stitt and Hurry 2002, Öquist and Hüner 2003, Savitch et al. 2005, Ensminger et al. 2006). Cold acclimation of winter rye, winter wheat (Hüner et al. 1981, 1985, Dahal et al. 2012), spinach (Boese and Hüner 1990) as well as *Arabidopsis thaliana* (Strand et al. 1999, Gorsuch et al. 2010a, 2010b) and *Brassica napus* (Savitch et al. 2005, Dahal et al. 2012) exhibit altered phenotype and growth habit. Growth and development of cold-tolerant plants at low temperature generally results in a compact, dwarf growth habit with leaves that exhibit increased thickness relative to NA controls (Hüner et al. 1981, 1985, Dahal et al. 2012). The increased leaf thickness associated with the cold acclimated state can be accounted for by either increases in leaf mesophyll cell size (Hüner et al. 1981, Gorsuch et al. 2010a) and/or increases in the number of palisade layers (Boese and Hüner 1990, Dahal et al. 2012).

Cold acclimation of cold tolerant species generally results in enhanced light-saturated rates of photosynthesis, A_{sat} . It has been suggested that the cold acclimation-induced increase in A_{sat} of cold-tolerant species such as wheat, rye, *Arabidopsis thaliana*, and *Brassica napus*, is correlated with a stimulation of carbon metabolism as a result of the enhanced activities of key regulatory photosynthetic enzymes such as Rubisco, cFBPase, and SPS in response to low growth temperatures (Hurry et al. 2000, Stitt and Hurry 2002, Savitch et al. 2005). Our recent study (Dahal et al. 2012) has revealed that the increased A_{sat} of CA winter wheat and winter rye, especially when measured on a leaf

area basis can, by and large, be accounted for by the increased specific leaf weight in response to growth at low temperature. There is a strong, positive correlation between the cold acclimation-induced increase in A_{sat} and the development of freezing tolerance as well as an increased resistance to low temperature-induced photoinhibition in winter rye and winter wheat (Hüner et al. 1993, Öquist et al. 1993, Pocock et al. 2001), spinach (Krause 1988, Somersalo and Krause 1989, Guy 1990, Boese and Hüner 1992, Gray et al. 1997), *Arabidopsis thaliana* (Savitch et al. 2001) and *Brassica napus* (Savitch et al. 2005). The increased resistance to photoinhibition and decreased temperature sensitivity of photosynthetic performance associated with cold acclimation are governed by changes at the cellular and biochemical levels rather than at the level of leaf anatomy and morphology and are characterized by an increased quantum requirement to close PSII reaction centers (Dahal et al. 2012).

What governs this complex, integrated phenomenon in cold tolerant plant species? It has been suggested that CBFs/DREBs (Cold- Binding Transcription Factors/Dehydration Responsive Element Binding Factors) appear to control the phenotypic plasticity, biochemical changes and photosynthetic performance in cold-tolerant species (Liu et al. 1998, Kasuga et al. 1999, Gilmour et al. 2000, 2004, Savitch et al. 2005). For instance, even at a growth temperature of 20°C, over-expression of *BnCBF17* (Savitch et al. 2005) and *AtCBF3* (Gilmour et al. 2000, 2004) mimics multiple phenotypic, physiological and biochemical changes observed upon cold acclimation of their wild type (WT) counterparts. Similar results have been reported for over-expression of *AtCBF1* in potato (Pino et al. 2008), tobacco (Yang et al. 2010), tomato *CBF1* in transgenic *Arabidopsis* (Zhang et al. 2004) and *EgucBF1* in *Eucalyptus* (Navarro et al. 2011). Our recent study has revealed that over-expression of *BnCBF17* in *B. napus* grown at 20°C mimics the effects of cold acclimation of winter rye and winter wheat with respect to increased SLW, increased leaf thickness, improved WUE, enhanced light-saturated rates of CO₂ assimilation and photosynthetic electron transport coupled with a decrease in the low temperature sensitivity of these processes (Dahal et al. 2012). Thus, over-expression of *B. napus* with a single transcription factor, *BnCBF17*, appears to cause the conversion of non-acclimated WT to a cold acclimated state without exposure to low growth temperature. CBFs/DREBs are a family of transcriptional

activators required to induce the expression of cold-regulated genes (*COR*) that enhance plant freezing tolerance (Liu et al. 1998, Kasuga et al. 1999, Gilmour et al. 2000, van Buskirk and Thomashow 2006, Chinnuswamy et al. 2007, Badawi et al. 2008). In addition to enhanced freezing tolerance (Savitch et al. 2005), over-expression of *BnCBF17* has much broader effects on plant phenotype, leaf anatomy, photosynthetic performance, water use efficiency and dry matter accumulation typically associated with cold acclimation of winter cereals and *Brassica napus* (Dahal et al. 2012). Thus, CBFs/DREBs appear to be critical factors that govern plant phenotypic plasticity during cold acclimation.

An immediate increase in the rates of net CO₂ assimilation has been observed following short-term shift of C₃ plants from ambient to elevated CO₂ (Cheng et al. 1998, Long et al. 2004, Ainsworth and Rogers 2007). This CO₂ stimulation of photosynthesis in C₃ plants is attributed to two factors. First, at current ambient CO₂ concentrations, Rubisco is CO₂-limited as the K_m (CO₂) for Rubisco is close to the current atmospheric CO₂ concentration (Long et al. 2004, Tcherkez et al. 2006). Thus, an increased CO₂ substrate availability for Rubisco immediately enhances carboxylation velocity. Second, elevated CO₂ competitively suppresses photorespiration because CO₂ is a competitive inhibitor of the oxygenation of RuBP by Rubisco (Long et al. 2004).

However, long-term growth and development of C₃ plants at high CO₂ concentration may lead to an end product inhibition of photosynthetic capacity due to accumulation of non-structural carbohydrates in the cytosol (Stitt and Quick 1989, Foyer 1990). The photosynthetic response of C₃ plants to CO₂ has been theoretically modeled by Farquhar et al. (1980). According to their model, at higher C_i, CO₂ assimilation is usually limited either by the capacity of photosynthetic electron transport to supply ATP and NADPH to regenerate RuBP, or by the capacity of starch and sucrose synthesis to utilize triose phosphates and consequently regenerate P_i.

The P_i regeneration-limited photosynthesis is governed by the balance between the source leaves to assimilate carbon and the sink strength to utilize photoassimilates (Arp 1991, Drake et al. 1997). It has been suggested that the increased carbon uptake

resulting from initial stimulation of photosynthesis alters the balance between supply and demand due to limited sink capacity to utilize carbohydrates and concomitant retardation of carbon export to the sinks (Kramer 1981, Arp 1991, Drake et al. 1997). This results in the accumulation of sucrose in the source leaves followed by inhibition of sucrose synthesis and a short-term decrease in utilization of phosphorylated intermediates and depletion in stromal P_i . Low availability of stromal P_i triggers inhibition of ATP synthesis and thereby a decrease in the rate at which PGA is converted to triose phosphate which results in feedback inhibition of CO_2 assimilation (Stitt and Quick 1989, Sharkey and Vadever 1989). In the long-term, the feedback inhibition of photosynthesis may result from the downregulation of the expression and activities of key regulatory photosynthetic enzymes (Harley & Sharkey 1991, Drake et al. 1997, Moore et al. 1999).

Previous studies have shown that over-expression of *BnCBF17* in *B. napus* mimics the effects of cold acclimation with respect to enhanced photosynthetic performance at ambient CO_2 (Savitch et al. 2005, Dahal et al. 2012). The objective of this study is to assess whether the enhanced photosynthetic performance observed for *BnCBF17*-OE as well as cold acclimated WT relative to non-acclimated WT *B. napus* at ambient CO_2 ($380 \mu\text{mol C mol}^{-1}$) is maintained upon long-term growth and development at elevated CO_2 ($700 \mu\text{mol C mol}^{-1}$). Since cold acclimated WT *B. napus* exhibits enhanced sink capacity and increased activities of major photosynthetic enzymes (Savitch et al. 2005, Dahal et al. 2012), we hypothesize first that, cold acclimation-induced increase in photosynthetic performance of *B. napus* at ambient CO_2 is maintained under long-term growth and development at elevated CO_2 . Second, we hypothesized that the *BnCBF17*-OE grown at 20°C should respond similarly to growth and development under elevated CO_2 as does cold acclimated WT *B. napus*.

4.2 Materials and methods

4.2.1 Plant growth

Brassica napus cv. Westar (wild type, WT) and the *B. napus* *BnCBF17*-over-expressing transgenic line (*BnCBF17*-OE) were used in all experiments. The *BnCBF17*-over-

expressing line was generated as described in detail by Savitch et al. (2005). Seeds of WT and *BnCBF17*-OE were grown in controlled environmental growth chambers (Model: GCW15 chamber, Environmental Growth Chambers, Chargin Falls, OH, USA) at either ambient CO₂ ($380 \pm 10 \mu\text{mol C mol}^{-1}$) or elevated CO₂ ($700 \pm 25 \mu\text{mol C mol}^{-1}$) with a PPFD of $250 \pm 20 \mu\text{mol photons m}^{-2} \text{ s}^{-1}$, 50 - 60% relative humidity and a 16 h photoperiod. The WT plants were grown at day/night temperature regimes of either 20/16°C (non-acclimated, NA) or 5/5°C (cold acclimated, CA) whereas the *BnCBF17*-over-expressing line was grown only at 20/16°C. Each CO₂ growth chamber was equipped with a computer-controlled CO₂ infra-red gas analyzer (Model: WMA-4 CO₂ Analyzer, PP Systems International, Inc. Amesbury, MA, USA) which monitored CO₂ concentrations continuously. In addition, the temperature, relative humidity, irradiance level and photoperiod in each chamber were computer-controlled and monitored continuously. The seedlings were grown in organic soil (Promix, Premier Horticulture, Quakertown, PA, USA) in 500 mL-sized plastic pots with one plant each and watered with all purpose fertilizer (Plant Prod 20-20-20, Sure-Gro IP Inc. Brampton, ON, Canada). The non-acclimated WT plants were grown for 3 weeks, the *BnCBF17*-OE for 4 weeks and the cold acclimated WT for 12 weeks. At these ages, the third leaves were fully expanded in non-acclimated WT, *BnCBF17*-OE and cold acclimated WT plants. Thus, all measurements of CO₂ gas exchange rates and Chl a room temperature fluorescence, and biochemical analyses were carried out on fully expanded third leaves of the 3-week-old non-acclimated WT, 4-week-old *BnCBF17*-OE and 12-week-old cold acclimated WT *B. napus*.

The shoot and root fresh biomasses were determined, and the tissues were dried at 80°C to constant weight for the determination of dry mass. Leaf blade area was measured by using a LI-COR portable area meter (LI-3000A, LI-COR Biosciences, Lincoln, NE, USA). Specific leaf weight (SLW) was calculated as leaf dry weight in g m⁻² leaf blade area. The photosynthetic pigments, Chl a and Chl b, were quantified according to Arnon (1949).

In order to confirm that the pot size did not limit rooting volume and sink growth, we carried out a pot size experiment for non-acclimated WT and *BnCBF17*-over-

expressing *B. napus*. Plants were grown at various pot sizes of 0.3 L, 0.5 L, 1 L and 1.5 L at elevated CO₂ ($700 \pm 30 \mu\text{mol C mol}^{-1}$) and at growth conditions described above. Root and shoot biomass were harvested from 3-week-old non-acclimated WT and 4-week-old *BnCBF17-OE*, and the tissues were dried at 80°C in order to get dry weight.

4.2.2 CO₂ gas exchange

CO₂ gas exchange rates were measured on attached fully expanded third leaves at either 380 $\mu\text{mol C mol}^{-1}$ or 700 $\mu\text{mol C mol}^{-1}$ and at a measuring temperature of 20°C irrespective of acclimation state. CO₂ gas exchange rates were measured on attached fully expanded third leaves by using the LI-COR portable infrared CO₂ gas analyzer (LI-6400 XRT Portable Photosynthesis System, LI-COR Biosciences, Lincoln, NE, USA). Light response curves were measured using 12 irradiance values ranging from 0 to 1300 $\mu\text{mol photons m}^{-2} \text{ s}^{-1}$ PPFD from high to low light intensity with 8 min of waiting time between each measurement. The apparent maximum quantum efficiency (Q) and the maximal photosynthetic capacity (A_{sat}) were determined as the maximum initial slope and the maximum light-saturated rates respectively from light response curves. CO₂ response curves were measured by supplying 11 different CO₂ values over the range of 50 to 1200 $\mu\text{mol C mol}^{-1}$ at a saturating irradiance of 1300 $\mu\text{mol photons m}^{-2} \text{ s}^{-1}$ PPFD at 20°C. Rubisco-limited carboxylation efficiency (CE) was calculated as the maximum initial slope and the CO₂-saturated photosynthesis as the plateau of the curves. The maximum Rubisco carboxylation capacity (V_{cmax}) and the maximum rates of electron transport (J_{max}) were calculated using the FCB photosynthesis model (Farquhar et al. 1980). Respiration rates (R_{dark}) were measured in the dark. Measurements were made inside the CO₂ enriched chambers, to reduce diffusion errors through the leaf blade and chamber seals as suggested previously (Jahnke 2001; Jahnke and Krewitt 2002). In addition, stomatal conductance and leaf transpiration rates were measured simultaneously with CO₂ gas exchange measurements at growth CO₂ and 20°C regardless of acclimation state. Leaf water use efficiency was calculated as $\mu\text{mol CO}_2$ fixed per mol of stomatal conductance (A/g_s). Stomatal density was estimated on both adaxial and abaxial leaf surfaces using a stage micrometer (1mm²) on a microscope (Leica ATC™ 2000, Buffalo, NY, USA). Stomata were counted at a magnification of 100X.

4.2.3 Room temperature Chl a fluorescence

In vivo Chl a fluorescence was measured to assess the effects of elevated CO₂ on maximum photochemical efficiency (F_v/F_m), maximum potential rates of photosynthetic electron transport (ETR), excitation pressure (EP), which estimates the relative reduction state of PSII reaction centers, and non-photochemical quenching (NPQ), an estimate of the capacity to dissipate energy as heat. Chl a fluorescence was measured simultaneously with CO₂ gas exchange on fully expanded third leaves using a LI-COR portable photosynthesis system (LI-6400 XRT, LI-COR Biosciences, Lincoln, NE, USA). Light response curves of electron transport rates, excitation pressure and non photochemical quenching of excess energy were measured at irradiance values ranging from 0 to 1500 $\mu\text{mol PPFd}$ at 700 $\mu\text{mol C mol}^{-1}$ and at a measuring temperature of 20°C irrespective of growth CO₂ and irrespective of growth temperature. All measurements of Chl a fluorescence were carried out by using the standard fluorescence leaf chamber (2 cm²). The leaves were dark-adapted for 20 min prior to fluorescence measurements. Minimum fluorescence (F_o) was measured by illuminating dark adapted leaves with a low irradiance measuring beam ($\text{PPFD} < 1 \mu\text{mol photons m}^{-2} \text{s}^{-1}$) from a light emitting diode. Maximal fluorescence (F_m) was determined by applying a flash of saturating light ($\text{PPFD} > 5000 \mu\text{mol photons m}^{-2} \text{s}^{-1}$) for pulse duration of 0.8 s. Afterwards, an actinic light ($\text{PPFD} 1300 \mu\text{mol photons m}^{-2} \text{s}^{-1}$) was applied. Superimposed on the actinic beam was a saturating light flash ($\text{PPFD} > 5000 \mu\text{mol photons m}^{-2} \text{s}^{-1}$; 0.8 s) applied repetitively at 20 s intervals to determine maximal fluorescence in the light-adapted state (F_m'). Light adapted steady state fluorescence (F_s) was determined by measuring the level of fluorescence during steady-state photosynthesis. Finally, minimal fluorescence (F_o') in the light-adapted leaf was measured by turning off the actinic light.

4.2.4 Determination of total leaf protein and immunodetection

The fully expanded third leaves were harvested, immediately frozen in liquid N₂ and stored at -80°C. The leaf samples for the protein determination were prepared as described in detail by Dahal et al. (2012). Total leaf protein content was quantified using the RC-DC protein assay kit (Bio-Rad, Hercules, CA, USA) according to the

manufacturer's instructions. While quantifying the total leaf protein content, the addition of 1 µg of bovine serum albumin (Invitrogen, Carlsbad, CA, USA) in the extraction buffer was used as an internal standard.

The extracted proteins were electrophoretically separated using NuPAGE Novex 10% (w/v) Bis-Tris precast, polyacrylamide gels (Invitrogen) with MES SDS running buffer (Invitrogen) in an XCell4 SureLock Midi Cell (Invitrogen) according to manufacturer's instructions. Samples were loaded for SDS-PAGE on either an equal Chl (0.5 µg Chl per lane) or on an equal protein (5 µg protein per lane) basis. Gels were electrophoresed at 80V for about 3 h. For immunodetection, separated polypeptides were electroblotted onto nitrocellulose membranes (0.2 µm pore size, Bio - Rad) in transfer buffer for 1 h at 100V. The membranes were blocked with 5% (w/v) fat free, dried milk powder overnight at 4°C and then probed with primary antibodies raised against the target proteins; rbcL (Hüner, University of Western Ontario, Canada), cFBPase and Lhcb1 (Agrisera, Sweden) at a dilution of 1:2000-5000. The blots were rinsed briefly and washed in TBS wash buffer at room temperature with agitation. The blots were probed with secondary antibody (anti-rabbit IgG Peroxidase antibody, Sigma-Aldrich, Steinheim, Germany) at a 1:10000-20000 dilutions for 1 h at room temperature with agitation. The blots were washed as described above and the target proteins were visualized with enhanced chemiluminescence immunodetection (ECL Detection Kit; GE Healthcare, Buckinghamshire, UK) on X-ray film (Fujifilm, Fuji Corporation, Tokyo, Japan). Immunoblots were quantified by using a computer software program (SCION IMAGE , Scion Corporation, Frederick, MD, USA). For quantification, exposure times were varied to ensure that signals from the immunoblots were not saturating.

4.2.5 Statistical analysis

The non-acclimated WT, *BnCBF17*-OE as well as cold acclimated WT each was grown in 30 replicate pots in a completely randomized design. Out of the 30 replicate pots, three pots for each line at each growth condition were randomly selected for all measurements. Thus, all data are the means of three replicate pots. Results were subjected to analysis of

variance (ANOVA). Means were compared at the 5% level of significance ($P \leq 0.05$) by using the statistical package SPSS version 17 (IBM, Armonk, NY, USA).

4.3 Results

4.3.1 Growth characteristics

In order to ensure that pot size did not limit rooting volume and sink growth at elevated CO₂, we carried out a pot size experiment for non-acclimated WT and *BnCBF17*-OE grown at elevated CO₂ (Appendix 4S1). Total dry matter accumulation was significantly lower when grown in 0.3L pot. Except for 0.3L, no differences were observed in total dry matter accumulation in various pot sizes of 0.5 L, 1 L and 1.5 L in both WT and transgenic *B. napus* (Appendix 4S1). Thus, to prevent rooting volume constraints and sink limitations, the plants were subsequently grown in 0.5 L-sized pots irrespective of growth CO₂ and growth temperatures in all experiments.

The *BnCBF17*-OE exhibited a compact, dwarf growth habit and altered leaf morphology as compared to the typical elongated growth habit for non-acclimated WT at ambient CO₂ (Figure 4.1). The growth habit and plant morphology observed for *BnCBF17*-OE were comparable to those observed for cold acclimated WT at ambient CO₂ (Figure 4.1). Although the *BnCBF17*-OE as well as cold acclimated WT *Brassica napus* were smaller plants, they exhibited comparable total dry matter accumulation as that of non-acclimated WT at fully expanded third leaf stage at ambient CO₂ (Table 4.1). Growth at elevated CO₂ significantly increased dry matter accumulation by 20, 40 and 35% for non-acclimated WT, *BnCBF17*-OE and cold acclimated WT, respectively relative to that at ambient CO₂ (Table 4.1). Thus, *BnCBF17*- over-expression as well as cold acclimation appeared to substantially increase the dry matter accumulation relative to that of non-acclimated WT at elevated CO₂. The specific leaf weight (SLW) increased by about 85% in *BnCBF17*-OE versus non-acclimated WT and by about 130% in cold acclimated WT versus non-acclimated WT at ambient CO₂ (Table 4.1). Elevated CO₂ significantly stimulated SLW by 33% in non-acclimated WT but had minimal effects in the *BnCBF17*-OE as well as in cold acclimated WT (Table 4.1). Consequently, at

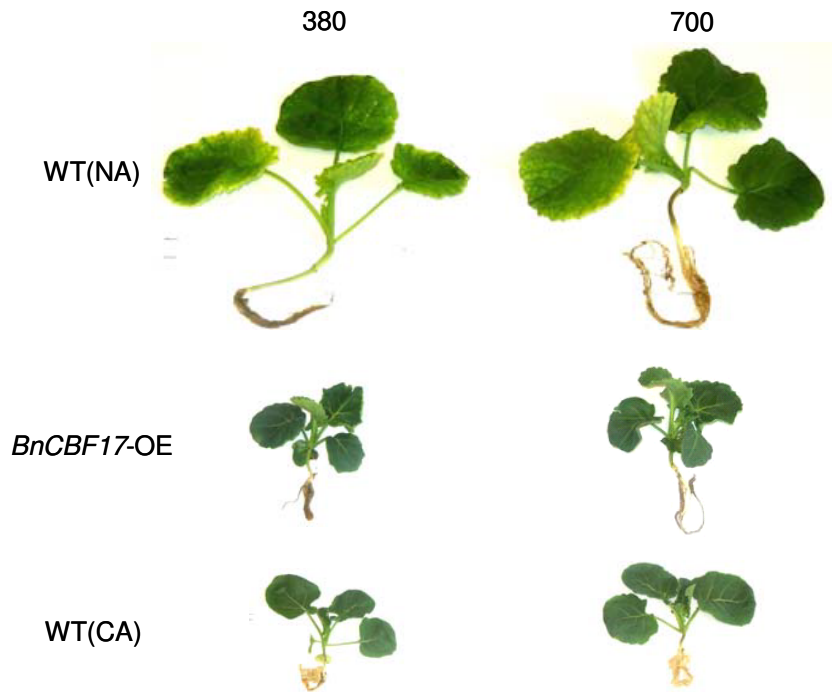


Fig. 4.1. Effects of cold acclimation and elevated CO₂ on plant morphology and growth habit of WT *B. napus* and *BnCBF17-OE*. The plants were grown at either 20/16°C (NA and *BnCBF17-OE*) or 5/5°C (CA Brassica WT) and at either ambient (380 $\mu\text{mol C mol}^{-1}$) or elevated (700 $\mu\text{mol C mol}^{-1}$) CO₂.

Table 4.1. Effects of cold acclimation and elevated CO₂ on morphological and photosynthetic characteristics of WT and *BnCBF17*-over-expressing *B. napus* grown at either ambient (380 μmol C mol⁻¹) or elevated (700 μmol C mol⁻¹) CO₂ and at either 20/16°C (Non-acclimated) or 5/5°C (Cold acclimated). All measurements were carried out on fully developed third leaves at their respective growth CO₂ at 20°C. Data represent the mean of three plants from three different pots ± SD. Significant differences of the means are indicated by the superscripted letters ($P \leq 0.05$).

Morphological and photosynthetic characteristics	Wild type (NA)		<i>BnCBF17</i> -OE		Wild type (CA)	
	380	700	380	700	380	700
Total dry mass (mg plant ⁻¹)	103 ± 6 ^a	124 ± 9 ^b	122 ± 10 ^{ab}	171 ± 14 ^c	117 ± 12 ^{ab}	158 ± 17 ^c
Specific leaf weight (g DM m ⁻² leaf area)	27 ± 3 ^a	36 ± 2 ^b	50 ± 6 ^c	61 ± 7 ^c	63 ± 5 ^{cd}	69 ± 6 ^d
Leaf chlorophyll (mg m ⁻² leaf area)	424 ± 21 ^a	491 ± 27 ^b	942 ± 63 ^e	808 ± 41 ^{cd}	866 ± 39 ^{de}	792 ± 24 ^c
Chl a/Chl b ratio	3.18 ± 0.21 ^b	2.47 ± 0.28 ^a	2.82 ± 0.31 ^{ab}	2.84 ± 0.16 ^{ab}	2.76 ± 0.17 ^{ab}	2.93 ± 0.23 ^{ab}
Total leaf protein (g m ⁻² leaf area)	3.65 ± 0.33 ^b	2.71 ± 0.24 ^a	16.30 ± 1.52 ^c	17.23 ± 0.64 ^c	17.46 ± 1.37 ^c	15.09 ± 0.93 ^c
Protein/Chl Ratio	8.61 ± 0.62 ^b	5.52 ± 0.36 ^a	17.30 ± 1.22 ^c	21.32 ± 1.51 ^d	20.16 ± 2.74 ^{cd}	19.05 ± 1.37 ^{cd}
Q (CO ₂ /photon)	0.045 ± 0.02 ^a	0.067 ± 0.04 ^c	0.054 ± 0.03 ^b	0.059 ± 0.03 ^{bc}	0.057 ± 0.05 ^b	0.063 ± 0.04 ^{bc}
CE (CO ₂ /mol ⁻¹ CO ₂)	0.081 ± 0.03 ^a	0.073 ± 0.05 ^a	0.109 ± 0.05 ^c	0.119 ± 0.06 ^c	0.102 ± 0.08 ^{bc}	0.093 ± 0.06 ^b
J _{max} (μmol e ⁻ m ⁻² s ⁻¹)	127 ± 7 ^b	101 ± 5 ^a	153 ± 8 ^c	148 ± 5 ^c	146 ± 6 ^c	152 ± 9 ^c
V _{cmax} (μmol m ⁻² s ⁻¹)	51 ± 4 ^b	39 ± 3 ^a	68 ± 7 ^{cd}	74 ± 9 ^d	63 ± 3 ^{cd}	60 ± 4 ^{bc}
R _{dark} (μmol C evolved m ⁻² s ⁻¹)	-2.19 ± 0.14 ^a	-2.81 ± 0.32 ^{bc}	-2.67 ± 0.20 ^b	-3.20 ± 0.11 ^c	-3.04 ± 0.19 ^{bc}	-4.08 ± 0.36 ^d

elevated CO₂, the *BnCBF17*-OE and cold acclimated WT exhibited about 70% and 90% higher SLW respectively compared to non-acclimated WT (Table 4.1).

Over-expression of *BnCBF17* substantially increased Chl per unit leaf area by about 125% as compared to non-acclimated WT at ambient CO₂ (Table 4.1). The increase in Chl in the *BnCBF17*-OE was at par with the cold acclimation- induced increase in Chl per unit leaf area (105%) for WT at ambient CO₂ (Table 4.1). Although, elevated CO₂ significantly increased Chl per unit leaf area by 16% for non-acclimated WT, it significantly decreased the Chl per unit leaf area for *BnCBF17*-OE as well as cold acclimated WT by 10 - 15% (Table 4.1). The Chl a/b ratios decreased by about 20% in non-acclimated WT but changed minimally in *BnCBF17*-OE and cold acclimated WT in response to growth at elevated CO₂ (Table 4.1).

The *BnCBF17*-OE as well as cold acclimated WT *B. napus* exhibited about 4.8-fold higher leaf protein content per unit leaf area relative to non-acclimated WT at ambient CO₂ (Table 4.1). Although elevated CO₂ had minimal effects on leaf protein content of the *BnCBF17*-OE as well as cold acclimated WT, elevated CO₂ appeared to significantly decrease leaf protein content by about 25% in non-acclimated WT relative to at ambient CO₂ (Table 4.1). The leaf protein to Chl ratio was about 2-fold higher in the *BnCBF17*-OE and cold acclimated WT *B. napus* relative to non-acclimated WT at ambient CO₂ (Table 4.1). Elevated CO₂ reduced this ratio by about 35% in non-acclimated WT but had minimal effects on this ratio in the *BnCBF17*-OE and cold acclimated WT *B. napus* relative to at ambient CO₂ (Table 4.1).

4.3.2 Light response curves for CO₂ assimilation

Consistent with our previous report (Dahal et al. 2012), over-expression of *BnCBF17* (Table 4.1, Figure 4.2b) mimicked cold acclimated WT Brassica (Figure 4.2c) with respect to the 25% and 40% increases in the apparent maximum quantum efficiency for CO₂ assimilation (Q) and the light-saturated rates of gross CO₂ assimilation (gross A_{sat}) respectively as compared to WT *B. napus* when grown and measured at ambient CO₂ (Table 4.1, Figure 4.2a).

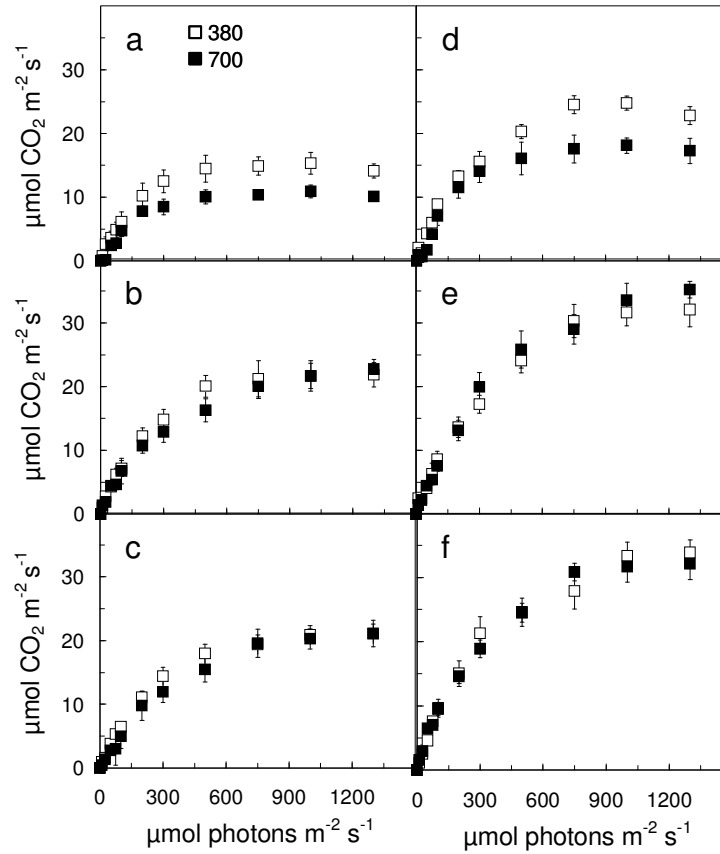


Fig. 4.2. Light response curves of gross CO₂ assimilation for WT *B. napus* (a, c, d, f) and the *BnCBF17-OE* (b, e) grown at either ambient (380 $\mu\text{mol C mol}^{-1}$, □) or elevated (700 $\mu\text{mol C mol}^{-1}$, ■) CO₂ and at either 20/16°C (a, b, d, e) or 5/5°C (c, f). All measurements were carried out on fully developed third leaves at 20°C at either 380 (a, b, c) or 700 (d, e, f) $\mu\text{mol C mol}^{-1}$. Data represent the mean of three plants from three different pots. Bars represent SD

The loss of photosynthetic capacity during growth at elevated CO₂ condition can be assessed by comparing CO₂ assimilation rates in plants grown under elevated (700 μmol C mol⁻¹) versus ambient CO₂ conditions (380 μmol C mol⁻¹) but measured at the same CO₂ concentration of either 380 or 700 μmol C mol⁻¹. Such a comparison revealed a significant inhibition of light-saturated rates of gross CO₂ assimilation in elevated versus ambient CO₂-grown non-acclimated WT (Figure 4.2a and d) but not in either the *BnCBF17*-OE (Figure 4.2b and e) or cold acclimated WT (Figure 4.2c and f). Compared to growth and development at ambient CO₂, the growth and development of non-acclimated WT *B. napus* at elevated CO₂ significantly inhibited the light-saturated rates of gross CO₂ assimilation by 27% when measured at an equal CO₂ concentration of 700 μmol C mol⁻¹ (Figure 4.2d). A similar inhibition of gross CO₂ assimilation (30%) was observed between elevated versus ambient CO₂-grown non-acclimated WT when measured at an equal CO₂ concentration of 380 μmol C mol⁻¹ (Figure 4.2a). In contrast, light-saturated rates of gross CO₂ assimilation for the *BnCBF17*-OE (Figure 4.2b and e) as well as cold acclimated WT *B. napus* (Figure 4.2c and f) exhibited minimal sensitivity to the elevated CO₂ concentration during long-term growth and development.

4.3.3 CO₂-response curves for CO₂ assimilation

Figure 4.3 illustrates the effects of cold acclimation and elevated CO₂ on the light-saturated CO₂ response curves of net CO₂ assimilation. *BnCBF17*-over-expression (Table 4.1, Figure 4.3b) mimicked cold acclimation of WT Brassica (Table 4.1, Figure 4.3c) with respect to a 26 to 37% increase in the carboxylation efficiency (CE) and a 35% increase in the light and CO₂-saturated photosynthetic rates as well as V_{cm_{max}} compared to non-acclimated WT grown at ambient CO₂ (Table 4.1, Figure 4.3a). These results are consistent with our previous reports (Dahal et al. 2012). No significant differences in the carboxylation efficiency were observed between elevated versus ambient CO₂-grown plants for all Brassica lines tested (Table 4.1, Figure 4.3). Elevated CO₂, however, significantly reduced the light and CO₂-saturated rates of net CO₂ assimilation and V_{cm_{max}} by 32% for non-acclimated WT (Table 4.1, Figure 4.3a,) but had minimal effects on these rates for *BnCBF17*-OE as well as cold acclimated WT (Table 4.1, Figure 4.3b, c). The decrease in light and CO₂-saturated rates of net CO₂ assimilation observed for elevated

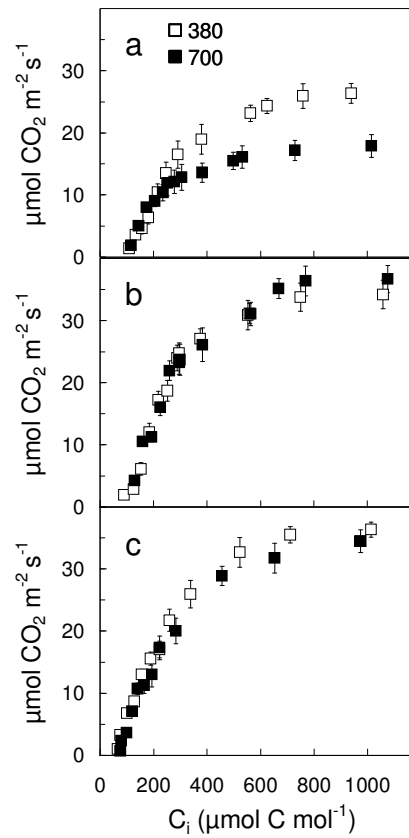


Fig. 4.3. CO₂ response curves of light-saturated net CO₂ assimilation for WT *B. napus* (a, c) and *BnCBF17-OE* (b) grown at either ambient (380 $\mu\text{mol C mol}^{-1}$, □) or elevated (700 $\mu\text{mol C mol}^{-1}$, ■) CO₂ and at either 20/16°C (a, b) or 5/5°C (c). All measurements were carried out on fully developed third leaves at a measuring temperature of 20°C and at a saturating irradiance of 1300 $\mu\text{mol m}^{-2} \text{ s}^{-1}$ PPFD. Data represent the mean of three plants from three different pots. Bars represent SD

versus ambient CO₂-grown non-acclimated WT was consistent with the decreased rates of light and CO₂-saturated electron transport in response to growth at elevated CO₂ (Table 4.1, J_{max}, Figure 4.4a, ETR).

4.3.4 Light response curves for ETR, EP and NPQ

Light response curves for electron transport rates (ETR), excitation pressure (EP), measured as 1-qP, and non-photochemical quenching (NPQ) (Figure 4.4) were generated to estimate the apparent quantum requirement for ETR, the apparent quantum requirement to close PSII reaction centers by EP, and the apparent quantum requirement to induce energy dissipation by NPQ, respectively (Rosso et al. 2009). Apparent quantum requirement is the inverse of apparent quantum efficiency and is estimated as the inverse of the initial slopes calculated from the linear portion of the light response curve for either ETR (Figure 4.4a,b,c), 1-qP (Figure 4.4d, e, f) or NPQ (Figure 4.4g, h, i).

In vivo Chl a fluorescence indicated that *BnCBF17*-OE (Figure 4.4b, open symbols) mimicked cold acclimated Brassica (Figure 4.4c, open symbols) and exhibited a small (15%) but significant increase in the light-saturated ETR but no change in the apparent quantum requirement for ETR (3.6 – 3.9 photons / e) compared to non-acclimated WT at ambient CO₂ (Figure 4.4a). The data for light saturated rates of ETR measured by room temperature Chl a fluorescence were consistent with the J_{max} based on CO₂ gas exchange (Table 4.1). However, the apparent quantum requirements for closure of PSII reaction centers (1414 photons to close 50% of PSII reaction centers) and the induction of NPQ (883 photons/unit NPQ) under ambient CO₂ conditions were 30 to 50% greater for the *BnCBF17*-OE (Figure 4.4e and h, open symbols) and cold acclimated WT Brassica (Figure 4.4f and i, open symbols) compared to non-acclimated WT (Figure 4.4d and g, open symbols).

Elevated CO₂ increased the apparent quantum requirement for ETR by 18% and significantly inhibited the light-saturated ETR by 22% in non-acclimated WT relative to at ambient CO₂ (Fig 4a). The data for ETR were consistent with the J_{max} based on CO₂ gas exchange (Table 4.1). However, the apparent quantum requirements for PSII closure decreased significantly by about 25% in elevated (826 photons to close 50% PSII

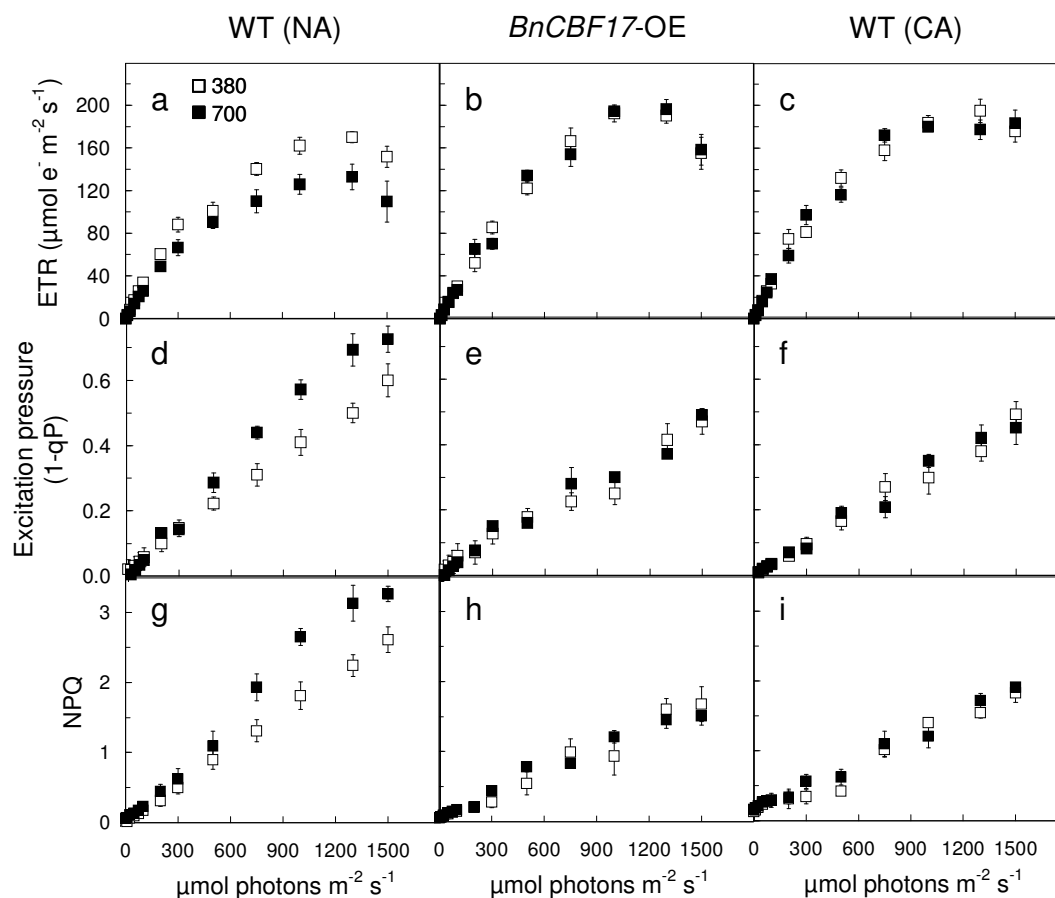


Fig. 4.4. Light response curves of electron transport rates (ETR; a, b, c), excitation pressures ($1-qP$; d, e, f) and non photochemical quenching of excess energy (NPQ; g, h, i) for non-acclimated WT (a, d, g), *BnCBF17*-OE (b, e, h) and cold acclimated WT (c, f, i) *B. napus* grown at either ambient ($380 \mu\text{mol C mol}^{-1}$, \square) or elevated ($700 \mu\text{mol C mol}^{-1}$, \blacksquare) CO_2 and at either $20/16^\circ\text{C}$ (NA) or $5/5^\circ\text{C}$ (CA). All measurements were carried out on fully developed third leaves at $700 \mu\text{mol C mol}^{-1}$ and at measuring temperature of 20°C . Data represent the mean of three plants from three different pots. Bars represent SD

reaction centers) versus ambient CO₂-grown, non-acclimated WT (1093 photons to close 50% PSII reaction centers) (Fig. 4.4d). Concomitantly, the quantum requirement to induce 1 unit of NPQ decreased by 30% from 573 photons / unit NPQ to 414 photons / unit NPQ in WT grown at elevated CO₂ compared at ambient CO₂ (Figure 4.4g). The decreased light and CO₂-saturated ETR for non-acclimated WT grown at elevated CO₂ was consistent with the decreased light and CO₂-saturated rates of CO₂ assimilation at elevated CO₂ (Figure 4.3a). In contrast, the light response curves of ETR, EP and NPQ for the *BnCBF17*-OE as well as cold acclimated WT were insensitive to growth at elevated CO₂ (Fig 4). This was consistent with the minimal changes in the CO₂ response curves for the *BnCBF17*-over-expressing line as well as cold acclimated WT grown under elevated versus ambient CO₂ conditions (Fig. 4.3b, c).

4.3.5 CO₂ response curves for ETR, EP and NPQ

The data for the effects of C_i on ETR for plants grown under ambient CO₂ (Figure 4.5a, b, c, open symbols) indicate that, under light-saturated conditions, the CO₂ saturated rates of ETR were 1.2-fold higher for *BnCBF17*-OE as well as cold acclimated WT than for NA WT Brassica. Furthermore, the efficiency of ETR estimated as the maximal initial slope of the ETR vs C_i response curves in either *BnCBF17*-OE or cold acclimated WT ($0.81 \mu\text{mol e}^- \text{m}^{-2} \text{s}^{-1} / \mu\text{mol CO}_2 \text{mol}^{-1}$) was 1.4-fold higher than that of NA Brassica ($0.57 \mu\text{mol e}^- \text{m}^{-2} \text{s}^{-1} / \mu\text{mol CO}_2$). Growth at elevated CO₂ decreased the CO₂ saturated rates of ETR by about 33% and the efficiency of ETR ($\mu\text{mol e}^- \text{m}^{-2} \text{s}^{-1} / \mu\text{mol CO}_2 \text{mol}^{-1}$) by 54% in NA Brassica (Figure 4.5a). In contrast, the CO₂ saturated rates of ETR as well as the efficiency of ETR were insensitive to growth of either *BnCBF17*-OE (Figure 4.5b) or CA Brassica (Figure 4.5c) at elevated CO₂. These trends were consistent with the data for the differential effects of elevated CO₂ on J_{max} in *BnCBF17*-OE and cold acclimated WT relative to non-acclimated WT Brassica (Table 4.1).

Consistent with the fact that CO₂ is the ultimate electron acceptor for photosynthetic carbon assimilation, increasing C_i decreased excitation pressure in all plants tested (Figure 4.5d, e, f) whether grown under ambient (open symbols) or elevated CO₂ (closed symbols). However, under light saturated conditions, excitation pressure at

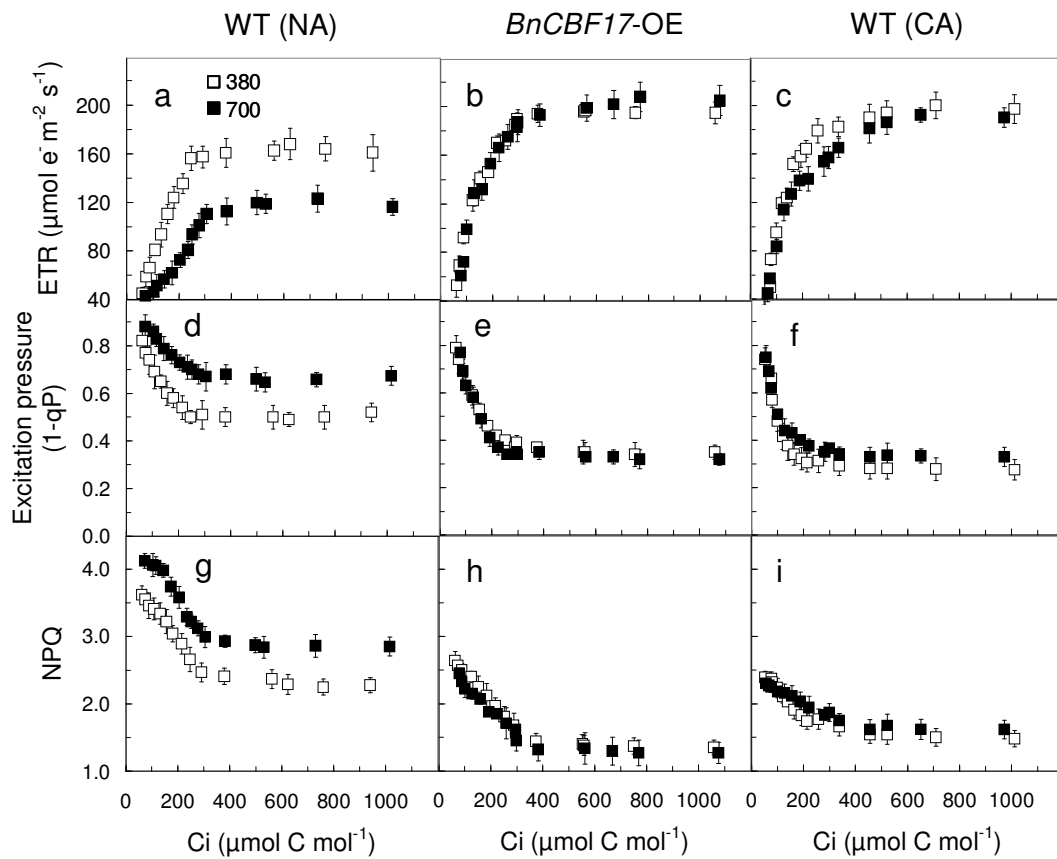


Fig. 4.5. CO₂ response curves of light-saturated electron transport rates (ETR; a, b, c), excitation pressures (1-qP; d, e, f) and non photochemical quenching of excess energy (NPQ; g, h, i) for non-acclimated WT (a, d, g), *BnCBF17*-OE (b, e, h) and cold acclimated WT (c, f, i) *B. napus* grown at either ambient (380 μmol C mol⁻¹, □) or elevated (700 μmol C mol⁻¹, ■) CO₂ and at either 20/16°C (NA) or 5/5°C (CA). All measurements were carried out on fully developed third leaves at 20°C and at a saturating irradiance of 1300 μmol photons m⁻² s⁻¹. Data represent the mean of three plants from three different pots. Bars represent SD.

CO₂ saturation was 1.4- to 1.6-fold lower in *BnCBF17*-OE (Figure 4.5e) and cold acclimated WT (Figure 4.5f) than NA controls (Figure 4.5d) grown at ambient CO₂ (open symbols). In addition, the efficiency with which PSII reaction centers were opened by increased CO₂, measured as the initial slope of the excitation pressure vs C_i response curves, was 1.7- to 1.9-fold greater in *BnCBF17*-OE and cold acclimated WT than in non-acclimated WT (Figure 4.5d, e, f).

Growth at elevated CO₂ not only increased the CO₂-saturated excitation pressure by about 1.4-fold in non-acclimated WT from a 1-qP of 0.48 upon growth at ambient CO₂ (open symbols) to 0.68 upon growth at elevated CO₂ (Figure 4.5d, closed symbols) but also inhibited the efficiency with which PSII reaction centers were opened as a function of increased C_i by about 1.6-fold relative to non-acclimated WT Brassica grown at ambient CO₂ (Figure 4.5d). In contrast, neither the CO₂ saturated excitation pressure nor the efficiency with which PSII reaction centers were opened by increased C_i were significantly affected by growth at elevated CO₂ in *BnCBF17*-OE (Figure 4.5e) as well as cold acclimated WT Brassica (Figure 4.5f).

To complement the CO₂ response curves for excitation pressure, we also assessed the effects of changes in C_i on NPQ (Figure 4.5g, h, i). Consistent with the fact that CO₂ is a substrate for the Rubisco-catalyzed carboxylation reaction of the Calvin cycle, increasing C_i resulted in the suppression of NPQ in non-acclimated WT (Figure 4.5g), *BnCBF17*-OE (Figure 4.5h) and cold acclimated WT Brassica (Figure 4.5i) irrespective of whether plants were grown at ambient (open symbols) or at elevated CO₂ (closed symbols). However, even at low C_i, NPQ was about 50% lower in *BnCBF17*-OE and cold acclimated WT Brassica compared to non-acclimated WT. Although the response of NPQ to increasing C_i was similar whether *BnCBF17*-OE and cold acclimated WT were grown at ambient or elevated CO₂ (Figure 4.5h, i, respectively), increasing C_i induced 26% higher levels of NPQ in non-acclimated WT grown at elevated CO₂ relative to non-acclimated WT grown at ambient CO₂ (Figure 4.5g).

4.3.6 Photosynthetic polypeptide abundance

The data in Table 4.1 indicate that either over-expression of *BnCBF17* or cold acclimation of WT *B. napus* resulted in a doubling of the protein / Chl ratio. When SDS-PAGE gels were loaded for immunoblot analyses on equal Chl basis (Figure 4.6a), *BnCBF17* as well as cold acclimated WT *B. napus* exhibited about 2-fold increase in the relative amount of major stromal photosynthetic enzyme (Rubisco, *rbcL*) and cytosolic FBPase (cFBPase) compared to non-acclimated WT Brassica grown at ambient CO₂ (Figure 4.6a). However, the relative amount of Lhcb1, the major protein of PSII light harvesting complex, changed minimally in *BnCBF17*-OE as well as cold acclimated WT compared to non-acclimated WT at ambient CO₂ (Figure 4.6a). However, when gels were loaded on an equal protein basis, the relative levels of *rbcL*, cFBPase and Lhcb1 changed minimally in *BnCBF17* as well as cold acclimated WT relative to non-acclimated WT at ambient CO₂ (Figure 4.6b). Thus, the data in Figure 4.6a and 6b are consistent with the increased protein / Chl ratio presented in Table 4.1.

Regardless of the basis upon which the SDS-PAGE gels were loaded, growth under elevated CO₂ decreased the relative levels of *rbcL* by about 35% and cFBPase by 40-70% yet increased the relative levels of Lhcb1 by about 20% in non-acclimated WT relative to at ambient CO₂ (Figure 4.6). In contrast, growth at elevated CO₂ appeared to have minimal effects on the abundance of *rbcL*, cFBPase and Lhcb1 in the *BnCBF17*-OE as well as cold acclimated WT relative to at ambient CO₂ irrespective of loading basis (Figure 4.6).

4.3.7 Stomatal Characteristics

The results summarized in Table 4.2 are consistent with previous reports which indicate that over-expression of *BnCBF17* and cold acclimation of *B. napus* resulted in a 30% and 80% increase in water use efficiency (WUE) compared to non-acclimated WT grown at ambient CO₂ (Dahal et al. 2012). This differential increase in WUE was accounted for, in part, by differential increase in CO₂ assimilation rates (Table 4.2).

Elevated CO₂ suppressed leaf stomatal conductance by 20 - 35% in non-acclimated, cold acclimated and the *BnCBF17*- over-expressing line of *B. napus* and, as a consequence, leaf transpiration rates decreased by 15 - 25% and WUE increased by 80 -

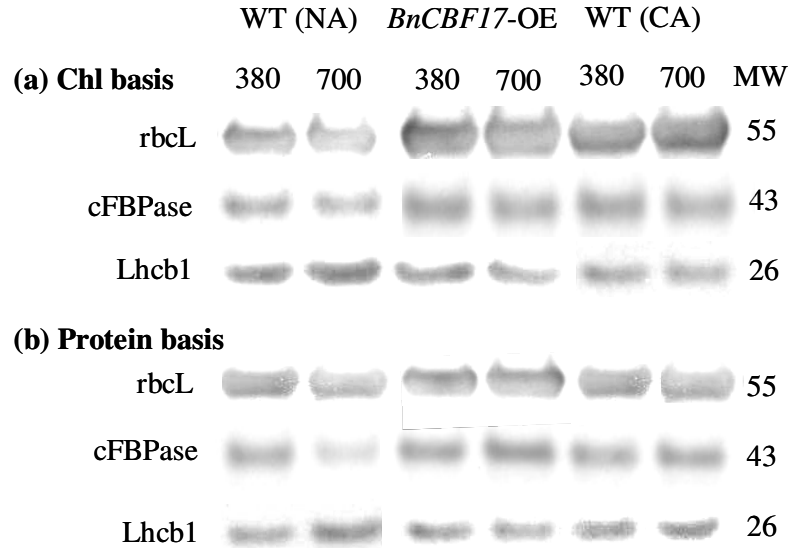


Fig. 4.6. Immunoblot analysis of SDS – PAGE probed with antibodies raised against: rbcL, cFBPase and Lhcb1, isolated from cold acclimated (CA) and non-acclimated (NA) wild type (WT) and *BnCBF17*-OE grown at either ambient (380 $\mu\text{mol C mol}^{-1}$) or elevated (700 $\mu\text{mol C mol}^{-1}$) CO_2 and at either 20/16°C (NA) or 5/5°C (CA). Lanes of SDS – PAGE were loaded on either equal Chl (a, 0.5 $\mu\text{g/lane}$) or on equal protein basis (5 $\mu\text{g protein/lane}$). The bovine serum albumin (1 $\mu\text{g/lane}$) was used as an internal control. Numbers on the right indicate molecular weight (MW, kDa) of markers

Table 4.2. Effects of cold acclimation and elevated CO₂ on stomatal characteristics of WT and *BnCBF17*-over-expressing *B. napus* grown at either ambient (380 μmol C mol⁻¹) or elevated (700 μmol C mol⁻¹) CO₂ and at either 20/16°C (Non-acclimated) or 5/5°C (Cold acclimated). All measurements were carried out on fully developed third leaves at their respective growth CO₂ at 20°C. Data represent the mean of three plants from three different pots ± SD. Significant differences of the means are indicated by the superscripted letters ($P \leq 0.05$)

Stomatal characteristics	Wild type (NA)		<i>BnCBF17</i> -OE		Wild type (CA)	
	380	700	380	700	380	700
Stomatal conductance (gs (mol m ⁻² s ⁻¹))	0.33 ± 0.02 ^c	0.21 ± 0.03 ^{ab}	0.37 ± 0.03 ^c	0.30 ± 0.04 ^c	0.26 ± 0.02 ^b	0.17 ± 0.04 ^a
Stomatal frequency (stomates mm ⁻² LA)						
Adaxial	77 ± 6 ^b	47 ± 8 ^a	175 ± 23 ^c	45 ± 6 ^a	67 ± 9 ^b	48 ± 7 ^a
Abaxial	153 ± 12 ^b	84 ± 11 ^a	240 ± 34 ^d	76 ± 7 ^a	125 ± 2 ^c	63 ± 14 ^a
Transpiration (mmol H ₂ O m ⁻² s ⁻¹)	2.16 ± 0.10 ^c	1.68 ± 0.14 ^{ab}	2.29 ± 0.11 ^c	1.87 ± 0.16 ^b	1.74 ± 0.19 ^{ab}	1.52 ± 0.12 ^a
Water Use Efficiency (WUE, A/gS)	48 ± 6 ^a	104 ± 8 ^c	63 ± 4 ^b	114 ± 16 ^c	87 ± 13 ^c	168 ± 31 ^d

115% (Table 4.2). It appears that the increased WUE induced by either cold acclimation or elevated CO₂ is primarily associated with an increase in light-saturated rates of CO₂ assimilation and a decrease in stomatal conductance in response to growth at either low temperature or under elevated CO₂.

The data in Table 4.2 indicate that the cold acclimation or elevated CO₂-induced suppression of stomatal conductance can be accounted for, in part, by a decrease in stomatal density on both the abaxial and adaxial leaf surfaces in response to growth at either low temperature or under elevated CO₂. For instance, cold acclimated WT exhibited about a 20% decrease in adaxial as well as abaxial stomatal densities as compared to non-acclimated WT. Similarly, elevated CO₂ decreased adaxial as well as abaxial stomatal densities by 30-75% relative to those of at ambient CO₂ for all Brassica plants tested (Table 4.2).

4.3.8 Dark respiratory rates

The *BnCBF17*-over-expressing line of *B. napus* exhibited a 22% increase in the dark respiratory rates (R_{dark}) as compared to non-acclimated WT at ambient CO₂ (Table 4.1). R_{dark} observed for the *BnCBF17*-OE was comparable to that of cold acclimated WT at ambient CO₂. The R_{dark} increased by 20-35% in non-acclimated WT, cold acclimated WT and *BnCBF17*-OE at elevated CO₂ relative to at ambient CO₂ (Table 4.1).

4.4 Discussion

Compared to non-acclimated WT, *BnCBF17*-OE grown at 20°C mimicked cold acclimated WT *B. napus* with respect to compact dwarf phenotype (Figure 4.1), increased SLW (Table 4.1), increased photosynthetic capacity (Figure 4.2), increased ETR as a function of irradiance (Figure 4.4) and C_i (Figure 4.5), improved WUE (Table 4.1) and enhanced levels of key photosynthetic enzymes and components of photosynthetic electron transport (Figure 4.6). These results are consistent with an increased quantum requirement to close PSII reaction centers and to induce energy dissipation by NPQ (Figure 4.4) coupled with a lower C_i requirement to open PSII reaction centers and a lower propensity to dissipate absorbed energy through NPQ under CO₂ saturated

conditions (Figure 4.5). Consequently, *BnCBF17*-OE and cold acclimated WT *B. napus* exhibited a lower excitation pressure for a given irradiance and a given CO₂ concentration, and thus, a greater capacity to keep Q_A oxidized compared to non-acclimated WT *B. napus*. This indicates that compared to non-acclimated WT, *BnCBF17*-OE as well as cold acclimated WT *B. napus* exhibit an enhanced capacity to utilize absorbed light energy and convert it to biomass as reflected in an increase in SLW with a concomitant decreased reliance on NPQ to dissipate absorbed energy for photoprotection. Thus, we show that over-expression of *BnCBF17* as well as cold acclimation enhances photosynthetic energy conversion efficiency into biomass in *B. napus* coupled with enhanced WUE during long-term growth at either ambient or elevated CO₂ conditions. We suggest that the enhanced photosynthetic capacity and energy conversion efficiency of *BnCBF17*-OE as well as cold acclimated WT relative to non-acclimated WT *B. napus* can be explained, in part, by the enhanced abundance, on a chlorophyll basis, of major regulatory photosynthetic enzymes such as stromal-localized Rubisco (rbcL) and cytosolic FBPase (cFBPase) important in regulating sucrose biosynthesis as well as components of the thylakoid membrane represented by Lhcb1 (Fig 6a). We suggest that the increased protein / Chl ratio (Table 4.1) reflects an increase in components of the thylakoid photosynthetic electron transport chain, Calvin cycle enzymes involved in the assimilation of CO₂ as well as cytosolic sucrose biosynthetic enzymes on a leaf area basis. These results for the *BnCBF17*-OE and cold acclimated *B. napus* are comparable to the enhanced photosynthetic performance reported recently for cold acclimated winter wheat and winter rye (Dahal et al. 2012). In the cold acclimated winter cereals, the enhanced photosynthetic performance was shown to be due to increased levels of photosynthetic proteins (eg. rbcL, psbA, psaA, cFBPase, Lhcb1) per leaf area combined with a decrease in the low temperature sensitivity of ETR and CO₂ assimilation (Dahal et al. 2012). *BnCBF17*-OE also exhibited similar low temperature insensitivity for ETR and CO₂ assimilation as did the cold acclimated winter cereals (Dahal et al. 2012). Therefore, we suggest that the enhanced photosynthetic performance and energy conversion efficiency of *BnCBF17*-OE and cold acclimated WT *B. napus* is due to increased levels of photosynthetic proteins per unit leaf area combined with a decrease in the low temperature sensitivity of ETR and CO₂ assimilation. This is

consistent with the report of Savitch et al. (2005) who reported that the *BnCBF17*-OE exhibited significant enhancement for the gene expression as well as enzyme activities of Rubisco, SPS and cFBPase. Thus, CBFs/DREBs appear to be critical factors that govern plant phenotypic plasticity associated with cold acclimation from the level of gene expression and freezing tolerance to whole plant architecture, WUE as well as photosynthetic energy conversion efficiency into biomass.

Sensitivity to feedback inhibition of photosynthesis at elevated CO₂ level can be assessed by comparing CO₂ assimilation of elevated versus ambient CO₂-grown plants measured at the same CO₂ concentration. The light response curves as well as CO₂ response curves clearly indicate that the growth and development of non-acclimated WT *B. napus* at elevated CO₂ significantly inhibited the light and CO₂-saturated rates of photosynthesis, with minimal changes in carboxylation efficiency, as compared to growth and development at ambient CO₂ (Figure 4.3a). This was consistent with the decreased CO₂-saturated rates of electron transport (Figure 4.4a) combined with decreased levels of major photosynthetic enzymes such as rbcL, cFBPase (Figure 4.6) as well as the maximum carboxylation velocity of Rubisco in elevated versus ambient CO₂-grown non-acclimated WT (Table 4.1). Consequently, the EP and NPQ at any given irradiance and CO₂ concentration increased significantly for non-acclimated WT in response to growth at elevated CO₂ (Figure 4.4, Figure 4.5). In contrast, *BnCBF17*-OE as well as cold acclimated WT did not exhibit inhibition of light and CO₂-saturated rates of photosynthesis in response to growth at elevated CO₂ (Figure 4.2, Figure 4.3). This was consistent with no changes in the light and CO₂-saturated rates of electron transport, excitation pressure and NPQ (Figure 4.4, Figure 4.5) and levels of rbcL and cFBPase (Figure 4.6) as well as the maximum carboxylation velocity of Rubisco (Table 4.1) in elevated versus ambient CO₂-grown *BnCBF17*-OE and cold acclimated WT *B. napus*. Thus, we report that the cold acclimated *B. napus* and the *BnCBF17*-OE are able to maintain enhanced photosynthetic performance and energy conversion into biomass even under long-term growth and development at elevated CO₂. This appears to be due to a decreased sensitivity to feedback limited photosynthesis in *BnCBF17*-OE as well as cold acclimated *B. napus* relative to non-acclimated WT plants.

How does *BnCBF17* over-expression and cold acclimation of WT *B. napus* differentially affect sensitivity to feedback inhibition of photosynthesis at elevated CO₂? Our results indicate that the *BnCBF17*-OE as well as cold acclimated WT exhibit a 1.7 - 1.9-fold higher specific leaf weight relative to non-acclimated WT at elevated CO₂ (Table 4.1). We have further shown that *BnCBF17*-over-expression as well as cold acclimation results in the enhanced amounts of rbcL and cFBPase (Figure 4.6) when corrected on a leaf area basis not only at ambient CO₂ but also at elevated CO₂. This is consistent with our previous reports that cold acclimation of winter cereals induces an increase in the amount of Rubisco and cFBPase with a concomitant stimulation of respiration and plant biomass production (Chapter 2). Furthermore, Savitch et al. (2005) reported that over-expression of *BnCBF17* in *B. napus* not only enhanced gene expression of the triose-P translocator and cFBPase but also increased the activity of Rubisco, cFBPase and SPS. Consequently, *BnCBF17*- over-expression as well as cold acclimation of *B. napus* result in enhanced P_i cycling and increased capacity for RuBP regeneration through increased utilization of phosphorylated intermediates. Thus, we suggest that the decreased sensitivity to feedback limited photosynthesis in cold acclimated *B. napus* as well as the *BnCBF17*-OE under conditions of elevated CO₂ reflects an improved capacity to maintain a high flux of carbon between source and sink even under elevated CO₂ conditions. This is further supported by the fact that in cereals, carbon export rates from source leaves to sink are also enhanced upon cold acclimation (Leonardos et al. 2003).

The improved WUE induced by either *BnCBF17*- over-expression or cold acclimation is primarily associated with an increase in A_{sat} and decrease in stomatal conductance. It appears that the suppressed stomatal conductance observed upon cold acclimation or *BnCBF17*- over-expression can be accounted for, in part, by a decrease in stomatal density on both the abaxial and adaxial leaf surfaces.

We conclude that the over-expression of *BnCBF17* and cold acclimation of *B. napus* enhances photosynthetic performance, the efficiency of energy conversion and WUE which is maintained even after long-term growth and development under elevated CO₂ conditions. Thus, we suggest that the transcription factor, *BnCBF17*, may be a central component which governs the regulation of photosynthetic capacity and energy

conversion efficiency of crop plants. This may provide important new insights into potential molecular and genetic approaches focussed on the maintenance or even the enhancement of plant productivity under suboptimal growth conditions associated with climate change.

Acknowledgements

This work was supported, in part, by the Natural Sciences and Engineering Research Council (NSERC) and industrial and government partners, through the Green Crop Research Network (GCN). NPAH also acknowledges research support through an individual NSERC Discovery Grant.

4.5 References

- Adams III WW, Demmig-Adams B, Rosenstiel TN, Brightwell AK, Ebbert V (2002) Photosynthesis and photoprotection in overwintering plants. *Plant Biol* 4: 545-557
- Ainsworth EA, Rogers A (2007) The response of photosynthesis and stomatal conductance to rising CO₂: mechanisms and environmental interactions. *Plant Cell Environ* 30: 258-270
- Arnon DI (1949) Copper enzymes in isolated chloroplasts. Polyphenoloxidases in *Beta vulgaris*. *Plant Physiol* 24: 1-15
- Arp WJ (1991) Effects of source–sink relations on photosynthetic acclimation to elevated CO₂. *Plant Cell Environ* 14: 869-875
- Badawi M, Reddy YV, Agharbaoui Z, Tominaga Y, Danyluk J, Sarhan F, Houde M (2008) Structure and functional analysis of wheat *ICE* (Inducer of CBF Expression) genes. *Plant Cell Physiol* 49: 1237-1249
- Boese SR, Hüner NPA (1990) Effect of growth temperature and temperature shifts on spinach leaf morphology and photosynthesis. *Plant Physiol* 94: 1830-1836
- Boese SR, Hüner NPA (1992) Developmental history affects the susceptibility of spinach leaves to in vivo low temperature photoinhibition. *Plant Physiol* 99: 1141-1145
- Cheng SH, Moore BD, Seemann JR (1998) Effects of short and long-term elevated CO₂ on the expression of Ribulose-1,5-bisphosphate carboxylase/oxygenase genes and

- carbohydrate accumulation in leaves of *Arabidopsis thaliana* (L.) Heynh. *Plant Physiol* 116: 715-723
- Chinnusamy V, Zhu J, Zhu JK (2007) Cold stress regulation of gene expression in plants *Trends Plant Sci* 12: 1360-1385
- Dahal K, Kane K, Gadapati W, Webb E, Savitch LV, Singh J, Sharma P, Sarhan F, Longstaffe FJ, Grodzinski B, Hüner NPA (2012) The effects of phenotypic plasticity on photosynthetic performance in winter rye, winter wheat and *Brassica napus*. *Physiol Plant* 144: 169-188
- Drake BG, González-Meler MA, Long SP (1997) More efficient plants: a consequence of rising atmospheric CO₂? *Annu Rev Plant Physiol Plant Mol Biol* 48:609–639
- Ensminger I, Busch F, Hüner NPA (2006) Photostasis and cold acclimation: sensing low temperature through photosynthesis. *Physiol Plant* 126: 28-44
- Farquhar GD, von Caemmerer S, Berry JA (1980) A biochemical model of photosynthetic CO₂ assimilation in leaves of C₃ species. *Planta* 149: 78-90
- Foyer C (1990) The effect of sucrose and mannose on cytoplasmic protein phosphorylation sucrose phosphate synthetase activity and photosynthesis in leaf protoplasts from spinach. *Plant Physiol Biochem* 28: 151–160
- Gilmour SJ, Fowler SG, Thomashow MF (2000) Arabidopsis transcriptional activators CBF1, CBF2 and CBF3 have matching functional activities. *Plant Mol Biol* 54: 767-781
- Gilmour SJ, Sebolt AM, Salazar MP, Everard JD, Thomashow MF (2004) Over-expression of the Arabidopsis CBF3 transcriptional activator mimics multiple biochemical changes associated with cold acclimation. *Plant Physiol* 124: 1854-1865
- Gorsuch PA, Pandey S, Atkin OK (2010a) Thermal de-acclimation: how permanent are leaf phenotypes when cold-acclimated plants experience warming? *Plant Cell Environ* 33: 1124-1137
- Gorsuch PA, Pandey S, Atkin OK (2010b) Temporal heterogeneity of cold acclimation phenotypes in Arabidopsis leaves. *Plant Cell Environ* 33: 244-258
- Gray GR, Chauvin LP, Sarhan F, Hüner NPA (1997) Cold acclimation and freezing tolerance. A complex interaction of light and temperature. *Plant Physiol* 114: 467-474

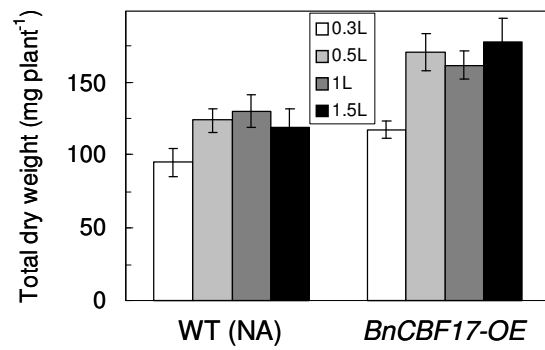
- Guy CL (1990) Cold acclimation and freezing tolerance: role of protein metabolism. *Ann Rev Plant Physiol Plant Mol Biol* 41: 187-223
- Harley PC, Sharkey TD (1991) An improved model of C₃ photosynthesis at high CO₂: reversed O₂ sensitivity explained by lack of glycerate re-entry into the chloroplast. *Photosynth Res* 27: 169-178
- Hüner NPA (1985) Morphological, anatomical and molecular consequences of growth and development at low temperature in *Secale cereale* L. cv Puma. *Amer J Bot* 72: 1290-1306
- Hüner NPA, Öquist G, Sarhan F (1998) Energy balance and acclimation to light and cold. *Trend Plant Sci* 3: 224-230
- Hüner NPA, Öquist G, Hurry VM, Krol M, Falk S, Griffith M (1993) Photosynthesis, photoinhibition and low temperature acclimation in cold tolerant plants. *Photosyn Res* 37: 19-39
- Hüner NPA, Palta JP, Li PH, Carter JV (1981) Anatomical changes in leaves of Puma rye in response to growth at cold hardening temperatures. *Bot Gaz* 142: 55-62
- Hurry V, Strand A, Furbank R, Stitt M (2000) The role of inorganic phosphate in the development of freezing tolerance and the acclimatization of photosynthesis to low temperature is revealed by the pho mutants of *Arabidopsis thaliana*. *Plant J* 24: 383-96
- Kasuga M, Liu Q, Miura S, Yamaguchi-Shinozaki K, Shinozaki K (1999) Improving plant drought, salt, and freezing tolerance by gene transfer of a single stress-inducible transcription factor. *Nat Biotech* 17: 287-291
- Kramer PJ (1981) Carbon dioxide concentration, photosynthesis and dry matter production. *Bio Sci* 31: 29-33
- Krause GH (1988) Photoinhibition of photosynthesis. An evaluation of damaging and protective mechanisms. *Physiol Plant* 74: 566-74
- Leonardos ED, Savitch LV, Hüner NPA, Öquist G, Grodzinski B (2003) Daily photosynthetic and C-export patterns in winter wheat leaves during cold stress and acclimation. *Plant Physiol* 117: 521-531
- Liu Q, Kasuga M, Sakuma Y, Abe H, Miura S, Yamaguchi-Shinozaki K, Shinozaki K (1998) Two transcription factors, DREB1 and DREB2, with an EREBP/AP2 DNA

- binding domain separate two cellular signal transduction pathways in drought- and low-temperature-responsive gene expression, respectively, in *Arabidopsis*. *Plant Cell* 10: 1391-1406
- Long SP, Ainsworth EA, Rogers A, Ort DR (2004) Rising atmospheric carbon dioxide: plants FACE the future. *Ann Rev Plant Biol* 55: 591-628
- Moore BD, Cheng SH, Sims D, Seemann JR (1999) The biochemical and molecular basis for photosynthetic acclimation to elevated atmospheric CO₂. *Plant Cell Environ* 22: 567-582
- Navarro M, Ayax C, Martinez Y, Laur J, Kayal WEI, Marque C, Teulieres C (2011) Two EguCBF1 genes over-expressed in *Eucalyptus* display a different impact on stress tolerance and plant development. *Plant Biotech J* 9: 50-63
- Öquist G, Hüner NPA (2003) Photosynthesis of overwintering evergreen plants. *Ann Rev Plant Biol* 54: 329-355
- Öquist G, Hurry VM, Hüner NPA (1993) Low-temperature effects on photosynthesis and correlation with freezing tolerance in spring and winter cultivars of wheat and rye. *Plant Physiol* 101: 245-250
- Pino M-T, Skinner JS, Jeknic Z, Hayes PM, Soeldner AH, Thomashow MF, Chen THH (2008) Ecotopic *AtCBF1* overexpression enhances freezing tolerance and induces cold acclimation-associated physiological modifications in potato. *Plant Cell Environ* 31: 393-406
- Pocock TH, Hurry VM, Savitch LV, Hüner NPA (2001) Susceptibility to low-temperature photoinhibition and the acquisition of freezing tolerance in winter and spring wheat: The role of growth temperature and irradiance. *Physiol Plant* 113:499-506
- Sarhan F, Ouellet F, Vazquez-Tello A (1997) The wheat *Wcs120* gene family: a useful model to understand the molecular genetics of freezing tolerance in cereals. *Physiol Plant* 101: 439-445
- Savitch LV, Allard G, Seki M, Robert LS, Tinker NA, Hüner NPA, Shinozaki K, Singh J (2005) The effect of over-expression of two Brassica CBF/DREB1-like transcription factors on photosynthetic capacity and freezing tolerance in *Brassica napus*. *Plant Cell Physiol* 46: 1525-1539

- Savitch LV, Barker-Astrom J, Ivanov A G, Hurry V, Oquist G, Hüner NPA (2001) Cold acclimation of *Arabidopsis thaliana* results in incomplete recovery of photosynthetic capacity which is associated with an increased reduction of the chloroplast stroma. *Planta* 214: 295-301
- Sharkey TD, Vanderveer PJ (1989) Stromal phosphate concentration is low during feedback limited photosynthesis. *Plant Physiol* 91: 679–684
- Somersalo S, Krause GH (1989) Photoinhibition at chilling temperatures: Fluorescence characteristics of unhardened and cold-hardened spinach leaves. *Planta* 177:409-416
- Stitt M, Hurry VM (2002) A plant for all seasons: alterations in photosynthetic carbon metabolism during cold acclimation in *Arabidopsis*. *Curr Opin Plant Biol* 5: 199-206
- Stitt M, Quick WP (1989). Photosynthetic carbon partitioning: its regulation and possibilities for manipulation. *Physiol Plant* 77: 633-641
- Strand A, Hurry VM, Henkes S, Hüner NPA, Gustafsson P, Gardeström P, Stitt M (1999) Acclimation of *Arabidopsis* leaves developing at low temperatures. Increasing cytoplasmic volume accompanies increased activities of enzymes in the Calvin cycle and in the sucrose-biosynthesis pathway. *Plant Physiol* 119: 1387-1398
- Tcherkez GGB, Farquhar GD, Andrews TJ (2006). Despite slow catalysis and confused substrate specificity, all ribulose biphosphate carboxylases may be nearly perfectly optimized. *Proc Nat Acad Sci* 103: 7246–7251
- Van Buskirk HA, Thomashow MF (2006) *Arabidopsis* transcription factors regulating cold acclimation. *Physiol Plant* 126:72-80
- Yang J-S, Wang R, Meng J-J, Bi Y-P, Xu P-L, Guo F, Wan S-B, He Q-W, Li X-G (2010) Overexpression of *Arabidopsis* CBF1 gene in transgenic tobacco alleviates photoinhibition of PSII and PSI during chilling stress under low irradiance. *J Plant Physiol* 167: 534-539
- Zhang X, Fowler SG, Cheng H, Lou Y, Rhee SY, Stockinger EJ, Thomashow MF (2004) Freezing-sensitive tomato has a functional CBF cold responsive pathway but a CBF regulon that differs from that of freezing tolerant *Arabidopsis*. *Plant J* 39: 905-919

4.6 Appendices

Appendix 4S1. Effects of pot size on total dry matter accumulation of non-acclimated WT and *BnCBF17-OE Brassica napus* grown at elevated CO₂ (700 $\mu\text{mol C mol}^{-1}$)



Chapter 5

Cold acclimated winter wheat and winter rye maintain enhanced photosynthetic performance, energy conversion efficiency and grain yield under long-term growth at elevated CO₂

5.1 Introduction

The effects of low cold hardening temperatures on the physiological, morphological and biochemical levels have been the subject of much research over the past few decades. Although cold-sensitive spring wheat (Hurry and Hüner 1991, Dahal et al. 2012a, 2012b), spring rye (Dahal et al. 2012a, 2012b), spring rape (Hurry et al. 1995) and tomato (Yakir et al. 1986, Sassernath and Ort 1990) can grow and develop at low cold hardening temperatures, they exhibit decreased photosynthetic capacity, estimated as the light-saturated rates of carbon assimilation (A_{sat}), during cold acclimation. The inhibition of photosynthetic capacity of cold acclimated spring cultivars is associated with limited sink strength and subsequent retardation of carbon export to the sinks in response to low growth temperature (Hurry et al. 1995). Consequently, cold acclimated spring cereals exhibit a reduction in sucrose synthesis and thus, decrease in utilization of phosphorylated intermediates and cytosolic P_i recycling which leads to feedback-limited photosynthesis (Hurry et al. 1995, Savitch et al. 2002). In addition, spring cultivars are susceptible to photoinhibition of photosynthesis induced by low growth temperature (Hüner et al. 2003, Hurry et al. 1995, Pockock et al. 2001) and are unable to overwinter (Sarhan et al. 1997).

In contrast, cold tolerant winter wheat, winter rye, barley, spinach, as well as *Arabidopsis thaliana*, and *Brassica napus* are able to maintain net CO₂ assimilation rates during cold acclimation that are comparable to or significantly higher than those rates observed for their NA controls (Krause 1988, Hüner et al. 1998, Adams et al. 2002, Stitt and Hurry 2002, Öquist and Hüner 2003, Ensminger et al. 2006, Dahal et al. 2012a, 2012b).

The cold acclimation-induced stimulation in A_{sat} of cold-tolerant herbaceous species, winter wheat, winter rye, *Arabidopsis thaliana*, and *Brassica napus* is, by and large, associated with increased specific leaf weight (Savitch et al. 2005, Dahal et al. 2012a) and enhanced activities of key regulatory photosynthetic and sucrose biosynthetic enzymes such as Rubisco, cFBPase, and SPS in response to low growth temperatures (Hurry et al. 2000, Stitt and Hurry 2002, Savitch et al. 2005). In addition, winter cultivars of wheat and rye (Savitch et al. 2002, Leonardos et al. 2003) and *Arabidopsis thaliana* (Stitt and Hurry 2002) have an ability to enhance sink capacity and concomitant carbon export to the sinks during cold acclimation. These cultivars store photosynthates as sucrose or fructans in the crown tissue as well as in the leaf vacuoles during cold acclimation. Concomitantly, cold acclimated winter wheat also exhibits a partial stimulation of carbon export from source leaf to sink and a two-fold increase in water use efficiency (Leonardos et al. 2003, Dahal et al. 2012a).

It has been well documented that cold tolerant species such as winter rye (Hüner et al. 1981, 1985, Dahal et al. 2012a), winter wheat (Dahal et al. 2012a), spinach (Boese and Hüner, 1990) as well as *Arabidopsis thaliana* (Strand et al. 1999, Gorsuch et al. 2010a, 2010b) and *Brassica napus* (Savitch et al. 2005) exhibit compact, dwarf growth habit with leaves that possess increased thickness relative to NA controls. The increased leaf thickness associated with the cold acclimated state can be accounted for by either increases in leaf mesophyll cell size (Hüner et al. 1981, Gorsuch et al. 2010a) and/or increases in the number of palisade mesophyll layers (Boese and Hüner 1990, Dahal et al. 2012a).

In addition, these changes at the physiological, biochemical and molecular levels during cold acclimation are associated with differential freezing tolerance in cold-tolerant versus cold-sensitive species (Pocock et al. 2001). Molecular and biochemical analyses have revealed that cold acclimation of *Arabidopsis thaliana*, barley, wheat and *Brassica napus* (Sarhan et al. 1997, Thomashow 2001, Savitch et al. 2005, Chinnuswamy et al. 2007, Rapacz et al. 2008) induces the expression of cold-regulated (COR) genes and subsequent accumulation of corresponding proteins associated with freezing tolerance. In fact, there is a strong, positive correlation between the cold acclimation-induced

stimulation in A_{sat} and the development of freezing tolerance measured as LT50, as well as an increased resistance to low temperature-induced photoinhibition in spinach (Krause 1988, Guy 1990, Boese and Hüner 1992), winter rye and winter wheat (Öquist et al. 1993, Gray et al. 1996, Pockock et al. 2001), *Arabidopsis thaliana* (Savitch et al. 2001) and *Brassica napus* (Savitch et al. 2005).

Short-term shift of C_3 species from ambient to elevated CO_2 results in an immediate stimulation of rates of CO_2 assimilation (Cheng et al. 1998, Long et al. 2004, Ainsworth and Rogers 2007, Dahal et al. 2012b). This stimulation of photosynthesis in C_3 plants due to elevated CO_2 results for two reasons. First, the $K_m(\text{CO}_2)$ for Rubisco is close to the current atmospheric CO_2 concentration (Long et al. 2004, Tcherkez et al. 2006) which indicate that Rubisco is CO_2 substrate-limited at ambient CO_2 . Thus, an immediate increase in carboxylation velocity can be expected by increased CO_2 substrate availability. Second, elevated CO_2 competitively inhibits photorespiration because CO_2 is a competitive inhibitor of the oxygenation of RuBP by Rubisco (Long et al. 2004).

In contrast to the short-term shift, long-term growth and development of plants at elevated CO_2 may lead to feedback inhibition of photosynthetic capacity due to accumulation of non-structural carbohydrates in the cytosol (Stitt and Quick 1989, Foyer 1990). It has been suggested that the increased carbon uptake resulting from initial enhancement of photosynthesis alters the balance between supply and demand due to limited sink capacity to utilize photosynthates for growth. Concomitantly, the amount of non-structural carbohydrates substantially increases in the cytosol due to retarded export of photosynthates to the sinks (Kramer 1981, Arp 1991, Drake et al. 1997). This results in inhibition of sucrose synthesis and short-term decrease in utilization of phosphorylated intermediates and P_i regeneration limitation in the cytosol. This may subsequently lead to depletion of stromal P_i due to reduced exchange of triose-P for P_i across the chloroplast. Low availability of stromal P_i inhibits ATP synthesis and subsequent RuBP regeneration and eventually feedback inhibition of photosynthesis (Stitt and Quick 1989, Sharkey and Vardaveer 1989). The low availability of stromal P_i may also lead to decreased activation state of Rubisco (Crafts-Brandner and Salvucci 2000). An alternate concept is that, in the long-term, the feedback inhibition of photosynthetic capacity is attributed to the

decreased transcript levels of major photosynthetic genes and subsequent amount and activities of corresponding proteins (Drake et al. 1997, Moore et al. 1999). Long et al. (2004) has suggested a sucrose cycling model for molecular control of Rubisco protein content. The increased level of sucrose in the source leaf is sensed by vacuolar invertase which hydrolyses sucrose to hexose (Long et al. 2004). The hexose stimulates the hexokinase sensing system that phosphorylates hexose to hexose-P which is used to resynthesize sucrose (Long et al. 2004). This hexokinase reduces Rubisco content by downregulation of *rbcL/S* gene expression at the levels of transcription, post-transcription, translation and post-translation (Webber et al. 1994, Long et al. 2004). This is reflected in decreased carboxylation efficiency in addition to decreased CO₂-saturated photosynthetic capacity (Drake et al. 1997, Moore et al. 1999).

It has been suggested that any factors that limit sink strength lead to a greater extent of feedback inhibition of photosynthesis induced by long-term growth at elevated CO₂. The development of sink capacity of a plant is primarily determined by its genetic makeup, environmental factors and experimental design. One of the most limiting experimental factors is the pot size. It has been reported that the feedback inhibition of photosynthetic CO₂ assimilation at elevated CO₂ would be severe in plants grown in small pot size due to inadequate sink size and rooting volume constraints (Arp 1991, Thomas and Strain 1991, Long et al. 2004, Ainsworth and Rogers 2007).

Earlier studies have suggested that cold acclimation of winter cereals enhances the light-saturated rates of CO₂ assimilation and energy conversion efficiency relative to NA controls at ambient CO₂ (Dahal et al. 2012a, 2012b). Can cold acclimated winter cereals maintain high A_{sat} and energy conversion efficiency under long-term growth and development at elevated CO₂ relative to non-acclimated controls? The feedback inhibition of photosynthesis induced by long-term growth and development at elevated CO₂ has been reported in a wide range of plant species grown under normal temperature (Long et al. 2004, Ainsworth and Rogers 2007). Does cold acclimation of winter wheat and rye decrease sensitivity to elevated CO₂-induced feedback inhibition of photosynthetic capacity? Since CA winter wheat and winter rye exhibit enhanced sink capacity and subsequent P_i recycling and RuBP regeneration as well as increased

activities of major photosynthetic enzymes and components of photosynthetic electron transport (Hurry 1995, Dahal et al. 2012a), I hypothesize first that, cold acclimation-induced increase in A_{sat} and energy conversion efficiency of winter wheat and rye at ambient CO_2 is maintained under long-term growth and development at elevated CO_2 . Second, cold acclimation of winter wheat and winter rye decreases the sensitivity to elevated CO_2 -induced feedback inhibition of photosynthetic capacity. I further hypothesize that cold acclimated spring cereals exhibit a decrease in photosynthetic capacity and energy conversion efficiency relative to non-acclimated controls upon long-term growth at elevated CO_2 .

To test our hypotheses, I compared CO_2 gas exchange rates and energy conversion efficiency coupled with photosynthetic gene expression assessed through Affymetrix wheat micro-array as well as polypeptide accumulation in NA and CA winter cultivars of wheat and rye grown at either ambient CO_2 ($380 \mu\text{mol C mol}^{-1}$) or at elevated CO_2 ($700 \mu\text{mol C mol}^{-1}$).

5.2 Materials and methods

5.2.1 Plant materials and growth conditions

Seeds of winter (cv Musketeer) and spring (cv SR4A) rye (*Secale cereale* L.) and winter (cv Norstar) and spring (cv Katepwa) wheat (*Triticum aestivum* L.) cultivars were grown in the controlled environmental growth chambers (Model: GCW15 chamber, Environmental Growth Chambers, Chagrin Falls, OH, USA) at either ambient CO_2 ($380 \pm 10 \mu\text{mol C mol}^{-1}$) or at elevated CO_2 ($700 \pm 25 \mu\text{mol C mol}^{-1}$). Non-acclimated (NA) plants were grown at day/night temperature regimes of 20/16°C and those of cold acclimated (CA) at 5/5°C from seed sowing. The plants were grown at a PPFD of $250 \pm 20 \mu\text{mol photons m}^{-2} \text{ s}^{-1}$, 50% to 60% relative humidity and a 16/8 hr photoperiod. The CO_2 concentrations in the growth chamber were monitored continuously with a computer-controlled CO_2 infra-red gas analyzer (Model: WMA-4 CO_2 Analyzer, PP Systems International, Inc. Amesbury, MA, USA) installed on each CO_2 growth chamber. In addition, the temperature, relative humidity, irradiance level and photoperiod in each chamber were computer-controlled and monitored continuously. The

seedlings were grown in coarse vermiculite in 4 L-sized plastic pots at a density of three plants per pot and fertilized with Hoagland solution.

5.2.2 Pot size experiment

To assess the potential effects of pot size on plant biomass, the NA and CA Musketeer were grown in pots of varying volume (0.5 L, 2 L, 4 L and 6 L) at either ambient ($380 \pm 10 \mu\text{mol C mol}^{-1}$) or elevated ($700 \pm 25 \mu\text{mol C mol}^{-1}$) CO_2 at growth conditions described above. Root and shoot biomass were harvested from 25-d-old NA and 75-d-old CA Musketeer, and the tissues were dried at 80°C in order to get dry weight.

5.2.3 Comparative growth kinetics

Comparative growth kinetics were performed to assess the effects of elevated CO_2 on growth characteristics and to ensure that NA and CA plants were assessed at a comparable physiological stage of development for photosynthetic measurements as well as biochemical analyses. Regardless of growth CO_2 , NA plants were harvested every week and CA plants every two weeks until the flag leaves were fully developed. Total tiller number, leaf number and leaf blade area were recorded on each harvest. Total root and shoot fresh biomass were weighed, and the tissues were dried at 80°C to constant weight for the determination of dry weight. Exponential growth rates ($\text{g g}^{-1} \text{dry mass day}^{-1}$) were calculated from the plots of the natural logarithm (\ln) of shoot dry mass over time in days. Specific leaf weight (SLW) was calculated as leaf dry weight in g m^{-2} leaf blade area. Leaf blade area was measured by using a LI-COR portable area meter (LI-3000A, LI-COR Biosciences, Lincoln, NE, USA). Chlorophyll a and b were determined according to Arnon (1949).

5.2.4 CO_2 gas exchange measurements

CO_2 gas exchange rates were measured on fully expanded third leaves of 25-d-old NA and 75-d-old CA plants for all four cultivars irrespective of growth CO_2 . At these ages, the NA and CA plants were at comparable physiological stages of development based on growth kinetics. All measurements of CO_2 gas exchange rates were carried out on fully expanded third leaves at either 380 or $700 \mu\text{mol C mol}^{-1}$ and at a measuring temperature

of 20°C regardless of growth temperature. CO₂ gas exchange rates were measured by using a LI-COR portable infrared CO₂ gas analyzer (LI-6400 XRT Portable Photosynthesis System, LI-COR Biosciences, Lincoln, NE, USA). The apparent maximum quantum efficiency (Q) and the maximal photosynthetic capacity (A_{sat}) were determined as the maximum initial slope and the maximum light-saturated rates respectively from the light response curves supplying 12 irradiance values over the range of 0 to 1500 μmol photons m⁻² s⁻¹ PPFD. Light response curves were measured from high to low light intensity with 8 min of waiting time between each measurement. CO₂ response curves were measured by providing 11 different CO₂ values over the range of 50 to 1200 μmol C mol⁻¹ at a saturating irradiance of 1300 μmol photons m⁻² s⁻¹ PPFD. Rubisco-limited carboxylation efficiency (CE) was calculated as the maximum initial slope and the CO₂-saturated photosynthesis as the plateau of the CO₂ response curves. The maximum Rubisco carboxylation capacity (V_{cmax}) and the maximum rates of electron transport for CO₂ gas exchange (J_{max}) were calculated using the FCB photosynthesis model (Farquhar et al. 1980). Respiration rates (R_{dark}) were measured in the dark. Measurements were made inside the CO₂ enriched chambers, to reduce diffusion errors through the leaf blade and chamber seals (Jahnke 2001, Jahnke and Krewitt 2002). In addition, stomatal conductance and leaf transpiration rates were measured simultaneously with CO₂ gas exchange measurements at either 380 or 700 μmol C mol⁻¹ and at 20°C regardless of growth temperature. Leaf water use efficiency was calculated as μmol CO₂ fixed per mol of stomatal conductance (A/g_s). Stomatal density was estimated on both adaxial and abaxial leaf surface using a stage micrometer (1mm²) on a microscope (Leica ATC™ 2000, Buffalo, NY, USA). Stomata were counted at a magnification of 100X.

5.2.5 Room temperature Chl a fluorescence

In vivo Chl a fluorescence was measured to assess the effects of elevated CO₂ and cold acclimation on maximum photochemical efficiency (F_v/F_m), maximum potential rates of photosynthetic electron transport (ETR), excitation pressure (EP), which estimates the relative reduction state of PSII reaction centers, and non-photochemical quenching (NPQ), an estimate of the capacity to dissipate excess energy as heat. Chl a fluorescence was measured simultaneously with CO₂ gas exchange on fully expanded third leaves

using a LI-COR portable photosynthesis system (LI-6400 XRT, LI-COR Biosciences, Lincoln, NE, USA). All measurements of Chl a fluorescence were carried out by using the standard fluorescence leaf chamber (2 cm²). The leaves were dark-adapted for 20 min prior to fluorescence measurements. Minimum fluorescence (F_o) was measured by illuminating dark adapted leaves with a low irradiance measuring beam (PPFD < 1 $\mu\text{mol photons m}^{-2} \text{s}^{-1}$) from a light emitting diode. Maximal fluorescence (F_m) was determined by applying second beam of saturating flash of light (PPFD >5000 $\mu\text{mol photons m}^{-2} \text{s}^{-1}$) for pulse duration of 0.8 s. Afterwards, an actinic light (PPFD 1300 $\mu\text{mol photons m}^{-2} \text{s}^{-1}$) was applied. Superimposed on the actinic beam was another saturating light flash (PPFD > 5000 $\mu\text{mol photons m}^{-2} \text{s}^{-1}$, 0.8 s) applied repetitively at 20 s intervals to determine maximal fluorescence in the light-adapted leaf (F_m'). Light adapted steady state fluorescence (F_s) was determined by measuring the level of fluorescence immediately before the saturating flash. Finally, minimal fluorescence (F_o') in the light-adapted leaf was measured by turning off the actinic light.

5.2.6 Determination of total leaf protein and immunodetection

The fully expanded third leaves were harvested, immediately frozen in liquid nitrogen and stored at -80°C. The total leaf protein of the leaf tissues was extracted and quantified by using the RC-DC protein assay kit (Bio-Rad, Hercules, CA) according to the manufacturer's specifications.

The extracted proteins were electrophoretically separated using NuPAGE Novex 10% (w/v) Bis-Tris precast, polyacrylamide gels (Invitrogen, Carlsbad, CA) as described in detail by Dahal et al. (2012a). Samples for SDS-PAGE were loaded on an equal protein basis (8 μg protein per lane). 1 μg of bovine serum albumin (Invitrogen) was added in the extraction buffer as an internal standard. The separated polypeptides were electroblotted onto nitrocellulose membranes (0.2 μm pore size, Bio - Rad). The blots were blocked with 5% (w/v) fat free, dried milk powder overnight at 4°C and then probed with primary antibodies raised against the target proteins; rbcL, cFBPase, Lhcb1, PsbA and PsaA at a dilution of 1:2000-5000. The blots were probed with secondary antibody (anti-rabbit IgG Peroxidase antibody, Sigma-Aldrich) at 1:10000-20000 dilutions

(depending on the target proteins) and visualized with enhanced chemiluminescence immunodetection (ECL Detection Kit, GE Healthcare, Buckinghamshire, UK) on X-ray film (Fujifilm, Fuji Corporation, Tokyo, Japan). Immunoblots were quantified by using a computer software program (Scion Image, Scion Corporation, Frederick, MD, USA). For quantification, exposure times were varied to ensure that signals from the immunoblots were not saturating.

5.2.7 Micro-array analysis

Leaf samples were ground in dry ice to a fine powder and total RNA was extracted with trizol (Invitrogen, Burlington, ON, Canada). Total RNA was cleaned using RNeasy plant minikit (Qiagen) and integrity was determined on agarose gel and on a bioanalyser (Agilent 2100). Synthesized cDNA were transcribed to cRNA with the 3'IVT labelling kit (Santa Clara, CA, USA) and hybridized to the Affymetrix wheat genome array (Santa Clara, Ca, USA) according to the McGill University and Génome Québec Innovation Centre (Montreal, Qc, CA). A total of 3 replicates for each of the 4 growth conditions mentioned above were used for hybridizations.

Cell files obtained from chip images were imported in Flexarray (<http://genomequebec.mcgill.ca/Flexarray>) and data were normalized, corrected for background in R2.5.1 environment with the robust multi-array (RMA) method. To identify the probe sets differentially regulated between two conditions, analysis of variance (ANOVA) were performed on the expression of three replicates for each condition. We compared the transcriptome between 3 pairs of conditions to assess the effects of: (i) cold acclimation at ambient CO₂ (ii) elevated CO₂ in non-acclimated plants, (iii) and elevated CO₂ in cold acclimated plants. The probe sets showing a fold change of 2 or more with a P value less than or equal to 0.05 were selected for gene annotation with HarvEST: Affymetrix wheat 1 array 1.12 (harvest.ucr.edu). Categorical classification of differentially regulated probe sets was made with MAPMAN (<http://gabi.rzpd.de/projects/MapMan>) and through blast search and manual annotation retrieval at NCBI.

5.2.8 Flowering time and grain yield

Changes in flowering time under growth at elevated CO₂ may influence plant size at flowering and thereby plant yield and productivity. Thus, flowering experiments were carried out in Norstar winter and Katepwa spring wheat in order to assess the effects of elevated CO₂ on flowering time. The plants were grown at either ambient (380 ± 13 μmol C mol⁻¹) or at elevated CO₂ (700 ± 20 μmol C mol⁻¹) at a PPFD of 250 ± 20 μmol photons m⁻² s⁻¹, 50 - 60% relative humidity and a 16/8 hr photoperiod. Katepwa was grown at 20/16°C until flowering initiation while Norstar was first grown at 5/5°C for 75 days and transferred to 20/16°C until flower initiation. In each growth condition, 56 plants were monitored from flag leaf stage to flower initiation on the main culm on a daily basis. Time to flowering was calculated from seed sowing to flower initiation (first visible flowers) for Katepwa. For Norstar, this was calculated from the days of shift from 5° to 20°C to flower initiation. Three pots for each of Norstar and Katepwa were grown until grain maturity. Plants were harvested at maturity and total tiller number, effective panicle number and grain number per panicle were counted and grains were weighed.

5.2.9 Statistical analysis

In all experiments, 20 replicate pots (4 L-sized) with three plants per pot for each cultivar were grown in a completely randomized design under the growth conditions described above. Out of the 20 replicate pots, three pots for each cultivar at each growth condition were randomly selected for all photosynthetic measurements and biochemical analyses. Thus, all data are the averages of measurements made on nine plants from three replicate pots. Results were subjected to analysis of variance (ANOVA). Means were compared at the 5% level of significance ($P \leq 0.05$) by using the statistical package SPSS version 17 (IBM, Armonk, NY).

5.3 Results

5.3.1 Effects of cold acclimation and elevated CO₂ on growth characteristics

In order to confirm that the pot size did not limit rooting volume and sink growth, we carried out a pot size experiment for Musketeer winter rye (Appendix 5S1). At ambient CO₂, pot size had minimal effects on total dry matter accumulation (Appendix 5S1)

regardless of growth temperature. However, at elevated CO₂, total dry matter accumulation was significantly affected by variations in pot sizes, such that the total dry matter increased substantially with increase in pot size from 0.5L to 4L in both NA and CA musketeer (Appendix 5S1). Thus, to prevent rooting volume constraints and sink limitations, all four cultivars were grown in 4L-sized pots in all experiments irrespective of growth CO₂ and growth temperatures.

Elevated CO₂ had minimal effects on the cold acclimation-induced compact, dwarf growth habit of winter cultivars as well as the typical elongated growth habit of spring cultivars (Appendix 5S2). Although elevated CO₂ had minimal effects on growth habit and leaf morphology of NA as well as CA cultivars, the plants grown at elevated CO₂, except for CA spring cultivars, were relatively larger with increased tiller number, total leaf number and, consequently, total leaf area relative to at ambient CO₂ (Appendix 5S2). Consistent with our previous reports (Dahal et al. 2012a, 2012b) cold acclimation inhibited the exponential growth rates by about 70% in all four cultivars at ambient CO₂ (Table 5.1). Except for CA SR4A and CA Katepwa, elevated CO₂ significantly increased exponential growth rates for all other NA and CA cultivars (Table 5.1). Consequently, all comparisons of CO₂ gas exchange and biochemical analyses were performed on fully expanded third leaves of 25-day-old NA versus 75-day-old CA plants regardless of growth CO₂.

The specific leaf weight (SLW, g dry weight m⁻² leaf area) increased by about 2.4-fold in CA versus NA winter cultivars, Musketeer and Norstar but changed minimally in CA versus NA spring cultivars, SR4A and Katepwa at ambient CO₂ (Table 5.1). Elevated CO₂ had minimal effects on the SLW for all NA and CA cultivars relative to at ambient CO₂ (Table 5.1). Elevated CO₂ significantly decreased the shoot to root ratios by 20 - 45% in all cultivars irrespective of growth temperature relative to that at ambient CO₂ (Table 5.1).

In the NA state, elevated CO₂ significantly increased Chl per unit leaf area for all

Table 5.1. Effects of cold acclimation and elevated CO₂ on growth characteristics of winter (cv Musketeer, cv Norstar) and spring (cv SR4A, cv Katepwa) cereals. Samples were collected from fully expanded third leaves grown at either ambient CO₂ (380 μmol C mol⁻¹) or elevated CO₂ (700 μmol C mol⁻¹) and at either 20/16°C or 5/5°C. Data represent the mean of nine plants ± SD. Significant differences of the means within each cultivar are indicated by the superscripted letters ($P \leq 0.05$).

Cultivars	Growth CO ₂ / Temperature	Exponential growth rates	Shoot dry mass (mg plant ⁻¹)	Specific leaf weight (gDW m ⁻² leaf area)	Shoot : Root ratio	Chlorophyll (mg m ⁻²)	Chl a/chl b ratio	Leaf protein (g m ⁻² leaf area)
Musketeer	380/20	0.225 ± 0.002 ^c	279 ± 12 ^a	37 ± 6 ^a	3.87 ± 0.19 ^b	642 ± 56 ^a	2.60 ± 0.16	3.67 ± 0.32 ^a
	700/20	0.235 ± 0.003 ^d	380 ± 26 ^b	44 ± 4 ^a	2.95 ± 0.34 ^a	704 ± 29 ^a	2.48 ± 0.27	3.12 ± 0.41 ^a
	380/5	0.074 ± 0.002 ^a	264 ± 32 ^a	90 ± 11 ^b	4.55 ± 0.27 ^c	933 ± 44 ^c	2.57 ± 0.14	10.62 ± 1.13 ^b
	700/5	0.079 ± 0.001 ^b	386 ± 21 ^b	95 ± 7 ^b	3.19 ± 0.21 ^a	829 ± 37 ^b	2.49 ± 0.25	9.96 ± 0.72 ^b
Norstar	380/20	0.222 ± 0.001 ^c	257 ± 20 ^{ab}	30 ± 5 ^a	3.54 ± 0.28 ^b	581 ± 31 ^a	2.82 ± 0.21 ^b	3.36 ± 0.24 ^a
	700/20	0.229 ± 0.002 ^d	328 ± 16 ^c	34 ± 6 ^a	2.89 ± 0.29 ^a	698 ± 44 ^b	2.31 ± 0.18 ^a	2.98 ± 0.17 ^a
	380/5	0.072 ± 0.002 ^a	226 ± 27 ^a	72 ± 9 ^b	4.37 ± 0.13 ^c	761 ± 65 ^b	2.67 ± 0.32 ^{ab}	8.13 ± 0.98 ^b
	700/5	0.076 ± 0.001 ^b	301 ± 20 ^{bc}	77 ± 6 ^b	3.32 ± 0.14 ^{ab}	736 ± 30 ^b	2.53 ± 0.26 ^{ab}	7.55 ± 0.60 ^b
SR4A	380/20	0.233 ± 0.003 ^b	337 ± 22 ^a	33 ± 5 ^a	4.54 ± 0.25 ^b	706 ± 33 ^b	2.86 ± 0.20 ^a	3.92 ± 0.44 ^b
	700/20	0.244 ± 0.003 ^c	487 ± 34 ^c	39 ± 4 ^{ab}	3.14 ± 0.22 ^a	807 ± 45 ^c	3.34 ± 0.12 ^b	3.61 ± 0.23 ^b
	380/5	0.078 ± 0.002 ^a	349 ± 42 ^{ab}	40 ± 4 ^{ab}	5.18 ± 0.18 ^c	665 ± 47 ^{ab}	3.29 ± 0.19 ^{ab}	3.53 ± 0.33 ^{ab}
	700/5	0.079 ± 0.001 ^a	405 ± 29 ^b	43 ± 2 ^b	2.95 ± 0.12 ^a	634 ± 18 ^a	3.32 ± 0.15 ^b	3.04 ± 0.19 ^a
Katepwa	380/20	0.220 ± 0.005 ^b	245 ± 38 ^a	36 ± 5 ^a	3.73 ± 0.16 ^b	620 ± 23 ^b	2.41 ± 0.36 ^a	4.47 ± 0.32 ^b
	700/20	0.233 ± 0.002 ^c	341 ± 20 ^b	40 ± 3 ^{ab}	2.81 ± 0.19 ^a	710 ± 49 ^c	3.12 ± 0.18 ^b	4.32 ± 0.17 ^b
	380/5	0.073 ± 0.001 ^a	233 ± 17 ^a	42 ± 7 ^{ab}	3.47 ± 0.40 ^b	580 ± 76 ^b	2.29 ± 0.29 ^a	4.03 ± 0.21 ^{ab}
	700/5	0.074 ± 0.002 ^a	262 ± 25 ^a	49 ± 5 ^b	2.76 ± 0.36 ^a	465 ± 37 ^a	2.67 ± 0.34 ^{ab}	3.64 ± 0.29 ^a

cultivars except Musketeer relative to that at ambient CO₂ (Table 5.1). In contrast, in the CA state, elevated CO₂ significantly decreased leaf Chl for Musketeer and Katepwa but had minimal effects for Norstar and SR4A. When grown at 20/16°C, the effects of elevated CO₂ on Chl a/b ratio were cultivar dependent such that elevated CO₂ had minimal effects on this ratio for Musketeer, significantly decreased for Norstar but significantly increased for SR4A and Katepwa relative to at ambient CO₂. However, when grown at 5/5°C, the effects of elevated CO₂ on Chl a/b ratio were minimal for all cultivars tested relative to that at ambient CO₂ (Table 5.1).

Elevated CO₂ significantly increased shoot dry matter accumulation by about 55% in winter cultivars, Musketeer (Fig. 5.1A, closed versus open circles) and Norstar (Appendix 5S3A, closed versus open circles) in the NA state. Although comparable CO₂ stimulation of dry matter accumulation was observed in the CA state (Fig. 5.1B, Appendix 5S3B, closed versus open circles) compared to in the NA state, CO₂-stimulated dry matter accumulation was 31% higher in CA versus NA Musketeer (Fig. 5.1A versus 1B, closed circles) and 12% higher in CA versus NA Norstar (Appendix 5S3A versus 5S3B, closed circles). Thus, cold acclimation further increased the CO₂-stimulated shoot dry matter accumulation for winter cultivars, Musketeer and Norstar relative to their NA counterparts.

Similar to winter cultivars, elevated CO₂ stimulated shoot dry matter accumulation by about 75% in spring cultivars, SR4A (Fig. 5.1C, closed versus open circles) and Katepwa (Appendix 5S3C, closed versus open circles) in the NA state. Unlike CA winter cultivars, CA spring cultivars, SR4A (Fig. 5.1D, closed versus open circles) and Katepwa (Appendix 5S3D, closed versus open circles) exhibited a minimal increase (15%) in shoot dry matter accumulation at elevated versus ambient CO₂ conditions. The CO₂-stimulated shoot dry matter accumulation was about 40% lower in CA versus NA SR4A (Fig. 5.1C versus 5.1D, closed circles) and in CA versus NA Katepwa (Appendix 5S3C versus 5S3D, closed circles). Thus, cold acclimation decreased the CO₂-stimulated shoot dry matter accumulation in spring cultivars, SR4A and Katepwa.

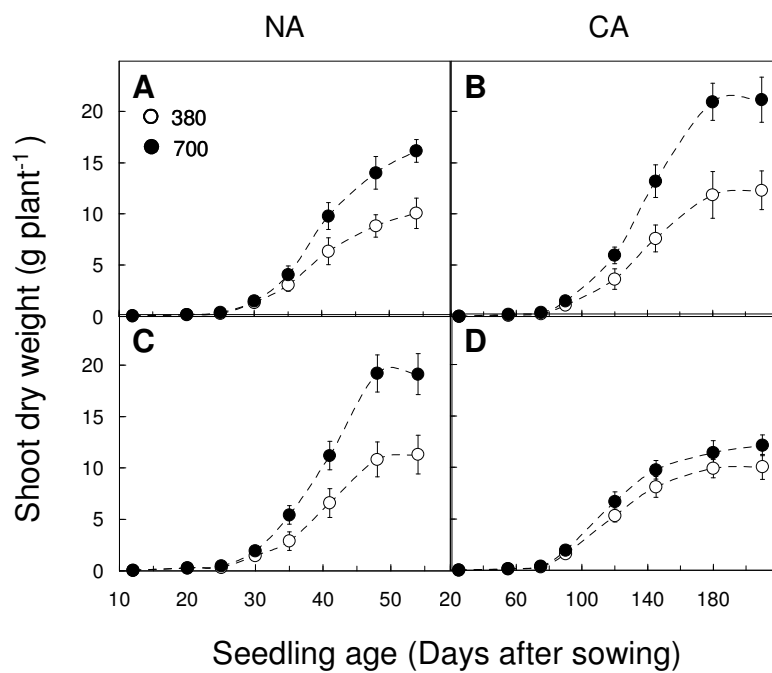


Fig. 5.1. Effects of cold acclimation and elevated CO₂ on shoot dry weight of Musketeer winter (A, B) and SR4A spring (C, D) rye. The plants were grown at either ambient CO₂ (380 μmol C mol⁻¹, ○) or elevated CO₂ (700 μmol C mol⁻¹, ●) and at either 20/16°C (NA, A, C) or 5/5°C (CA, B, D). Each point represents the mean of nine plants from three different pots. Bars represent SD.

5.3.2 Effects of cold acclimation and elevated CO₂ on photosynthetic light response curves

Figure 5.2 and Appendix 5S4 illustrate the light response curves of gross CO₂ assimilation for NA and CA winter and spring cultivars measured at their respective growth CO₂. Consistent with our recent report (Dahal et al. 2012a), cold acclimation increased light-saturated rates of gross photosynthesis (gross A_{sat}) by about 35%, with minimal change in apparent maximum quantum efficiency for CO₂ assimilation (Q) in winter cultivars (Fig. 5.2A vs 2B, Appendix 5S4A vs S4B, open circles) but inhibited Q as well as gross A_{sat} by 25-45% in spring cultivars (Fig. 5.2C vs 2D, Appendix 5S4C vs S4D, open circles) at ambient CO₂. Elevated CO₂ significantly increased Q by 30-45% in all NA cultivars (Fig. 5.2A, C, Appendix 5S4A, C, closed circles) as compared to those values observed at ambient CO₂ (Fig. 5.2A, C, Appendix 5S4A, C, open circles). In contrast, Q values changed minimally in elevated versus ambient CO₂ conditions for all CA cultivars (Fig. 5.2B, D, Appendix 5S4B, D, closed versus open circles).

Elevated CO₂ stimulated gross A_{sat} by 53% in NA Musketeer winter rye (Fig. 5.2A, closed circles) relative to at ambient CO₂ (Fig. 5.2A, open circles). Comparable CO₂-stimulation of gross A_{sat} (46%) was observed for NA Norstar winter wheat (Fig. 5S4A, closed versus open circles) as well as for NA SR4A spring rye (41%, Fig. 5.2C, closed versus open circles) and NA Katepwa spring wheat (56%, Appendix 5S4C, closed versus open circles). Thus, in the NA state, all four cultivars exhibited a similar stimulation of gross A_{sat} when grown and measured at elevated CO₂ relative to those rates observed when grown and measured at ambient CO₂.

Growth at elevated CO₂ further enhanced the CO₂-stimulation of gross A_{sat} for CA Musketeer rye and Norstar wheat. For instance, CA Musketeer exhibited an average 66% stimulation of gross A_{sat} at elevated CO₂ (Fig. 5.2B, closed circles) relative to that observed at ambient CO₂ (Fig. 5.2B, open circles). The CO₂-stimulated gross A_{sat} was 42% higher for CA Musketeer (Fig. 5.2B, closed circles, $40.7 \pm 2.3 \mu\text{mol CO}_2 \text{ m}^{-2} \text{ s}^{-1}$) as compared to that of NA Musketeer (Fig 5.2A, closed circles, $28.6 \pm 2.2 \mu\text{mol CO}_2 \text{ m}^{-2} \text{ s}^{-1}$).

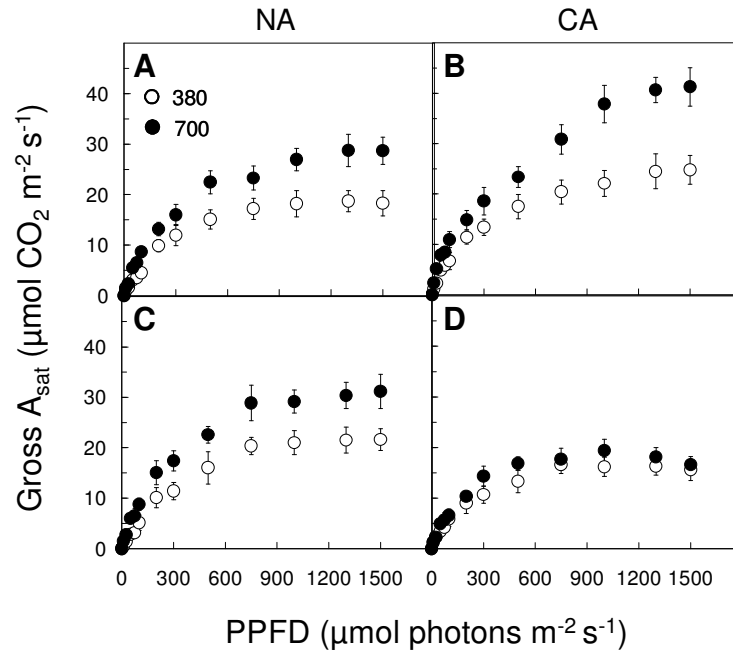


Fig. 5.2. Light response curves of gross CO₂ assimilation for Musketeer winter (A, B) and SR4A spring (C, D) rye. The plants were grown at either ambient CO₂ (380 μmol C mol⁻¹, ○) or elevated CO₂ (700 μmol C mol⁻¹, ●) and at either 20/16°C (NA, A, C) or 5/5°C (CA, B, D). Measurements were carried out on attached, fully developed third leaves at their respective growth CO₂ and at measuring temperatures of 20°C. Each point represents the mean of nine plants from three different pots. Bars represent SD.

¹). Similar trends were observed for Norstar winter wheat (Appendix 5S4A versus 5S4B). In contrast to CA Musketeer winter rye, CA SR4A spring rye exhibited minimal stimulation of gross A_{sat} at elevated CO_2 (Fig. 5.2D, closed circles) relative to those rates observed at ambient CO_2 (Fig. 5.2D, open circles). However, since cold acclimation substantially inhibited gross A_{sat} of CA SR4A, this minimal stimulation of gross A_{sat} of CA SR4A at elevated CO_2 (Fig. 5.2D, closed versus open circles) was not sufficient to compensate for the cold acclimation-induced inhibition of A_{sat} at ambient CO_2 (Fig. 5.2C versus 2D, open circles). The CO_2 -stimulated rate of gross CO_2 assimilation was about 35% less for CA spring rye (Fig. 5.2D, closed circles, $22.9 \pm 3.2 \mu\text{mol CO}_2 \text{ m}^{-2} \text{ s}^{-1}$) as compared to the stimulation observed for NA spring rye measured at the same temperature (Fig 5.2C, closed circles, $34.1 \pm 2.4 \mu\text{mol CO}_2 \text{ m}^{-2} \text{ s}^{-1}$). We observed similar trends for CA Katepwa spring wheat (Appendix 5S4C versus 5S4D) relative to CA Norstar winter wheat.

5.3.3 Effects of cold acclimation and elevated CO_2 on photosynthetic CO_2 response curves

As reported previously (Dahal et al. 2012a, 2012b), CA winter cultivars exhibited 10-40% increase in carboxylation efficiency (CE) as well as carboxylation capacity (light and CO_2 -saturated rates of photosynthesis) whereas CA spring cultivars, exhibited 25-35% inhibition in CE as well as carboxylation capacity relative to their NA counterparts at ambient CO_2 (Table 5.2, Fig. 5.3, Appendix 5S5, open circles). Elevated CO_2 had minimal effects on CE, CO_2 -saturated photosynthesis, J_{max} as well as V_{cmax} in all four cultivars irrespective of growth temperature (Table 5.2, Fig. 5.3, Appendix 5S5, closed vs open circles).

Table 5.2. Effects of cold acclimation and elevated CO₂ on the maximum Rubisco carboxylation capacity (V_{cmax}), maximum rates of electron transport (J_{max}), the apparent maximum quantum efficiency (Q) and the carboxylation efficiency (CE) for winter and spring cereals grown at either ambient CO₂ (380 $\mu\text{mol C mol}^{-1}$) or elevated CO₂ (700 $\mu\text{mol C mol}^{-1}$) and at either 20/16°C or 5/5°C. Measurements were carried out on fully expanded third leaves at 700 $\mu\text{mol C mol}^{-1}$ and at 20°C. Data represent the mean of nine plants from three different pots \pm SD. Significant differences among the means within each cultivar are indicated by the superscripted letters ($P \leq 0.05$).

Cultivars	Growth CO ₂ /temperature	V_{cmax} ($\mu\text{mol CO}_2 \text{ m}^{-2} \text{ s}^{-1}$)	J_{max} ($\mu\text{mol e}^- \text{ m}^{-2} \text{ s}^{-1}$)	Q (CO ₂ /photon)	CE (CO ₂ m ⁻² s ⁻¹ / mol ⁻¹ CO ₂)
Musketeer	380/20	66 \pm 5 ^a	132 \pm 15 ^a	0.046 \pm 0.003 ^a	0.075 \pm 0.09 ^a
	700/20	71 \pm 8 ^{ab}	147 \pm 11 ^a	0.059 \pm 0.005 ^b	0.068 \pm 0.06 ^a
	380/5	95 \pm 10 ^c	183 \pm 16 ^b	0.052 \pm 0.007 ^{ab}	0.098 \pm 0.08 ^b
	700/5	83 \pm 7 ^{bc}	166 \pm 9 ^b	0.061 \pm 0.005 ^b	0.105 \pm 0.11 ^b
Norstar	380/20	57 \pm 4 ^a	143 \pm 12 ^{ab}	0.041 \pm 0.006 ^a	0.070 \pm 0.05 ^a
	700/20	54 \pm 9 ^a	134 \pm 7 ^a	0.060 \pm 0.005 ^b	0.079 \pm 0.08 ^{ab}
	380/5	76 \pm 8 ^b	165 \pm 13 ^b	0.048 \pm 0.002 ^{ab}	0.085 \pm 0.04 ^b
	700/5	69 \pm 5 ^{ab}	152 \pm 17 ^{ab}	0.053 \pm 0.004 ^b	0.071 \pm 0.05 ^a
SR4A	380/20	71 \pm 13 ^b	140 \pm 10 ^b	0.049 \pm 0.004 ^b	0.082 \pm 0.08 ^b
	700/20	62 \pm 6 ^b	126 \pm 12 ^b	0.071 \pm 0.005 ^c	0.089 \pm 0.04 ^b
	380/5	39 \pm 3 ^a	113 \pm 9 ^a	0.035 \pm 0.004 ^a	0.064 \pm 0.07 ^a
	700/5	36 \pm 5 ^a	103 \pm 7 ^a	0.041 \pm 0.006 ^{ab}	0.061 \pm 0.05 ^a
Katepwa	380/20	63 \pm 3 ^b	148 \pm 18 ^b	0.053 \pm 0.004 ^b	0.069 \pm 0.07 ^b
	700/20	70 \pm 9 ^b	159 \pm 15 ^b	0.066 \pm 0.005 ^c	0.063 \pm 0.05 ^b
	380/5	35 \pm 4 ^a	97 \pm 8 ^a	0.033 \pm 0.005 ^a	0.045 \pm 0.04 ^a
	700/5	28 \pm 6 ^a	108 \pm 10 ^a	0.040 \pm 0.006 ^a	0.051 \pm 0.04 ^a

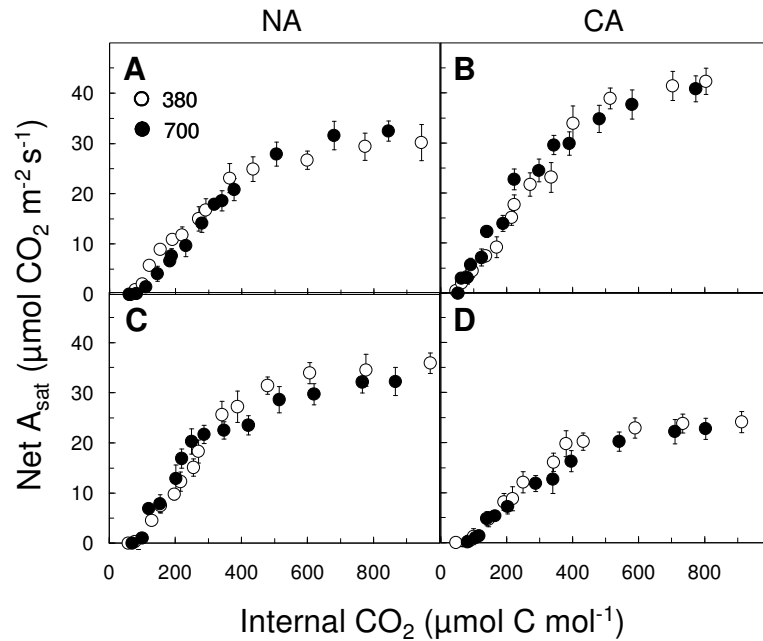


Fig. 5.3. CO₂ response curves of light-saturated net CO₂ assimilation for Musketeer winter (A, B) and SR4A spring (C, D) rye. The plants were grown at either ambient CO₂ (380 μmol C mol⁻¹, ○) or elevated CO₂ (700 μmol C mol⁻¹, ●) and at either 20/16°C (NA, A, C) or 5/5°C (CA, B, D). Measurements were carried out on attached, fully developed third leaves at measuring temperature of 20°C. Each point represents the mean of nine plants from three different pots. Bars represent SD.

5.3.4 Effects of cold acclimation and elevated CO₂ on light response curves for ETR, EP and NPQ

The apparent quantum requirement for electron transport rates (ETR), the apparent quantum requirement to close PSII reaction centers by excitation pressure (EP), measured as 1-qP and apparent quantum requirement to induce energy dissipation by non-photochemical quenching (NPQ), were estimated from the light response curves for electron transport rates, excitation pressure and non-photochemical quenching respectively (Fig. 5.4, Appendix 5S6). Apparent quantum requirement, which is the inverse of apparent quantum efficiency, was estimated from the linear portion of the light response curves for either ETR (Fig. 4A, B, C, D), 1-qP (Fig. 5.4E, F, G, H) or NPQ (Fig. 4I, J, K, L) obtained through *in vivo* Chl *a* fluorescence measured at 20°C and at 700 $\mu\text{mol C mol}^{-1}$.

Cold acclimation significantly decreased the apparent quantum requirement for ETR by about 25% but significantly increased the light-saturated ETR by about 40% for Musketeer winter rye grown at ambient CO₂ (Fig. 5.4A vs 4B, Appendix 5S6A vs 5S6B, open circles). However, the apparent quantum requirements for PSII closure (Fig. 5.4E vs 4F, Appendix 5S6E vs 5S6F, open circles) and the apparent quantum requirements to induce NPQ (Fig. 5.4I vs 4J, Appendix 5S6I vs 5S6J, open circles) under ambient CO₂ conditions were about 50% higher in CA relative to NA Musketeer. In contrast, cold acclimation increased the apparent quantum requirements for ETR by about 10% but significantly decreased the light-saturated ETR by about 30% for SR4A spring rye grown at ambient CO₂ (Fig. 5.4C vs 4D, open circles). This was associated with a 40% decrease in the apparent quantum requirements for PSII closure (Fig. 5.4G vs 4H, open circles) and a 35% decrease in the apparent quantum requirements to induce NPQ (Fig. 5.4K vs 4L, open circles) in CA versus NA SR4A grown at ambient CO₂. Comparable trends for light response curves of ETR, EP and NPQ were observed in NA and CA Norstar winter wheat versus NA and CA Katepwa spring wheat grown at ambient CO₂ (Appendix 5S6).

The light response curves of ETR, EP and NPQ were insensitive to growth at elevated CO₂ in all four cultivars irrespective of growth temperatures (Fig. 5.4, Appendix

5S6, closed vs open circles). This was consistent with the minimal changes in the CO₂ response curves of all four cultivars grown under elevated versus ambient CO₂ conditions irrespective of growth temperatures (Fig. 5.3, Appendix 5S5, closed vs open circles).

5.3.5 Effects of cold acclimation and elevated CO₂ on photosynthetic CO₂ response curves for ETR, EP and NPQ

The efficiency of ETR estimated as the maximal initial slope of the ETR vs C_i response curves as well as the CO₂ saturated rates of ETR were about 1.4-fold higher in CA versus NA Musketeer grown under ambient CO₂ conditions (Fig. 5.5A vs 5B, open circles). In contrast, the efficiency of ETR and the CO₂ saturated rates of ETR were 30% and 50% lower respectively in CA versus NA SR4A grown at ambient CO₂ (Fig. 5.5C vs 5D, open circles). Growth at elevated CO₂ had minimal effects on the efficiency of ETR as well as the CO₂ saturated rates of ETR in both Musketeer and SR4A rye (Fig. 5.5A, B, C, D).

Increasing C_i decreased excitation pressure in both Musketeer and SR4A (Fig. 5.5E, F, G, H), regardless of growth CO₂ which is consistent with the notion that CO₂ is the ultimate electron acceptor for photosynthetic carbon assimilation. However, excitation pressure at CO₂ saturation was 45% lower in CA Musketeer compared to NA Musketeer (Fig. 5.5E, F) grown at ambient CO₂. In addition, the efficiency with which PSII reaction centers were opened by increased CO₂, measured as the initial slope of the excitation pressure vs C_i response curves, was about 30% greater in CA Musketeer relative to NA Musketeer grown at ambient CO₂ (Fig. 5.5E, F). In contrast, the efficiency to open PSII reaction centers as a function of CO₂ was 70% lower and the CO₂ saturated excitation pressure were 55% higher in CA versus NA SR4A (Fig. 5.5G, H). Growth at elevated CO₂ had minimal effects on the efficiency to open PSII reaction centers as well as the CO₂ saturated excitation pressure in both Musketeer and SR4A rye (Fig 5.5E, F, G, H).

Increasing C_i resulted in the suppression of NPQ in both Musketeer and SR4A irrespective of growth CO₂, which is consistent with the fact that CO₂ is a substrate for the Rubisco-catalyzed carboxylation reaction of the Calvin cycle (Fig. 5.5I, J, K, L).

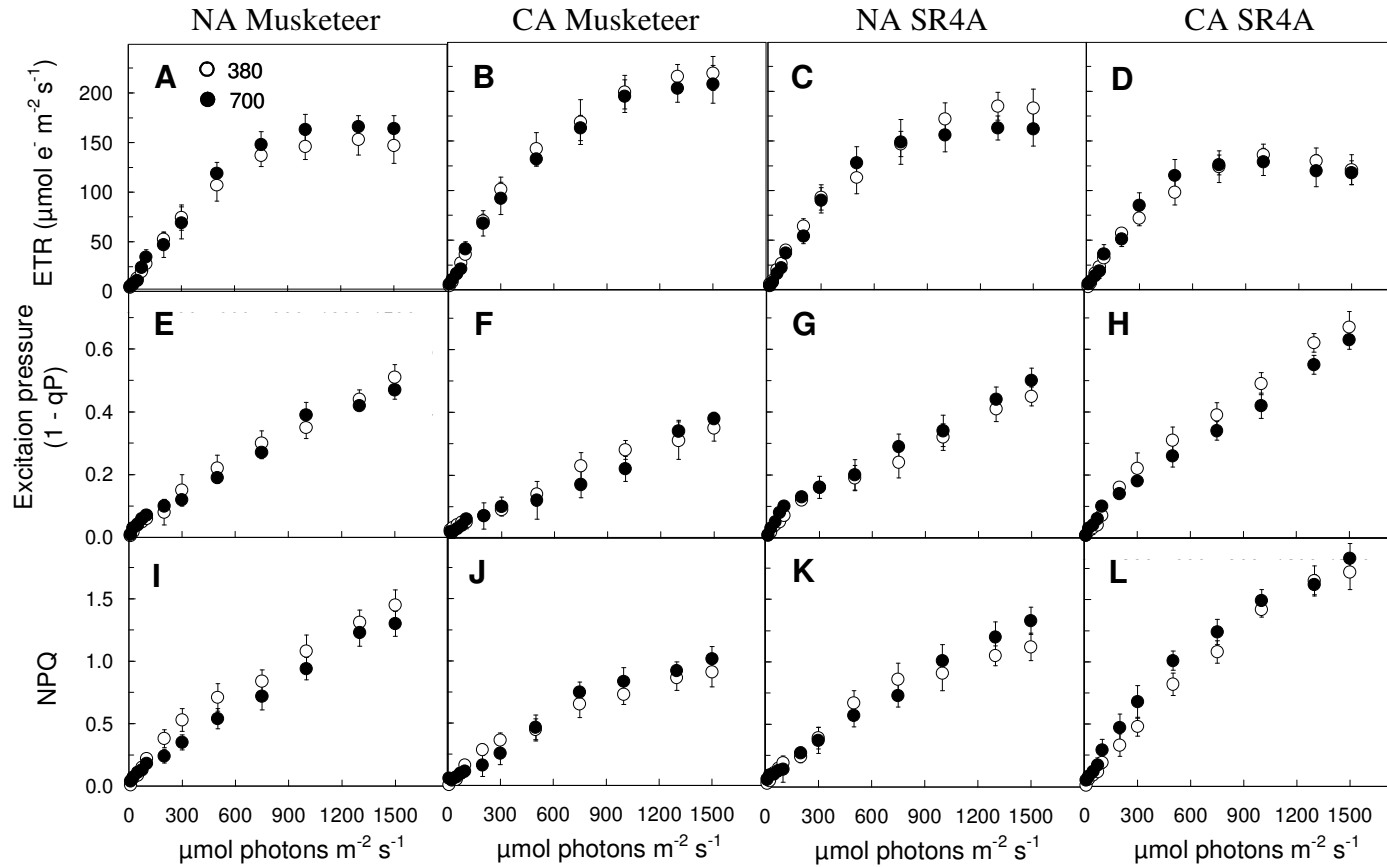


Fig. 5.4. Light response curves of electron transport rates (ETR, A, B, C, D), excitation pressures (1-qP, E, F, G, H) and non photochemical quenching of excess energy (NPQ, I, J, K, L) for Musketeer winter (A, B, E, F, I, J) and SR4A spring rye (C, D, G, H, K, L) grown at either 20/16°C (NA) or 5/5°C (CA) and at either ambient CO₂ (380 $\mu\text{mol C mol}^{-1}$, ○) or elevated CO₂ (700 $\mu\text{mol C mol}^{-1}$, ●). Measurements were carried out on attached, fully developed third leaves at measuring temperature of 20°C and at 700 $\mu\text{mol C mol}^{-1}$. Each point represents the mean of nine plants from three different pots. Bars represent SD.

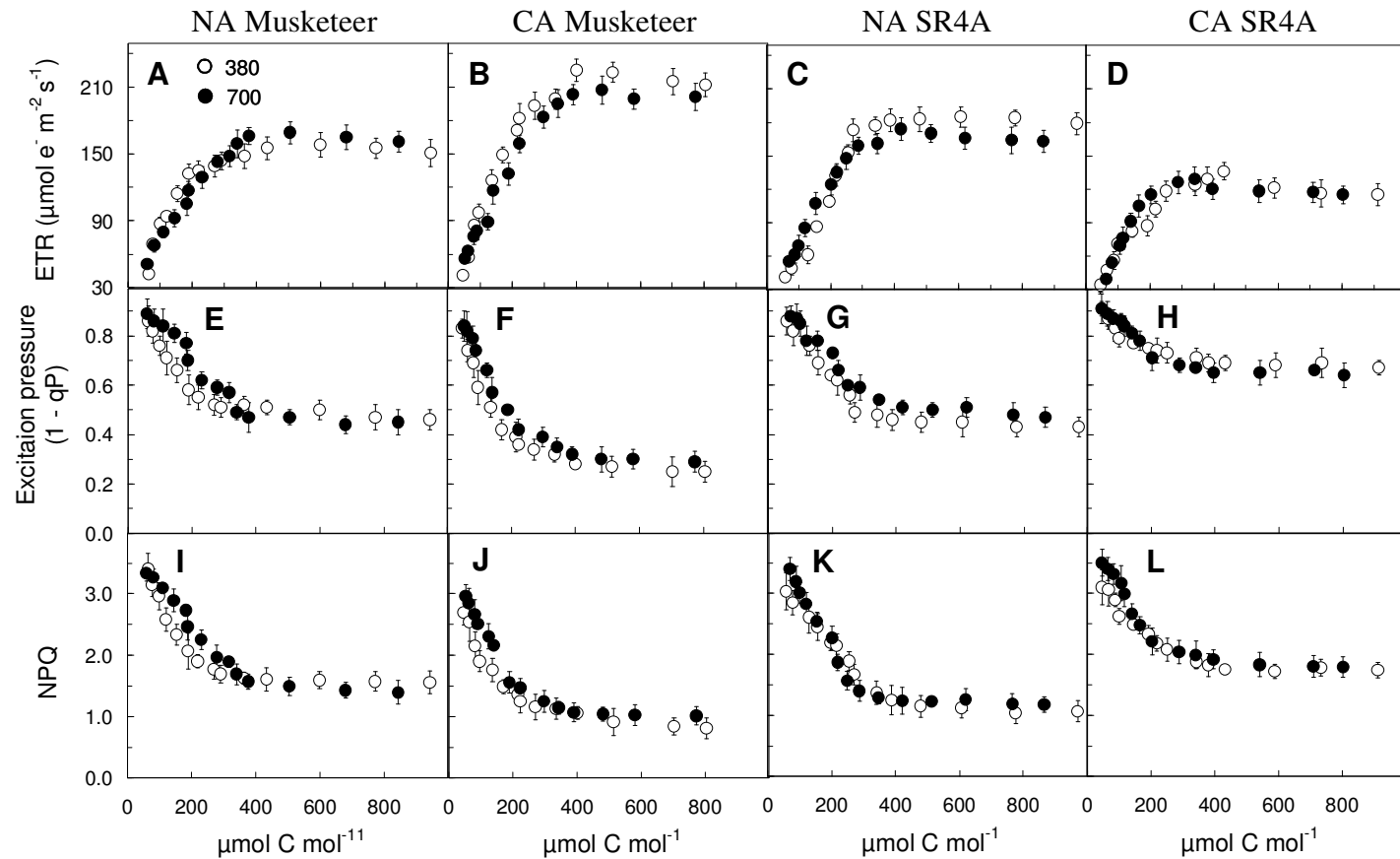


Fig. 5.5. CO₂ response curves of light-saturated electron transport rates (ETR, A, B, C, D), excitation pressures (1-qP, E, F, G, H) and non photochemical quenching of excess energy (NPQ, I, J, K, L) for Musketeer winter (A, B, E, F, I, J) and SR4A spring (C, D, G, H, K, L) rye grown at either 20/16°C (NA) or 5/5°C (CA) and at either ambient CO₂ (380 μmol C mol⁻¹, ○) or elevated CO₂ (700 μmol C mol⁻¹, ●). Measurements were carried out on attached, fully developed third leaves at 20°C and at saturating irradiance of 1300 μmol m⁻² s⁻¹ PPFD. Each point represents the mean of nine plants from three different pots. Bars represent SD.

However, even at low C_i , NPQ was about 30% lower in CA Musketeer than in NA counterpart grown at ambient CO_2 (Fig. 5.5I, J). The CO_2 saturated NPQ was 50% lower in CA versus NA Musketeer at ambient CO_2 (Fig. 5.5I, J). In contrast, the NPQ was 25% and 60% higher at low CO_2 and CO_2 saturation respectively in CA versus NA SR4A grown at ambient CO_2 (Fig. 5.5 K, L). Growth at elevated CO_2 had minimal effects on CO_2 response curves of NPQ in both Musketeer and SR4A rye (Fig. 5.5I, J, K, L). Comparable trends for CO_2 response curves of ETR, EP and NPQ were observed in NA and CA Norstar winter wheat versus NA and CA Katepwa spring wheat grown at either ambient or elevated CO_2 (Appendix 5S7).

5.3.6 Effects of cold acclimation and elevated CO_2 on stomatal characteristics

Growth at elevated CO_2 suppressed stomatal conductance by 30 - 55% in all NA cultivars and, as a consequence, leaf transpiration rates decreased by 25 - 35% in all NA cultivars in response to growth at elevated CO_2 (Table 5.3). In contrast, elevated CO_2 induced minimal changes in stomatal conductance, as well as leaf transpiration rates in all CA cultivars (Table 5.3). WUE of all NA cultivars increased by 130 - 210% and that of CA winter cultivars by 40 - 85% at elevated CO_2 relative to at ambient CO_2 (Table 5.3). Elevated CO_2 had minimal effects on WUE for CA spring cultivars (Table 5.3).

It appears that elevated CO_2 -induced suppression of g_s of all cultivars can be accounted for, in part, by a decrease in stomatal density on both abaxial and adaxial leaf surfaces in response to growth at elevated CO_2 (Table 5.3). These data indicate that the enhancement of WUE induced by elevated CO_2 is primarily associated with increase in light-saturated CO_2 assimilation and decrease in stomatal conductance in elevated versus ambient CO_2 -grown plants.

5.3.7 Effects of cold acclimation and elevated CO_2 on dark respiratory rates

In the NA state, all cultivars exhibited a 10 - 25% increase in the R_{dark} upon growth at elevated CO_2 relative to those rates observed at ambient CO_2 (Appendix 5S8). In the CA state, unlike photosynthesis, the R_{dark} appeared to be insensitive to growth at elevated CO_2 for all four cultivars (Appendix 5S8).

Table 5.3. Effects of cold acclimation and elevated CO₂ on stomatal characteristics of winter and spring cereals. The plants were grown at either ambient CO₂ (380 μmol C mol⁻¹) or elevated CO₂ (700 μmol C mol⁻¹) and at either 20/16°C or 5/5°C.

Measurements were carried out on fully expanded third leaves at their respective growth CO₂ and at 20°C. Data represent the mean of nine plants from three different pots ± SD. Significant differences among the means within each cultivar are indicated by the superscripted letters ($P \leq 0.05$).

Cultivars	Growth CO ₂ / Temperature	Stomatal density (stomates mm ⁻² leaf area)		Stomatal conductance (mol m ⁻² s ⁻¹)	Transpiration (mmol H ₂ O m ⁻² s ⁻¹)	WUE (A/gS)
		Adaxial	Abaxial			
Musketeer	380/20	148 ± 16 ^b	161 ± 19 ^c	0.48 ± 0.03 ^b	2.68 ± 0.36 ^b	34 ± 5 ^a
	700/20	90 ± 11 ^a	127 ± 10 ^b	0.29 ± 0.05 ^a	1.78 ± 0.29 ^a	89 ± 14 ^b
	380/5	102 ± 19 ^a	92 ± 8 ^a	0.23 ± 0.04 ^a	1.92 ± 0.22 ^a	94 ± 12 ^c
	700/5	83 ± 13 ^a	99 ± 7 ^a	0.28 ± 0.03 ^a	1.87 ± 0.31 ^a	131 ± 19 ^d
Norstar	380/20	109 ± 3 ^b	122 ± 18 ^b	0.59 ± 0.06 ^c	3.28 ± 0.19 ^c	28 ± 4 ^a
	700/20	73 ± 4 ^a	67 ± 6 ^a	0.39 ± 0.03 ^b	2.38 ± 0.12 ^b	64 ± 6 ^b
	380/5	71 ± 12 ^a	76 ± 11 ^a	0.35 ± 0.02 ^{ab}	2.05 ± 0.15 ^a	48 ± 9 ^b
	700/5	78 ± 12 ^a	68 ± 16 ^a	0.31 ± 0.02 ^a	2.23 ± 0.25 ^{ab}	89 ± 21 ^c
SR4A	380/20	135 ± 20 ^b	163 ± 25 ^b	0.67 ± 0.04 ^c	2.32 ± 0.31 ^c	29 ± 5 ^a
	700/20	93 ± 6 ^a	105 ± 18 ^a	0.31 ± 0.05 ^a	1.73 ± 0.20 ^b	88 ± 10 ^c
	380/5	106 ± 10 ^a	117 ± 10 ^a	0.42 ± 0.02 ^b	1.66 ± 0.14 ^b	32 ± 4 ^{ab}
	700/5	102 ± 9 ^a	121 ± 20 ^a	0.38 ± 0.03 ^{ab}	1.32 ± 0.19 ^a	39 ± 3 ^b
Katepwa	380/20	105 ± 5 ^b	128 ± 11 ^c	0.43 ± 0.04 ^b	3.43 ± 0.33 ^b	44 ± 9 ^a
	700/20	65 ± 20 ^a	88 ± 18 ^{ab}	0.31 ± 0.05 ^a	2.54 ± 0.43 ^a	96 ± 14 ^b
	380/5	80 ± 18 ^a	107 ± 13 ^b	0.32 ± 0.03 ^a	2.74 ± 0.24 ^a	34 ± 8 ^a
	700/5	76 ± 11 ^a	81 ± 10 ^a	0.36 ± 0.02 ^{ab}	2.25 ± 0.28 ^a	38 ± 10 ^a

5.3.8 Effects of cold acclimation and elevated CO₂ on gene expression in wheat

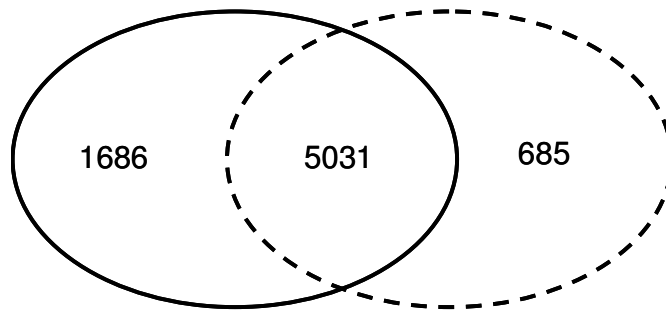
Wheat micro-array analysis has indicated that CA Norstar grown under ambient CO₂ condition exhibited at least a 2-fold change in expression of 6717 genes representing about 10.5% of total genes on the micro-array relative to NA Norstar (Fig. 5.6A). Under elevated CO₂, CA Norstar exhibited differential expression of 5716 genes compared to NA Norstar (Fig. 5.6A). A total of 5031 genes appeared to be differentially regulated in CA versus NA Norstar under both ambient and elevated CO₂ conditions (Fig. 5.6A). Compared to growth at ambient CO₂, a total of 1022 genes were differentially expressed upon growth at elevated CO₂ for NA Norstar (Fig. 5.6B). However, growth at elevated CO₂ appeared to change the expression of only 372 genes for CA Norstar relative to that at ambient CO₂ condition (Fig. 5.6B). A total of 77 genes appeared to be differentially regulated in elevated versus ambient CO₂-grown Norstar under both NA and CA state (Fig. 5.6B).

Table 5.4 shows the list of the genes encoding the major photosynthetic as well as sucrose, fructan and starch biosynthetic enzymes, respiratory enzymes and components of photosynthetic and mitochondrial electron transport, assessed through micro-array analysis using the Affymetrix wheat micro-array. Cold acclimation up-regulated the expression of several genes involved in the Calvin cycle and in sucrose and fructan biosynthesis, however, it down-regulated most of the genes for the dicarboxylic acid cycle and for starch synthesis at ambient CO₂ (Table 5.4). Cold acclimation differentially regulated the expression of the genes for components of photosynthetic electron transport such that cold acclimation up-regulated *psaA*, *psaB*, *petD* and *petL* gene expression, had minimal effects for *psbA* and down-regulated *Lhcb* and other PSI components at ambient CO₂ (Table 5.4). The expression of the genes involved in mitochondrial electron transport (MET) was up-regulated in CA versus NA Norstar at ambient CO₂ (Table 5.4).

Elevated CO₂ up-regulated the expression of genes for Rubisco and components of photosystem I, however, it down-regulated the expression of the genes involved in sucrose as well as fructan biosynthesis and dicarboxylic acid cycle for NA Norstar

A Genes regulated by low temperature

○ 380 (CA Vs NA)
⋯ 700 (CA Vs NA)



B Genes regulated by elevated CO₂

○ NA (700 Vs 380)
⋯ CA (700 Vs 380)

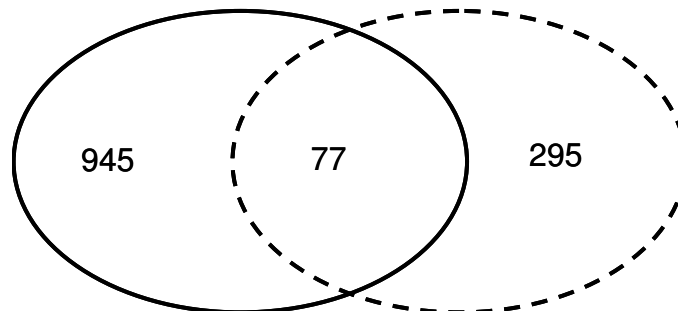


Fig. 5. 6. Number of genes differentially expressed by cold acclimation at either ambient or elevated CO₂ conditions (A) and by elevated CO₂ at either NA or CA state (B) for Norstar winter wheat obtained through micro-array analysis using the Affymetrix wheat micro-array. The plants were grown at either ambient CO₂ (380 μmol C mol⁻¹), or elevated CO₂ (700 μmol C mol⁻¹) and at either 20/16°C (NA) or 5/5°C (CA).

Table 5.4. List of the genes differentially expressed upon growth at low temperature (5/5°C vs 20/16°C) or at elevated CO₂ (700 versus 380 μmol C mol⁻¹) or combination of both for Norstar winter wheat obtained through micro-array analysis using the Affymetrix wheat micro-array. N = nucleus, C = chloroplast, M = mitochondrion.

Protein/subunit name	Gene name/ location	Fold change due to low growth temperature or elevated CO ₂			Associated with
		380/5	380/20	380/5	
		vs 380/20	vs 700/20	vs 700/5	
Photosynthetic electron transport					
LHCII Chl a/b-binding protein	<i>Lhcb</i> , N	-3.21	NS	-1.45	LHCII
Photosystem I P700 chlorophyll a apoprotein (PsaA)	<i>psaA</i> , C	2.04	1.18	-3.40	PS1, RC
Photosystem I P700 chlorophyll a apoprotein (PsaB)	<i>psaB</i> , C	2.24	2.02	-2.19	PS1, RC
Photosystem I reaction center subunit III (PSI-F)	<i>PsaF</i> , N	-1.51	1.18	1.15	PS1
Photosystem I reaction center subunit N (PSI-N)	<i>PsaN</i> , N	-1.88	1.12	NS	PS1
Photosystem I reaction center subunit (PSI-K)	<i>PsaK</i> , N	-1.99	1.25	NS	PS1
Photosystem I reaction center subunit XI (PSI-L)	<i>PsaL</i> , N	-1.85	1.38	1.41	PS1
Photosystem II Reaction center D1 protein (PsbA)	<i>psbA</i> , C	NS	1.26	NS	PSII, RC
Photosystem II 10 kDa polypeptide (PSII-R)	<i>PsbR</i> , N	-154.70	NS	NS	OEC
Cytochrome b6-f complex iron-sulfur subunit	<i>petC</i> , C	-1.26	-1.08	1.16	<i>Cyt b6f</i>
Cytochrome b6/f complex subunit IV	<i>petD</i> , C	2.49	NS	-1.34	<i>Cyt b6f</i>
Cytochrome b6-f complex subunit 6	<i>petL</i> , C	4.19	NS	NS	<i>Cyt b6f</i>
Carbon metabolic pathway					
Rubisco large subunit (RbcL)	<i>rbcL</i> , C	1.25	1.47	1.26	C ₃ cycle
Rubisco small subunit (RbcS)	<i>RbcS</i> , N	1.28	1.35	1.17	C ₃ cycle
Phosphoenolpyruvate carboxylase	<i>Pepc</i> , N	-2.77	-1.30	1.49	C ₄ cycle
NADP-dependent malate dehydrogenase	<i>Nadp-mdh</i> , N	2.98	-1.18	-1.40	C ₄ cycle
NADP-dependent malic enzyme	<i>Nadp-me</i>	2.98	-1.18	-1.40	C ₄ cycle

Table 5.4. Contd.

Protein/subunit name	Gene name/ location	Fold change due to low growth temperature or elevated CO ₂			Associated with
		380/5 vs 380/20	380/20 vs 700/20	380/5 vs 700/5	
Cytosolic fructose 1,6-bisphosphatase (cFBPase)	<i>cFBPase</i> , N	-2.11	-1.19	1.14	Sucrose biosynthesis
Sucrose phosphate synthase (SPS)	<i>SPS</i> , N	1.30	-1.34	-1.13	Sucrose biosynthesis
Fructan:fructan 1-fructosyltransferase	<i>1-FFT</i> , N	2.80	-3.09	NS	Fructan biosynthesis
Sucrose:fructan 6-fructosyltransferase	<i>6-SFT</i> , N	-4.38	-4.09	NS	Fructan biosynthesis
Fructan exohydrolase	<i>D3I</i> , N	-1.46	1.33	1.65	Fructan hydrolysis
Glucose-6-phosphate 1-dehydrogenase	<i>G6pdh</i> , N	10.44	-1.41	-1.30	Phosphogluconate pathway
ADP-glucose pyrophosphorylase small subunit	<i>AGP_{sma}</i> , N	-2.81	NS	NS	Starch synthesis
Mitochondrial electron transport (MET)					
Cytochrome c oxidase subunit 1	<i>COX1</i> , M	1.33	-9.87	-2.59	MET
Cytochrome c oxidase subunit 2	<i>COX2</i> , M	-1.31	NS	1.25	MET
Cytochrome c oxidase subunit 3	<i>COX3</i> , M	1.62	NS	-1.71	MET
Cytochrome c oxidase subunit 5C	<i>COX5C</i> , N	1.19	NS	NS	MET
Alternative oxidase	<i>Waox1a</i> , N	8.65	-1.26	-1.55	MET
Respiratory pathway					
Pyruvate dehydrogenase E1 component alpha subunit	<i>PDHE1-A</i> , N	NS	-2.48	NS	glycolysis
Pyruvate kinase	<i>PK</i> , N	2.02	-1.49	-1.24	glycolysis
Malate dehydrogenase	<i>MDH</i> , N	-1.56	1.21	1.17	citric acid cycle
PPi-PFK (PPi-dependent phosphofructokinase)	<i>PPi-PFK</i> , N	-1.36	NS	NS	glycolysis

(Table 5.4). The expression of the genes for PSII complex, cytochrome *b6f* complex (Cyt *b6f*), starch synthesis and mitochondrial electron transport were minimally changed in elevated versus ambient CO₂-grown NA Norstar. In contrast to NA Norstar, CA Norstar was less sensitive to growth at elevated CO₂ for expression of several genes (Table 5.4). The genes down-regulated by elevated CO₂ in the NA state were minimally changed in the CA state. Thus, cold acclimation of Norstar appeared to prevent the down-regulation of several genes induced by long-term growth at elevated CO₂.

5.3.9 Effects of cold acclimation and elevated CO₂ on leaf protein and polypeptide contents

Elevated CO₂ had minimal effects on leaf protein content of all NA and CA cultivars relative to at ambient CO₂ (Table 5.1).

Cold acclimation induced minimal changes (<15%) in the protein levels of *rbcL*, *cFBPase*, *Lhcb1*, *psbA* and *psaA* in either winter or spring cultivars at ambient CO₂ (Fig. 5.7, Appendix 5S9). This can be explained by the fact that the loading for SDS-PAGE and immunoblotting was based on leaf protein. Our leaf protein results (Table 5.1) have clearly indicated that CA winter cultivars exhibited a 3-fold increase in leaf protein content per unit leaf area relative to NA controls (Table 5.1). Hence, the increased leaf protein content is likely to reflect the enhanced levels of *rbcL*, *cFBPase*, *Lhcb1*, *PsbA* and *PsaA* on a leaf area basis for CA winter cultivars, Norstar and Musketeer. In contrast, CA spring cultivars, Katepwa wheat and SR4A rye exhibited minimal changes in leaf protein content (Table 5.1) and would likely reflect minimal changes in the levels of all five proteins on a leaf area basis. Elevated CO₂ had minimal effects on the levels of *rbcL*, *cFBPase*, *Lhcb1*, *PsbA* and *PsaA* expressed on leaf protein basis for all four cultivars tested (Fig. 5.7, Appendix 5S9).

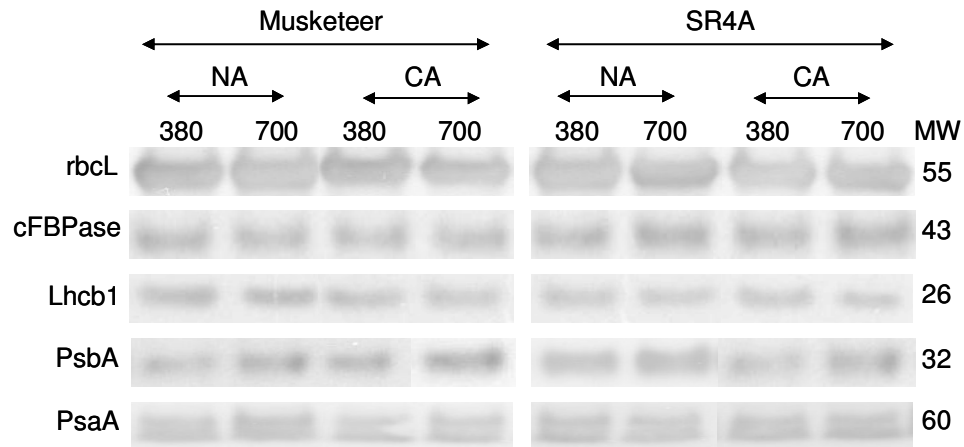


Fig. 5.7. Effects of elevated CO₂ on immunoblot analysis of SDS – PAGE probed with antibodies raised against: rbcL, cFBPase, Lhcb1, psbA and psaA isolated from Musketeer winter and SR4A spring rye. Samples were collected from fully expanded third leaves grown at either ambient CO₂ (380 μmol C mol⁻¹) or elevated CO₂ (700 μmol C mol⁻¹) and at either 20/16°C (NA) or 5/5°C (CA). Lanes of SDS – PAGE were loaded on equal protein basis (8 μg protein/lane). The bovine serum albumin (1μg on each lane) was used as an internal control. Numbers on the right indicate molecular weight (MW, kD) of protein markers.

5.3.10 Effects of elevated CO₂ on flowering time and grain yield

It has been well documented that nutrients, photoperiod and temperature substantially affect flowering time (Hadley et al. 1984, Ofir and Kiegel, 2006, Craufurd and Wheeler, 2009). The studies done to date have suggested that the effects of elevated CO₂ on flowering time differ extensively among species as well as within species such that elevated CO₂ may advance, delay or not change the flowering time (Reviewed by Springer and Ward, 2007, Springer et al. 2008, Craufurd and Wheeler, 2009).

We assessed the effects of elevated CO₂ on flowering time of Norstar winter and Katepwa spring wheat. In each growth condition of either ambient or elevated CO₂, 56 plants were monitored from the flag leaf stage to flowering initiation on the main culm on a daily basis. Flowering time was calculated from seed sowing to flower initiation (first visible flowers) for Katepwa. For Norstar, this was calculated from the days of the shift from 5° to 20°C to flower initiation. Elevated CO₂ significantly delayed flowering initiation by 3 days for Norstar such that, in 50% of the plants, the flowers initiated 52 ± 2 days after vernalization (shift from 5°C to 20°C) at elevated CO₂ in comparison to 49 ± 2 days after vernalization at ambient CO₂ (Fig. 5.8A). Similar results were obtained for Katepwa in which elevated CO₂ significantly delayed flowering initiation by 5 days (Fig. 5.8B) such that, in 50% of the plants, the flowers initiated 62 ± 3 days after seed sowing at elevated CO₂ as compared to 57 ± 2 days after seed sowing at ambient CO₂.

Elevated CO₂ significantly increased the grain yield per plant by about 60% and 40% in Norstar and Katepwa wheat respectively on a per plant basis relative to that at ambient CO₂ (Table 5.5). The enhanced grain yield under elevated CO₂ condition was associated with increased number of panicles per plant and thus, increased grain number per plant as well as increased grain size for both cultivars in response to growth at elevated CO₂ (Table 5.5, Appendix 5S10).

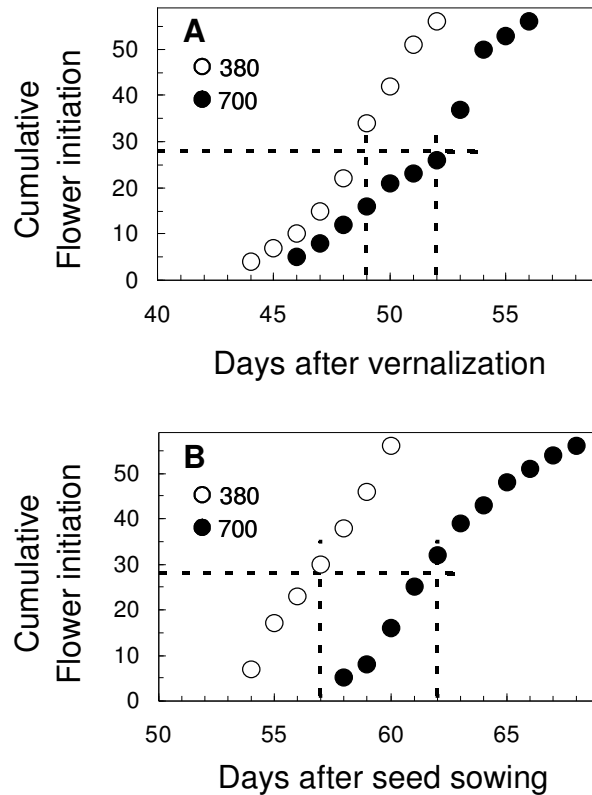


Fig. 5.8. Effects of elevated CO₂ on flowering time of Norstar winter (A) and Katepwa spring (B) wheat. The plants were grown at either ambient CO₂ (380 μmol C mol⁻¹, ○) or elevated CO₂ (700 μmol C mol⁻¹, ●). Katepwa was grown at 20/16°C until flowering initiation while Norstar was first grown at 5/5°C for 75 days and transferred to 20/16°C until flowering initiation. In each growth condition, 56 plants were monitored from flag leaf stage to flower initiation on the main culm on daily basis. Time to flowering was calculated from seed sowing to flower initiation (First visible flowers) for Katepwa and from shifting at 20/16°C to flower initiation for Norstar. Broken lines represent the days to flower 50% of the plants.

Table 5.5. Effects of elevated CO₂ on grain yield and its components in winter and spring wheat. The plants were grown at either ambient CO₂ (380 μmol C mol⁻¹) or elevated CO₂ (700 μmol C mol⁻¹). Katepwa was grown at 20/16°C until grain maturity while Norstar was first grown at 5/5°C for 75 days and transferred to 20/16°C until grain maturity. Data represent the mean of nine plants from three different pots ± SD. Significant differences due to growth CO₂ within each cultivar are indicated by the symbol* ($P \leq 0.05$).

Cultivars	Growth CO ₂ (μmol C mol ⁻¹)	Tiller No. plant ⁻¹	Effective panicle No. plant ⁻¹	Grain No. panicle ⁻¹	Grain yield (g plant ⁻¹)
Norstar	380	15 ± 2	14 ± 2	30 ± 3	9.2 ± 1.2
	700	21 ± 2*	18 ± 1*	32 ± 2	14.8 ± 2.1*
Katepwa	380	12 ± 1	8 ± 1	35 ± 2	6.6 ± 0.4
	700	17 ± 3*	9 ± 2	38 ± 3	9.4 ± 0.9*

5.4 Discussion

Consistent with our hypothesis, the low temperature-induced increase in photosynthetic capacity of winter cultivars, Norstar and Musketeer, at ambient CO₂, was maintained under growth and development of plants at elevated CO₂. In fact, the CA winter cultivars exhibited about 1.4-fold higher A_{sat} than NA controls when grown at elevated CO₂ (Fig. 5.2, Appendix 5S4). This 1.4-fold enhancement of photosynthetic capacity in CA versus NA winter cultivars at elevated CO₂ was associated with increased SLW (Table 5.1,) and, as a consequence, increase in total leaf protein content and subsequent levels of major photosynthetic enzymes such as Rubisco (rbcL), cFBPase and components of photosynthetic electron transport, Lhcb1, PsbA and PsaA on a leaf area basis upon cold acclimation (Table 5.1, Fig. 5.7, Appendix 5S9). These were consistent with increased quantum requirements to close PSII reaction centers as well as to induce energy dissipation by NPQ (Fig. 5.4, Appendix 5S6) coupled with a lower C_i requirement to open PSII reaction centers and a lower tendency to dissipate absorbed energy through NPQ under CO₂ saturated conditions in CA versus NA winter cultivars irrespective of growth CO₂ (Fig. 5.5, Appendix 5S7). Consequently, CA winter cultivars, Musketeer and Norstar exhibited a lower excitation pressure for a given irradiance and a given CO₂ concentration, and thus, a greater capacity to keep Q_A oxidized compared to NA counterparts (Fig. 5.4, Appendix 5S6, 5S7). This indicates that compared to NA winter cultivars, CA winter cultivars exhibit an enhanced capacity to utilize absorbed light energy and convert it to biomass as reflected in an increase in SLW with a concomitant decrease in dissipation of absorbed energy through NPQ. The increased energy conversion efficiency at ambient as well as elevated CO₂-grown winter wheat is translated into increased biomass (Fig. 5.1, Appendix 5S3) and enhanced seed production (Table 5.5).

In contrast to CA winter cultivars, the low temperature-induced decrease in A_{sat} of CA spring cultivars at ambient CO₂ translated into decreased photosynthetic capacity at elevated CO₂ relative to NA controls (Fig. 5.2, Appendix 5S4). This inhibition of photosynthetic capacity for CA spring cultivars was associated with decreased rates of electron transport in response to growth at low temperature (Fig. 5.4, Appendix 5S6,

5S7). These were consistent with decreased quantum requirements to close PSII reaction centers as well as to induce energy dissipation by NPQ coupled with increased C_i requirement to open PSII reaction centers in CA versus NA spring cultivars regardless of growth CO_2 (Fig. 5.4, Appendix 5S6, 5S7). Consequently, CA spring cultivars exhibited a higher excitation pressure for a given irradiance as well as given C_i concentration and thus, a lower capacity to keep Q_A oxidized compared to NA counterparts (Fig. 5.4, Appendix 5S6, 5S7). This is coupled to an enhanced dissipation of absorbed light as heat via NPQ to protect the photosynthetic apparatus from excess irradiance. Thus, compared to NA counterparts, CA spring cultivars exhibit a reduced capacity to convert absorbed light energy to biomass. Similar to our previous report that short-term elevated CO_2 can not overcome the cold acclimation-induced inhibition of A_{sat} in spring wheat and rye (Dahal et al. 2012b), long-term growth of spring wheat and rye does not compensate for the cold acclimation-induced inhibition of A_{sat} in spring cereals. We suggest that the decreased photosynthetic performance and energy conversion efficiency of CA spring cereals at either ambient or elevated CO_2 is due to feedback inhibition of CO_2 assimilation induced by growth at low temperature (Hurry et al. 1995, Savitch et al. 2002) rather than a CO_2 effect.

Since CA winter cultivars exhibit increased sink capacity, increased P_i cycling, and subsequent ATP synthesis and RuBP regeneration as well as enhanced activities of the key regulatory photosynthetic enzymes relative to NA winter cultivars grown at ambient CO_2 (Hurry et al. 1995, Dahal et al. 2012a), we hypothesized that the cold acclimation of winter wheat and winter rye decreases the sensitivity to feedback inhibition of photosynthetic capacity induced by long-term growth at elevated CO_2 . The CO_2 response curves indicate no feedback inhibition of photosynthetic capacity in response to growth at elevated CO_2 for both Norstar and Musketeer regardless of growth temperature (Fig. 5.3, Appendix 5S5). The light-saturated carboxylation efficiency as well as light and CO_2 -saturated carboxylation capacity appears to be minimally sensitive to growth at elevated CO_2 relative to at ambient CO_2 for both cultivars irrespective of growth temperature (Fig. 5.3, Appendix 5S5). These data are consistent with minimal changes in the quantum requirement as well as C_i requirement to close PSII reaction centers by EP (Fig. 5.4, Appendix 5S6, 5S7, 1-qP) and to induce energy dissipation by

NPQ (Fig. 5.4, Appendix 5S6, 5S7, NPQ) in elevated versus ambient CO₂-grown plants. The minimal changes in the carboxylation efficiency as well as carboxylation capacity were associated with minimal changes in the levels of major photosynthetic enzymes and components of photosynthetic electron transport in elevated versus ambient CO₂-grown plants (Fig. 5.7, Appendix 5S9). This was further supported by the fact that elevated CO₂ caused minimal changes in the light and CO₂-saturated rates of electron transport (Fig. 4, 5, Appendix 5S6, 5S7, ETR) as well as J_{max} and V_{cmax} (Table 5.2) for elevated versus ambient CO₂-grown plants. Similar trends of CO₂ effects were observed for spring cultivars, Katepwa wheat and SR4A rye in the NA state. However, in the CA state, spring cultivars exhibited feedback inhibition of photosynthesis induced by low growth temperature. The growth CO₂ has minimal effects on the cold-acclimation induced feedback-limited photosynthesis of spring cultivars. Thus, cold acclimation, but not elevated CO₂, appears to trigger the feedback inhibition of photosynthesis in the spring cultivars.

What enables these cultivars to overcome feedback inhibition of photosynthesis induced by long-term growth at elevated CO₂? Much of the previous information on feedback inhibition of photosynthetic capacity in responses to growth at elevated CO₂, has been derived from plants grown in small pots. Recent studies have shown that these apparent decreases in photosynthetic capacity upon growth at elevated CO₂ are likely an artifact of the pot size used in the experiments (Ainsworth and Rogers 2007). Small pots restrict the rooting volume, impede nutrient uptake, especially N and eventually limit sink strength (Arp 1991, Drake et al. 1997). In our experiment we used 4 L-sized pots which were large enough for maximum rooting volume and subsequent plant growth as confirmed by our pot size experiment (Appendix 5S1). Furthermore, the CA winter cultivars as well as all NA cultivars appeared to have an ability to enhance sink capacity, as reflected by increased respiratory rates and dry matter accumulation at elevated CO₂ relative to at ambient CO₂ (Fig. 5.1, Appendix 5S3, Appendix 5S8). In addition, the enhanced sink capacity under growth at elevated CO₂ resulted in increased grain yield associated with increased panicle number per plant and thus, increased grain number per plant as well as increased grain size in Norstar and Katepwa wheat (Table 5.5). We conclude that the increased sink capacity for CA winter cultivars as well as NA

controls at elevated CO₂ enable these cultivars to utilize the increased photoassimilates under elevated CO₂. Consequently, all cultivars were likely to overcome P_i regeneration limitation and thus, feedback inhibition of CO₂-saturated photosynthetic capacity at elevated CO₂. Moreover, elevated CO₂ had minimal effects on total protein content per unit leaf area (Table 5.1) as well as the amount of photosynthetic enzymes and components of thylakoid proteins for all four cultivars tested regardless of growth temperature (Fig. 5.7, Appendix 5S9). As a consequence, we did not observe feedback inhibition of photosynthetic capacity in response to growth at elevated CO₂. Cold acclimation but not the elevated CO₂ appeared to induce the feedback-limited photosynthesis in spring cultivars due to limited sink capacity and subsequent depletion of P_i during cold acclimation (Hurry et al. 1995).

Although cold acclimation significantly inhibited A_{sat} in spring cultivars, cold acclimation appears to increase the respiration rates in these cultivars. This stimulation of dark respiration rates by either cold acclimation or elevated CO₂ may be a consequence of increased metabolic demand, enhanced activities of respiratory enzymes, increased substrate availability or increased mitochondrial density and mitochondrial cristae per mitochondria during cold acclimation as well as growth upon elevated CO₂ (Talts et al. 2004, Campbell et al. 2007).

Although cold acclimation substantially up-regulated the expression of *rbcL* and *psaA* and substantially down-regulated the expression of *cFBPase* and *Lhcb* at the transcript level (Table 5.4), cold acclimation appeared to have minimal effects on the protein levels for corresponding genes relative to NA counterparts at ambient CO₂ (Appendix 5S9). Based on the results obtained at the transcript level, one could expect the increased protein levels for *rbcL* and *PsaA* and decreased protein levels for *cFBPase* and *Lhcb* in CA versus NA plants, which were not observed. In fact, contrary to down-regulation of *cFBPase* and *Lhcb* transcript levels, cold acclimation tended to enhance the rates of photosynthesis as well as electron transport in Norstar wheat. This suggests that the transcription of *cFBPase*, *Lhcb* and is not limiting the protein levels of a corresponding genes and associated functions. Thus, while interpreting the results, one

should not only entirely rely on gene expression data but should also consider results obtained at the functional level.

Although elevated CO₂ differentially regulated the expression of several genes associated with photosynthetic and mitochondrial electron transport, carbon metabolic pathway and respiratory pathway in NA Norstar, CA Norstar appeared to be less sensitive to growth at elevated CO₂ for gene expression (Table 5.4). The genes down-regulated by elevated CO₂ in the NA state were changed minimally in the CA state (Table 5.4). Thus, cold acclimation of Norstar appeared to prevent the elevated CO₂-induced down-regulation of several genes of photosynthetic and mitochondrial electron transport, carbon metabolic pathway and respiratory pathway. Although elevated CO₂ differentially regulated the expression of *rbcL*, *cFBPase*, *Lhcb*, *psbA* and *psaA* (Table 5.4), the protein levels for corresponding genes, were minimally changed upon growth at elevated CO₂ relative to at ambient CO₂ for both CA and NA Norstar (Appendix 5S9). Furthermore, at the functional level of corresponding genes, growth at elevated CO₂ appeared to cause minimal changes for rates of CO₂ assimilation and electron transport.

In summary, compared to NA counterparts, CA winter cultivars, Musketeer and Norstar exhibited an enhanced potential for CO₂ assimilation, increased energy conversion efficiency and grain yield at ambient CO₂ which is maintained during long-term growth and development at elevated CO₂. In contrast, compared to NA counterparts, CA spring cultivars, SR4A and Katepwa exhibited a decreased capacity for CO₂ assimilation and energy conversion efficiency not only at ambient CO₂ but also under long-term growth and development at elevated CO₂. I conclude that long-term growth and development at elevated CO₂ does not lead to the feedback inhibition of photosynthesis in winter cereals, Norstar and Musketeer as well as spring cereals, Katepwa and SR4A. Cold acclimation, however, appears to trigger the feedback-limited photosynthesis in spring cultivars, Katepwa and SR4A which can not be overcome by long-term growth and development at elevated CO₂.

Acknowledgements

This work was supported, in part, by the Natural Sciences and Engineering Research Council (NSERC) and industrial and government partners, through the Green Crop Research Network (GCN). NPAH and FS also acknowledge research support through their individual NSERC Discovery Grants.

5.5 References

- Adams III WW, Demmig-Adams B, Rosenstiel TN, Brightwell AK, Ebbert V (2002) Photosynthesis and photoprotection in overwintering plants. *Plant Biol* 4: 545-557
- Ainsworth EA, Rogers A (2007) The response of photosynthesis and stomatal conductance to rising CO₂: mechanisms and environmental interactions. *Plant Cell Environ* 30: 258-270
- Arnon DI (1949) Copper enzymes in isolated chloroplasts. Polyphenoloxidases in *Beta vulgaris*. *Plant Physiol* 24: 1-15
- Arp WJ (1991) Effects of source-sink relations on photosynthetic acclimation to elevated CO₂. *Plant Cell Environ* 14: 869-875
- Boese SR, Hüner NPA (1990) Effect of growth temperature and temperature shifts on spinach leaf morphology and photosynthesis. *Plant Physiol* 94: 1830-1836
- Boese SR, Hüner NPA (1992) Developmental history affects the susceptibility of spinach leaves to *in vivo* low temperature photoinhibition. *Plant Physiol* 99: 1141-1145
- Campbell C, Atkinson L, Zaragoza-Castells J, Lundmark M, Atkin O, Hurry V (2007) Acclimation of photosynthesis and respiration is asynchronous in response to changes in temperature regardless of plant functional group. *New Phytol* 176: 375-389
- Cheng SH, Moore BD, Seemann JR (1998) Effects of short and long-term elevated CO₂ on the expression of Ribulose-1,5-bisphosphate carboxylase/oxygenase genes and carbohydrate accumulation in leaves of *Arabidopsis thaliana* (L.) Heynh. *Plant Physiol* 116: 715-723
- Chinnusamy V, Zhu J, Zhu JK (2007) Cold stress regulation of gene expression in plants. *Trends Plant Sci* 12: 444-451

- Crafts-Brandner SJ, Salvucci ME (2000) Rubisco activase constrains the photosynthetic potential of leaves at high temperature and CO₂. *Proc Natl Acad Sci* 97: 13430-13435
- Craufurd PQ, Wheeler TR (2009) Climate change and the flowering time of annual crops. *J Exp Bot* 60: 2529-2539
- Dahal K, Kane K, Gadapati W, Webb E, Savitch LV, Singh J, Sharma P, Sarhan F, Longstaffe FJ, Grodzinski B, Hüner NPA (2012a) The effects of phenotypic plasticity on photosynthetic performance in winter Rye, winter wheat and *Brassica napus*. *Physiol Plant* 144: 169-188
- Dahal K, Kane K, Sarhan F, Grodzinski B, Hüner NPA (2012b) Cold acclimation inhibits CO₂-dependent stimulation of photosynthesis in spring wheat and spring rye. *Botany (in press)*
- Drake BG, González-Meler MA, Long SP (1997) More efficient plants: a consequence of rising atmospheric CO₂? *Annu Rev Plant Physiol Plant Mol Biol* 48: 609-639
- Ensminger I, Busch F, Hüner NPA (2006) Photostasis and cold acclimation: sensing low temperature through photosynthesis. *Physiol Plant* 126: 28-44
- Farquhar GD, Caemmerer S, Berry JA (1980) A biochemical model of photosynthetic CO₂ assimilation in leaves of C₃ species. *Planta* 149: 78-90
- Foyer C (1990) The effect of sucrose and mannose on cytoplasmic protein phosphorylation sucrose phosphate synthetase activity and photosynthesis in leaf protoplasts from spinach. *Plant Physiol Biochem* 28: 151-160
- Gorsuch PA, Pandey S, Atkin OK (2010a) Thermal de-acclimation: how permanent are leaf phenotypes when cold-acclimated plants experience warming? *Plant Cell Environ* 33: 1124-1137
- Gorsuch PA, Pandey S, Atkin OK (2010b) Temporal heterogeneity of cold acclimation phenotypes in *Arabidopsis* leaves. *Plant Cell Environ* 33: 244-258
- Gray GR, Savitch LV, Ivanov A, Hüner NPA (1996) Photosystem II excitation pressure and development of resistance to photoinhibition II. Adjustment of photosynthetic capacity in winter wheat and winter rye. *Plant Physiol* 110: 61-71
- Guy CL (1990) Cold acclimation and freezing tolerance: role of protein metabolism. *Ann Rev Plant Physiol Plant Mol Biol* 41: 187-223

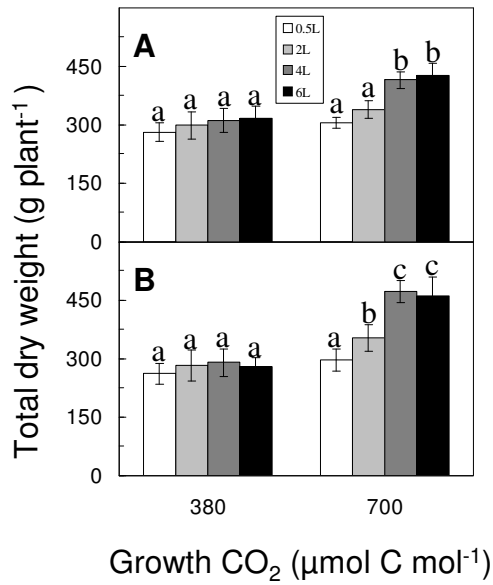
- Hadley P, Roberts EH, Summerfield RJ, Minchin FR (1984) Effects of temperature and photoperiod on flowering in soya bean [*Glycine max* (L.) Merrill]: a quantitative model. *Ann Bot* 53: 669-681
- Hüner NPA (1985) Morphological, anatomical and molecular consequences of growth and development at low temperature in *Secale cereale* L. cv Puma. *Amer J Bot* 72: 1290-1306
- Hüner NPA, Öquist G, Sarhan F (1998) Energy balance and acclimation to light and cold. *Trend Plant Sci* 3: 224-230
- Hüner NPA, Öquist G, Melis A (2003) Photostasis in plants, green algae and cyanobacteria: the role of light harvesting antenna complexes. In: Green BR, Parson WW (eds) *Advances in Photosynthesis and Respiration Light Harvesting Antennas in Photosynthesis*. Kluwer Academic Publishers, Dordrecht, pp 401–421
- Hüner NPA, Palta JP, Li PH, Carter JV (1981) Anatomical changes in leaves of Puma rye in response to growth at cold hardening temperatures. *Bot Gaz* 142: 55-62
- Hurry VM, Hüner NPA (1991) Low growth temperature effects a differential inhibition of photosynthesis in spring and winter wheat. *Plant Physiol* 96: 491-497
- Hurry V, Strand A, Furbank R, Stitt M (2000) The role of inorganic phosphate in the development of freezing tolerance and the acclimatization of photosynthesis to low temperature is revealed by the pho mutants of *Arabidopsis thaliana*. *Plant J* 24: 383-396
- Hurry VM, Strand A, Tabiaeson M, Gardeström P, Öquist G (1995) Cold hardening of spring and winter wheat and rape results in differential effects on growth, carbon metabolism, and carbohydrate content. *Plant Physiol* 109: 697-706
- Jahnke S (2001). Atmospheric CO₂ concentration does not directly affect leaf respiration in bean or poplar. *Plant Cell Environ* 24: 1139–1151
- Jahnke S, Krewitt M (2002) Atmospheric CO₂ concentration may directly affect leaf respiration measurement in tobacco, but not respiration itself. *Plant Cell Environ* 25: 641–651
- Kramer PJ (1981) Carbon dioxide concentration, photosynthesis and dry matter production. *Bio Sci* 31: 29-33

- Krause, GH (1988) Photoinhibition of photosynthesis. An evaluation of damaging and protective mechanisms. *Physiol Plant* 74: 566-74
- Leonardos ED, Savitch LV, Hüner NPA, Öquist G, Grodzinski B (2003) Daily photosynthetic and C-export patterns in winter wheat leaves during cold stress and acclimation. *Plant Physiol* 117: 521-531
- Long SP, Ainsworth EA, Rogers A, Ort DR (2004) Rising atmospheric carbon dioxide: plants FACE the future. *Ann Rev Plant Biol* 55: 591-628
- Moore BD, Cheng SH, Sims D, Seemann JR (1999) The biochemical and molecular basis for photosynthetic acclimation to elevated atmospheric CO₂. *Plant Cell Environ* 22: 567-582
- Ofir M, Kiegel J (2006) Opposite effects of daylength and temperature on flowering and summer dormancy of *Poa bulbosa*. *Ann Bot* 97: 659-666
- Öquist G, Hüner NPA (2003) Photosynthesis of overwintering evergreen plants. *Ann Rev Plant Biol* 54: 329-355
- Öquist G, Hurry VM, Hüner NPA (1993) Low-temperature effects on photosynthesis and correlation with freezing tolerance in spring and winter cultivars of wheat and rye. *Plant Physiol* 101: 245-250
- Pocock TH, Hurry VM, Savitch LV, Hüner NPA (2001) Susceptibility to low-temperature photoinhibition and the acquisition of freezing tolerance in winter and spring wheat: The role of growth temperature and irradiance. *Physiol Plant* 113: 499-506
- Rapacz M, Wolanin B, Hura K, Tyrka M (2008) The effects of cold acclimation on photosynthetic apparatus and the expression of COR14b in four genotypes of barley (*Hordeum vulgare*) contrasting in their tolerance to freezing and high-light treatment in cold conditions. *Ann Bot* 101: 689-699
- Sarhan F, Ouellet F, Vazquez-Tello A (1997) The wheat *Wc55S100* gene family: a useful model to understand the molecular genetics of freezing tolerance in cereals. *Physiol Plant* 101: 439-445
- Sassenrath GF, Ort DR (1990) The relationship between inhibition of photosynthesis at low temperature and the inhibition of photosynthesis after rewarming in chill-sensitive tomato. *Plant Physiol Biochem* 28: 457-465

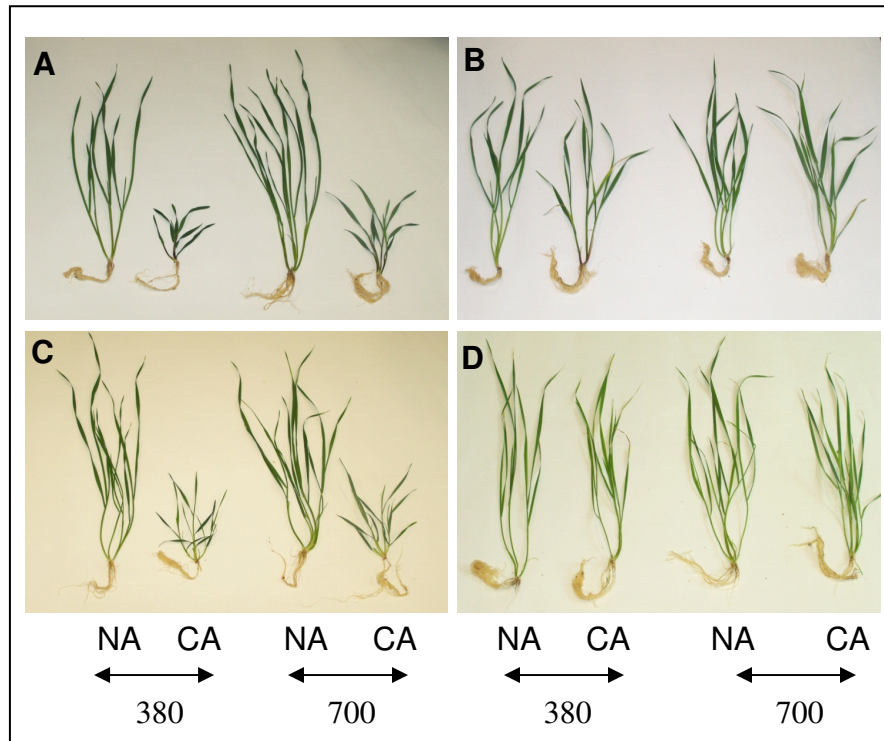
- Savitch LV, Barker-Astrom J, Ivanov A G, Hurry V, Oquist G, Hüner NPA (2001) Cold acclimation of *Arabidopsis thaliana* results in incomplete recovery of photosynthetic capacity which is associated with an increased reduction of the chloroplast stroma. *Planta* 214: 295-301
- Savitch LV, Allard G, Seki M, Robert LS, Tinker NA, Hüner NPA, Shinozaki K, Singh J (2005) The effect of overexpression of two Brassica CBF/DREB1-like transcription factors on photosynthetic capacity and freezing tolerance in *Brassica napus*. *Plant Cell Physiol* 46: 1525-1539
- Savitch LV, Leonardos ED, Krol M, Jansson S, Grodzinski B, Hüner NPA, Öquist G (2002) Two different strategies for light utilization in photosynthesis in relation to growth and cold acclimation. *Plant Cell Environ* 25: 761-771
- Sharkey TD, Vanderveer PJ (1989) Stromal phosphate concentration is low during feedback limited photosynthesis. *Plant Physiol* 91:679-684
- Springer CJ, Ward JK (2007). Flowering time and elevated atmospheric CO₂. *New Phyto* 176: 243-255
- Springer C, Orozco R, Kelly J, Ward J (2008). Elevated CO₂ influences the expression of floral-initiation genes in *Arabidopsis thaliana*. *New Phyto* 178: 63–67
- Stitt M, Quick WP (1989). Photosynthetic carbon partitioning: its regulation and possibilities for manipulation. *Physiol Plant* 77: 633-641
- Stitt M, Hurry VM (2002) A plant for all seasons: alterations in photosynthetic carbon metabolism during cold acclimation in *Arabidopsis*. *Curr Opin Plant Biol* 5: 199-206
- Strand A, Hurry VM, Henkes S, Hüner NPA, Gustafsson P, Gardeström P, Stitt M (1999) Acclimation of *Arabidopsis* leaves developing at low temperatures. Increasing cytoplasmic volume accompanies increased activities of enzymes in the Calvin cycle and in the sucrose-biosynthesis pathway. *Plant Physiol* 119: 1387-1398
- Talts P, Parnik T, Gardeström P, Keerberg O (2004) Respiratory acclimation in *Arabidopsis thaliana* leaves at low temperature. *J Plant Physiol* 161: 573–579
- Tcherkez GGB, Farquhar GD, Andrews TJ (2006). Despite slow catalysis and confused substrate specificity, all ribulose biphosphate carboxylases may be nearly perfectly optimized. *Proc Nat Acad Sci* 103: 7246-7251

- Thomas RB, Strain BR (1991) Root restriction as a factor in photosynthetic acclimation of cotton seedlings grown in elevated carbon dioxide. *Plant Physiol* 96: 627-634
- Thomashow MF (2001) So what's new in the field of plant cold acclimation? Lots! *Plant Physiol* 125: 89-93
- Webber AN, Nie G-Y, Long SP (1994) Acclimation of photosynthetic proteins to rising atmospheric CO₂. *Photosyn Res* 39: 413-425
- Yakir D, Rudich J, Bravdo BA (1986) Adaptation to chilling: Photosynthetic characteristics of the cultivated tomato and a high altitude wild species. *Plant Cell Environ* 9: 477-484

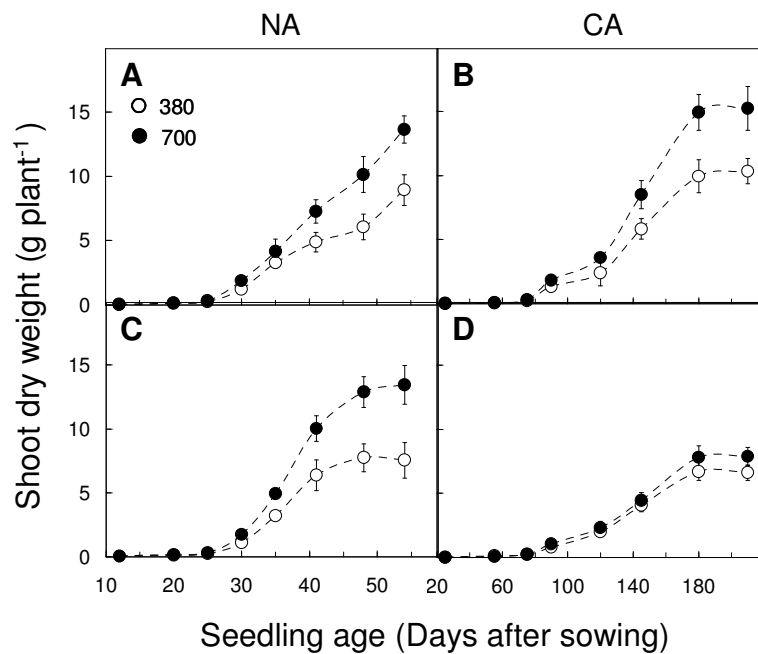
5.6 Appendices



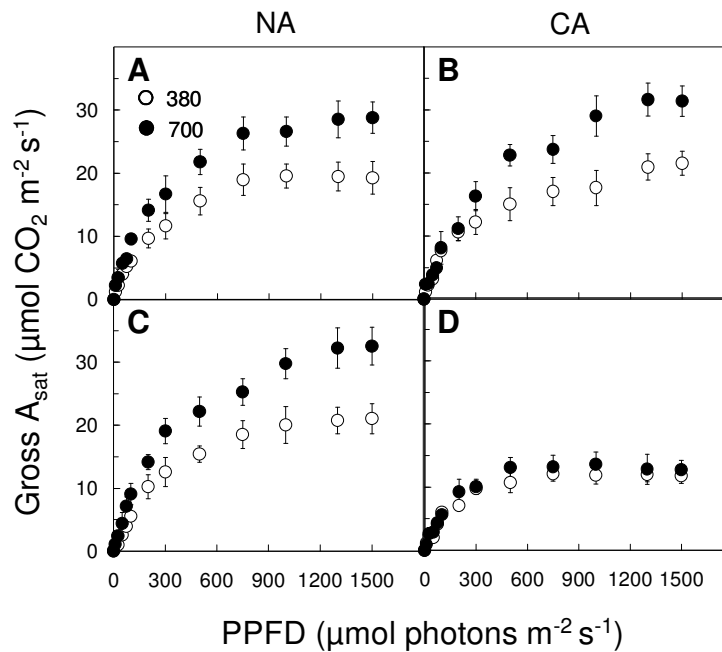
Appendix 5S1. Effect of pot size on total dry matter accumulation (shoot and root). Musketeer winter rye was grown in 0.5L, 2L, 4L and 6L-sized pots at either ambient CO₂ (380 μmol C mol⁻¹) or elevated CO₂ (700 μmol C mol⁻¹) and at either 20/16°C (NA, A) and 5/5°C (CA, B). The shoot and root samples were harvested from 25-d-old NA and 75-d-old CA plants regardless of growth CO₂. Each point represents the mean of nine plants from three different pots. Bars represent SD. Significant differences among different pot sizes are indicated by the superscripted letters (P ≤ 0.05).



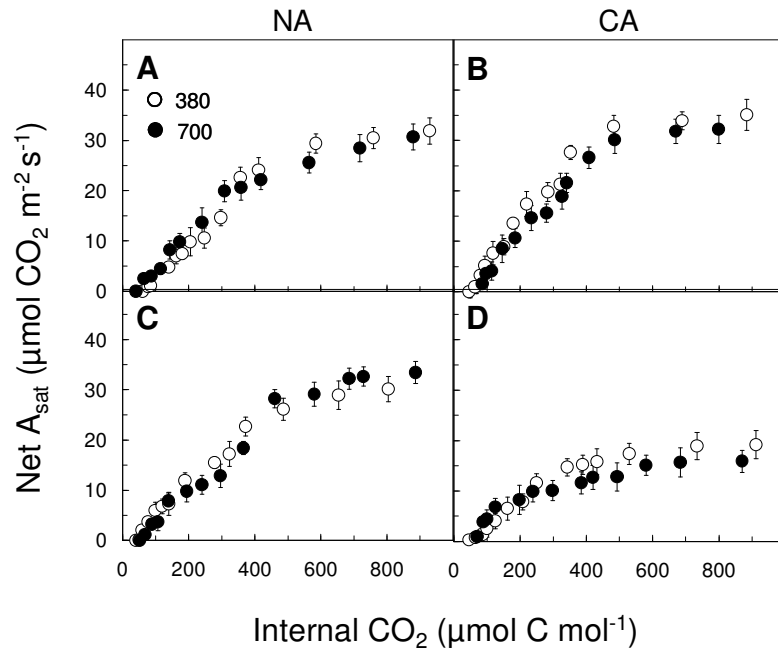
Appendix 5S2. Effects of elevated CO₂ and growth temperatures on plant morphology and growth habit of winter (cv Musketeer rye, A, cv Norstar wheat, C) versus spring cultivars (cv SR4A rye, B, cv Katepwa wheat, D). Plants were grown at either ambient CO₂ (380 μmol C mol⁻¹) or elevated CO₂ (700 μmol C mol⁻¹) and at either 20/16°C (NA) or 5/5°C (CA). Photographs were taken together for each cultivar from 25-d-old NA and 75-d-old CA plants grown at either ambient or elevated CO₂.



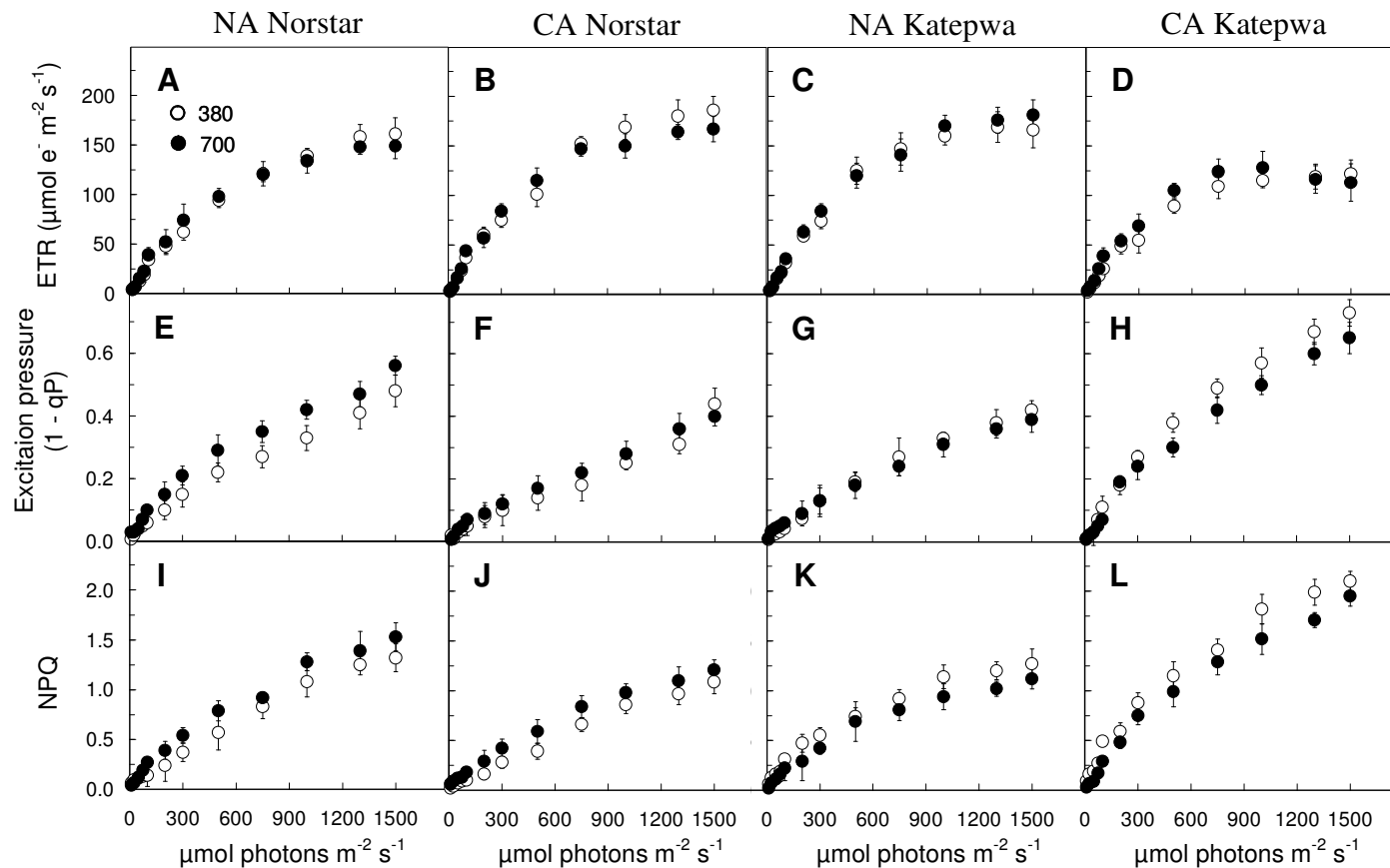
Appendix 5S3. Effects of cold acclimation and elevated CO₂ on shoot dry weight of Norstar winter (A, B) and Katepwa spring (C, D) wheat. The plants were grown at either ambient CO₂ (380 μmol C mol⁻¹, ○) or elevated CO₂ (700 μmol C mol⁻¹, ●) and at either 20/16°C (NA, A, C) or 5/5°C (CA, B, D). Each point represents the mean of nine plants from three different pots. Bars represent SD.



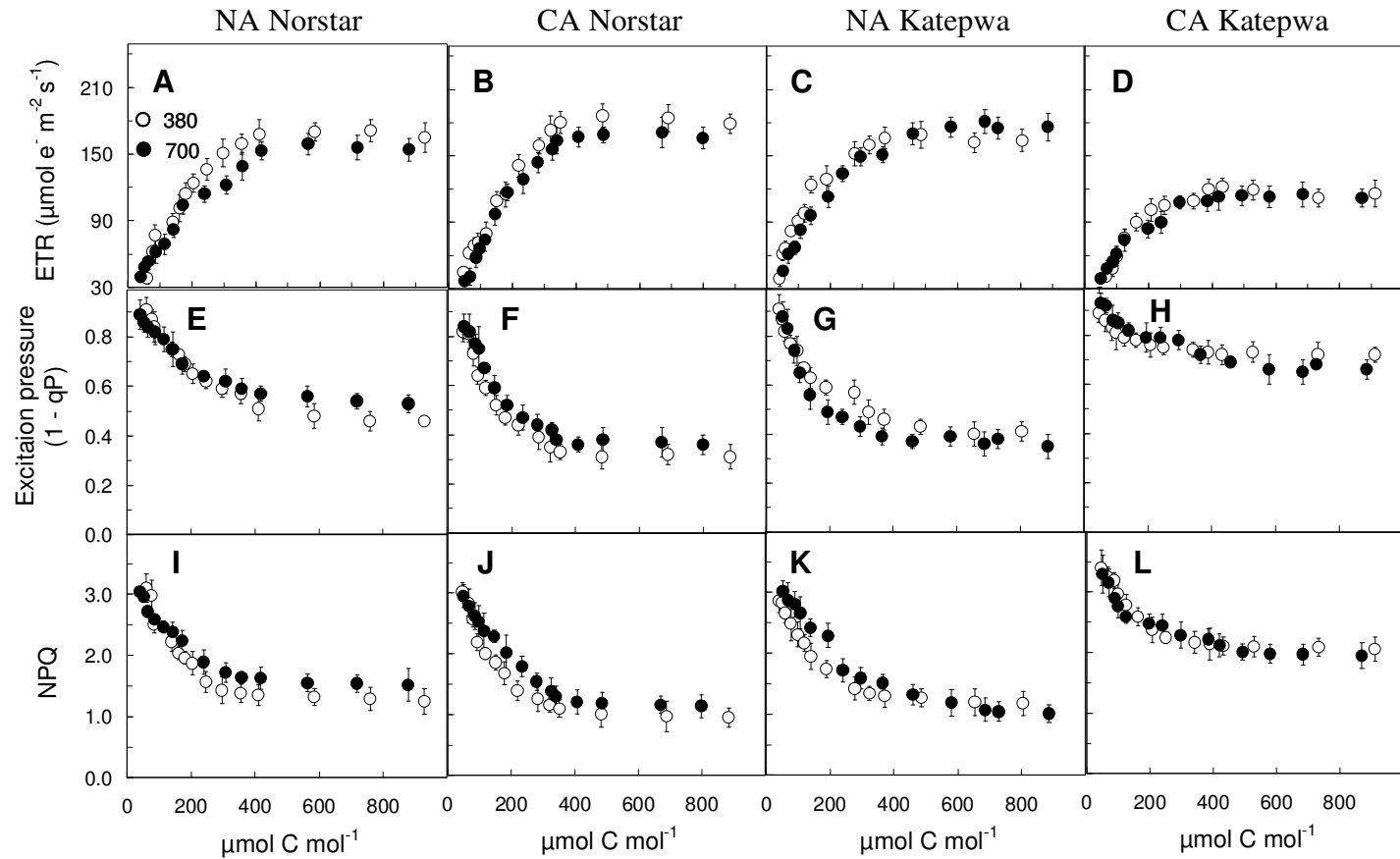
Appendix 5S4. Light response curves of gross CO₂ assimilation for Norstar winter (A, B) and Katepwa spring (C, D) wheat. The plants were grown at either ambient CO₂ (380 μmol C mol⁻¹, ○) or elevated CO₂ (700 μmol C mol⁻¹, ●) and at either 20/16°C (NA, A, C) or 5/5°C (CA, B, D). Measurements were carried out on attached, fully developed third leaves at their respective growth CO₂ and at measuring temperatures of 20°C. Each point represents the mean of nine plants from three different pots. Bars represent SD.



Appendix 5S5. CO₂ response curves of light-saturated net CO₂ assimilation for Norstar winter (A, B) and Katepwa spring (C, D) wheat. The plants were grown at either ambient CO₂ (380 μmol C mol⁻¹, ○) or elevated CO₂ (700 μmol C mol⁻¹, ●) and at either 20/16°C (NA, A, C) or 5/5°C (CA, B, D). Measurements were carried out on attached, fully developed third leaves at measuring temperature of 20°C. Each point represents the mean of nine plants from three different pots. Bars represent SD.



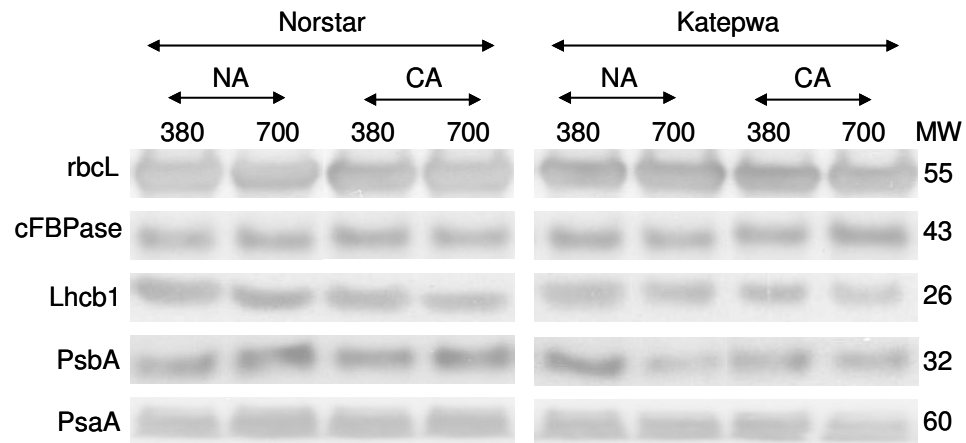
Appendix 5S6. Light response curves of electron transport rates (ETR, A, B, C, D), excitation pressures (1-qP, E, F, G, H) and non photochemical quenching of excess energy (NPQ, I, J, K, L) for Norstar winter (A, B, E, F, I, J) and Katepwa spring wheat (C, D, G, H, K, L) grown at either 20/16°C (NA) or 5/5°C (CA) and at either ambient CO₂ (380 μmol C mol⁻¹, ○) or elevated CO₂ (700 μmol C mol⁻¹, ●). Measurements were carried out on attached, fully developed third leaves at measuring temperature of 20°C and at 700 μmol C mol⁻¹. Each point represents the mean of nine plants. Bars represent SD.



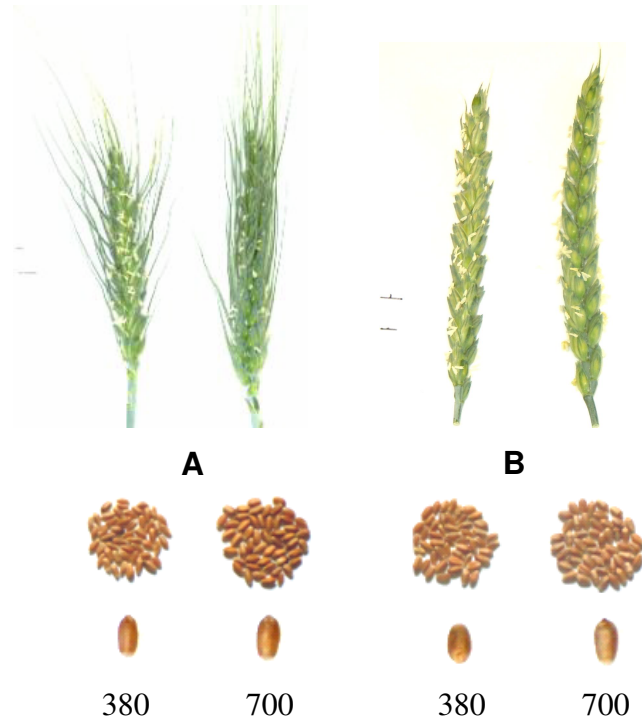
Appendix 5S7. CO₂ response curves of light-saturated electron transport rates (ETR, A, B, C, D), excitation pressures (1-qP, E, F, G, H) and non photochemical quenching of excess energy (NPQ, I, J, K, L) for Norstar winter (A, B, E, F, I, J) and Katepwa spring (C, D, G, H, K, L) wheat grown at either 20/16°C (NA) or 5/5°C (CA) and at either ambient (380 μmol C mol⁻¹, ○) or elevated (700 μmol C mol⁻¹, ●) CO₂. Measurements were carried out on fully developed third leaves at 20°C and at saturating irradiance of 1300 μmol m⁻² s⁻¹ PPFD. Each point represents the mean of nine plants. Bars represent SD.

Appendix 5S8. Effects of elevated CO₂ on dark respiratory rates (R_{dark}) of winter and spring cereals. The plants were grown at either ambient CO₂ (380 $\mu\text{mol C mol}^{-1}$) or elevated CO₂ (700 $\mu\text{mol C mol}^{-1}$) and at either 20/16°C (NA) or 5/5°C (CA). Measurements were carried out on fully expanded third leaves at their respective growth CO₂ and at 20°C. Data represent the mean of nine plants from three different pots \pm SD. Significant differences among the means within each cultivar are indicated by the superscripted letters ($P \leq 0.05$).

R_{dark} ($\mu\text{mol C evolved m}^{-2}\text{s}^{-1}$)				
Cultivars	NA		CA	
	380	700	380	700
Musketeer	2.48 $\pm 0.12^a$	2.87 $\pm 0.16^b$	3.64 $\pm 0.27^c$	3.79 $\pm 0.22^c$
Norstar	3.07 $\pm 0.23^a$	3.41 $\pm 0.31^{ab}$	3.88 $\pm 0.18^b$	3.97 $\pm 0.43^b$
SR4A	2.42 $\pm 0.12^a$	2.99 $\pm 0.25^b$	2.96 $\pm 0.39^b$	3.02 $\pm 0.42^b$
Katepwa	1.93 $\pm 0.22^a$	2.26 $\pm 0.31^a$	2.35 $\pm 0.12^b$	2.19 $\pm 0.10^{ab}$



Appendix 5S9. Effects of elevated CO₂ on immunoblot analysis of SDS – PAGE probed with antibodies raised against: rbcL, cFBPase, Lhcb1, PsbA and PsaA isolated from Norstar winter and Katepwa spring wheat. Samples were collected from fully expanded third leaves grown at either ambient CO₂ (380 μmol C mol⁻¹) or elevated CO₂ (700 μmol C mol⁻¹) and at either 20/16°C (NA) or 5/5°C (CA). Lanes of SDS – PAGE were loaded on equal protein basis (8 μg protein/lane). The bovine serum albumin (1μg on each lane) was used as an internal control. Numbers on the right indicate molecular weight (MW, kD) of protein markers.



Appendix 5S10. Effects of elevated CO₂ on panicle and grain size in Norstar winter (A) and Katepwa spring (B) wheat. The plants were grown at either ambient CO₂ (380 μmol C mol⁻¹) or elevated CO₂ (700 μmol C mol⁻¹). Katepwa was grown at 20/16°C until grain maturity while Norstar was first grown at 5/5°C for 75 days and transferred to 20/16°C until grain maturity. Pictures were taken for a single seed as well as 50 seeds together.

Chapter 6

General discussions and future perspectives

6.1 Major contributions

In the present study, I assessed the effects of cold acclimation and long-term elevated CO₂ on photosynthetic performance and energy conversion efficiency of winter and spring wheat and rye as well as wild type and *BnCBF17*-over-expressing line of *Brassica napus* cv Westar. Following are the major contributions of my PhD research.

6.1.1 CBF enhances energy conversion efficiency

Atmospheric CO₂ is projected to rise from present 380 $\mu\text{mol C mol}^{-1}$ to ca. 700 $\mu\text{mol C mol}^{-1}$ which may likely be coupled with an increase in average global temperature by the end of the next century (IPCC 2007). These changes in atmospheric CO₂ and temperature may have considerable effects on photosynthetic performance of plants and therefore on plant biomass and grain yield. Global concerns regarding food security have highlighted an urgent need to double yield and productivity of major food crops such as rice and wheat to feed the increasing population over the next 50 years (Murchie et al. 2009). In order to achieve this rising food demand to keep pace with a growing population, we need to identify specific characteristics to develop and exploit new cultivars with increased biomass and seed yield potentiality under projected future adverse environmental conditions.

The maximum potential biomass and grain yield a plant can produce is determined by a number of variables. They are amount of solar radiation absorbed, light interception efficiency, energy conversion efficiency, translocation of photosynthate to sinks, sink strength and partitioning efficiency also termed harvest index (Long et al. 2006, Amthor 2007, Zhu et al. 2010). The increase in potential yield of major crops over the past 50 years was, by and large, accounted for by the improved partitioning efficiency and light interception efficiency. Increased partitioning efficiency has chiefly resulted through the release of dwarf cultivars producing higher numbers of seeds per plant.

Whereas increased light interception efficiency has resulted as a consequence of increased leaf area index (LAI) associated with larger-leafed cultivars as well as through the development of dwarf cultivars with improved lodging resistance against the adverse weather conditions, such as rain, wind and hail (Long et al. 2006, Murchie et al. 2009).

Since partitioning efficiency and light interception efficiency have approached the theoretical upper limit (Amthor 2007, Zhu et al. 2008, 2010), further increase in yield potential can only be achieved by an increase in energy conversion efficiency, that is, the efficiency of conversion of the intercepted light energy in biomass and seed production. Since plant dry matter consists of about 40% carbon by weight, an enhancement in total biomass production can be achieved through enhancement of photosynthetic carbon assimilation (Murchie et al. 2009). Although photosynthesis is the ultimate basis of yield, improving photosynthetic efficiency has played only a minor role in enhancing plant biomass and seed yield to date (Long et al. 2006, Zhu et al. 2010).

Research on CBF over-expression in plants has been primarily focussed on freezing tolerance at the molecular level. Although increasing energy conversion efficiency is critical for plant biomass and seed yield, few studies have attempted to integrate CBF- over-expression with photosynthetic efficiency. In the present study, I have shown that CBFs appear to be critical factors that govern energy conversion efficiency of a plant from the level of gene expression to the changes at the whole plant architecture, carbon metabolism and sink capacity. Thus, my present studies on Brassica *BnCBF17* transcription factor have advanced our understanding of CBF as a central component that plays a vital role to produce superior hardy crops that can not only withstand multiple abiotic stresses but also exhibit outstanding photosynthetic performance and energy conversion efficiency under high CO₂ environment. I have shown that over-expression of *BnCBF17* in *B. napus* grown at 20°C mimics the effects of cold acclimation in wild type *B. napus* as well as winter cereals with respect to increased photosynthetic performance, enhanced energy conversion efficiency to biomass as well as seed yield and improved water use efficiency. Thus, the over-expression in *B. napus* of a single transcription factor, *BnCBF17*, appears to convert the non-acclimated WT to a cold acclimated state without prior exposure to low temperature. This is a very

incredible finding suggesting that instead of growing plants for a longer period of time at low temperature to acquire CA state, we can over-express CBF transcription factors and achieve plants with similar photosynthetic performance without being exposed to low temperature. This is a useful and time-saving approach to enhance capacity to utilize absorbed light energy and convert it to biomass and grain yield. Thus, this study provides exciting new insights into the molecular basis for enhanced plant productivity under conditions of elevated CO₂ associated with global warming and climate change.

Targeting the CBF pathway in major crop species will be a novel approach to improve crop yield and productivity that help meet the nutritional demands of a rising population. This may provide important new insights into potential molecular approaches focussed on the maintenance or even the enhancement of plant productivity under suboptimal growth conditions associated with global warming and climate change. In addition, this research has helped identify novel wheat, rye and *Brassica* cultivars that can sustain stress or even perform better under changing environmental conditions. Winter cereals such as Musketeer and Norstar and *B. napus* exhibit an unusual capacity to enhance CO₂ assimilation and energy use efficiency as a result of phenotypic and metabolic adjustments to low temperature. Thus, this study has provided new insights into the central role of the CBF transcription factor (s) and the identification of novel characteristics in wheat, rye and *B. napus* that offer considerable potential for breeding programmes aimed at enhancing or monitoring crop productivity in response to global warming and climate change.

In conclusion, CBF transcription factor (s) plays a pivotal role in enhancing energy conversion efficiency in biomass and grain yield. However, the precise way by which CBF regulates this mechanism is still not fully understood. Therefore, future research on CBF transcription factor should pay attention to determine the underlying mechanisms for CBF-regulation of energy conversion efficiency.

6.1.2 CO₂-induced feedback-limited photosynthesis is species dependent

The feedback inhibition of photosynthesis induced by long-term growth and development at elevated CO₂ has been reported in a wide range of plant species (Long et al. 2004,

Ainsworth and Rogers, 2007). My present study has indicated that although WT *Brassica napus* grown at 20°C exhibits the feedback inhibition of photosynthesis upon growth at elevated CO₂, both winter and spring cereals are insensitive to feedback-limited photosynthesis in response to growth at elevated CO₂. I suggest that the elevated CO₂-induced differential sensitivity to feedback-limited photosynthesis may be associated with differential stimulation of sink capacity as reflected in differences in biomass accumulation in cereals versus *Brassica* in response to growth at elevated CO₂. Elevated CO₂ appears to enhance the dry matter accumulation by about 65% in cereals as opposed to 20% in *Brassica napus* in the NA state. This tremendous increase in biomass accumulation of cereals upon growth at elevated CO₂ may be a consequence of an increased sink capacity enabling these species to utilize the increased photoassimilates resulting from initial CO₂ stimulation of photosynthesis. Consequently, all cereal cultivars are likely to overcome P_i regeneration limitation and thus, feedback inhibition of photosynthetic capacity at elevated CO₂. This is further supported by the fact that elevated CO₂ had minimal effects on the amount of key photosynthetic enzymes and components of photosynthetic electron transport for all cereals tested.

In contrast to cereals, elevated CO₂ enhances the dry matter accumulation by only 20% in WT *Brassica* which may not be sufficient to utilize the increased photoassimilates resulted from initial CO₂ stimulation of photosynthesis. This is further supported by the fact that elevated CO₂ appears to significantly inhibit the level of key regulatory Calvin cycle enzyme, *rbcL* and sucrose biosynthetic enzyme, *cFBPase* in WT *Brassica*. I suggest that the WT *Brassica* exhibits sensitivity to feedback-limited photosynthesis due to insufficient sink demand and concomitantly decreased P_i recycling and inhibition of expression of major photosynthetic enzymes upon growth at elevated CO₂. Cold acclimation and/or *BnCBF17*-over-expression appear to overcome the CO₂-induced feedback-limited photosynthesis. I suggest that the decreased sensitivity to feedback-limited photosynthesis in CA *Brassica* as well as in *BnCBF17*-OE under elevated CO₂ conditions is due to increased sink capacity as reflected in increased respiration rates and biomass accumulation. Consequently, CA *Brassica* and *BnCBF17*-OE exhibit improved capacity to maintain a high flux of carbon between source and sink even under elevated

CO₂ conditions. This is further supported by the fact that in cereals, carbon export rates from source leaves are also enhanced upon cold acclimation (Leonardos et al. 2003).

Thus, I suggest that the sensitivity to feedback-limited photosynthesis induced by growth at elevated CO₂ is species dependent. CBF plays a crucial role in reducing sensitivity of photosynthesis to feedback inhibition during long-term growth of *B. napus* at elevated CO₂. However, the molecular mechanisms that differentially regulate the feedback-limited photosynthesis in cereals versus *Brassica* upon growth at elevated CO₂ are not fully understood. Thus, it is imperative that future research be focused on identifying the molecular mechanisms governing feedback limitation of photosynthesis in order to enhance crop yield and productivity under projected sub-optimal environmental conditions.

6.1.3 Phenotypic plasticity accounts for the increased CO₂ assimilation

Previous studies have suggested that the increased photosynthetic capacity measured on a leaf area basis for CA winter cereals can be accounted for solely on the basis of reprogramming of the carbon metabolic pathways upon cold acclimation (Hurry 1995, Savitch et al. 2002). However, in the present study, I have shown that the increased photosynthetic capacity of CA winter cereals as well as *BnCBF17*-OE *Brassica napus* is, by and large, accounted for by altered leaf morphology, leaf anatomy and SLW associated with increased photosynthetic apparatus per unit leaf area. However, phenotypic plasticity could not account for the difference in the temperature sensitivity (Q₁₀) of CO₂ assimilation and photosynthetic electron transport as well as the differences in the light response curves for ETR, excitation pressure and NPQ. The changes in Q₁₀ and the decreased efficiencies of PSII closure and the induction of NPQ as a function of irradiance in either CA winter cereals or in the *BnCBF17*- OE Brassica reflect, in part, the inherent flexibility in energy utilization by photosynthetic electron transport (McDonald et al. 2011) rather than changes in leaf anatomy and plant phenotype.

6.1.4 Elevated CO₂ can not compensate for decreased A_{sat} of CA spring cereals

Consistent with a cold acclimation-induced decrease in A_{sat} at ambient CO_2 , spring cereals exhibit decreased CO_2 assimilation during a short-term shift to elevated CO_2 upon cold acclimation. In fact, CA spring wheat and spring rye are not able to recover from the low temperature-induced inhibition of A_{sat} through a short-term exposure to elevated CO_2 . Therefore, even though spring cereals grow and develop at low temperature, cold acclimation not only inhibits photosynthetic rates at ambient CO_2 but also inhibits the stimulation of photosynthetic rates by short-term exposure to elevated CO_2 . In addition, my long-term CO_2 experiment has indicated that CA spring cultivars exhibit decreased photosynthetic performance and consequently reduced capacity to utilize absorbed light energy and convert it to biomass upon growth at elevated CO_2 relative to NA counterparts.

In conclusion, although spring cereals can grow and develop at low temperature, unlike winter cereals, they inhibit the photosynthetic capacity in response to growth at low temperature. However, spring cereals appear to enhance the respiratory rates during cold acclimation. What are the mechanisms of differential stimulation of photosynthetic capacity and respiratory rates in winter versus spring cereals upon cold acclimation? Future research should provide an answer to this question.

6.1.5 CBF is a master regulator: A model

In the present study, I have revealed that the CBF transcription factor (s) plays a key role in enhancing energy conversion efficiency to biomass and grain yield through morphological, physiological and biochemical adjustments. Hence, I present a model on CBF-regulation of enhanced energy conversion efficiency based on results obtained from CA winter cereals and *BnCBF17*- over-expressing *Brassica napus* (Fig 6.1). I further propose the model for CBF pathways regulating freezing tolerance, growth habit and flowering time based on the previous reports (Fig 6.1).

Plants sense low temperature through cell membrane rigidification which activates Ca^{2+} channels resulting in an accumulation of Ca^{2+} in the cytosol (Chinnusamy et al. 2007) (Fig 6.1). Such accumulation of Ca^{2+} in the cytosol activates a protein kinase which phosphorylates ICE1 (inducer of CBF expression1). Low temperature-induced

phosphorylation of ICE1 is necessary to induce the expression of CBF transcription factors (Zarka et al. 2003, Gilmour et al. 2004). The CBF transcription factors bind to the promoter region of CBF-regulons and initiate the expression of CBF-regulons necessary to acquire freezing tolerance (Jaglo-Ottosen et al. 1998, Chinnusamy et al. 2007) (Fig 6.1). In addition to playing a central role in enhancing freezing tolerance (Jaglo-Ottosen et al. 1998, Savitch et al. 2005), my present studies show that CBF transcription factor has a much broader effect on enhancing energy conversion efficiency as reflected in increased biomass and seed yield through morphological, physiological and biochemical adjustments (Fig 6.1). As illustrated in figure 6.1, I propose that the CBF-induced enhancement of energy conversion efficiency is associated with increased CO₂ assimilation as consequences of (i) altered plant architecture (ii) suppressed photorespiration (iii) increased expression and activities of key regulatory photosynthetic enzymes and (iv) increased sink capacity.

Plant architecture such as the dwarf, compact phenotype observed for CA winter cereals as well as *BnCBF17*-over-expressing *B. napus* results in increased CO₂ assimilation due to enhanced SLW and associated photosynthetic apparatus per unit leaf area. It has been suggested that the success of the green revolution was achieved through the dwarf phenotype which resulted in short stem length with concomitant increase in the potential number of seeds (Reviewed by Long et al. 2006). This suggests that CBF-induced change in phenotypic plasticity accounts, by and large, for increased CO₂ assimilation and concomitant increased energy conversion efficiency in CA winter cereals as well as *BnCBF17*-over-expressing *B. napus*.

Savitch et al. (2000) reported that cold acclimation of winter wheat results in the suppression of photorespiration, thus, diverting ATP and NADPH from oxygenation to carboxylation. Thus, as observed upon cold acclimation of winter wheat, I propose that CBF is involved in repressing photorespiration and thus, enhancing photosynthetic efficiency and ability to convert intercepted solar energy into biomass and grain yield.

I suggest that the increased energy conversion efficiency of CA winter cereals as well as *BnCBF17*-OE is associated with CBF-induced improved capacity to maintain an

increased sink capacity, for instance, increased respiratory rates and increased specific leaf weight (Fig. 6.1). This is further supported by the fact that in cereals, carbon export rates from source leaves are also enhanced upon cold acclimation (Leonardos et al. 2003). Thus, to meet the increased sink demand, CA winter cereals as well as *BnCBF17*-OE exhibit increased CO₂ assimilation through increased levels of key regulatory photosynthetic enzymes such as Rubisco (rbcL) and cytosolic FBPase (cFBPase) important in regulating sucrose biosynthesis as well as components of the thylakoid membrane represented by Lhcb1, PsbA and PsaA on a leaf area basis.

Consistent with a previous study (Savitch et al. 2005), over-expression of *BnCBF17* in *Brassica napus* mimics the effects of cold acclimation in winter cereals. Thus, the results obtained for CA winter cereals and *BnCBF17*-over-expressing *B. napus* indicate that CBFs/DREBs appear to be critical factors that govern energy conversion efficiency of plants from the level of gene expression to changes in whole plant architecture, carbon metabolism and sink capacity. In addition to enhanced energy conversion efficiency obtained in the present study, previous studies have suggested that CBF pathways regulate freezing tolerance, growth habit and flowering.

The CBF-over-expressing transgenic lines of *Arabidopsis* exhibit growth retardation at normal temperature through down-regulation of the expression of gibberellins (GA) biosynthetic genes as well as up-regulation of GA catabolizing genes (GAox) (Achard et al. 2008). This indicates that CBF has an antagonistic relationship with GA. The reduced GA levels cause a dwarf phenotype through accumulation of DELLAs, a family of proteins that suppress plant growth (Achard et al. 2008). This dwarf phenotype has been reversed by either exogenous application of GA or by generating a DELLAs deficient mutant in *Brassica napus* (Jaglo et al. 2001). In addition, salicylic acid (SA), a growth inhibitor, is also suggested to be involved in suppressing plant growth. SA-deficient mutants exhibit a larger phenotype compared to wild type *Arabidopsis* suggesting that SA accumulation induces dwarf phenotype in *Arabidopsis* (Scott et al. 2004). Thus, I propose that CBF- induced GA/DELTA and SA signalling pathways are involved in repressing plant growth in CA winter cereals and *BnCBF17*-OE *Brassica* (Fig. 6.1).

Previous studies have suggested that the vernalisation and CBF pathways have an antagonistic relationship in both Arabidopsis and cereals. If Arabidopsis plants are exposed to cold stress before vernalization they induce CBF-activated FLOWERING LOCUS C (FLC) expression, which delays flowering and enhances resistance to freezing winter conditions (Oliver et al. 2009, Trevaskis 2010). After the vernalisation requirement is fulfilled, the VRN1 gene is expressed and the CBF pathway is suppressed by the floral activator SUPPRESSOR OF OVEREXPRESSION OF CO1 (SOC1) or FLOWERING LOCUS T (FT) and thus decreases freezing tolerance after transition from vegetative to reproductive stage (Sung and Amasino 2005, Trevaskis et al. 2007, Chew et al. 2011). Consistent with the previous reports for Arabidopsis and cereals, I propose that the *BnCBF17*-over-expression in *B. napus* induces FLC expression and subsequently delays flowering through suppression of SOC1 or FT expression (Fig. 6.1).

CBF-induced increase in abiotic stress tolerance has been reported in cold resistant as well as some of the cold sensitive major crop species such as rice, wheat, maize, tomato and potato (Reviewed by Medina et al. 2011). In addition, other food crops, forage and trees such as barley, sorghum, oat, rye, perennial rye grass, sweet cherry alfalfa, *Medicago truncatula*, poplar, birch and cotton also exhibit increased abiotic tolerance through CBF mediated pathways (Medina et al. 2011). For instance, transgenic Arabidopsis and tobacco over-expressing CBF homologues from rice, perennial ryegrass, maize, barley and wheat plants result in dwarf phenotype, increased freezing tolerance and expression of suites of cold-regulated genes suggesting that the CBF regulon is conserved in a wide range of higher plants (Medina et al. 2011). On the other hand, the over-expression of Arabidopsis *AtCBFs* in rice, wheat and bahia grass also enhances freezing tolerance. A number of studies have identified wheat CBFs that are expressed in winter but not in spring cultivars. As a consequence, winter wheat but not spring wheat is able to overcome freezing winter. In rice, *OsDREB1A* and *OsDREB1B* genes, which have functional overlap with Arabidopsis *CBF3/DREB1A* and *CBF1/DREB1B*, are induced by low temperature that subsequently leads to enhanced stress tolerance to drought, high salt and cold (Duboujet et al. 2003). In addition, over-expression of barley *HvCBF4* in transgenic rice also results in improved tolerance to drought, high-salinity and low temperature stresses (Oh et al. 2007). In tomato, the CBF

pathway has been shown to be important for the induction of chilling tolerance in the mature fruit (Zhao et al. 2009). In addition, over-expression of CBFs in *Arabidopsis* and *Brassica napus* enhances tolerance to dehydration, high salt and freezing stress (Kasuga et al. 1999, Savitch et al. 2005, Medina et al. 2011).

Taken together, these findings lead me to propose that CBFs activate multiple mechanisms of morphological, physiological and biochemical adjustments associated with abiotic stress tolerance (Fig. 6.1). However, the underlying molecular mechanisms by which CBFs regulate these adjustments are still not fully understood. Future research should be focused on addressing the precise mechanisms governing the CBF-regulation of morphological, physiological and biochemical adjustments.

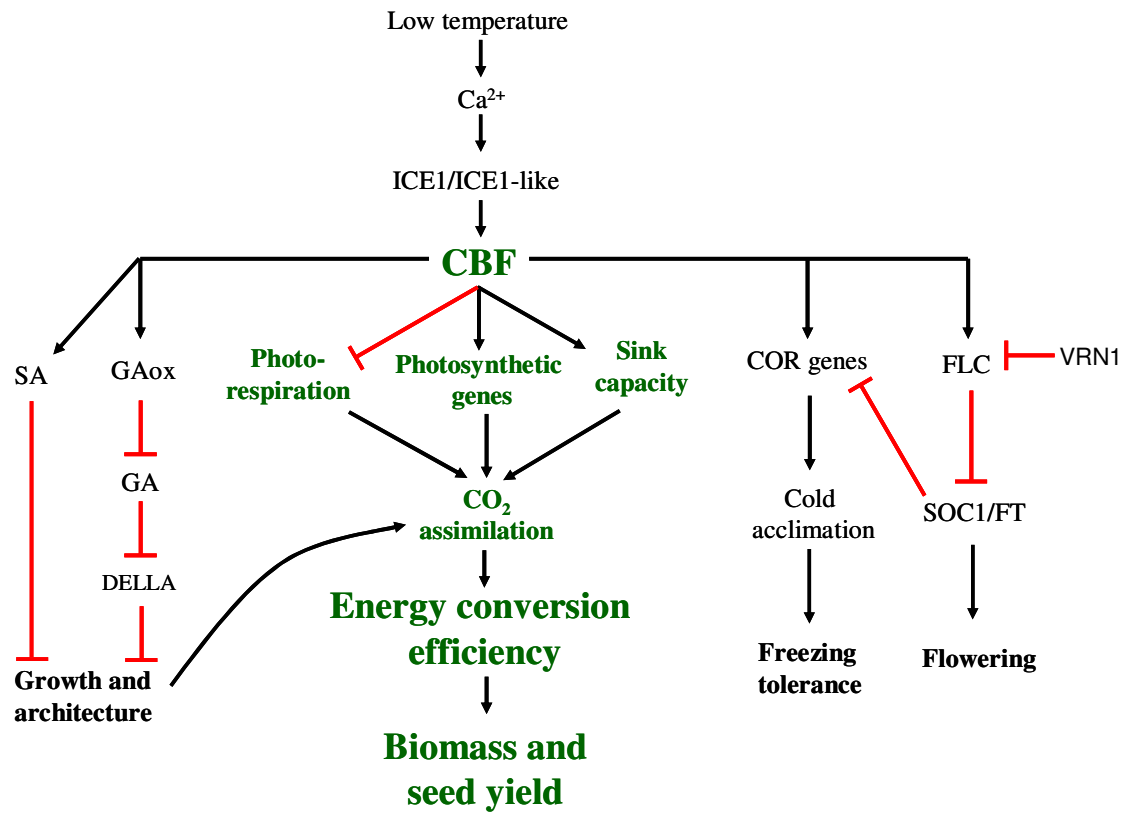


Fig. 6.1. Proposed model for CBF as a master regulator of morphological, physiological and biochemical adjustments. The CBF transcription factor plays important roles in energy conversion efficiency, freezing tolerance, hormone signaling and flowering. CBF expression increases energy conversion efficiency through enhanced CO₂ assimilation as a consequence of altered plant architecture, decreased photo-respiration, enhanced sink strength and increased expression and activities of key regulatory photosynthetic genes. The enhanced energy conversion efficiency is reflected in increased biomass and seed yield. CBF expression increases freezing tolerance through expression of COR genes. CBF expression induces dwarf phenotype due to accumulation of DELLA proteins through suppression of GA. CBF expression induces FLC expression that suppresses transcription of floral promoter, FT/ SOC1. Vernalization represses FLC transcription through VRN1 expression. FT/ SOC1 expression suppresses transcription of COR genes deteriorating cold acclimation capacity and subsequently freezing tolerance. Black arrowheads and red end lines indicate positive and negative regulation, respectively. The green font represents proposed model based on results obtained from my research work whereas black font represents model based on literature review.

6.2 References

- Achard P, Gong F, Cheminant S, Alioua M, Hedden P, Genschik P (2008) The cold-inducible CBF1 factor-dependent signaling pathway modulates the accumulation of the growth-repressing DELLA proteins via its effect on gibberellins metabolism. *Plant Cell* 20: 2117-2129
- Ainsworth EA, Rogers A (2007) The response of photosynthesis and stomatal conductance to rising CO₂: mechanisms and environmental interactions. *Plant Cell Environ* 30: 258-270
- Amthor JS (2007) Improving photosynthesis and yield potential. In *Improvements of Crop Plants for Industrial End Uses*, ed. P Ranalli, pp. 27–58. Dordrecht, Netherlands: Springer
- Chew YH, Halliday KJ (2011) A stress-free walk from Arabidopsis to crops. *Cur Opin Biot*: 22: 281-286
- Chinnusamy V, Zhu J, Zhu JK (2007) Cold stress regulation of gene expression in plants. *Trends Plant Sci* 12: 444-451
- Dubouzet JG, Sakuma Y, Ito Y, Kasuga M, Dubouzet EG, Miura S, Seki M, Shinozaki K, Yamaguchi-Shinozaki K (2003) *OsDREB* genes in rice. *Oryza sativa* L., encode transcription activators that function in drought-, high-salt- and cold-responsive gene expression. *Plant J* 33: 751-763
- Gilmour SJ, Fowler SG, Thomashow MG (2004) Arabidopsis transcriptional activators CBF1, CBF2, and CBF3 have matching functional activities. *Plant Mol Biol* 54: 767-781
- Hüner NPA, Öquist G, Sarhan F (1998) Energy balance and acclimation to light and cold. *Trend Plant Sci* 3: 224-230
- Hurry VM, Strand A, Tabiaeson M, Gardeström P, Öquist G (1995) Cold hardening of spring and winter wheat and rape results in differential effects on growth, carbon metabolism, and carbohydrate content. *Plant Physiol* 109: 697-706
- IPCC, 2007: *Climate Change 2007: The Physical Science Basis. Contribution of Working Group I to the Fourth Assessment Report of the Intergovernmental Panel on Climate Change* [Solomon, S., D. Qin, M. Manning, Z. Chen, M. Marquis, K.B. Averyt, M.

- Tignor and H.L. Miller (eds.)]. Cambridge University Press, Cambridge, United Kingdom and New York, NY, USA, 996 pp.
- Jaglo KR, Kleff S, Amundsen K.L, Zhang X, Haake V, Zhang JZ, Deits T, Thomashow MF (2001) Components of the Arabidopsis C-repeat/dehydration responsive element binding factor cold-response pathway are conserved in *Brassica napus* and other plant species. *Plant Physiol* 127: 910-917
- Kasuga M, Liu Q, Miura S, Yamaguchi-Shinozaki K, Shinozaki K (1999) Improving plant drought, salt, and freezing tolerance by gene transfer of a single stress inducible transcription factor. *Nat Biotech* 17: 287-291
- Jaglo-Ottosen KR, Gilmour SJ, Zarka DG, Schabenberger O, Thomashow MF (1998) Arabidopsis CBF1 overexpression induces COR genes and enhances freezing tolerance. *Science* 280: 104-106
- Leonardos ED, Savitch LV, Hüner NPA, Öquist G, Grodzinski B (2003) Daily photosynthetic and C-export patterns in winter wheat leaves during cold stress and acclimation. *Plant Physiol* 117: 521-531
- Long SP, Ainsworth EA, Rogers A, Ort DR (2004) Rising atmospheric carbon dioxide: plants FACE the future. *Ann Rev Plant Biol* 55: 591-628
- Long SP, Zhu XG, Naidu SL, Ort DR. 2006. Can improvement in photosynthesis increase crop yields? *Plant Cell Environ* 29: 315-30
- McDonald A, Ivanov AG, Bode R, Maxwell D, Rodermel SR, Hüner NPA (2011) Flexibility in photosynthetic electron transport: the physiological role of plastoquinol terminal oxidase (PTOX). *Biochim Biophys Acta (Bioenergetics)*, *in press*.
- Medina J, Catalá R, Salinas, J (2011) The CBFs: Three Arabidopsis transcription factors to cold acclimate. *Plant Sci* 180: 3-11
- Murchie EM, Pinto M, Horton P (2009) Agriculture and the new challenges for photosynthesis research. *New Phytol* 181: 532-552
- Oh SJ, Kwon CW, Choi DW, Song SI, Kim JK (2007) Expression of barley *HvCBF4* enhances tolerance to abiotic stress in transgenic rice. *Plant Biotech J* 5: 646-656
- Oliver SN, Finnegan EJ, Dennis ES, Peacock WJ, Trevaskis B (2009) Vernalization-induced flowering in cereals is associated with changes in histone methylation at the vernalization1 gene. *Proc Nat Acad Sci* 106: 8386-8391

- Pocock TH, Hurry VM, Savitch LV, Hüner NPA (2001) Susceptibility to low-temperature photoinhibition and the acquisition of freezing tolerance in winter and spring wheat: The role of growth temperature and irradiance. *Physiol Plant* 113: 499-506
- Sarhan F, Ouellet F, Vazquez-Tello A (1997) The wheat *Wcs120* gene family: a useful model to understand the molecular genetics of freezing tolerance in cereals. *Physiol Plant* 101: 439-445
- Savitch LV, Allard G, Seki M, Robert LS, Tinker NA, Hüner NPA, Shinozaki K, Singh J (2005) The effect of overexpression of two Brassica CBF/DREB1-like transcription factors on photosynthetic capacity and freezing tolerance in *Brassica napus*. *Plant Cell Physiol* 46: 1525-1539
- Savitch LV, Leonardos ED, Krol M, Jansson S, Grodzinski B, Hüner NPA, Öquist G (2002) Two different strategies for light utilization in photosynthesis in relation to growth and cold acclimation. *Plant Cell Environ* 25: 761-771
- Scott IM, Clarke SM, Wood JE, Mur LA (2004) Salicylate accumulation inhibits growth at chilling temperature in *Arabidopsis*. *Plant Physiol* 135: 1040-1049
- Sung S, Amasino RM (2005) Remembering winter: Toward a molecular understanding of vernalization. *Ann Rev Plant Biol* 56: 491-508
- Trevaskis B (2010) The central role of the vernalization1 gene in the vernalization response of cereals. *Funct Plant Biol* 37: 479-487
- Trevaskis B, Hemming MN, Dennis ES, Peacock WJ (2007) The molecular basis of vernalization-induced flowering in cereals. *Trend Plant Sci* 12: 352-357
- Zarka DG, Vogel JT, Cook D, Thomashow MF (2003) Cold induction of *Arabidopsis* CBF genes involves multiple ICE (Inducer of CBF expression) promoter elements and a cold-regulatory circuit that is desensitized by low temperature. *Plant Physiol* 133: 910-918
- Zhao DY, Shen L, Fan B, Yu MM, Zheng Y, Lv SN, Sheng JP (2009) Ethylene and cold participate in the regulation of *LeCBF1* gene expression in postharvest tomato fruits. *FEBS Lett* 583:3329-3334
- Zhu XG, Long SP, Ort DR (2008) What is the maximum efficiency with which photosynthesis can convert solar energy into biomass? *Curr Opin Biotech* 19: 153-59

Zhu XG, Long SP, Ort DR. (2010) Improving photosynthetic efficiency for greater yield.
Annu Rev Plant Biol 61: 235-61

Curriculum Vitae

Name: Keshav Dahal

Post-secondary Education and Degrees: Tribhuvan University,
Rampur, Chitwan, Nepal
1991-1995 Bachelors in Agricultural Sciences

University of Bonn
Bonn, Germany
2002-2004 Masters in Agricultural Sciences

The University of Western Ontario
London, Ontario, Canada
2007-2012 Ph.D.

Honours and Awards: Dr. Irene Uchida Fellowship in Life Sciences, UWO
2011-2012

Western Graduate Research Scholarship (WGRS)
2007-2012

German Academic Exchange Service (DAAD) Award to pursue
M. Sc. Ag. at the University of Bonn, Germany, 2002-2004

Related Work Experience Teaching Assistant/Research Assistant
The University of Western Ontario
2007-2012

Publications:

Dahal K, Kane K, Gadapati W, Webb E, Savitch LV, Singh J, Sharma P, Sarhan F, Longstaffe FJ, Grodzinski B, Hüner NPA (2012a) The effects of phenotypic plasticity on photosynthetic performance in winter rye, winter wheat and *Brassica napus*. *Physiol Plant* 144: 169-188

Dahal K, Kane K, Sarhan F, Grodzinski B, Hüner NPA (2012b) Cold acclimation inhibits CO₂-dependent stimulation of photosynthesis in spring wheat and spring rye. *Botany (in press)*

Dahal K, Gadapati W, Savitch LV, Singh J, Hüner NPA (2012c) Cold acclimation and *BnCBF17*-over-expression enhance photosynthetic performance and energy conversion efficiency during long-term growth of *Brassica napus* under elevated CO₂ conditions. *Planta (in press)*

Dahal K, Weraduwege SM, Kane K, Rauf SA, Gadapati W, Savitch LV, Singh J, Marillia EF, Taylor DC, Micallef MC, Knowles V, Plaxton W, Barron J, Sarhan F, Hüner NPA, Grodzinski B and Micallef, BJ (2012d) Enhancing biomass production and yield by maintaining enhanced capacity for CO₂ uptake in response to elevated CO₂. Submitted to Canadian Journal of Plant Science

Dahal K, Kane K, Sarhan F, Hüner NPA (2012e) Cold acclimated winter wheat and winter rye maintain enhanced photosynthetic performance, energy conversion efficiency and grain yield under long-term growth at elevated CO₂. *In preparation* (to be submitted to Plant Physiology)

Kane K, **Dahal K**, Houde M, Badawi M, Hüner NPA, Sarhan F (2012) Elevated CO₂ down regulates the plant defense responses at normal growing temperature but not in cold-acclimated wheat. *In preparation* (to be submitted to Plant Physiology)

Oral Presentations

4 oral presentations in international seminars/workshops in Europe and South Asia. Several university level presentations while pursuing PhD, Masters and Bachelors degree.

Poster presentations

Presented 19 posters in several international seminars/conferences in North America, Europe and South Asia.

Others

- ❖ Nominated by Ministry of Agriculture, Government of Egypt (2006) to participate in the intensive training on Agricultural Extension Activities.
- ❖ Humboldt University Award (2006) to participate in the training on Project Cycle Management, Conflict Management and Leading Peoples under European Capacity Building Program for International Development Cooperation at Humboldt University, Faculty of Agriculture and Horticulture, Berlin, Germany.
- ❖ Europe-Asia Link Award (2005-2006) to participate in the intensive training on Basic Soil Parameters (Soil physical, mechanical and chemical properties) at the University of Kiel, Institute of Plant Nutrition and Soil Sciences, Kiel, Germany.
- ❖ Nominated by Japan International Cooperation Agency (JICA) to participate in the intensive training on improving food productivity 2005.
- ❖ Award of excellence on securing first position with distinction on training of trainers organized by the Directorate of Agriculture Training, Department of Agriculture. 22nd November to 3rd December 2004. Kathmandu, Nepal. Ranked first best participant with 95% marks.
- ❖ Nominated by Wageningen University, Netherland to participate in the intensive training on Agriculture Extension Activities and Gender Analysis 2001-02.
- ❖ A silver jubilee medal awarded by His Majesty's Government of Nepal on the occasion of 25th coronation's anniversary of late King Birendra, 1997.
- ❖ Received other many merit scholarships/awards while pursuing Bachelors in Agricultural Sciences, Nepal. 1991-1995.